Cape Peninsula
University of Technology

THERMAL ELECTRIC SOLAR POWER CONVERSION PANEL DEVELOPMENT

by

JANVIER KAMANZI

Thesis submitted in fulfilment of the requirements for the degree

Doctor of Engineering: **Electrical, Electronic and Computer** **Engineering**
in the Faculty of Engineering

at the Cape Peninsula University of Technology

Supervisor: Prof MTE Kahn

Bellville
January 2017

CPUT copyright information
The dissertation/thesis may not be published either in part (in scholarly, scientific or technical journals), or as a whole (as a monograph), unless permission has been obtained from the University

DECLARATION

I, Janvier Kamanzi, declare that the contents of this thesis represent my own unaided work, and that the dissertation/thesis has not previously been submitted for academic examination towards any qualification. Furthermore, it represents my own opinions and not necessarily those of the Cape Peninsula University of Technology.

Signed **Date**

ABSTRACT

The world has been experiencing energy-related problems following pressuring energy demands which go along with the global economy growth. These problems can be phrased in three paradoxical statements: Firstly, in spite of a massive and costless solar energy, global unprecedented energy crisis has prevailed, resulting in skyrocketing costs. Secondly, though the sun releases a clean energy, yet conventional plants are mainly being run on unclean energy sources despite their part in the climate changes and global warming. Thirdly, while a negligible percentage of the solar energy is used for power generation purposes, it is not optimally exploited since more than its half is wasted in the form of heat which contributes to lowering efficiency of solar cells and causes their premature degradation and anticipated ageing. The research is geared at addressing the issue related to unsatisfactory efficiencies and anticipated ageing of solar modules.

The methodology adopted to achieve the research aim consisted of a literature survey which in turn inspired the devising of a high-efficiency novel thermal electric solar power panel. Through an in-depth overview, the literature survey outlined the rationale of the research interest, factors affecting the performance of PVs as well as existing strategies towards addressing spotted shortcomings.

While photovoltaic (PV) panels could be identified as the most reliable platform for sunlight-to-electricity conversion, they exhibit a shortcoming in terms of following the sun so as to maximize exposure to sunlight which negatively affects PVs' efficiencies in one hand. On the other hand, the inability of solar cells to reflect the unusable heat energy present in the sunlight poses as a lifespan threat. Strategies and techniques in place to track the sun and keep PVs in nominal operational temperatures were therefore reviewed.

The literature then revealed that various sun-tracking technologies could grant the power increases ranging between 14 % and 45 % over static solar panels. They were however found short on important issues such as reliability, implementation and cost-effectiveness. Concerning the heat effects on PVs' performance, the literature indicated that exisiting research has mostly focused on concentrated PVs (CPVs) perhaps because of their high operation temperatures and need of cooling thereof. Little was therefore directed to common flat and static solar panels of which the tight mounting on the roof undoubtedly poses as a major cause of temperature rises. These findings from the literature were referred to in the process of devising a novel PV design that yielded an optimal use both the light and heat in the generation of the power.

The design of a novel sun-tracking system was informed by an approach consisting of having at least a façade of the PV system facing the sun in its apparent motion from sunrise

to sunset. Multisided was the qualification of the design of such PV systems formed with regular-sized sub panels, adjoined together at regular angles producing polygonal and half-polygonal shaped PV systems respectively named closed-structure-multisided (CSM) and open-structure-multisided (CSM). Structural models were first conceived and then ad hoc novel mathematical models developed for both OSM and CSM PV systems for performance evaluation purposes. Mathematical models were first verified, validated for a once and newly conducted study to grant a solid base to its results. The models were then translated in MATLAB (Matrix Laboratory) codes and applied to a well-picked sample of OSM and CSM PV systems so as to ensure reliability and accuracy of the results. Results led to a conclusion that the OSM PV systems would provide an average increase of 32 % in collecting the sunlight as compared to flat and fixed-tilt panels of same area, while CSM PV systems proved to receive a stable and consistent sunlight distribution during the daytime of which the average level is the same as that of a flat and fixed-tilt panels. In the same context, it was demonstrated that a double-sided with 60^0 joint angle could guarantee an even irradiance collection distribution which is 32 % more than the reference panel. The findings on the novel sun-tracking schemes served as the basis of the power panel.

Design requirements, limitations, constraints were first established in the design process of the proposed power panel. This ultimate phase of the research was explored and completed at panel and cell scales respectively. In the first place, the design considered two PV panels were assembled together with a 60^0junction angle. With such configuration, the exposed area is twofold that of a laid-flat solar panel, so is the sunlight collected further to the boost of OSM systems on the average harvested power. In the second place, cells were assembled in the same consideration was applied to cells, and resulting assemblies were integrated on one solar panel base. The PV panel thus formed served as the base to thermoelectric (TE) devices that would provide the cooling effect. At the end, the performance comparison between the developed power panel and the flat-fixed-tilt solar panel was established, and the developed panel proved its worth in terms of efficiency and preserving lifespan of solar cells. The research outcome is a novel printable 3D model provided with all measurements, specifications and is ready for prototyping. The research aim was met and the research questions answered.

Overall, this condensed research with a variety of novelties significantly contributes a high-impact knowledge in the field of energy.

ACKNOWLEDGEMENTS

Glory and praise be to the Almighty God for inspiring me in the completion of this work and keeping my family in safe hands.

Special thanks go to Professor Mohamed Tariq Ekeramodien Kahn. Inspiring guidance, encouragements, flexibility and collegial atmosphere were characteristics which enabled a successful research work. Such a blend of qualities is uncommon to be found in one person. So, I was abundantly blessed. I hereby send my thanks to the Centre of Distributed Power and Electronic Systems (CDPES) especially Dr Marco Adonis and Dr Atanda K Raji for advice and encouragement. In the same line, I also convey my gratitude to Martial Giraneza and Mohamed Esmail for keeping me updated on academic schedules and information, Chris Willis and Deon Kallis for technical assistance.

I also take this opportunity to extend my acknowledgment to the management and colleagues at Mechanical Engineering department.

Mathew Sibanda has been a distinguished friend, may he accept my sincere thanks. Valuable, constructive and life-transforming ideas he freely shared have borne fruits and set a good foundation to a sustainable future.

My appreciation extends to Dr Ben Mvuyekure, Christophe Nsengiyaremye as well as Eugene Liberakurora who have been beyond where I could expect them for me.

Last but not least, I acknowledge the good work and all the love and care from Marie Nyirampitiye, my mother, Mercy Kileo, my wife, and the warming smiles from my little angels, Nathan Cornerstone and Aemy Imani Kamanzi.

May God you bless all!

DEDICATION

Aemy Imani, Nathan Cornerstone and Mercy, you are deservedly honoured with this dedication. May also the families of T. Munyanshongore and K. Kileo witness greatness through this work.

CONTENTS

LIST OF FIGURES

LIST OF TABLES

GLOSSARY

Acronyms

^{0} C	:	Celsius degrees
1 G	:	First generation
2 G	:	Second generation
3 D	:	Three dimensions
3 G	:	Third generation
A	:	Ampere
AC	:	Alternating current
Ag	:	Silver
ARC	:	Anti-reflective coating
ARCO	:	Atlantic Ritchfield company
ATO	:	Aluminium-doped tin oxide
CdS	:	Cadmium sulphide
CdTe	:	Cadmium telluride
CHAPS	:	Combined heat and power solar
COP	:	Coefficient of performance
CPV	:	Concentrated PV
c-Si	:	Monocrystalline Silicon
CSM	:	Closed structure multisided
Cu	:	Copper
Cu_2O	:	Copper oxide
CuI	:	Copper iodide
DC	:	Direct current
DHET	:	Department of higher education and training
DoE	:	Department of energy
DSSC	:	Dye-sensitised solar cells
EMF	:	Electromagnetic force

ESKOM	:	South African power utility
FTO	:	Fluorine-doped tin oxide
Ge	:	Germanium
HVDC	:	High voltage direct current
I^-	:	Iodine negative ion
IAEA	:	International atomic energy agency
IEA	:	International energy agency
ITO	:	Iodine-doped tin oxide
J	:	Joules
K	:	Kelvin
kW	:	Kilowatt
LCOE	:	Levelized cost of energy
m	:	Meter
m^2	:	Square meter
MATLAB	:	Matrix laboratory
mc-Si	:	Multicrystalline Silicon
MPP	:	Maximum power point
n-	:	Electron-doped
NASA	:	National aeronautics and space administration
NOCT	:	Nominal operating cell temperature
NREL	:	National renewable energy laboratory
NSPDA	:	National space development agency
OSM	:	Open structure multisided
p-	:	Hole-doped
P	:	Phosphorous
PCM	:	Phase change material
Pt	:	Platinum
PV	:	Photovoltaic

PVT	:	Photovoltaic thermal
PVT/a	:	Photovoltaic thermal hybrid / air
PVT/w	:	Photovoltaic thermal hybrid / liquid
PV-TE	:	Photovoltaic-TE
RCA	:	Radio Corporation of America
Se	:	Selenium
Si	:	Silicon
Si-C-Ge-H	:	Silicon-Carbon-Germanium-Hydrogen
TE	:	TE
TEG	:	TE generator
Ti_2O	:	Titanium oxide or Titania
UNFCCC	:	United Nations framework convention on climate change
USA	:	United States of America
UV	:	Ultra violet
V	:	Volt
W	:	Watt
WWWII	:	World war two
zT	:	Figure of merit

Equation symbols

A	:	Area
D	:	Diameter
G	:	Irradiance
G_M	:	Nominal irradiance
G_{avg}	:	Average irradiance
H	:	Height
k	:	Boltzmann constant
i	:	Iteration order
I	:	Current
I_{ph}	:	PV current
I_S	:	Cell's saturation of dark current
N	:	Ideality factor
m	:	Number of iterations
n	:	Number of sides
p_n	:	Power at noon
p_s	:	Power at sunrise/sunset
q	:	Electronic charge
r	:	Radius
R_S	:	Series resistor
R_{sh}	:	Shunt resistor
t	:	Time
T_C	:	Cell's temperature
V	:	Voltage
V_{oc}	:	Open- circuit voltage

φ	:	Phase angle
ω	:	Angular velocity
$\sum$	:	Summation symbol
$\in$	:	Belongs to

CHAPTER ONE

OVERVIEW

1.1. Chapter summary

1.2. Statement of the research problem

1.3. Background to the research problem

1.4. Research questions

1.5. Aim and objectives

1.6. Methodology

1.7. Delineation of the research

1.8. Significance of the research

1.9. Deliverables

1.10. Publications

1.10.1. Journal articles

10.1.2. Conferences

1.1. Chapter summary

Chapter one gives the reader a broad but full overview of the thesis contents. The rational of the research is highlighted and substantiated with solid arguments in the background of the problem. The research questions that set the path to strategies that were used to successfully complete the research are part of this chapter as well. Aim and objectives and the methodology used to achieve them were meticulously discussed. The end-product and all the expected outcomes of this research were concisely outlined. The publications that derived from this work were listed as well.

1.2. Statement of the research problem

The world has been faced with unprecedented energy-related problems. These problems, with a paradoxical aspect, can be three-fold stated: Firstly, the world is undergoing a critical energy crisis responsible of energy cost exponential hikes. Secondly, power plants are still mainly running on polluting conventional primary sources of energy though the sun covers the earth's surface with a huge amount of clean energy every day of which a negligible percentage is exploited for power generation purposes. Thirdly, of that negligible portion used in power generation, more than its half is heat waste and breaks cells' junction causing premature degradation and ageing. Although solar energy has been deservedly identified as one of the solutions to the mentioned issues given its cleanness and abundant availability, its utilization needs a review in terms of optimization. Only light, a portion equivalent to 25 % of the solar energy spectrum is ready for conversion into electricity whereas the major part of the remaining energy is a waste that degrades photovoltaic (PV) cells and affects their efficiencies. Furthermore, common PV technology is limited to making use of about 30 % of the readily available sunlight due to their inability of tracking the sun which results in low efficiencies. The issues pertaining to PVs low efficiencies are the focus of this research.

1.3. Background to the research problem

Forecast suggests that the global demands in electricity might double by the year 2030 (Crabtree & Lewis, 2007). It was also indicated that (Narendrasinh Parmar et al., 2015)a major part of electric energy demands has been fulfilled by means of steam plants. Furthermore, the demand for fuel and heat involved in electricity generation could increase by 60% by a decade and half. The resulting increase of the environmental degradation and of global warming (IAEA, 2012) would worsen state of climate changes due to the increase usage of fossil fuels in running steam plants main generators of electric power worldwide (Kyono, et al., 2012). The preliminary

literature also indicated that the efficiencies at electric power generation stage are low and efforts to improve these efficiencies should be encouraged. The efficiency at the output of the steam boiler is 100 % and drops to 90 % when evaluated at the input of the turbine. In the process of converting the mechanical energy from the turbine into electrical energy, the efficiency tremendously fall from 90 % to as low as 30-40 % (Honorio, et al., 2003).

Alternative sources of energy in the form of solar and wind have therefore been identified as means of addressing the shortcomings encountered in conventional systems. Keeping within solar boundaries, substantial research initiatives have been invested into taking advantages of solar energy merits, and interesting results have been achieved as solar energy could be double-folded exploited from both light and heat perspectives. Applications such as electric power generation, water heating and air-conditioning (Jingcheng, 1959) are at the core of solar-based technologies that are fast growing given the global prevalent energy demands in mentioned areas; and alarming effects of conventional energy generation systems on the environment and the society.

From illumination perspective, the invention of PV cells in 1883 as a conversion platform of light into electricity, was one of the biggest achievements of the century (Fraas, 2014). Research initiatives have been ipso facto taken up for efficient use of the clean energy from the sun and promising results have been gradually recorded. Highly efficient PV cells (Santra & Kamat, 2012) have thus been invented and their use has seen a rapid growth in terms of electrification proving the worth of solar-based electricity in the solution to the global energy preoccupations. Indeed, the power utilities in most countries of the globe have invested in putting in place strategies aiming at enabling the integration of solar energy in national power grids.

From the heat point of view, water heating and air conditioning systems working through absorption or adsorption processes are counted among the major applications. With buildings holding 40 % of the global energy consumption (Kamal, 2012), heating and cooling claim a share estimated to 10 % (Lain & Hensen, 2006) and solar energy-based air conditioning systems have been worthily viewed as viable and cost saving alternative to electric heaters and air conditioning systems.

However, solar-energy-run systems are disadvantaged by low efficiencies, firstly due to the low ability to absorb the sunlight, quality strictly dependent on the material playing the role of rectification in a solar cell (Ismail & Ahmed, 2009). An ideal rectifier, normally a photodiode was meant to transfer an electricity charge per

phonon, but experiments ironically showed low performance. Lab results suggested that only 30 % of phonons are converted into electricity for a good quality diode whereas practical results showed a conversion percentage of 10 % (Green, 2002). Solar panels commonly used for electricity supply, have efficiencies generally less than 20 % though some laboratory experiments suggest that up to 40 % efficiency could be achieved with concentrated cells (Green et al., 2011). In addition, the efficiency of solar systems-subject of this study- is further lowered by the solar modules' inability to make full use of the incident sunlight. Solar panels are conventionally laid on buildings' roofs in a way they cannot track the East-to-West sun's apparent movement. Same applies to solar collectors and solar concentrators. At sunrises and sunsets, the incident radiation is parallel to the receiving plan of the panels or collectors, yielding a Gaussian-shaped overall irradiance. In the mix of platforms that are used to harvest and directly transform solar energy in electric or heat energy, PV systems have been taken as a study case. Since the problem resides in solar energy capturing and the principle being the same irrespective of the end-use, findings for PV systems can be used to analogically approximate expected findings for solar collectors.

Beside the uneven distribution of the irradiance, ageing, weather, shading, temperature increase and physical defects are other factors that affects PV cells in general.

Solar panels' performance is understood to naturally decline as they age. Studies suggest that cells are subject to degradation rate of about 0.5 % per year; whereas a 20 % degradation of a solar module is qualified for failure; though the figure may be debatable (Jordan & Kurtz, 2013). Even though ageing is natural and unavoidable, there are factors that haste it through the degradation of cells.

Heats beyond prescribed limits are the major reason of a progressive deterioration of cells that are meant to operate within safe boundaries of nominal operational temperatures. Silicon-based cells, when serving as primary power supply to spacecraft, are expected, beside the ageing, to undergo a change of temperature of up to 180^{o} C between the extreme temperatures (-80 ^{0}C and 100 ^{0}C) in the space environment while the efficiency sees 0.5 % drop for each ^{0}C increase (Ovchinnikov et al., n.d.). It should be then understood that the efficiency would decline for positive temperature gradients in one hand whereas it would rise for positive temperature gradients referring to the nominal operating temperature.

While solar cells' efficiency is an adequate indicator to quantitatively evaluate the performance of cells in terms of the output power they can deliver, power parameters (explicitly the current and voltage of the cells at the maximum point) are the ones directly influenced by thermal conditions of the environment. The literature has shown that for a degree Celsius increase inflicts a 0.37 % drop on the open circuit voltage and 0.05 % increase on the short circuit current for the crystalline silicon cells; and this lead to an assertion that open-circuit voltages are more affected by the temperature where the change rate is about 8 times higher than the change rate of the short circuit current. Temperature rises are a result of the heat energy which forms a major part of the incident solar energy spectrum that PVs cannot convert in electricity or reflect. While the PVs can convert a maximum of 25 % of the sunlight, waste heat energy is estimated at above 50 %; the remaining percentage representing the reflected portion of the spectrum (Chow, 2010). One of the feature of this research is to recover that heat energy and reconvert it into electricity in one hand and to pump the heat out thus keeping the PVs operated at their nominal operating cell temperature (NOCT) (Ibrahim, 2011).

In previous paragraphs, heat has been proven to be problematic with regards to PVs lifespan and efficiencies. However, referring to space applications, there should be suggestions concerning the way of exploiting the massive thermal energy since it is quasi impractical to get steam or nuclear plants due to diverse reasons including the inexistence of water in space and of the supporting physical environment. Heat-to-electricity conversion power panel could be identified as a good alternative to PVs with regard to spacecraft primary power systems. PVs deficiencies related to the degradation (Jordan & Kurtz, 2012) and the dependence of the efficiency on the sunlight can be overcome by a material capable to guarantee power supply even during the absence of the sun like in orbit eclipse. TE conversion would be also a suitable solution to thermal issues observed in small satellites. In this category of satellites, the smallness of the volume is the source of the high temperature gradients that in turn can sabotage the whole working of the spacecraft (Martinez, 2014; Baturkin, 2012). In this regard, TE conversion would be playing a twofold role: power supply and cooling effect.

For manufacture-related defects, there are those occurring when cells are being strung together, those observable in the process of laying out cells and defects happening during the lamination and defects directly inherent to the basic component, the cell.

Cells are typically strung together by means of soldering. When the soldering is not properly done, cases like poor soldering can give room to high contact resistance between cells, which can also be linked to temperature increase on the solder ribbon. Thus, the cells are connected in series in the layout process using wires. At this stage, possibilities of cells movement can have cell-connecting wires unwantedly joined together occasioning short circuits in the array. The lamination is phase consisting of encapsulating cells with a membrane in a high temperature process that should take place in vacuum-free and isothermal conditions. Failure to comply with the conditions, lead to bubbles between the membrane and the cells and a premature crack in the formed glass is expected due to the presence of the vacuum and to the thermal uneven distribution in the lamination process. This may also be accompanied with cells disjunction and hence to poor power conversion and arrays' low efficiency. Other defects in PV cells world directly relate to the base component of the array, and commonly characterised by the antireflective coating (ARC) peeling off the silicon surface or simply by cells breaking during the fabrication process, shipping and installation. Such types of defects are understood to be dealt with by the manufacturers and companies in-charge of shipment.

1.4. Research questions

- How do I design a simple and competitive sun-tracking PV system?
- How do I design a system that cools PVs and converts heat into electricity?
- How do I design a compact panel that meets the research aims?

1.5. Aim and objectives

The purpose of this research is to develop a highly efficient solar power panel that fully exploits solar energy spectrum.

In the process of the panel development, focus was put on the efficiency. The efficiency was presumed to be raised by:

- Developing a reliable and cost-effective sun-tracking system.
- Applying a simple and suitable cooling technique.
- Developing a platform for heat- into- electrical energy conversion.

1.6. Methodology

The methodology followed in developing the thermal electric solar power panel is broken as follows:

- Investigative literature on sun-tracking methods with emphasis on their performances, advantages and disadvantages. This helped evaluate the

designed system in terms of capturing the irradiance as compared to existing methods. In the power panel development process, the methods proposed were first conceived, modelled mathematically, then coded using Matrix Laboratory (MATLAB) which provided results. The mathematical model was in each case verified and validated for results' integrity and reliability sake. Both the mathematical models and codes were developed in a way it could accommodate a large sample possible so as to ensure the accuracy of the findings. From (Leite, 2010), MATLAB was developed in USA by MathWorks, Inc, Natick. The first version was released in 1984 and was essentially geared at performing mathematical computation especially complex matrix-related equations. With time, MATLAB has been adapted to accommodate a variety of applications such as control systems, power plant systems, aerospace, bioinformatics, statistics to name just a few. MATLAB has been an essential tool for simulating systems in universities around the world. It has also seen its application in high-profile firms such as NASA and General Motors.

- Sun-tracking using a multisided approach: Two types of structural configurations were explored and their performance quantified in terms of irradiance capturing ratio. Mathematical models for open and close-structure multisided PV systems were developed in the first place and the irradiance dynamics of respective PV systems were then profiled in MATLAB 2014 release.

- System evaluation and selection: To evaluate the performance of multisided PV systems, key parameters were considered namely the average value, the deviation from the mean value and the irradiance collection ratio. These parameters were computed for a variety of open-structure multisided (OSM) PV systems and closed-structure multisided (CSM) PV systems. The parameters were assessed against those of a flat-plate-fixed tilt solar panel of the same area and ratings.

- Investigation on PV cooling systems and heat-to-electricity conversion: The purpose of cooling PVs is to keep the PV systems within their operating temperatures. Thus, their efficiency is unaffected or improved when operated in a colder surrounding environment. The panel design was therefore made such that passive cooling can keep cells aerated. As for converting heat in electricity, an extensive literature was conducted. Thermoelectric (TE) and PV-thermal (PVT) hybrid systems attracted more attention and showed

closeness to the research in question. TEs were regarded for offering a double advantage. With their ability of directly changing heat into electricity while cooling the hot side at the same time, a TE-based-material was recommended to be placed at the back of each cell.

- Power panel design: The design was done into major steps. The design of the sun-tracking structure was the basis of the overall panel design. Based on the chosen structure, a macrostructure consisting of a multisided assembly of solar panels was first studied and developed. Microstructures made of PV cells were then joined and laid on a solar base through Solidworks and the model was developed.

1.7. Delineation of the research

The research project was limited on the development of a physical model for high efficient PV systems' design. Developed model was primarily developed for terrestrial applications though it could provide a massive insight in the design of spacecraft's primary power supply.

1.8. Significance of the research

The significance of this research is of high importance as it aligns with the policies aiming at lifting the burdening energy crisis and its skyrocketing as well as associated issues of global warming and climate change in terrestrial applications. As for space applications, from the literature point of view, this research suggests the optimal use of the abundant solar thermal energy present in space and on other planets while addressing the deficiencies of the current methods used as primary source of energy.

The output of this research project may directly benefit the Department of Energy (DoE), power producers and utilities.

1.9. Deliverables

The primary end-product of this research, a power panel, is a model with full measurements and specifications that can be referred to by manufacturers for prototyping. The work done in the process of the model development comprise a thesis and five journal articles of which some are accredited by the department of higher education and training (DHET).

1.10. Publications

Publications related to this research project are chronologically listed as follows:

1.10.1. Journal articles

Kamanzi, J. & Kahn, M. 2015. Development of a Renewable Energy-Based Cooling System for a Mobile Ground Station. IEEE Aerospace & Electronics Magazine, 30(2): 6–13. **DHET accredited.**

Kamanzi, J. & Kahn, M. 2016. Multisided approach for photovoltaics regulated outputs : computer-based simulations. Journal of Energy Challenge and Mechanics, 3(2): 93–99.

Kamanzi, J. & Kahn, M.T. 2016. Closed-structure multisided PV systems for evenly distributed irradiance collection. International Journal of Electronics and Communication Engineering, 5(6): 29–36.

Kamanzi, J. & Kahn, M.T. 2017. Development of a model for highly efficient solar power panels. International Journal of Applied Engineering Research.12(10):2171-2181. **DHET accredited**.

10.1.2. Conferences

Kamanzi, J. & Kahn, M. 2013. Low energy cooling technology for a cubesat mobile ground station. Proceedings of the 10th annual conference on Industrial and Commercial Use of Energy, 19-21 August 2013, Cape Town: CPUT: 183-188.

Kamanzi, J. & Kahn, M. 2013. Low energy cooling technology for a cubesat mobile ground station. Award-winning presentation at the centre of postgraduate studies (CPGS) conference of the 5th November 2013.

CHAPTER TWO

LITERATURE REVIEW

2.1. Chapter summary

The literature review conducted highlighted the background of the global energy crisis and PVs efficiency and degradation issues in detail. The causes affecting the PV performance were discussed and graphically modelled where possible. Thermal effects, PV's weather-dependence, shading and irradiance collection ratio topped the list among the causes. Thermal effects and PVs' weather-dependence were simulated and results conformed to those proposed by other authors. Advances in sun-tracking technologies with their efficiencies were overviewed, their functioning, advantages and disadvantages discussed. Current sun-tracking systems with moving parts and electronic involvement were found to be unreliable beside post-installation maintenance costs. A section on PV technologies, their historical, functioning and types was compiled in order to get the knowledge of what was available and what was suitable for this study. A review on PV cooling technologies was synthetized with regard to cooling PVs, and TE cooling was found to suit best the aim of this project. TE technologies were therefore brushed up, their operation mode and applications outlined. The light was shed on TE poor efficiencies as well.

2.2. Introduction

The unprecedented time of energy crisis and its consequences on both the society and environment (Sthel, 2013) has instigated remarkable research in the domain of alternative sources of energy. Fossil fuels dominating the pool of primary energy supply are faced with depletion due to exponential increase in energy demands in one hand and critics of the big role they in the alarming global warming and climate change on the other hand.

The global demand in energy is deemed to double within the next two decades (Crabtree & Lewis, 2007); which implies an imminent increase use of complementary energy sources with more focus on green and renewable type (Wright, 2015). In this regard, Global Market Outlook (Photovoltaics, 2014) indicated that solar-based power would increase from 138.8 GW (2013 figures) to 1700 GW within two a decade and half (2030), whereas a further remarkable increase up to 4670 GW should be expected by 2050. In parallel, the same author highlighted there would be an increase in the implantation of wind-supplied power generators with a bit lower impact observable than solar-powered generators.

With the sun providing about 2 MWh/m^2 to the earth (Systems, 2015), which is way far higher than any other source of energy (Mittal V, Kasana KS, 2005) and being by

excellence IEA compliant, solar energy has proven its worth in terms alternative power generation platform for all the time.

In the context of South Africa, the Department of Energy (DoE), along with public power utility (ESKOM) in addition to private companies, have made significant progress towards a full and optimal use of available energy sources and integration of the latter in the national grid. Policies involving independent power producers (IPP) were adopted with regard to adopting distributed energy sources in electric power systems (Carter-brown et al., 2015; Wasiak & Hanzelka, 2010). To make this a success, smart techniques for grid automation and management of power distributed systems were given a priority research wise (Diamandis, 2015).

Solar energy's unique qualities have therefore seen notable research initiatives being directed to its exploitation. Interesting results have been achieved as solar energy could be double-folded exploited from both light and heat perspectives. Applications such as electric power generation, water heating and air-conditioning (Jingcheng, 1959) are at the core of solar-based technologies that are fast growing worldwide given the global prevalent energy demands and alarming effects of conventional energy generation systems on the environment and the society. However, energy-conversion platforms developed so far, including PV panels, solar collectors and solar concentrators, have been criticized for low efficiencies. In the mix of platforms that are used to harvest and directly transform solar energy in electric or heat energy, PV systems have been taken as a study case. Since the problem resides in solar energy capturing and the principle being the same irrespective of the end-use, findings for PV systems could be used to analogically approximate expected findings for solar collectors and solar concentrators. PV systems were then thoroughly investigated in their area of low efficiency and the reasons behind were deeply discussed in the first chapter.

However, with focus on solar energy, low efficiency and inconsistent power outputs of PV cells remain an intricate concern to address. This has been a major and long-time handicap to the successful implementation of a PV-based grid by power utilities. A lot of studies and initiatives from various perspectives have been carried out with encouraging results; of which some have been spotlighted.

Efficiency improvement has been targeted by much research in an attempt to make PV technology more viable and an increase of 5% could be gained by using Magnesium-doped quantum dot sensitized solar cells (Santra & Kamat, 2012). Thin

film is another technology which was brought forth to increase the PV efficiency yielding an increase of about 5 % (Santra & Kamat, 2012)

2.3. PV technologies

The sunlight has to be absorbed by solar cells for the light to convert into electricity. Inside solar cells, there is a structure that absorbs photons and then generates free electrons through a PV effect. The energy conversion material is a semiconductor junction which is the basic solar cell technology. The junction is made of an electron-doped region (n) and hole-doped region (p) on the other side. The electricity generation follows the principle of photodiode (Floyd, 2012). For electric energy generation, the sunlight energy strikes the cells and raises the energy levels of valence electrons and frees them. A potential barrier that develops around the pn-junctions results in a voltage capable of driving currents in electrical circuits.

2.3.1. Brief PV historical

From the study conducted by Green (2002), research on PV effects started in 1876 by Adams and Day when they were investigating photoconductivity in Selenium (Se). Seven years later, the first Se-thin-film PV were fabricated by Fritts. Until the 1940s, efficient solar cells exploited copper oxide (Cu_2O) and titanium sulfide (TI_2S) as a light-absorbing layer and a metal contact as rectifying layer. In photo electronics, rectification refers to the conversion of photons in electricity (Floyd, 2012).

Semiconductor-based solar cells were first developed in 1941 by Russel Ohl at Bell Laboratories. A hole-doped region (p) and an electron-doped region (n) are put together to form a junction which plays a rectifier role. Normally, a p-region is created by doping a quadrivalent element with a trivalent element, thus creating holes. Conversely, an n-region is obtained by doping a quadrivalent element with a pentavalent element which results in free electrons in the region. In the1970s, the advances in PV technologies were characterised by the introduction of crystographic texture on cells' top surfaces as means of minimizing reflection losses in the incident sunlight.

However, the history of solar energy in general dates before Christ (BC) era. Ã et al., (2011) provide milestones in the historical development of solar technology in general as briefed in the following:

Between the 7^{th} and 2^{nd} centuries BC, solar energy could be used to produce fire when sun rays are concentrated through magnifying lenses. Greeks and romans exploited the discovery for setting alight torches for religious purposes. Greek

scientist Archimedes exploited bronze properties to burn belligerent's wooden ships during their war against Romans.

A time period between the 1st and 4th century anno domini (AD) was characterised by the development of a bathhouse by Romans which was having the windows facing the sun's daily apparent motion. Two centuries later, sun rights were instituted by guaranteeing sun rooms in houses even in public places. North Americans only started living in South-facing houses in order to enjoy winter sun in 1200 AD. More serious discoveries were yet to come at this stage.

The 18th century was marked by the invention and development of the first ever solar collector by a Swiss scientist Horace de Saussure. The developed device was later used by Sir John Herschel during his 1830s South African expedition.

In the 19th century, 1816 precisely, 86-year-old Robert Stirling, a minister in the Church of Scotland, built a heat engine that was named after him and which he applied a patent for. The invention found applications in a solar thermal technology applying sun rays concentration system to generate power. Its model was also used by Lord Kelvin in his university classes.

In 1839, Edmond Becquerel, a French scientist discovered the PV effect. He was conducting experiments on an electrolyte cell with electrodes placed in a good electricity conducting solution. He could realize that electricity production was increasing was he exposed the cell to the light.

In 1860, an idea of a solar-powered steam engine was proposed by August Mouchet, French mathematician. The idea proposal came to mature two decades later when he, assisted by Abel Pifre, developed the first multipurpose solar-power engines which paved the way for parabolic solar collectors.

In 1873, selenium conductivity was discovered by Willoughby Smith, facts confirmed by William Grylls Adams and Richard Evans. Thus, the concept of light-to-electricity conversion was proved with no resort to moving parts but by just using solid-state material.

In 1880, a balometer was invented by Samuel Langley. The device used to measure light from stars and sun's heat rays, is made of a wire connected to an electrical circuit. Observations showed that the resistivity of the wire to electricity was increasing as it was hit by sun's rays heat.

In 1883, Charles Fritts, an American inventor, laid down the description of Selenium-made solar cell wafers. Eight years later, the first commercial solar water heater was patented for a Baltimore inventor, Clarence Kemp.

Furtherrmore, Wilhelm Hallwacks discovered the photosensitivity of Copper and Cuprous oxide in 1904. A year later, Albert Einstein published a paper concerning PV effect.

In 1908, a solar collector formed by copper coils and as heating material was invented by William J. Bailey.

Robert Millikan concluded on the photoelectricity effect in 1916, two years after the existence of a potential barrier was brought to light (in 1914); which was followed by Polish scientist Jan Czochralski work on growing single-crystal silicon PVs. In 1921, Albert Einstein won the Nobel Prize as a result of his work and publications on PV effect during the same year. The latter (effect) was discovered in Cadmium Sulfide (CdS) eleven years later (1932) by Audobert and Stora.

In 1947, passive solar technology in buildings was in demand in USA to accommodate the energy scarcity caused by World War Two (WWII). Participation of about 50 architects were part of the initiative of which a book titled Your Solar House was published by Libbey-Owens-Ford Glass Company.

In 1953, Dr. Dan Trivich of Wayne State University established calculations on the efficiency and band-gap width of various PV materials with regards to solar energy spectrum.

In 1954, Americans celebrated the invention of Silicon PV cells by Daryl Chaplin, Calvin Fuller and Gerard Pearson at Bell Laboratories. Developed PVs could produce a much higher power with efficiencies of 4 % which grew up to 11 % with time. Western Electric in 1955 started selling licences for commercial PVs. The first commercial building fitted with solar water heating and running on passive methods was implanted by architect Frank Bridgers.

In 1956, the idea of developing PVs for earth-orbiting satellites was tabled by William Cherry of the US Signal Corps Laboratories. In 1957, Hoffman Electronics developed PV cells with 8 % efficiency which he scaled up to 9 % two in the following two years.

In 1958, US Signal Corps Laboratories manufactured pn- based Silicon PV cells excellently suitable for space applications given their resistance to radiation. The same year was characterized by significant advances in space engineering which saw numerous PV-powered satellites being launched. The Vanguard I and II,

Explorer III and Sputnik 3 were successfully launched during 1958. Explorer VI was put on orbit the following year. Si-solar cells thus became approved as a primary power source for satellites.

A year later (1959), 10 %-efficiency for commercial Si-cells were manufactured at Hoffman Electronics. With one year only, the efficiency was scaled up to a stunning figure of 14 %. Silicon Sensors, Inc., is founded dealing with Se and Si PV cells production in 1960.

In 1962, the first PV-powered telecommunication satellite was launched by Bell Telephone Laboratories with 14Watt-initial power. A year later, Sharp Corporation produced PV practical modules. The world's largest PV of that era array was installed on a lighthouse by in Japan.

In 1965, the National Aeronautics and Space Administration (NASA) launched a 470-Watt-PV-powered satellite, Nimbus, while Peter Glaser came up with the idea of solar power satellite station.

The following year, NASA launched the first orbiting astronomical observatory power-supplied by 1-Kw PV array with the mission of gathering data on sun's radiation in UV and X-rays that pass through the atmosphere to earth.

In 1969, a solar furnace running on parabolic mirror was built in Odeilo, France. Further developments were observed in 1970s with the design of significantly low-price cells. Price cut down from $100 to $20 a Watt could be achieved by Dr Elliot Berman with the collaboration of Exxon Corporation. This has prompted the extensive of PVs in numerous applications especially for remote areas which are not connected to the utility's grid.

In 1972, research on the development of thin-film PVs was initiated at the Institute of Energy Conversion of the University of Delaware which became the world's first laboratory exclusively oriented to research on PV development. The following year, the first solar-powered residences called Solar One were built at the research institute. A PV/Thermal hybrid integrated in the roof was used to feed metered electric power to the utility network during the day and relayed by the utility power at night. It was also serving as a flat-plate solar thermal collector.

In 1976, NASA disseminated 83 PV systems over all the continents but Australia. Mentioned systems were intended to assist in various medical applications such as vaccine refrigeration, medical clinic lighting, telecommunication, classroom lighting and so forth. The project initiated in 1976, it was accomplished in 1995. It is during

the same year that David Carlson and Christopher Wronski of the Radio Corporation of America (RCA) Laboratories fabricated the first thin film Si-PV cells.

In 1977, the US DoE put in place the Solar Energy Institute specializing in renewable energy with focus on the exploitation of the power from the sun. More than 500 kW power could be produced from PVs then manufactured.

In 1978, Papago Indian Reservation in Arizona became the world's first village to use PV systems for residential electricity supply and to run water pumps. The 3.5-kW PV system was installed by the NASA's Lewis Research Center in 15 homes which were not grid-connected yet.

In 1980, Atlantic Richfield Company (ARCO) set a record by manufacturing more than a Megawatt PVs in a year. University of Delaware managed to fabricate PVs using Copper Sulfide/Cadmium Suflide with an efficient exceeding 10 %.

Year 1981 was marked by a first solar-powered aircraft, the Solar Challenger, built by Paul McCready which he used to fly across the English Channel from France to England. The aircraft carried 3-kW- electric power through in 16000 PV cells spread on its wings.

In 1982, a high-scale PV power station became operational in Hisperia, California. A MW dual-axis-sun-tracking system of 108 modules was built by ARCO solar. Elsewhere, in Australia, the first solar-powered car, the Quiet Achiever, was driven by the Hans Tholstrup. The car was twice faster than a gasoline-powered one based on the speed that was put to cover the distance between Sydney and Perth. At the same time in US, Solar One, a 10-MW central-receiver demonstration project became operational. The project considered developing power-tower systems using solar thermal electric or solar concentrating technology. In Germany, Volkswagen begins the testing of PVs for ignition system for Dasher station wagons using 160-W-roof-mounted arrays. During that year, PV production exceeded 9.3 MW power worldwide.

In 1983, ARCO Solar implant 6-MW-PV substation in central Carolina, an unmanned facility that has the capacity of supplying the power to 2500 homes. In the Hudson River Valley, a 4-kW-powered home was built by Solar Design Associate. The power production stunningly increased to 21.3 MW, more than twofold previous year figures with more than $250-million sales worldwide.

Year 1984 was marked by Sacramento Municipality Utility's first one-megawatt PV facility.

In 1985, the efficiency barrier for Si solar cells that was set at 20 % under 1-sun conditions was broken by the University of South Wales.

In 1986, the world's largest solar thermal facility was developed in Kramer Junction, California. The purpose of the facility was to produce the steam and run conventional electricity plants. This could be performed by through rows of mirrors that would concentrate the sun's heat energy into pipe system that would circulate the heat fluid in turn. ARCO solar releases the G-4000, the world's first commercial thin film power module.

Two years later, in 1988, Lepcon and Lumeloid, two solar power technologies invented by Dr Alvin Marks were patented. Lepcon technology is made of super-thin aluminium or copper strings covering a glass panels. As the sunlight hits the metal trips, electrons flow from one end to the other thus producing electricity. Lumeloid technology is similar to Lepcon with the exception that the former used a cheaper material in the form of thin-film, or a plastic in the place of glass panels which is covered with conductive polymers or long chains of molecular plastic units.

In 1991, the US DoE was renamed as the National Renewable Energy (NREL) by then US President George Bush.

In 1992, 15.9 %-efficient thin film PVs made of Cadmium Telluride (CdTe) were produced at the University of South Florida, making them to be the first to lift the 15 % efficiency technology barrier.

In 1994, the NREL had a Solar Energy Research Facility completed. The building exploiting solar energy and passive design earned a recognition of being the most-energy efficient of US government buildings in the world. It is during this year that the first solar dish generator running on a Sterling engine without piston was connected to the utility grid and the efficiency-record-breaking (>30 %) cells made of Gallium Indium Phosphide and Gallium Arsenide were developed by NREL.

In 1996, a high technology airplane Icare powered with very high efficiency PV cells was developed at the University of Stuttgart, Germany. Three thousand cells were laid on wings and tail covering an area of 21 m^2. In US, the DoE with the collaboration of the industry consortium made operational Solar Two, an upgrade of Solar One. It proved and showed techniques of storing solar energy usable to produce power even in the absence of the sunshine.

In1998, Pathfinder, an aircraft that was remote-controlled and powered with solar cells, flew as high as eight thousand feet in Monrovia, Carolina, setting a record

altitude for that matter. Meanwhile, scientist Subhendu Guha study on amorphous cells yielded the invention of solar shingles, a roofing material.

In 1999, the tallest skyscraper of New York City was built based on the most-energy efficient technologies of the time. With regards to PV cells' efficiencies, Spectrolab, Inc. and NREL produced a 32.3 %-efficiency PV using three-layer solar cells, and a combination of devices that would concentrate sun's rays and track the sun. NREL also recorded an efficiency of 18.8 % for thin film cells. PVs' installation reach 1 GW-power worth.

In 2000, Perrysburg, Ohio had the biggest PV manufacturing plant with the capacity of producing 100 MW power yearly, the International Space Station initiated the development of the largest PV arrays launched in space. Furthermore, Sandia National Laboratories developed a new inverter which was deemed to ensure the safety of the systems during the power blackout. In the thin film domain, BP Solarex realised largest power modules which could produce a power of order 91.5 W. Furthermore, the largest residential PV installation was observed in Colorado, where the electricity needs were mostly catered for based on PVs.

In 2001, many events came forth with regards to PVs advances. Home Depot opened more than 60 stores in US. Meanwhile NASA developed Helios, the tallest a solar-powered aircraft of the time with more than 18 miles- height. In Japan, the National Space Development Agency (NSPDA) initiated an idea of supplying solar power via a satellite covered with solar panels. The power would be supplied to earth via an airship that would have received by means of laser form the satellite. It is also during the same year that TerraSun LLC came with a technology based on holographic films which enables the concentration of sunlight on PV cells. The inventor of the technology stated that holographic films offer selectivity in terms of light allowed to or not to pass through transparent modules; which was an advantage over Fresnel-based sun concentrating technology. It was also claimed that holographic films could be integrated in buildings and act as skylights. Solar-wind largest power system was put in place by PowerLight Corporation in Hawaii in order to make use of the available power at maximum. More advances in PV technology materialized in Indianapolis in the invention of a solar-electric canopy having glasses coated with thin films.

In 2002, NASA scientists successfully tested an unmanned and solar-powered aircraft, Pathfinder, which was flown at a highest altitude and operating as a telecommunication platform. In Canada, Automated Tooling Systems Inc. put on

market a PV technology known as Spheral Solar. PV cells made of tiny Si beads and kept together with two sheets of aluminium foil. The technology was envisaged as low cost given the use of reduced amount of Si as compared to multicrystalline solar Si cells.

Advances in the area of PV technologies were further favoured by global efforts to preserve the climate within acceptable limits. The outcome the 21st Conference of Parties (COP) held in Paris by end 2016 about the United Nations Framework Convention on Climate Change (UNFCCC) emphasises on keeping the temperature rises as low as 1.5 ^{0}C (Jäger-waldau, 2017). Paris Agreement strongly recommended the use of renewable energy for residential and commercial electric power as well as friendly synthetic fuels for transport applications. While the energy sector was 81 % lead by fossil fuels in 2014, PV production costs have significantly improved. A decrease of 85 % in production cost was achieved between 2008 and 2016. In 2015, the Levelized-Cost-of-Energy (LCOE), a metric of assessment of lifetime costs and returns was found to range between $0.07 and $0.13/kWh in US; the figures are a function of parameters such as location and federal as well as state incentives (Jones-albertus et al., 2016). The DoE SunShot Initiatives aims at levelling PVs' costs relative to conventional energy sources by 2020. The aim is to achieve a LCOE of $0.07/kWh and $0.09/kWh for commercial and residential applications respectively.

Therefore, there is an imperative need of exploring existing technologies in the perspective of functioning, costs and efficiencies.

2.3.2. Semiconductor-based cells

In semiconductor-based cells, the phenomenon of light-to-energy conversion is based on the pn-junction (diode) working principle (Green, 2002). With no voltage applied to its terminal, a diode absorbs a fraction of incident blackbody which is transmitted according to the spectral absorptance. The absorbed light rises level of valence electrons' energy until the band-gap energy is overcome. Excited electrons enter the conduction band where a hole-electron recombination process occurs concurrently along with the reflection of a small amount of the absorbed energy. The active material in the whole process is technically referred to as rectifying material. Significant advances have been gradually observed concerning the its development by combining heterogenous rectifying materials and form higher efficiency multijunction cells. As such, double or triple pn junctions stacked on top of each other are integrated in one cell to ensure each junction deals with the sunlight energy suited to its band gap and spectrum. Hence, spectrum-related energy losses

occurring in the conversion process are minimized. Thus-formed rectifying material have a merit of providing more electrical power than single-junction cells using a small surface area. In fact, III group and V group elements were the ones involved in the doping of quadrivalent elements such as Silicon (Si) and Germanium (Ge).

Further progress in PVs materialized through the development of thin films on the basis of group II-group VI compounds, such is the case for the CdS. Thin films are deposited via chemical bath in a heterojunction window layer (Thompson et al., 2008; Dharmadasa et al., 2014) whereas heterojunction amorphous cells made from the Silicon-Carbon-Germanium-Hydrogen (Si-C-Ge-H) alloy (Solesvik Oppedal, 2013; Hegedus, 2005). As semiconductor-based cells involve high production costs, research initiatives have shifted focus and targeted cost-effective technologies. Dye-sensitized nanocrystalline (Jiao et al., 1991) and organic semiconductors were further developments from the homo or heterogeneous semiconductors.

2.3.3. Dye-sensitized solar cells

Dye-sensitized solar cells (DSSCs) differ from the ordinary pn-junction based cells from the energy conversion point of view (Jiao et al., 1991; Green, 2002) . While both light absorption and charge carrier take place side-by-side in pn- junction cells, the processes occur separately in dye-sensitized cells. The sunlight is collected by dye molecules adsorbed on a nanocrystalline, the Titania (Ti_2O) being the most utilized. The charge transport is done in a separate photosynthesis process through a lower cost and wider band-gap oxide than Si-cells and III-V group compounds. In terms of cost, dye-sensitized cells have proven to be about 40 % cheaper than the Si-cells, they exhibit a particular feature of flexibility and transparency (Rawal et al., 2016) while providing same efficiency range as amorphous cells.

For the working principle, the energy conversion is performed by a series of essentials as follows: glass substrate, transparent conducting layer, TiO_2 nanoparticles, dyes, electrolyte, a counter electrode and a gasket.

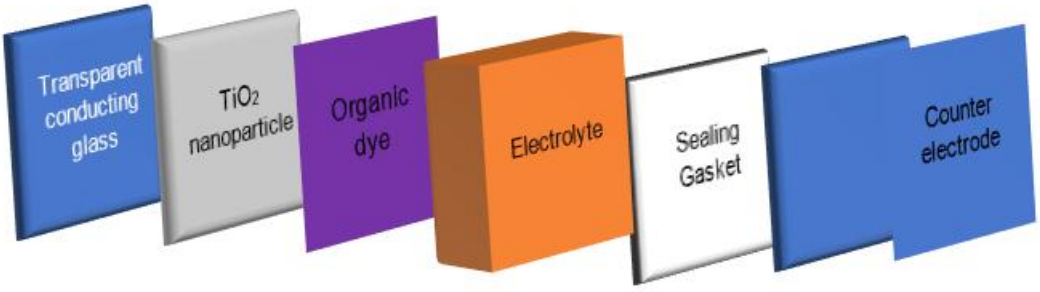

Figure 2. 1: DSSC essentials (adopted from Jiao et al. (1991))

- The glass substrate: material at the front of the DSSC made in glass that performs transmission of the light in the cell and ensures transmission of electrons to the circuit.
- The transparent conductive oxide: a negatively-doped layer of Ti_2O used for its high photosensitivity, structure stability and cost-effectiveness. Other elements such as Fluorine-doped tin oxide (FTO), Iodine-doped-tin oxide (ITO) and Aluminium-doped-tin oxide (ATO) could be also successfully used. Before the introduction of Titania by Gratzel, DSCC's efficiency was as low as 1 % (Jiao et al., 1991). The Titania also offers an advantage of operating at significantly high band-gap (~3.2 V) for a maximum particle size of 30 mm diameter and 20 µm thickness. Therefore, the fact that they only absorb the UV portion of the sunlight estimated at about 5 % of the solar spectrum, dyes guarantee the optimal use of solar energy spectrum.
- Dye molecules: with their ability to absorb much of visible light photons, dye molecules form a key essential that contributes to the improvement of DSSCs' efficiencies. At the beginning, DCCS were operating on transitional metal coordinated compounds such as ruthenium polyprydil as sensitizers (Grätzel, 2003). Ruthenium complexes could rise the cells efficiencies to a height of 11 % but high costs posed as a shortcoming that triggered search for alternative sensitizers with quite good photon absorption ability. Organic dyes, natural pigments and synthetic organic dyes were then found to be a solution based on their donor-acceptor structure which is also known as push-pull. They improve the light absorption in the red and infrared regions and increase the short current density. Natural pigments present in leaves, flowers and fruits, could grant 7.1 % efficiency DSSCs (Campbell et al., 2007). Synthetic organic dyes do not involve metal ion and could offer efficiencies as high as 10 %. They exist in several kind of acids such as Indolic dyes and Cynocrylic acids while being ten times cheaper than ruthenium-based dyes (Zeng et al., 2010) .
- Electrolyte: There are three types of electrolytes: organic solvents, inorganic solvents, and solid electrolytes. Organic solvents essentially consist of iodine negative ions such as I^- and I^{3-} which play a role of facilitating the transport of electrons. Electrolytes such as Acetronite Lithium ease the electrons' diffusion and penetration in the film of Titania. However, their performance suffers from instability as the electrolytes are prone to natural volatilization despite the initial good efficiencies. Inorganic solvents are ionic liquids composed by salts

and salt mixtures. They are known to do well while their liquid properties are still preserved. Efficiencies go declining otherwise. Solid electrolytes of which spiro-MEOTAD and copper iodide (CuI) are the most used present instability in their performance as well. They suffer from state instability and crystallization; and they cannot duly fill in the porous Titania film as such. They require addition of ionic liquids to regain their properties. With spiro-MEOTAD, DSSC efficiency of about 5 % could be attained.

- Counter electrode: It is a glass substrate at the back of the DSSC covered by a thin layer of Platinum (Pt). It serves as a catalyst in the generation of iodine negative ions and as a cathode material. Despite the good performance of Pt, high costs lead to considering alternative material; and carbon cathodes were found to be the suitable substitutes. 9.1 % could be achieved (Grätzel, 2003).

With the efficiency and production costs being the driving factors, the need of a more realistic approach of manufacturing PVs was imminently being sought for. Depending on application requirements, and efficiency levels required, PVs were categorized in three generations.

2.4. PV technology generations

Kibria et al. (2014) and Bagnall & Boreland (2008) have discussed the classification of PVs according to generations: first generation (1 G), second generation (2 G) and third generation (3 G). Generations have been outlined based on the correlation between production-cost and PV cells' efficiency.

2.4.1. First-generation PV cells

1 G is the oldest generation of PVs based on single crystal silicon cells (c-Si) and multi-crystal Silicon (mc-Si) produced on wafers. For 2 to 3 W power each wafer, many cells are put together to form a panel according of a specified power. In terms of crystals, single or mono crystal cells are the ones made with only one crystal grains, whereas multi crystal cells consist of a multitude of crystal grains each. Despite the high efficiencies of mono crystal over mc-Si cells, the latter dominate the word market at a rate of 63 % due to their low production cost (Bagnall & Boreland, 2008). 1 G PV lab efficiencies could hit the high of 24.7% whereas best module efficiencies are limited at 21.7 % (Kibria et al., 2014). However, in their previous work, Bagnall & Boreland (2008) had indicated that 1 G PV efficiencies would be of order 18-21 % in general. They also stipulated that the efficiencies of mc-Si cells would range between 13-14 %. However, the latter authors still highlighted concerns about

costs involved in 1 G PV production. They indicated that half of that cost was due to the mechanical work involved in developing thick silicon wafer (200-500 µm). The authors suggested that the reduction of the Si wafer could be followed by the reduction of the production cost.

2.4.2. Second-generation PV cells

Second generation (2 G) PVs was thought of as a PV design that would help alleviate costs involved in the development of 1 G PVs while keeping close to the efficiencies figures. The approach was deemed to retrench the unnecessary material possible from the production budget. 2 G technology focused on a variety of material including amorphous Silicon cells (a-Si) thin film solar cells, mc-Si cells, CdTe solar cells, CuIn(Ga)Se_2 (CIS/CGIS) solar cells. Their efficiencies are lower than those of 1 G PV cells, so is their production cost, since the active material is deposited on low-cost substrates, a glass for instance. With a little thickness (1-10 µm), the active material could capture much light and a stunning 10 % efficiency could be recorded. Lab tests showed 16.5 % and 18.4 % efficiencies for CdTe and CIGS respectively, and module efficiencies as low as 10. 7 % (Green, 2011). According to Segal et al. (2004), 2 G PVs have been praised for their visual aesthetic and their ability to be applied on cars and windows. Thin films also offer an advantage of being deposited on flexible substrates, thus enlarging the field of applications unlike wafer cells. They can be applied to walls, car windows and so forth. Furthermore, 2 G PVs can be reproduced in larger area up to 6 m^2 while wafer cells can only be generated in wafer dimensions (Bagnall & Boreland, 2008).

2.4.3. Third-generation PVs

Third-generation (3 G) PVs aims at ultrahigh efficiencies for the same production costs as 1 G and 2 G PVs. 3 G targets at making use of proven and viable technologies such as nanocrystal-based cells, polymer-based cells, dye-sensitized cells and concentrated photovoltaic cells (CPV) (Kibria et al., 2014). Though not commercially available yet, hopes are high referring to 32 % efficient GaInP/GaAs/Ge triple junction limited to space applications due to too high development costs (Bagnall & Boreland, 2008).

2.4.4. PVs in power cogeneration

Electrical power is generated by solar panels or solar arrays which consist of cells put together by mechanical and electrical means according to size and power requirements. PVs are rated referring to the peak power they can produce when the sun is directly overhead on a clear sky day. For applications, PVs can be used in

stand-alone mode in residences generating the power of order of kW, or in grid-connected mode along with conventional coal, gas plants where they are power requirements are of order of GW.

From a review conducted by Parida et al. (2011), PVs have been involved in a variety of cogeneration or hybrid systems with great success. Hybrid power generation refers to a combination of PVs with conventional forms of power generation (such as coil, gas, hydro) or a renewable energy source (like wind, fuel cells, to name just a few). With remote area in the mind, studies conducted, showed that a stand-alone PV-wind stand-alone power generator was more effective than the PV and wind in independent stand-alone modes. PV-Fuel cell hybrid system utilising an electrolyser to generate the hydrogen and a fuzzy regression model for maximum power point tracking could also be implemented.

However, producing high efficiency PV cells with low-production costs poses as a tough challenge referring to the material, manufacture process plus external factors affecting cells' efficiency.

2.5. External causes of PVs poor efficiencies

In terms of external factors that further affect PV cells efficiencies, the following are viewed as the main factors:

- Poor irradiance capturing ratio (Yilmaz et al., 2015).
- Manufacture or factory related defects and ageing (Bhushan, 1999; Jordan & Kurtz, 2013).
- Heat effect (Sabri et al., 2007).
- Unfriendly weather and shading (Pachpande & Jalgaon, 2012).

2.5.1. Poor irradiance capturing ratio

PV modules, typically fixed-tilt ones which are laid flat on buildings' rooftops, are characterised by the inability of making use of the available irradiance. As such, they cannot synchronise with the sun's apparent movement over daytime and cannot take advantage of the available light to ensure maximum electrical energy conversion.

PV arrays as traditionally laid on the roof of buildings at a fixed angle can receive the maximum sun irradiation at noon over a whole day (Figure 2.1). Moreover, the sun shuttling between the two tropics yearly exposes the shortcoming of fitting PV modules at fixed tilt angle. Figure 2.2 shows combined effect of sun's daily and yearly apparent movements on the output power dynamics. The PV output power was simulated with respect to the irradiance set at 1 kW/m^2 for convenience purposes; the

sun moving from one tropic to another i.e. between -23.45^0 and 23.45^0 (You et al., n.d.).

The sun's movement double effect is also shown on a three-dimension (3D) plot in Figure 2.3. The PV output power shown in Figure 2 reflects a moderated case with a minimum of 92 % of the expected output for an observer located in the equatorial region. With the tropic being the limits of observation, the best in terms of irradiance will occur when one tropic is experiencing the solstice whereas the opposite tropic is at the worse since having the longest night producing an output drop down to 72% of the nominal output. Figure 2.4 portrays a 3D-plot of the irradiance distribution between the two global poles. Simulations were done assuming the solar panel laid flat and tangential to the equator. The model followed to produce the plots was based on a sine-shaped distribution governing the amount of irradiance collected by a fixed-tilt solar panel from morning to evening. The conditions were set ideal with a sunrise at 6:00 and the sunset at 18:00. The irradiance was assumed to be uniform and equal to the nominal irradiance of 1 kW/m^2.

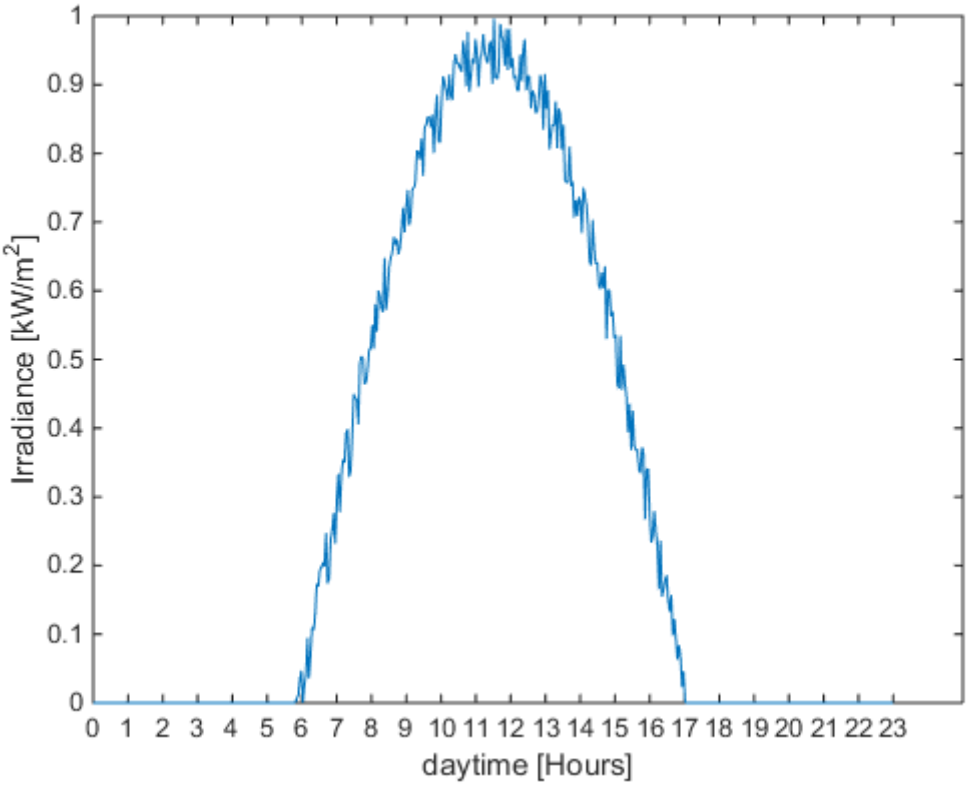

Figure 2. 2: Daily irradiance ideal distribution of a PV panel

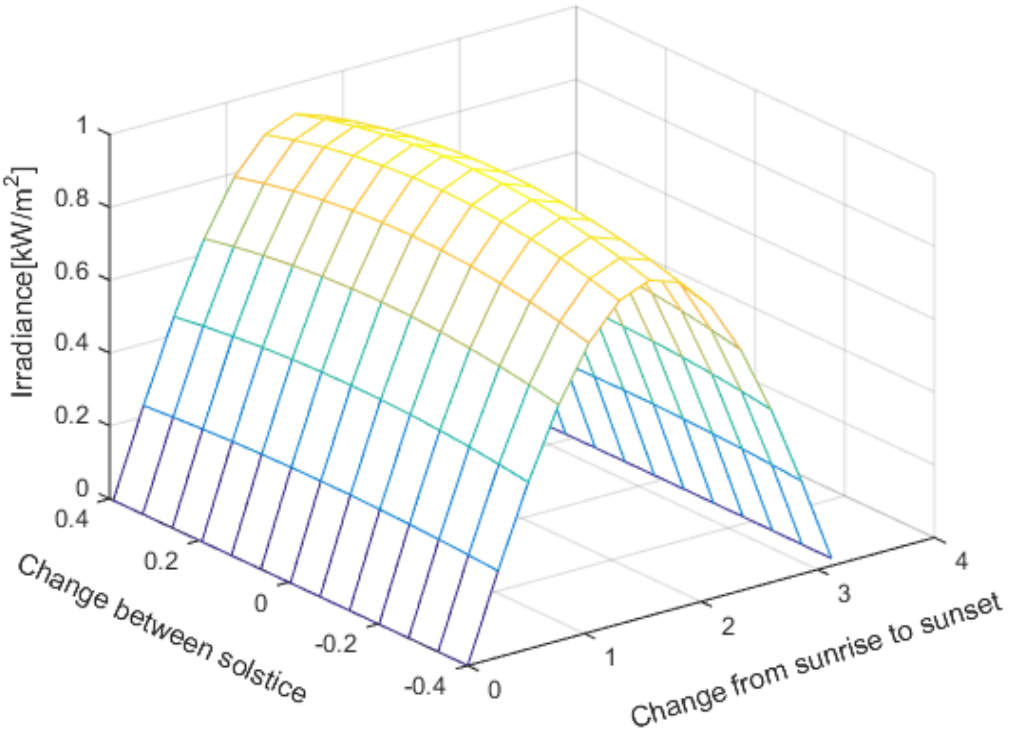

Figure 2. 3: Effect of sun's intertropical motion on flat and fixed-tilt PV panels

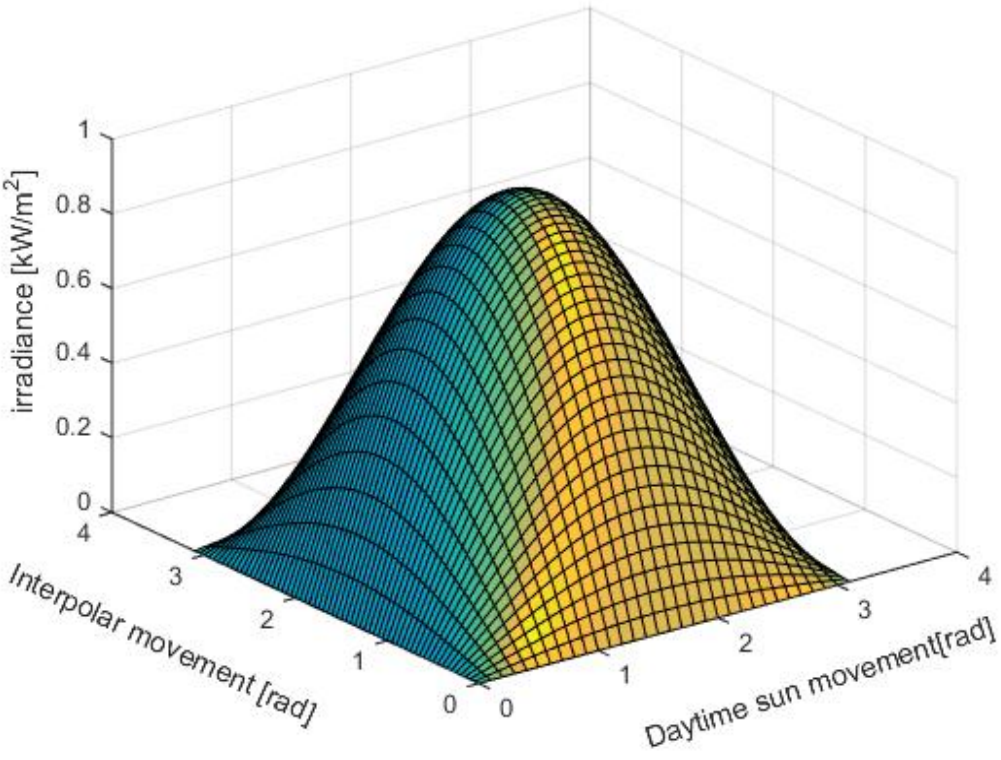

Figure 2. 4: Effects of interpolar sun's movement on flat and fixed-tilt PV panels

2.5.2. Heat effects on PV efficiency

Only a little amount of the solar energy contained in the light spectrum is converted into electricity while a huge portion of heat spectrum negatively impact on energy conversion efficiencies performance PV cells and is responsible of their degradation and early ageing. Chow (2010) indicated that common PV cells could only exploit the light which is estimated to 17 % of the incident solar energy. After deduction of reflected energy, an amount above 50 % of incoming energy is absorbed by the cells in the form of heat. If not dissipated, the heat or thermal energy could affect cells' efficiency and cause permanent structural damages at the cells junction. The author mentioned a 0.4 % efficiency fall for each Celsius degree increase though others converged on a bit higher figure of 0.5 % decrease per a Celsius degree rise (Moharram et al., 2013; Jordan & Kurtz, 2013). Also, studies conducted showed that the open-circuit voltage *(Voc)* changes much higher than the short-circuit current *(Isc)* at respective rates of 0.37 % and 0.05 %; which yields a 0.5 % in the maximum power point (MPP). Given a PV cell parameters, the impact of temperature effects, the characteristics of the current or power against the voltage of a PV module have to be obtained following mathematical and electrical models, a solar simulator or through experimental measurements.

Solar cell models

For scientific analysis of PV cells parameters behaviours with respect of factors such temperature, illumination, the cells physical models have translated to their equivalent electrical models which were suitable for a mathematical representation. There are three types models referred to when it comes to studying and analysing PV cell performance.

Ideal model

In the ideal model, PV cells are represented as a current source in parallel with a diode, and is mathematically represented as per equation 2.1.

$$I = I_{ph} - I_S\left[\exp\left(\frac{V}{NV_T}\right) - 1\right] \qquad \textbf{Equation 2. 1}$$

$$V_T = kT_c / q \qquad \textbf{Equation 2. 2}$$

Non-ideal model with a resistor placed in series with the diode (Equation 2.3)

$$I = I_{ph} - Is\left[\exp\left(\frac{V + IR_S}{NV_T}\right) - 1\right] \qquad \textbf{Equation 2. 3}$$

Non-ideal model with both series and shunt resistors (Equation 2.4)

$$I = I_{ph} - Is\left[\exp\left(\frac{V + IR_S}{NV_T}\right) - 1\right] - \left[\frac{V + IR_S}{R_{sh}}\right] \qquad \textbf{Equation 2. 4}$$

Where: I_s is the cell saturation of dark current, k is Boltzmann constant equal to $1.38*10^{-23} J/K$ (Boltzmann constant), $q = 1.6*10^{-19} C$ (Electronic charge), R_s is a series resistor, R_{sh} is a shunt resistor, T_c is the cell's temperature, and $N = 1.1$ is the ideality factor).

The last two models with resistors included are more practical. The first one has a series resistor. The shunt resistor, very large, represents the surface quality along the periphery whereas the series resistor, very small derives from the ohmic contact between metal and semiconductor internal resistance. The three models have the electrical representations as per Figures 2.5-2.7.

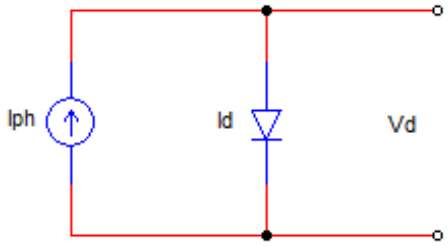

Figure 2. 5: Ideal model

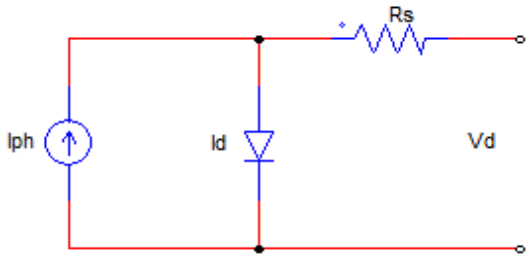

Figure 2. 6: Model with series resistor

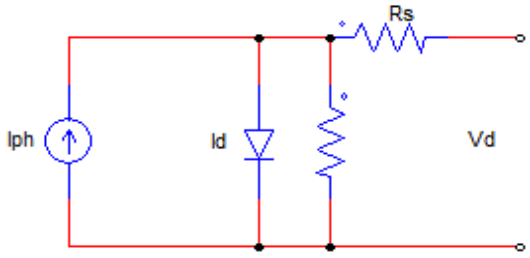

Figure 2. 7: Model with shunt and series resistors

2.5.3. Thermal effects in graphs (PV cells' performance vs thermal fluctuations)

The performance of PV cells is basically estimated based on electrical equivalent circuit. This section portrays the effects of temperature on the output of a fictive PV module given some parameters. A complete model consisting of a diode in parallel with a shunt resistor and a series resistor was used. The open circuit voltage and short-circuit current are respectively 32.9 V and 8. 21 A. The nominal irradiance generally set equal 1000 W/m^2 is maintained and the nominal operating temperature of 25^0 C is considered. The performance of the module was studied for both positive and negative temperature gradients in two dimensions (2D) and three dimensions (3D).

In 2D, only two parameters can be evaluated against each other whereas the third one must be kept constant. For instance, the plot of the change in the current of the module versus the change in the voltage has to be made when the temperature is kept at a certain constant value. The same applies for the power versus voltage. The voltage-current (V-I) and the voltage-power (P-V) curves are shown in Figures 2.8 and 2.9

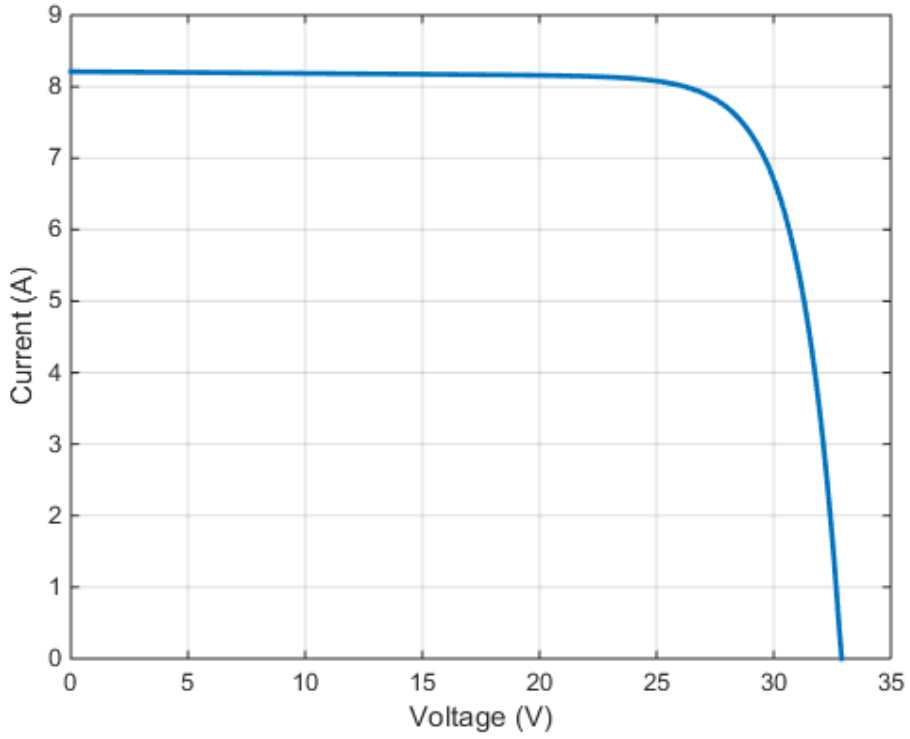

Figure 2. 8: Current-Voltage characteristic at operating temperature

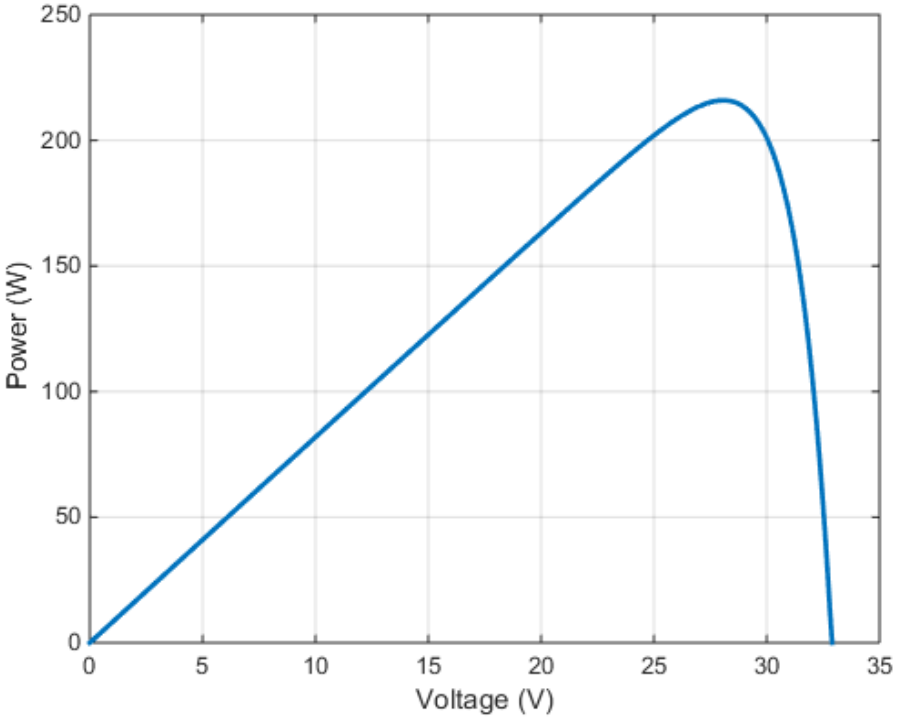

Figure 2. 9: Power-voltage characteristic at operating temperature

To evaluate the performance of the module in 2D over a range of temperatures, one has to repeat the process for each discrete value of temperature in order to sketch V-I and P-V curves. Figures 2.10 and 2.11 illustrate the change in the V-I and V-P characteristics if the module was operated in extreme temperatures of the space environment (Sunlight and eclipse). From the graphs, with reference to the nominal operation temperature, a gain of about 8 V can be gained when the module is operated at 180 K whereas a loss of more than 10 V may be incurred when the module's temperature rises to 360 K. Similarly, a gain of 30 W and a loss of up to 70 W are expected for the mentioned extreme temperatures.

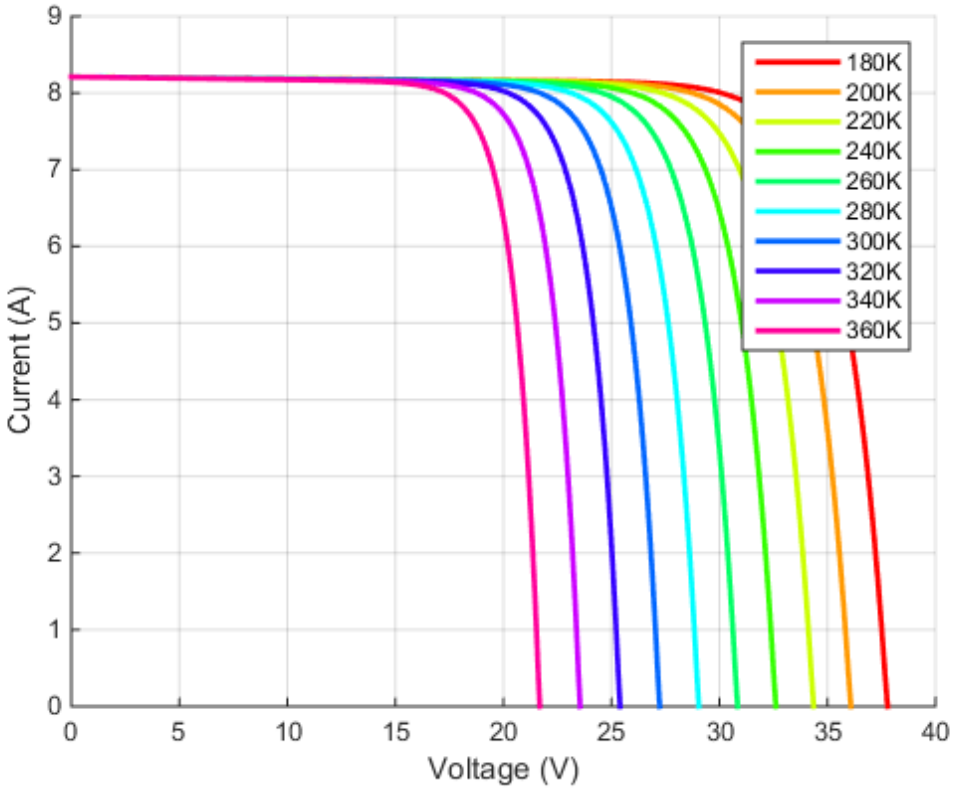

Figure 2. 10: Thermal effects on the open-circuit voltage between 280 K and 460 K

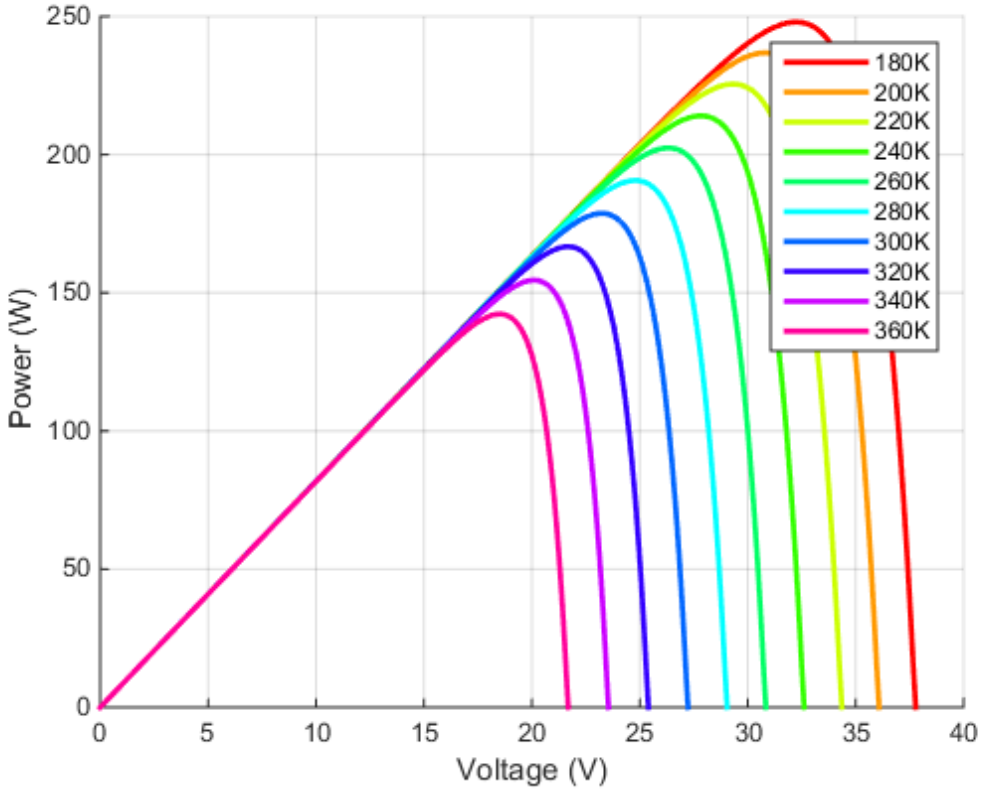

Figure 2. 11: Thermal effect on the power for temperature between 280 K and 460 K

The performance curves of PV modules have mostly been graphically represented in 2D, only relating to parameters per curve at a time. In this study, the researcher has introduced the possibility of relating three changing parameters of PV modules in one graph. Parameters taken into consideration are the voltage, the current, the power and the temperature. Thus, V-I-T graphs (relating the voltage change with respect to the current and temperature) P-I-V graph (evaluating the power against the current and voltage), and P-I-T (reflecting the power change with regards to the temperature and current) are displayed in Figures 2.12, 2.13 and 2.14. 3D graphs are plotted based on a temperature range of 180 K to 500 K.

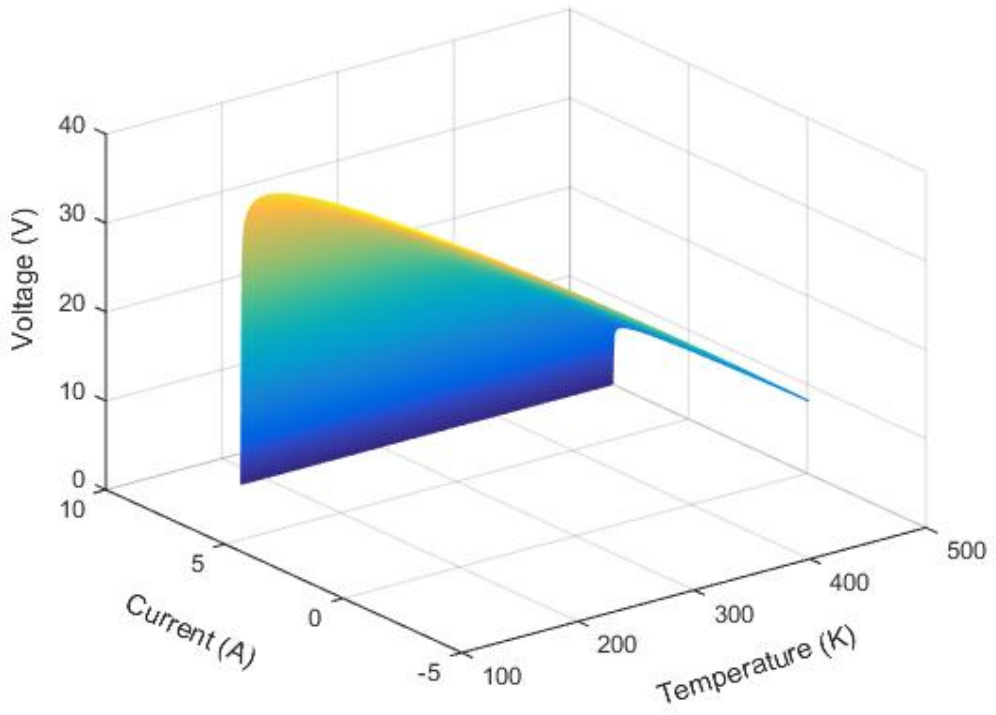

Figure 2. 12: 3D plot of Voc versus current and temperature when PV cooled between 460 K and 100 K

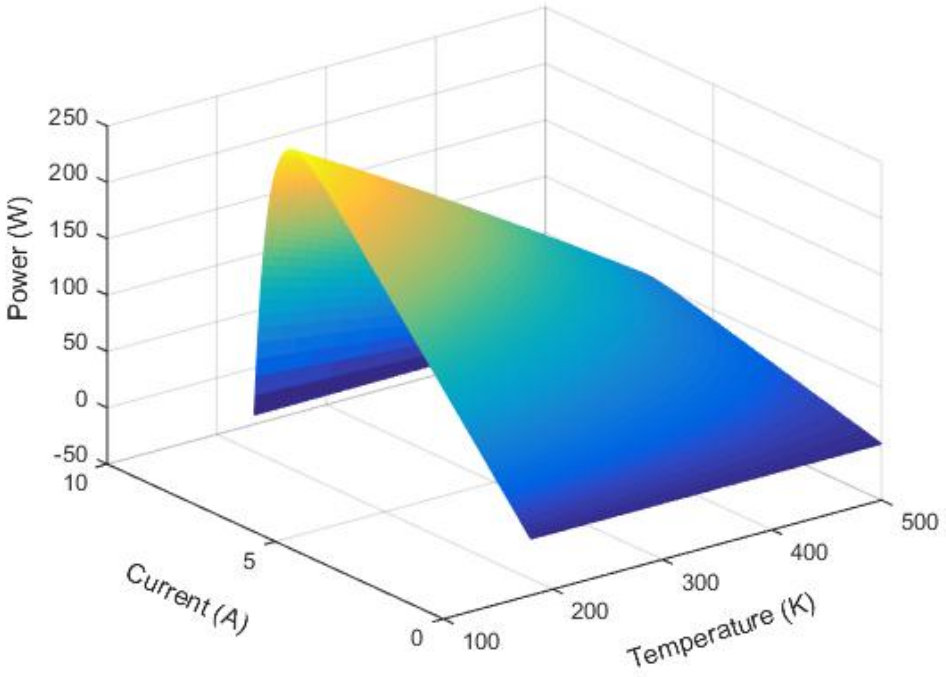

Figure 2. 13: 3D plot of the power versus the current and temperature when PV cooled

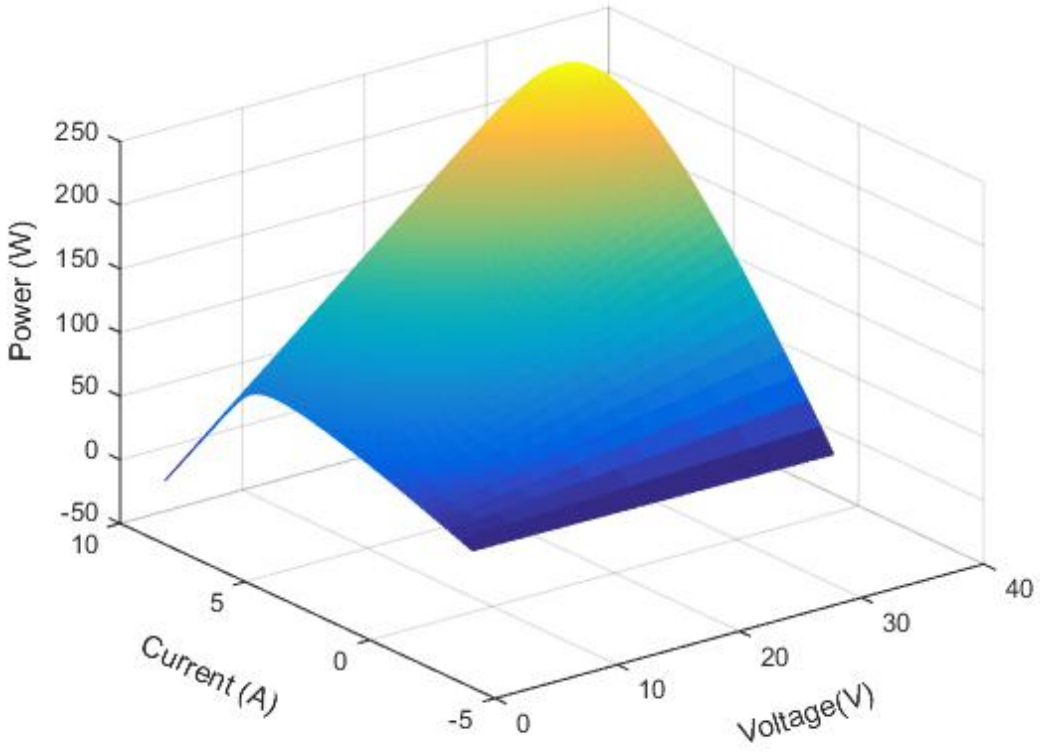

Figure 2. 14:3D plot for power versus current and voltage when PV cooled between 460 K to 180 K

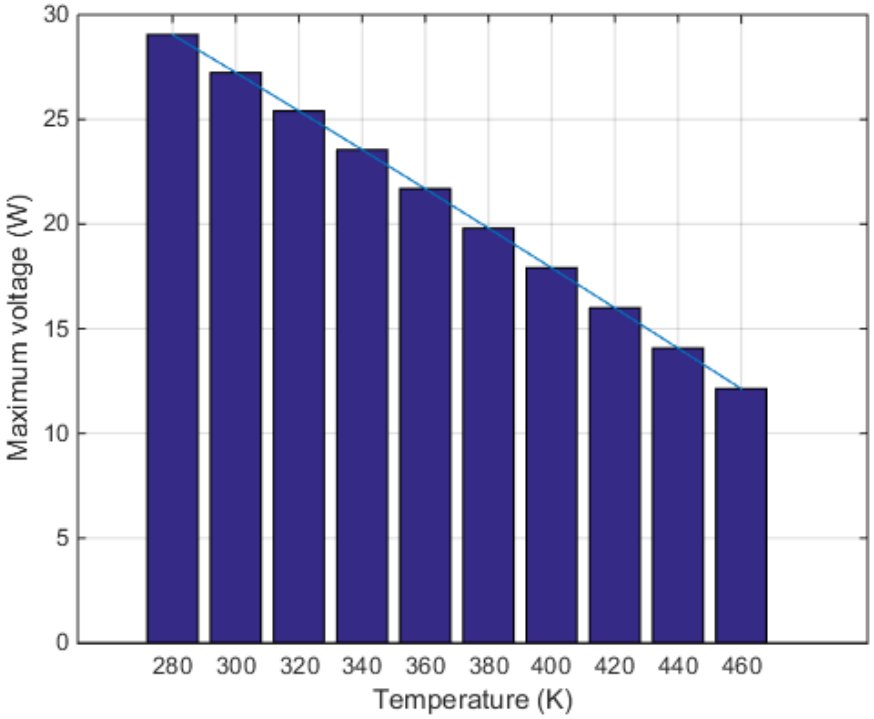

Figure 2. 15: Maximum voltages vs temperature progression

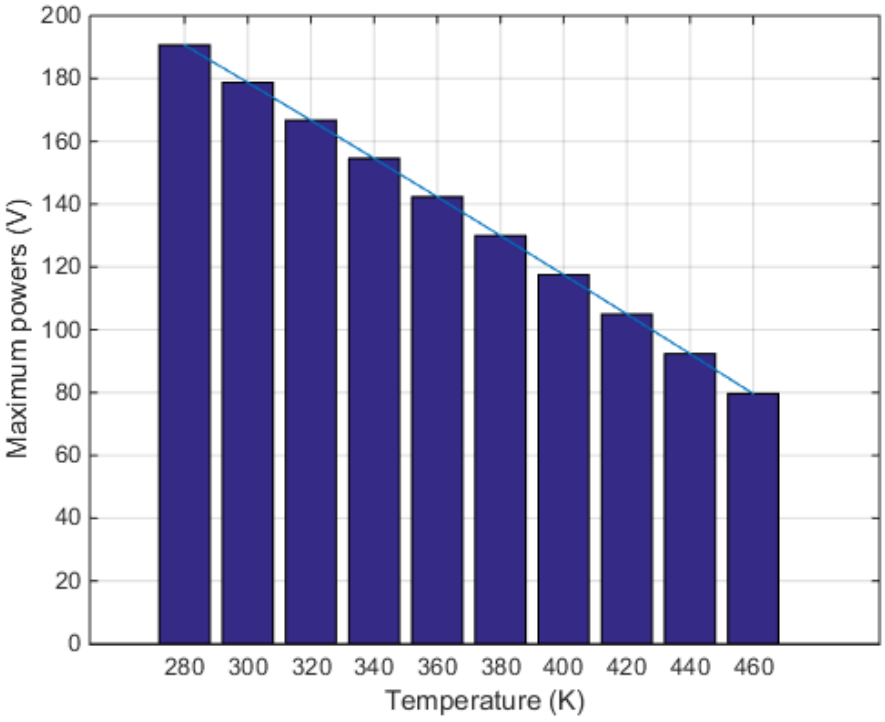

Figure 2. 16: Maximum powers vs temperature progression

2.5.4. Observations

Maximum values of voltage and power as gathered in Table 2.1 and graphically represented in Figures 2.18 and 2.19 show that both power and voltage have

significantly regressed for a temperature increase between 280 K and 460 K. It was also observed that from 32.9 V, the open-circuit voltage could go as low as 12 V and the power to 143 W when the PV was operated between 280 K and 460 K. The maximum power was also found to drop from 247 W to 143 W per Celsius degree was found to be 0.58 W. The power drop rate of 0.56 % was computed thereof, a rate too close to other research findings (Natarajan et al., 2011; Chow, 2010).

Table 2. 1: Maximum power, voltage and temperatures

Maximum Voltage (V)	29.048	27.234	25.401	23.551	21.685	19.803	17.906	15.995	14.071	12.134
Maximum Powers (W)	190.629	178.724	166.697	154.556	142.306	129.955	117.507	104.967	92.340	79.631
Temperature (K)	280	300	320	340	360	380	400	420	440	460

2.5.5. Weather effects effects on PV efficiency

Weather conditions where PV arrays are fielded have a big impact on their performance as the sunlight depends on the moment weather (Ibrahim, 2011). It is also noteworthy to highligt that the sunlight intensity is time-dependent on a daily basis. It is weak in mornings and evenings and maximum at noons. The sunlight, a portion of the electromagnetic radiation released by the sun, is first filtered by the atmosphere before it reaches the earth in the form of sunshine. On its way down through the atmosphere, the sunlight can be interfered by seasonal or day-based weather conditions or any other obstacles in the form air molecules, aerosols, duster, water drops and ice crystals (Rekioua & Matagne, 2012). A resulting sunlight is designated as diffuse due to eventual scatterings it undergoes before it reaches the PVs. On the contrary, in a clear sky, the sunlight is intense and direct during its travel as it relatively encounters no hindrance. It becomes evident when the appears at horizon in the morning (at sunrise) and its intensity gradually strengthens to hit the peak in noon hours, and progressively regresses to hit the minimum in the evening at sunset, when the sun disappears at horizon in the evening. This can only be observed if there is no weather change on the course of the day like rain and clouds. In terms of energy for PV applications, the amount of power received by a surface per unit area is well-known standard which is tehnically called the irradiance and its value is determined based on the sunlight intensity at noon. So, given a PV array area, the

amount of hosted sunlight power can be determined. Figures 2.18 and 2.19 portray the impact of the irradiance on the output power and current of the module.

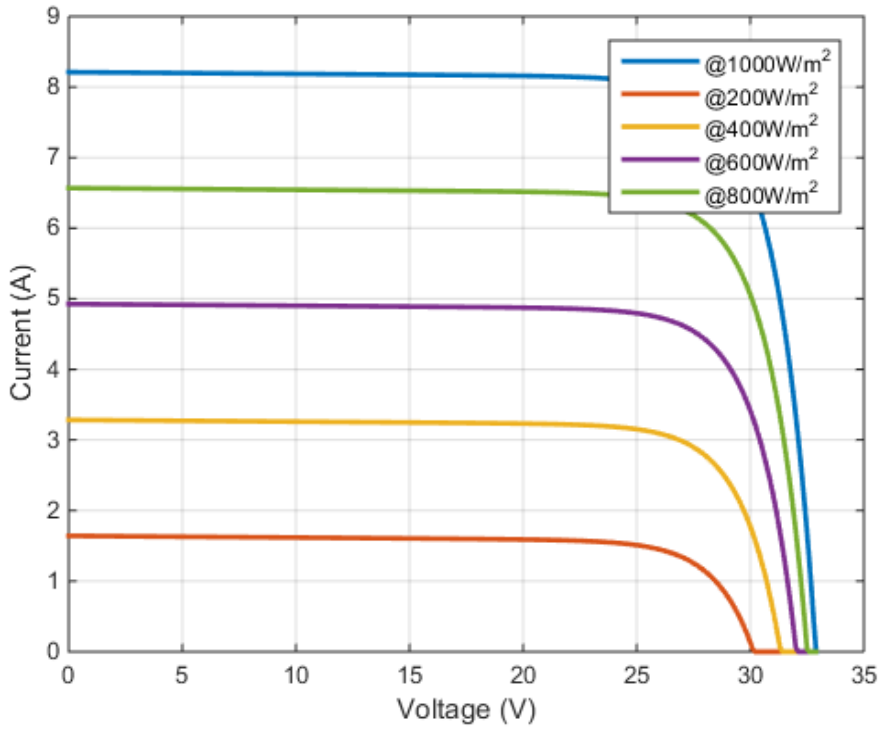

Figure 2. 17: Effect of irradiance variation on the current

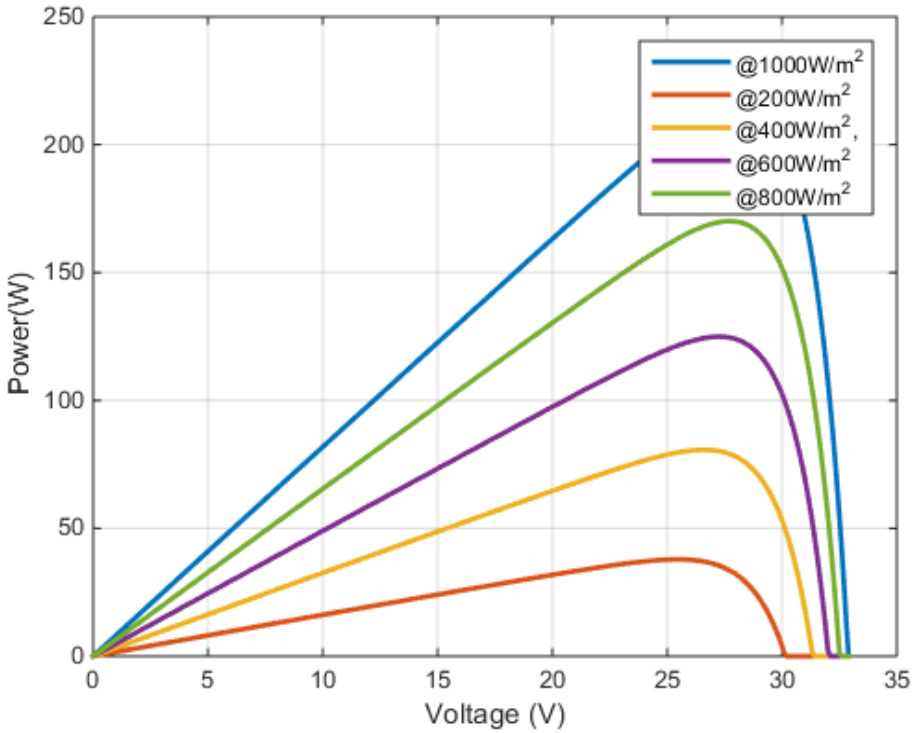

Figure 2. 18: Effects of the irradiance variation on the power

The variation of the of the maximum currents and powers at irradiance of 200, 400, 600, 800 and 1000 kW/m^2 are depcited in above graphs and data for current, power and irradiance are gathered in Table 2.2. Barcharts were also used to disctinctly provide module parameters' peak values for selected irradiance levels (Figures 2.19 and 2.20).

Table 2. 2: Currents, power and irradiance

Irradiance (W/m^2)	**Current (A)**	**Power (W)**
200	1.642	37.852
400	3.284	80.000
600	4.926	124.935
800	6.568	171.090
1000	8.210	215.904

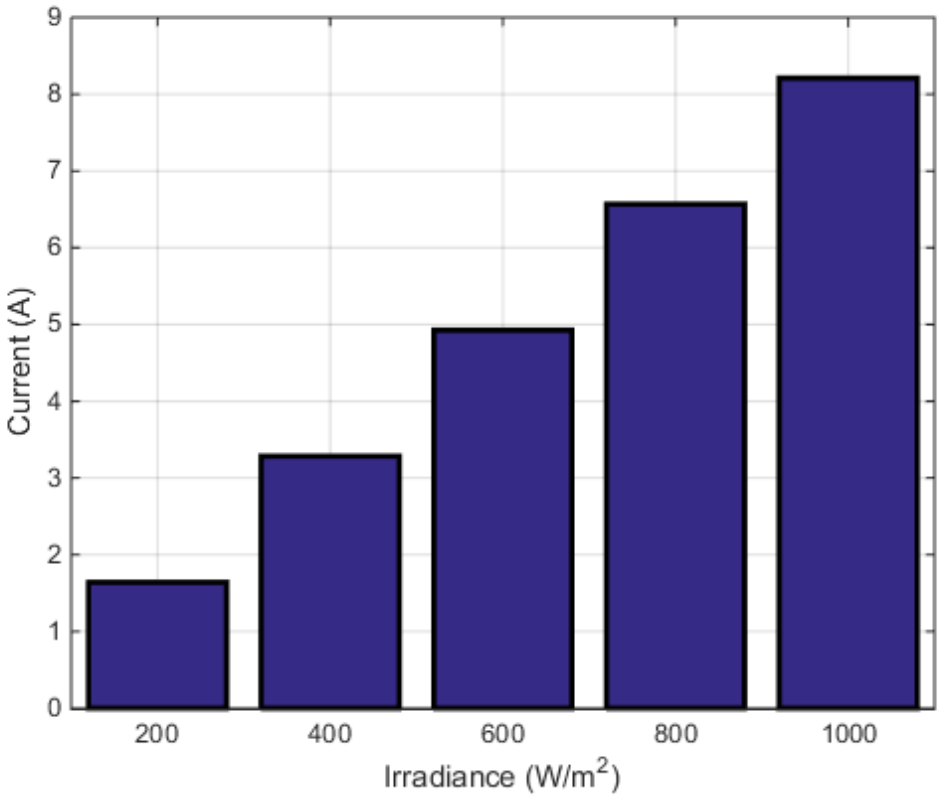

Figure 2. 19: Current vs irradiance in bar charts

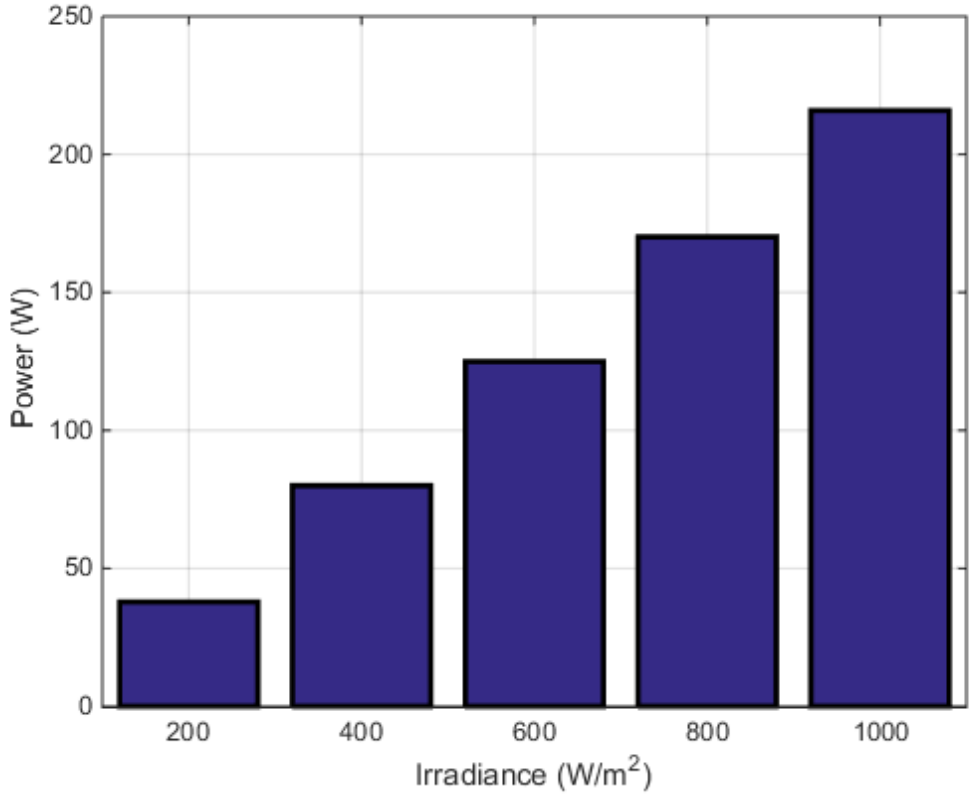

Figure 2. 20: Power vs irradiance in bar charts

2.5.6. Observations

Both power and current increase linearly with the increase of the irradiance at a rate of 0.223 W and 0.008 A per unit irradiance respectively. These values do also represent the slopes of straight lines in Figures 2.21 and 2.22. The rate of change obtained by computing the increase over the minimum values for the current and the power are 0.6 % and 0.5 % per unit irradiance respectively.

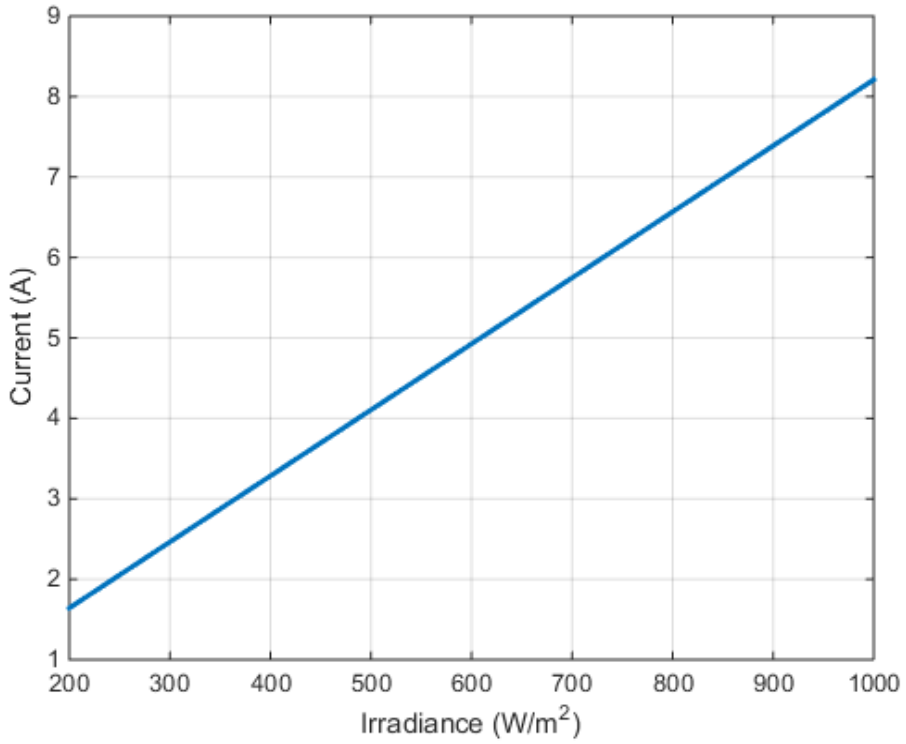

Figure 2. 21: Linear correlation of current vs irradiance

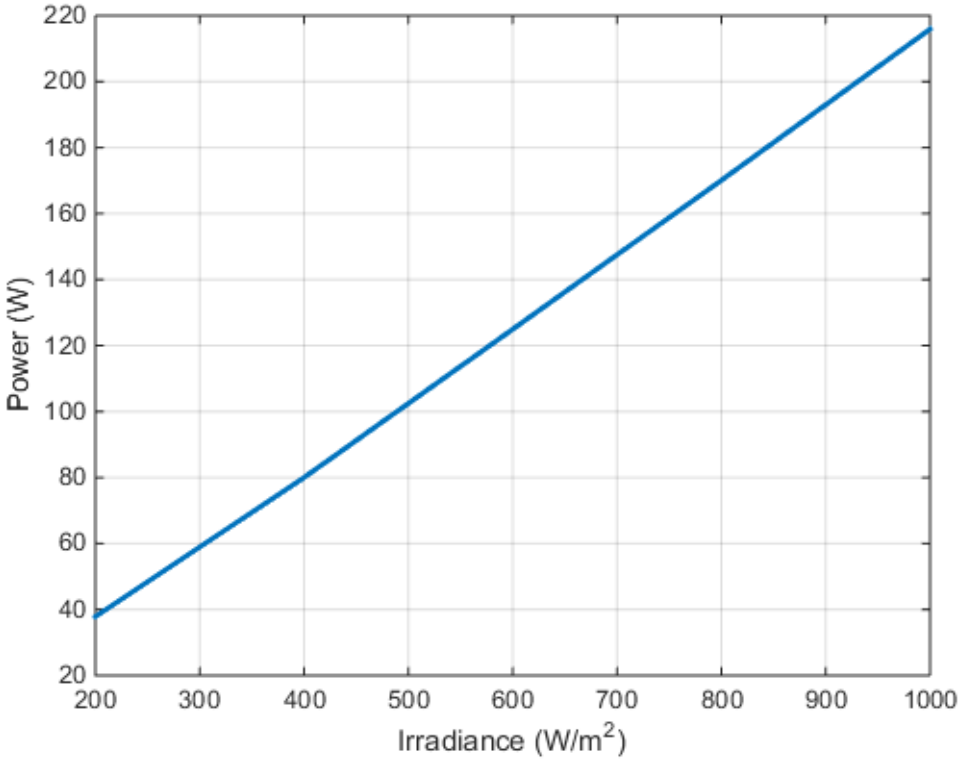

Figure 2. 22: Linear progression of power vs irradiance

2.6. Techniques for efficiency improvement

The technique targeting at addressing the causes that are behind low energy conversion of PV cells in following subheading.

2.6.1. Sun-tracking technologies

Sun-tracking PV systems can be described as technologies that aim at following the sun in its apparent movement so as to ensure the sunlight intensity is maximum for the cells at any time of the day. By tracking sun movement, the irradiance is optimally received by the cells and thus optimizing the sunlight capturing ratio. High-tech sun-tracking systems have been a concern of much research and significantly contributed to improving solar cells' efficiency. PV systems following the sun in its seasonal move (yearly) between Cancer and Capricorn tropics, and daily move from East to West could then be adpted. Single-axis systems tracking the sun from East to West and dual-axis tracking systems adding a North-to-South dimension were designed, developed and implemented yielding notable energy conversion increases. However, little interest was found in single-axis systems for intertropical sun's movement since the power gains prove to add no significant value (Figure 2.2) as corroborated by the literature carried out in the sun-tracking area. Gains in power ranging between 14 % up to 45 % as compared to single flat fixed-tilt panels were recorded (Juang & Radharamanan, 2014; Zhang et al., 2015; Yılmaz & Kentli, 2015; Narendrasinh Parmar et al., 2015; Bazyari et al., 2014; Lee et al., 2009; Yilmaz et al., 2015).

Two types of sun-tracking systems, active and passive, could be identified in the reading process.

2.6.2. Electronic controlled sun-tracking systems

The main essentials involved in an electronic-controlled sun-tracking system consist of two motors (only one for single-tracking), a microcontroller, a comparator and a power supply (Yilmaz et al., 2015; Juang & Radharamanan, 2014). Microcontrolled motors command the navigation of PV arrays latitudinally and longitudinally whereas the comparator ensures the irradiance collection is maximum. A power supply is also required to drive the electromechanical system in the process of rotating PV arrays.

The involvement of electronic devices in the operations of sun-tracking systems implies a robust and well-designed structure to ensure the whole assembly is not affected by vibrations due to winds and weather fluctuations. Active sun-tracking systems are also reproached for the parasitic aspect in terms of the power they consume.

2.6.3. Passive sun-tracking systems

This type of systems are purely passive and purely mechanical (Clifford & Eastwood, 2004; Narendrasinh Parmar et al., 2015). The rotation of the PV arrays is governed by the gravity principle. Such mechanical systems mainly comprise two metallic communicating cylinders placed at either side of the solar panel, a fluid and a damper. A pivot which is placed at equal distance from the assembly's ends (Clifford & Eastwood, 2004). The rotation of the assembly supporting the PV system takes place when the fluid moves from one cylinder to the other. The sun heats the fluid which evaporates and the mass imbalance causes the movement of the PV arrays. The damper is used to limit the speed of the solar panels. Mechanical systems are delicate to set up especially with fluid use requiring a careful attention. In terms of efficiencies, passive systems provide 23 % increase (Clifford & Eastwood, 2004) even more than 25 % (Narendrasinh Parmar et al., 2015) over fixed panels.

2.6.4. Disadvantages of sun-tracking systems

While their advantages are obvious, sun-tracking systems have also shortcomings. Lapidot et al., (2014) highlighted some disadvantages of using sun-tracking systems and concluded that stand alone PV home kits are still a better, reliable, simple source of energy production minor maintenance requirements. His critics of sun-tracking systems were based on the cost involved in their development, the involvement of moving parts (such as gears, motors), maintenance costs required for eventual broken parts in addition to consuming electrical power. The reliability of such systems was hence put to question. Juang & Radharamanan (2014) provided the requirements and limitations in the design of his systems. Error at levels of hardware and software design should be eliminated or controlled to ensure system stability and resistance to weather during stability. He also spoke about resistance to temperature and to minor mechanical stresses.

When it comes to temperature, all the electronic devices part of the system are naturally sensitive to temperature increase like any electronic component (Kim et al., 2008; Wang & Chen, 2009; Megahed, n.d.), foretells risks of control system's failure and short system's lifespan. The reliability of sun-tracking systems is put in doubt if they can only withstand minor mechanical stresses. Thus, their effectiveness should be understood to be good in zones of fair weather and less wind as high temperature gradients acts opposing PVs efficiency.

2.7. Cooling of PV systems

2.7.1. PV cooling techniques review

From the literature above, one can deduce that PV cells performance can be improved by fielding them in low temperature environments in order to have increase in the open circuit voltage while a slight decrease is inflicted on the short-circuit current. For this purpose, cooling technologies are deemed to help keep cells at low operating temperatures and keep on receiving the same radiation flux.

A literature survey on PVs cooling was conducted and summarized. Most research conducted has aimed at exploiting both the electric and heating aspects of the solar energy.

A review article by Chow (2010) discusses the PV thermal (PVT) hybrid technologies. Solar and thermal components are combined in an integrated unit to produce electricity and heat. Like previous work on similar topic, the rationale of his research was the effects of temperature raise on PV performance. He indicated that the PV efficiency would drop by 0.4 % per ^{0}C for concentrated Si cells while high temperatures could cause permanent damages on PV structure. PVTs have also been extensively researched on and have proven to contribute heat services and improve electricity efficiency of the PV modules; thus, saving allowing for on air-conditioning electricity especially in winter time and gaining on electricity production at the same time. Temperature rises of 5 to 7^0 C could be added to the ambient through an air-type PVT while maintaining the efficiency of Si cells at 10.4 % (Long & Memik, 2010)

Chow (2010) discussed a variety of PVT systems in detail including flat-plate-collector systems, PVT heat pumps and concentrator-type PVT systems. With regards to the flat-plate PVT collectors, two types were debated: Air-type and liquid-type collector systems. The efficiencies of the air-type PVT (PVT/a) have been found in the range between 38 % and 75 % whereas liquid-types (PVT/w) proved to be significantly more efficient with percentages lying between 55 % and 80 % according to data collected at the University of Patra in Greece during noon hours (Zondag, 2008). Higher values were claimed to be attained when reflectors were involved in PVTs design. On the other hand, Zhu et al. (2011) conducted a study on cooling PV cells under higher concentration using deionized water. Under one sun, 30 ^{0}C of cooling water and 17 ^{0}C ambient temperature, PV modules could be maintained at a temperature of 45 ^{0}C. Similar results could be realized by the latter author (Zhu et al.,2010), by using dimethyl Silicon to cool CPV through in an immersive process.

Heat transfer of 3 kW/m^2 and maximum acceptable temperature of 45 ^{0}C could be accomplished by immersing the module in the liquid circulated in a pipe-pump-valve system.

As for the development of the concentrated type PVTs from the 90s, concentrated PVTs were found to be more efficient than the flat PVTs and to involve lower costs attributable to higher efficiency cell. CPVTs have in fact the ability of increasing the radiation intensity, thus performing thermal wise, while negatively impacting on the concentrated PV module's efficiency. Therefore, the design of CPVTs requires a cooling circuit in order to keep the temperatures low and uniform. Though dedicated to handling high temperatures, the circuit should be kept as simple and less parasitic in electricity consumption as possible. In terms of efficiencies, a single-tracing combined heat and power solar (CHAPS) collector developed in Australia exhibited a thermal efficiency of about 58 %, an electrical efficiency of 11 % and an overall efficiency of 69 %.

Impinging jets and microchannels were other cooling system proposed for cooling CPVs (Royne & Dey, 2007). The authors also suggested a two-phase forced convection as an alternative. Active cooling was ultimately recommended given the intensity higher than 150 suns the modules may be subjected to when under high concentration especially in hot countries mostly found in desert regions. The study focussed on minimizing water used to cool CPV modules as to maintain them to the operating temperature of 35 ^{0}C, 45 ^{0}C being the maximum acceptable temperature (MAT).

Miniature parabolic dishes concentrating light into small CPV cells were suggested (Feuermann & Gordon, 2001). This was mainly due to challenges posed by developing CPVs operating in the order of 1000 suns. The design is such that the small CPV is placed behind the paraboloid; and the sunlight gathered in a short glass rod. Concentrated sunlight is then transported and homogenized in a small kaleidoscope glass coupled to the high efficiency small PV cell coupled to a passive heat sink for cooling purposes.

Segal et al. (2004) worked on cooling concentrated solar cells by means of spectral splits. Given that solar cells only use a band between 600 and 900 nm of the whole solar spectrum to generate energy, spectrum splitter can be resorted to ensure the spectrum out of the desired band is reflected and does not interfere with electricity generation efficiency and does not affect the module's lifespan. A monocrystalline PV cell can perform the energy conversion lying between of 55 % to 60 % when operated

within the spectrum band containing the light only. The rest of the spectrum conveying thermal energy could be used for various applications including further electric power generation. The authors have recommended a hyperboloid tower reflector as band splitter of which the mirrors are made of transparent fused silicon and coated with a dielectric; thus fulfilling the function of a band pass filter. The transmitted light is directed to a focal zone and then to the PV array while the reflected band is taken to another focal zone whereby thermal energy is concentrated and recovered.

Phase shift materials (PCM) were also investigated as one of the means of preventing PV cells' temperature hikes (Hasan et al., 2016; Marco, 1849). PCMs are well known as heat transfer agents which change their state depending on whether they are receiving or releasing heat energy. Hasan et al. (2016) further proposed the use of with PCM technique assisted with fins for a better performance. An increase in electricity efficiency of 1.3 % and 41 % thermal energy recovery were observed despite the authors acknowledging the need of a further investigation on PCMs for PV cells cooling.

While the focus of most research is on cooling, Meneses-Rodríguez et al. (2005) have taken the journey of improving solar cells efficiency in the opposite direction. The authors advised that cells be operated at temperatures ranging between 100 ^{0}C and 200 ^{0}C. The excessive heat energy would be to be part of the second stage of a hybrid system for efficiency increase sake. The second stage being a TE generator or heat engine, efficiencies of order 30 %-40 % were recorded when PV arrays were operated in the temperature interval of 25 ^{0}C to 170 ^{0}C.

On the other hand, PV-TE technologies have made possible a broader use of solar spectrum. Zhu et al. (2016) have manufactured a PV-TE hybrid system where the heat flow was controlled through a TE having a copper plate on one side. With such a design, the copper side of the TE material is at a very high temperature, while the other one is at a very low temperature. The resulting high thermal difference yields a proportional amount of electric power. The hybrid system could perform with an efficiency as high as 23 % outdoors, a yield of 25 % more power than the flat plate PV cells, plus a residual heat energy.

With regards to the development of the solar power panel and from the literature, cooling types for PVs are categorized as active and passive in one hand. Active cooling systems can thus be criticized from the power consumption perspective and as such, they should not be on the top list of candidates for the development of the

solar power in question. Passive cooling systems can deliver with no power passive cooling which is an advantage. Yet their low coefficient of performance (COP) and their inability to make use of the dissipated heat energy are setbacks. On the structural point of view, systems that do not fit to form one compact panel along with PV arrays are not recommendable. The development of the solar power panel will therefore be implemented around TE technology for its capacity of providing the cooling effect while generating extra power.

2.8. TE technology

The ability of a material converting heat energy in electrical energy or vice-versa is referred to as TE effect (Kim et al., 2013; Lin et al., 2016). A composite material made of two different types of conductors joined together has been serving as an adequate basic model to illustrate TE effect (Camargo et al., 2011). Research has explored TE materials in various ways. Some have studied TE materials based on the ability of converting temperature differences into electricity known as Seebeck effect using thermocouples (Gaultier, et al., 2013; Snyder & Toberer, 2008). However, challenges in using TE materials were observed with regard to the figure of merit zT (Alam & Ramakrishna, 2013; Chen, et al., 2012; Lu, et al., 2011). For a better efficiency, TE material lattices should have low thermal conductivity and high electric conductivity, which is difficult to achieve with the interdependence of the two properties. The authors suggested rather the use of nano-TE materials than bulk materials in the attempt to enhance the zT.

2.8.1. TE effect manifestation

TE effect has a twofold manifestation: Conversion of thermal energy or temperature gradient in electrical energy or a conversion of electrical energy into a temperature gradient resulting in a cooling effect. A temperature gradient between the junction and the conductors' surrounding generates an electromotive force (EMF) at the conductors' terminal whereas the flow of current in the conductor provides a cooling or heating effect. The whole TE conversion process takes place directly with no intermediate energy converter involved (Zhang & Zhao, 2015). Thus, TE process is referred to as a direct conversion process.

TE conversion has been the focus of researchers and yielded results early nineteenth century through Thomas Johann Seebeck in 1821 (Seebeck & Coefficient, 1821), Jean Athanasius Peltier in 1834 (Wang & Chen, 2009) and William Thomson (Lord Kevin) in 1855 (Marco, 1849). The findings were named after their authors respectively yielding Seebeck effect, Peltier effect and Thomson effect.

Though differently named, the three effects present similarities and complete each other. Seebeck effect states that the presence of a temperature between hot and cold junctions of two dissimilar conductors generates a voltage named Seebeck voltage. Conversely, Peltier effect indicates that the flow of the current through a conductor with a temperature gradient creates a heating or a cooling effect on the conductor depending on the current's flow direction.

The performance of TE materials is assessed referring to an energy conversion parameter. The Seebeck effect, also known as thermopower coefficient, is used to evaluate the electrical performance of a material. It is used to classify a material's ability to generate electric power. Regarding TE cooling performance, materials are classified with respect to the coefficient of performance (COP), the heat pumping rate, the maximum temperature difference achievable and the current required to maximise the use of the input energy.

The compound name TE implies a combination or an interaction between thermal and electrical effects. The concepts of thermodynamics apply then for thermal part of the conversion whereas the electrical concepts are essential for power generation. When two objects are paced in contact, there are two possible scenarios thermal wise. Either heat exchange will take place from the hottest material to the coldest via the junction or there will be no heat exchange if both objects have the same temperature. The absence of heat exchange between objects in contact is technically referred to as thermal equilibrium. In thermodynamics, this phenomenon makes the zeroth law of thermodynamics. On the contrary, when objects in contact are at different temperatures they exchange heat. The heat lost by one object is won by the other and there the principle of energy conservation is observed. This makes the first law of thermodynamics.

Similarly, the concepts of electricity apply to two objects in contact with electrical charges moving between two objects due to an external source of energy. Heat is one of the sources of energy capable of making electrical charges move through a junction between two different objects as a result of a temperature gradient. The concept of interaction between charges is an interesting topic with regard to the design of TE materials. The design's ideal is to have a compound material capable to allow as much as current flow possible through the junction subjected to a temperature gradient or to move as much as quantity of heat from the cold side to the hot side of the junction. Here it becomes imperative to shed the light on the process of heat and electric exchange. The idea on TE concepts was primarily explored using

two dissimilar metals having two junctions at different temperatures. A more viable and efficient technology was then realised through some work on electronic properties of semiconductors.

2.8.2. TE atomic theory

TE process is primarily performed at atomic level, the smallest particle of the matter. Atoms are composed of a nucleus surrounded by negatively charged electrons distributed on orbits or shells. The nucleus itself comprises positively charged protons and charge free neutrons. The number of protons is the same as the number of electrons, which yields a neutrally charged atom in normal conditions. For electric and thermal conduction to take place, free electrons are needed and this requires an external source of energy. The electrons on the outermost shell also known as the valence electrons are less tight to the nucleus since the attraction force is inversely proportional to square of the distance between the shell and the nucleus.

On the outermost shell, the gravitational force is also proportional to the number of valence electrons. The less the number the less the gravitational force exerted on valence electrons; therefore, there are more chances of having free electrons with the presence of an external energy source such as heat. On the contrary, the larger the number on the valence, the larger the gravitational force from the nucleus and the more the chance for an atom to capture a free electron in order to have the valence shell complete. An atom releasing an electron becomes a positive ion since the number of negative charges has gotten smaller than the number of positive charges. In this process, the total charge of an atom is no more neutral but positive. An atom releasing electrons is also called donor. Conversely, when an atom captures an electron, it becomes negatively due to the superiority of negative charges. In such a case, the atom is designated as negative ion and is also known as acceptor. In a material, the process of exchanging charges is done via valence electrons moving in conduction mode. Charge exchange occurs from one atom to the neighbouring one and propagates through the whole material and this happens naturally for good conducting materials such as copper (Cu), silver (Ag) just to name few.

Coming back to the flow of electric charges through the junction, the suitable TE design should be the one having a material featured to releasing electrons on one side of the junction and another material excellent at accepting electrons on the other side of the junction. Such design can be better achieved using semiconductors, such as Silicon (Si) and Germanium (Ge). Semiconductors made of valence 4 atoms are mixed with materials having pentavalent atoms to create a free electron per atom.

The material thus obtained is negatively charged and called n-type. Inversely, positively charged materials are obtained when a material consisting of trivalent atoms is mixed with a semiconductor resulting in valence 7 atoms therefore forming a p-type material. The p-type and n-type materials put together form a p-n junction.

The resulting TE material is susceptible to allow electrons cross over the junction from certain temperature levels. Electrons will be at the same time attracted by atoms working on filling their peripheral shell short of one electron to be complete. In this case, the TE material operates as a power generator. A source of voltage connected between the p- n material makes a flow of electrons pass across the junction taking heat from the cold side to the hot side along hence providing a cooling effect.

2.8.3. TE power generation

With concerns over global energy crisis and use of unfriendly technologies to the environment and human beings, TE power generation has been identified as one of the potential candidate. A TE generator is known as a solid state device performing direct energy conversion from a thermal form to an electrical one based on the Seebeck effect (Ismail & Ahmed, 2009). It works as heat pump where electrons, charge carriers act as the working fluid in a similar way as in heat engines. TE generators have a long lifespan, have no moving parts, are noise free and produce no greenhouse gases. They are furthermore suitable to small scale and remote areas applications due to their size (Schock et al., 2011).

However, TE promise is hampered by its low conversion rate; and has therefore been kept out of contention when it comes to large scale power generation. The efficiency of about 5 % (Steinfeld et al., 2010) is too low when compared to more than 30 % of steam plants and 10-20 % of PV panels (Green et al., 2011). In fact, 60 % of the sun radiation is reradiated while only about 20 % is available for electricity conversion. TE should only rely on operating with very high temperature differences so to generate a high potential difference but it is not advisable to do so in order to avoid damaging the device (Steinfeld et al., 2010). Instead, TE technology was highly welcome in applications where reliability and mobility in power supply are much more important than the energy conversion efficiency. The technology was then used in aerospace for deep space missions where there is no solar energy but heat. It had been also used in specific applications military and in systems where mobile supply is demanded.

Nevertheless, TE technology remain appreciated for its unique ability of converting low grade temperature into electricity and research has been conducted with regards

to improving the overall efficiency of conventional power plants. The latter are known for a huge heat waste estimated to 60-70% of the input heat energy (Ekama et al., 2003). The loss or waste occurs in the process of conversion from heat energy in mechanical energy at the turbine level. Through cogeneration with the existing plant, the author here suggests that TE technology be used to recover electricity from the waste heat and whereby raising the efficiency of the whole plant. TE generators would perform better when operated at high temperature gradient but this could require stacking various devices operating at different temperature differences as a single device cannot effectively manage large temperature gradients.

In terms of cost, TE power generators offer an advantage of running with no operating and maintenance cost unlike conventional power generators; only the device's cost is involved. They do not require fuel and personnel for their working. Therefore, though the initial cost may be high, it will be compensated on a long run.

2.8.4. TE possible applications

In the context of this research project, a TE panel is being suggested to be the platform of energy conversion because a surface of contact needed to capture as much as heat in an environment. TE direct power conversion Could be envisaged as a way of increasing the efficiency in conventional power generation plants as well as in the modern high voltage direct current-based power generation (HVDC) (Rudevall, et al., 2000).

2.8.5. TE in conventional steam plant

Conventional steam power plants have been criticized for their very low efficiencies. This shortcoming can be addressed by means of TE direct power conversion. The route between the boiler and the alternator in steam plants costs a lot of energy and therefore affects the system's efficiency (Figure 2.23). Only about 40 % of the heat energy is converted into electricity while 60 % of the input energy is wasted (Honorio, et al., 2003). By cutting short this route and just replace the energy requiring elements within it by a direct current (DC) power convertor panel (Figure 2.24), there is possibility of having a more efficient power plant. In this case, a power invertor would be needed to take the output of the power panel, which is DC, into an alternating current (AC) (Vignola, et al., n.d). Alternatively, TE technology can be applied within the conventional existing plant by converting the heat energy, usually wasted, into electric useful energy partaking into the overall output of the power generation plant (Ono & Suzuki, 1998; Sivitava, et al., 2011) (Figure 2.25).

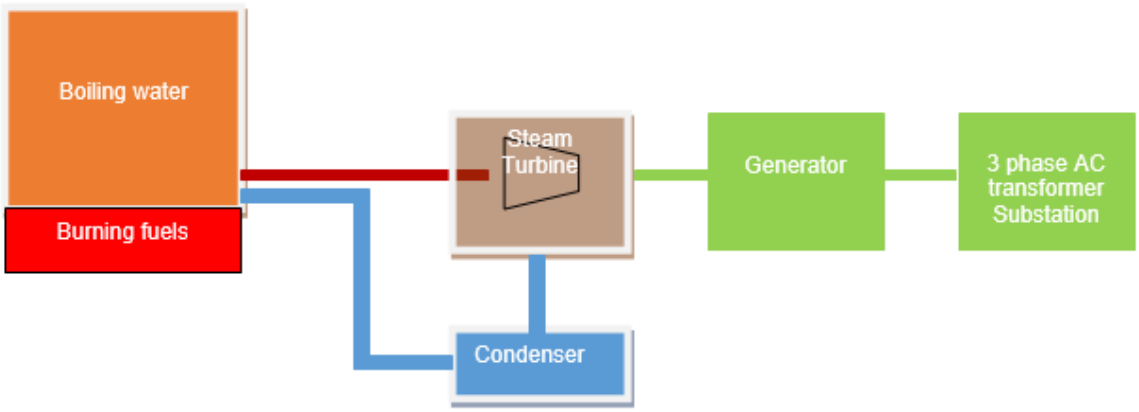

Figure 2. 23: Conventional steam power plant layout

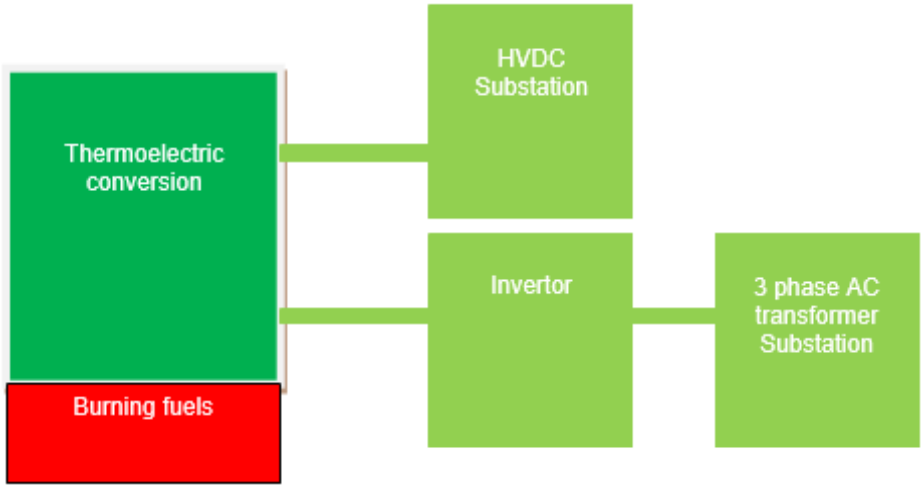

Figure 2. 24: Direct TE conversion in a steam plant

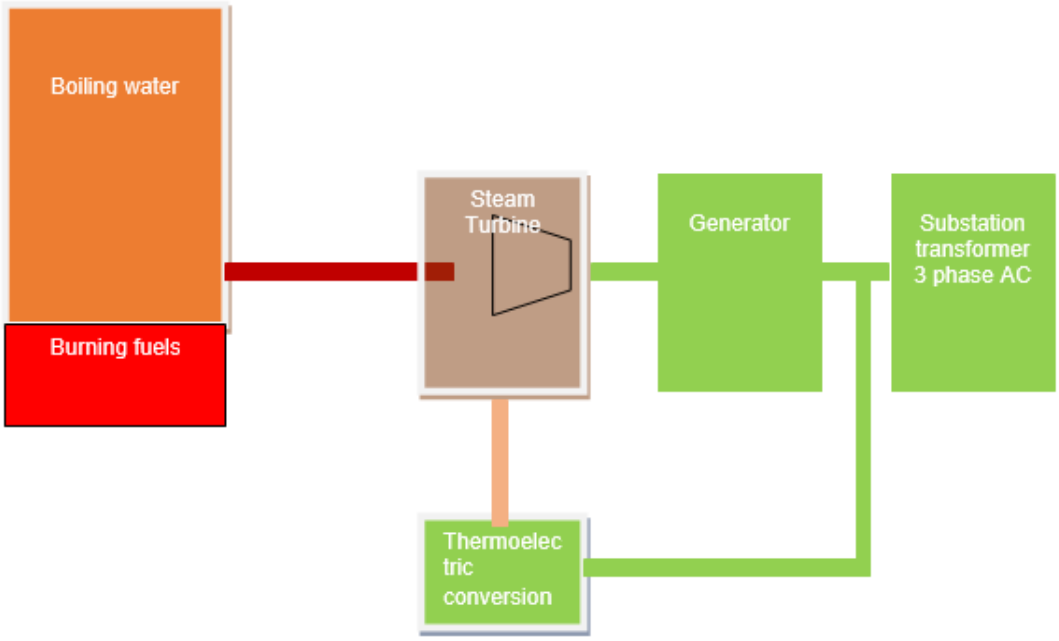

Figure 2. 25: Waste energy recovery in a steam power plant

2.8.6. TE as renewable energy solution to the power shortage

A renewable energy based approach should be one of the better ways to address the negative impacts of conventional steam power plants with regard to environment degradation and climate changes. TE plants using solar and ground energy as the source of heat should be envisaged as viable solution with solar energy as the major primary source of renewable energy. An amount of energy estimated to $1.2 * 10^5$ Terawatts is regularly radiated to the earth but its utilization is still low (Mittal, et al., 2005). However, when utilized to produce electricity, solar energy contributes only 0.015 % of the world's electricity demands. TE direct conversion can make use of the abundant solar thermal energy to alleviate the energy crisis and its consequences.

TE based plants could offer a unique advantage of converting any temperature gradient (Srivitava, et al., 2011). TE conversion can take place at positive or negative temperature gradients. This advantage can make TE technology profitable to countries with so-called extremely unfair weathers either naturally too hot like most Asian countries or too cold countries.

2.8.7. Current status on usage of the solar thermal energy

From its history, solar energy has been explored and it is only in the 18^{th} century that it got exploited for human welfare (Renewable, n.d). Solar energy has been studied to be utilised for two main purposes: Water and surface heating in the first place and electric power generation in the second place. Scientists' efforts were rewarded with inventions capable of performing the conversion of solar energy in either suitable thermal or electric energies. The solar collector was invented in the 1860's and the PV some decades later. The solar concentrator was only discovered in the 1960's, two centuries later.

When it comes to electric energy, the most popular platform for directly converting solar energy into electricity is the PV panel commonly known as solar panel. PVs operate rather by converting the sunlight than sun thermal energy. Also, with their dependence on the weather; solar panels could not be fully relied on. Solar concentrators could be seen as an indirect way of generating electricity. Using the concentrating lenses, they have the ability of producing high thermal energy capable of driving a conventional steam plant. However, the same problem of energy waste will still be encountered.

Beside thermal solar energy, there are numerous other unused sources of thermal energy such as the heat generated in production industries, and the heat generated from the ground during night time.

2.9. Conclusion

From the literature above-explored, topics paramount to this research were deeply studied and discussed. Research uptake on alternative sources of energy should be given high priority in order to overcome the energy crisis and its consequences. With regard to PV technologies, sun-tracking systems in place so far have been associated with high efficiencies over flat laid and fixed-tilt solar panels. However, on the other side, they face criticism in terms of reliability, implementation and cost effectiveness. Research on thermal effects has mostly focused on CPVs due to high operation temperatures; little was directed to common rooftop solar panels of which the mounting on the roof may be the major cause of temperature rises. This research was conducted in order to bring a novel means of tracking the sun and cooling the solar panels while generating extra electric power. TEG were identified to suit the best to the power panel development.

CHAPTER THREE

OPEN-STRUCTURE MULTISIDED PV SYSTEMS

3.1. Chapter summary

Chapter three focuses on increasing the efficiency of PV cells by addressing the issue of poor irradiance collection ratios discussed in chapters one and two. Multisided PV systems were proposed, both structural and mathematical models were developed. With open-structure and closed-structure PV systems being considered to boost the irradiance collection ratio, this chapter targets the open-structure multisided (OSM) PV systems. The mathematical, base of the system evaluation, was verified and validated before proceeding with further design steps. A MATLAB code was used to generate results which were graphically presented while values for systems evaluation parameters were gathered in a Table. A well-picked sample of OSM PV systems was used to ensure reliability and integrity of the results. Few-number, medium-number and large-number OSM PV systems were considered. The OSM PV systems were qualified for providing a 32 % increase in collecting the sunlight as compared to flat and fixed-tilt panels of same area.

3.2. Aims and methods

The aim of this chapter is to provide a novel and simple technology of achieving competitive results as compared to most sun-tracking PV systems while minimizing the cost, risks of failure and eliminating the system running power. The proposed technique consists of PV panel systems assembled with regular joint angles to ensure there is at least a facade of the PV system facing the sun.

Since the PV system is a structure having more than a side, it was named multisided. Figure 3.1 portrays the shape of double-sided. In the study of the performance of the proposed technique, multisided topologies have been explored in order to identify which one is highly efficient one in terms of sun's irradiance collection. The results were obtained based on a developed mathematical model for a multisided PV system. The model was then translated into a code that generated graphs and a results' table.

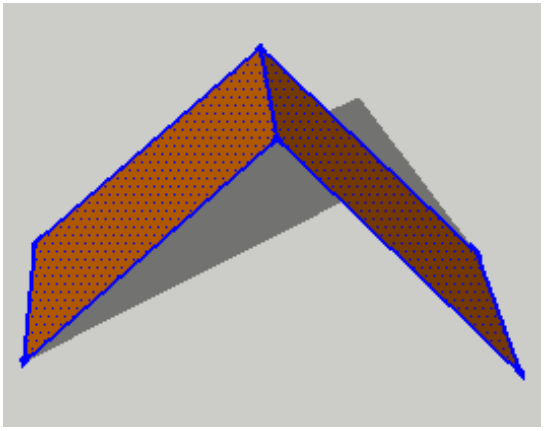

Figure 3. 1*: Illustration of a double-sided system*

In the process of system development, the study explored possible PV structures that could ensure that the irradiance is collected at full throughout the daytime. For a classic single fixed-tilt panel, the irradiance is close to zero when the direction of light is tangential to the array's plane and this occurs at sunset; and the maximum at noon when the incident sun rays form a right angle with the PV plane. Multisided structured systems were thus thought of as one of the solutions. Two types of multisided PV systems were then taken into consideration: the open and closed multisided structures. The open structure is in the form of a longitudinally halved prism, while the closed structure is in the form of a normal but hollowed prism. A double-sided may derive from a cubic or rectangular prism, a three-sided from a hexagonal prism and so forth. According models (mathematical and structural) for both kinds of topologies were established in order to quantitatively determine their performance with regard to collecting the sun avails on a daily basis.

3.3. Development of PV Multisided models

Though the study investigated both multisided closed and open structures as mentioned in the introductory section, open structure models are the focus of this chapter.

3.3.1. Model for open-structure PV systems

Both physical and mathematical models for the open-structure (OSM) PV systems were developed in this section. The system was designed as to have a side or more facing the sun during its apparent movement from morning to evening. The side of the structure that will have no view to the sun is left open and without cells.

The mathematical model development for the open structure system was governed by the need of having at least a side collecting the sunlight during the day. Sides will not therefore face the sun at the same as some will be doing it with a certain advance

while others doing it with delay. Hence, with respect to the sunlight incidence angle varying all day long following the sun's apparent motion, phase angles between the PV system sides relatively to their exposure to the sun were evaluated. Assuming the phase angle is regular, the fundamental angle could be determined as described by equation 3.1.

$$\varphi = \frac{\pi}{n} \qquad \textbf{Equation 3.1}$$

where π is the maximum angle reachable by the sun at sunset PV structure and *n* is the number of sides.

Though the sun provides a direct irradiance of 1 kW for an earth area of 1 m^2, the incident angle of the sunlight to a side of the PV structure affects the amount of irradiance received. Also, given that the sun moves while a side of the PV structure remains stationary, the irradiance ideally describes a half sine function for each side. The resulting mathematical model was therefore found to be defined as in equation 3.2.

$$G = \frac{1}{n}\left(G_M \sin(\omega t - i\varphi)\right) \qquad \textbf{Equation 3. 2}$$

Where $\omega t \in [0, \pi]$, $i \in \left[-\frac{m}{2}, \frac{m}{2}\right]$, $m = n - 1$ and G_M is the nominal irradiance.

The total contribution of a multisided structure in collecting the irradiance is the sum of individual sides contributions and is therefore given in Equation 3.3:

$$G = G_M \sum_{i=-\frac{m}{2}}^{\frac{m}{2}} \frac{1}{n} \sin(\omega t - i\varphi) \qquad \textbf{Equation 3. 3}$$

As an example, for a three-sided OSM PV system (Figure 3.2), the fundamental phase angle is $\pi/3$, $m = 2$. It can thus be mathematically modelled as per equation 3.4.

$$G = \frac{1}{3} G_M \sum_{i=-1}^{1} \sin(\omega t - i\varphi) = \frac{1}{3} G_M \left(\sin(\omega t + \pi/3) + \sin(\omega t) + \sin(\omega t - \pi/3)\right) \qquad \textbf{Equation 3. 4}$$

3.3.2. Model verification and validation

Before proceeding with the development of the OSM PV system, the proposed mathematical model had first to be validated and a three-sided model was used as an

example (Figure 3.2). Looking at various sides of a three-sided system, the middle panel will see the whole day. It was ideally assumed the sunrise to be at 6:00 and the sunset to occur at 18:00. In the morning, the sunlight will be zero until the sun appears at the horizon, it will then increase and reach the maximum at 12:00 when the sunlight is normal to the middle side. The irradiance will start decaying in the afternoon and becomes zero at sunset (moment when the sunlight is parallel to the panel).

For the side facing the East, the sunlight will land with an angle of 120^0 ($2\pi/3$), and the irradiance will be equal to 0.27 kW/m^2. It will cease to see the sun at 14:00. The side facing the West will only see the light at 10:00, time corresponding to $\pi/3$ phase delay with respect to the middle side. At the sunset, the sunlight will be landing to the West side at a120^0, which makes the irradiance to be equal at 0.27 kW/m^2. The model was verified and thus validated referring to Figure 3.5.

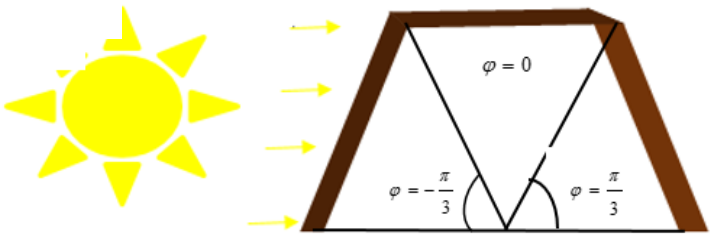

Figure 3. 2*: Illustration of the three-sided OSM PV system at sunrise*

3.4. OSM PV systems profiles

The validated mathematical was used to generate the dynamics of the irradiance and compute key parameters needed to evaluate the performance of OSM PV systems. MATLAB 2014 release, as a renowned graphical and computing tool, was used to generate an ad hoc code meant to accommodate limitless OSM systems having a limitless number of sides (theoretically) so as to ensure the reliability and accuracy of the results. The code was however applied on strategically chosen sample of OSM systems for practical reasons (Figures 3.2 – 3.17). Since the aim of the study was to improve the performance of single-sided and fixed-tilt solar panels, the total area of a multisided PV system was assumed to be equal to the area of a single-sided fixed-tilt system. Thus, the area of a side of a multisided system was set equal to the area of a single sided system divided by the number of sides. The reference area was purposely set equal to 1 m^2 for convenience, visual and easy understanding purposes.

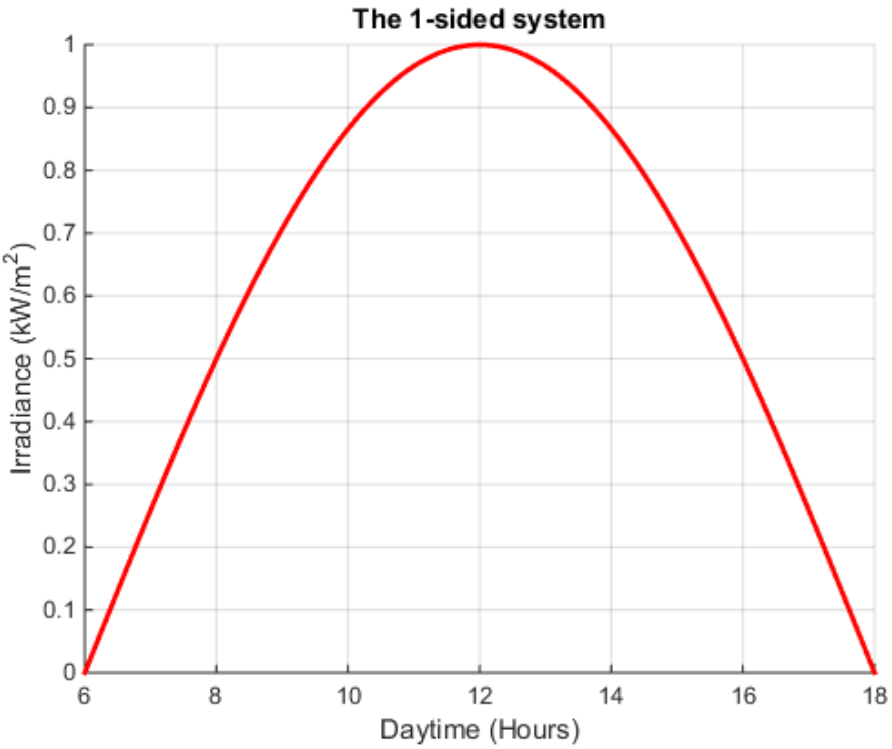

Figure 3. 3: Flat-fixed-tilt irradiance dynamics

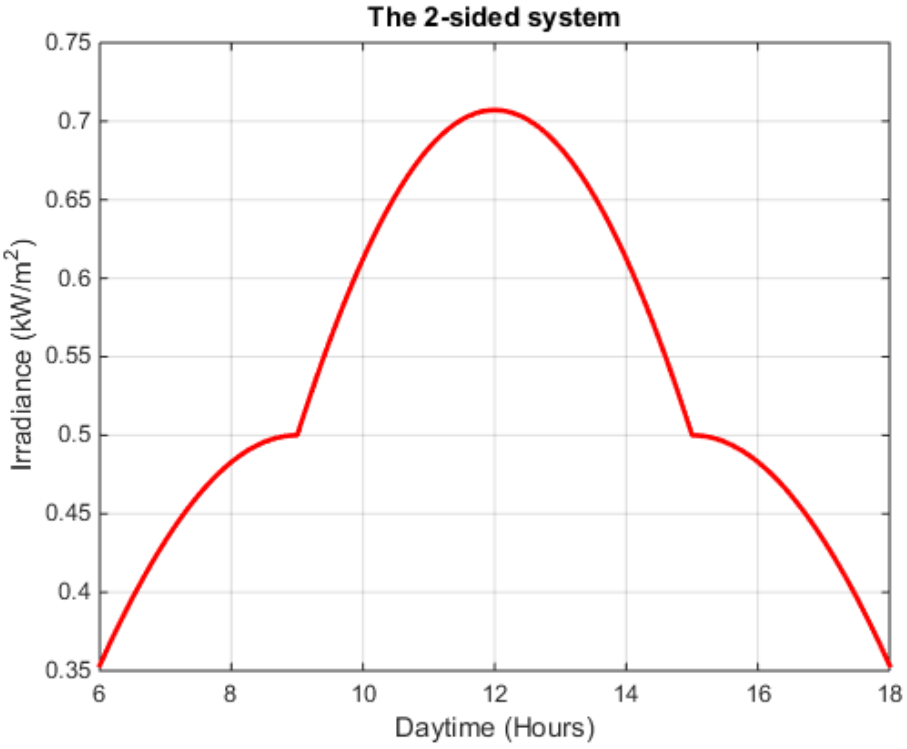

Figure 3. 4: Double-sided OSM irradiance dynamics

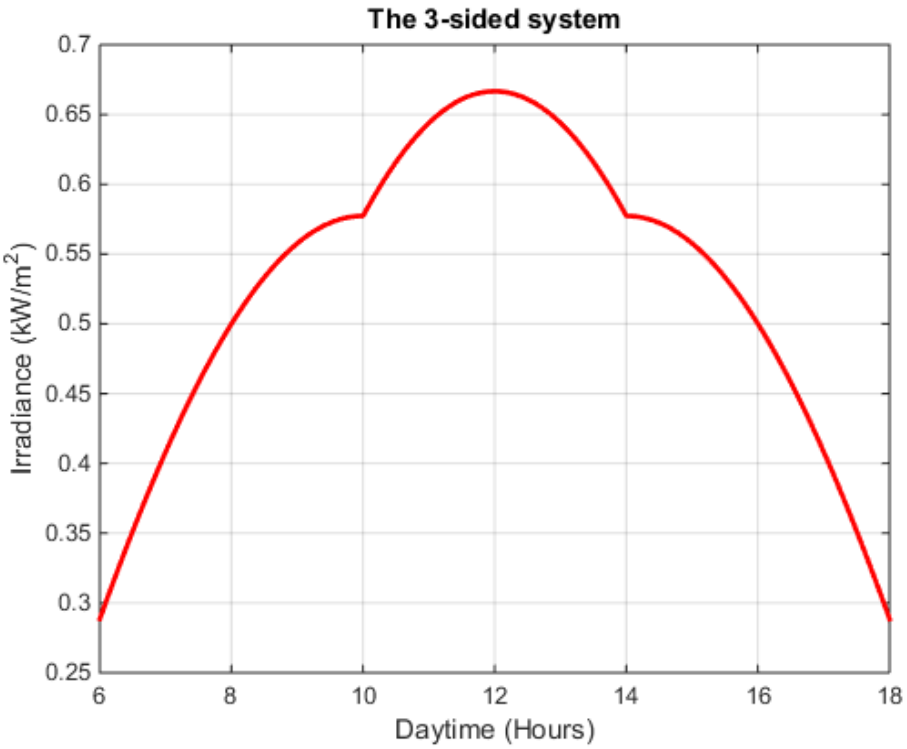

Figure 3. 5: Three-sided OSM irradiance dynamics

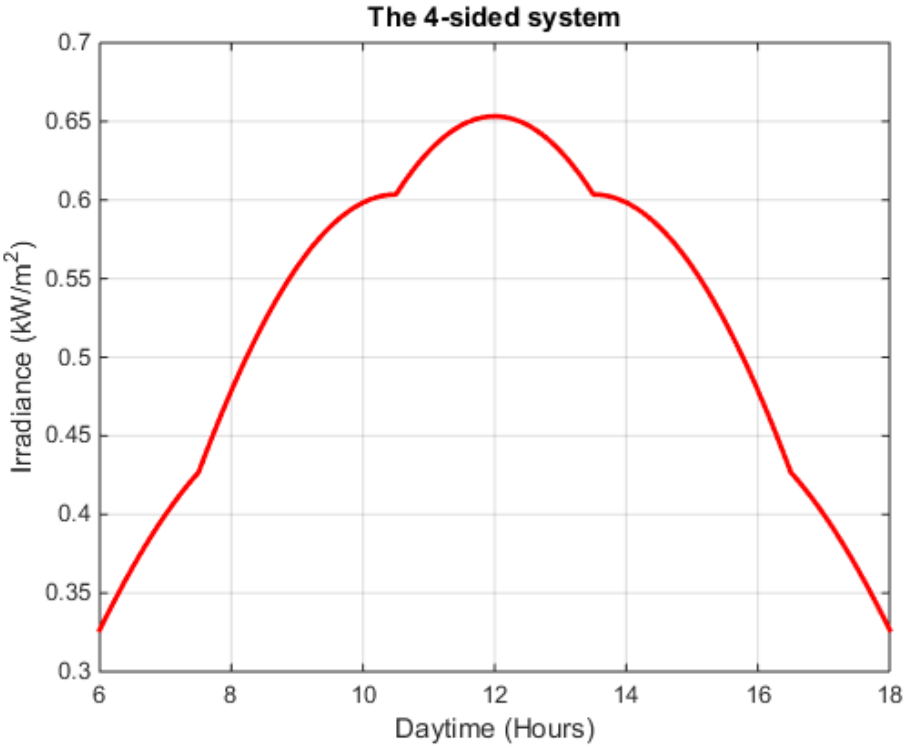

Figure 3. 6: Four-sided OSM irradiance dynamics

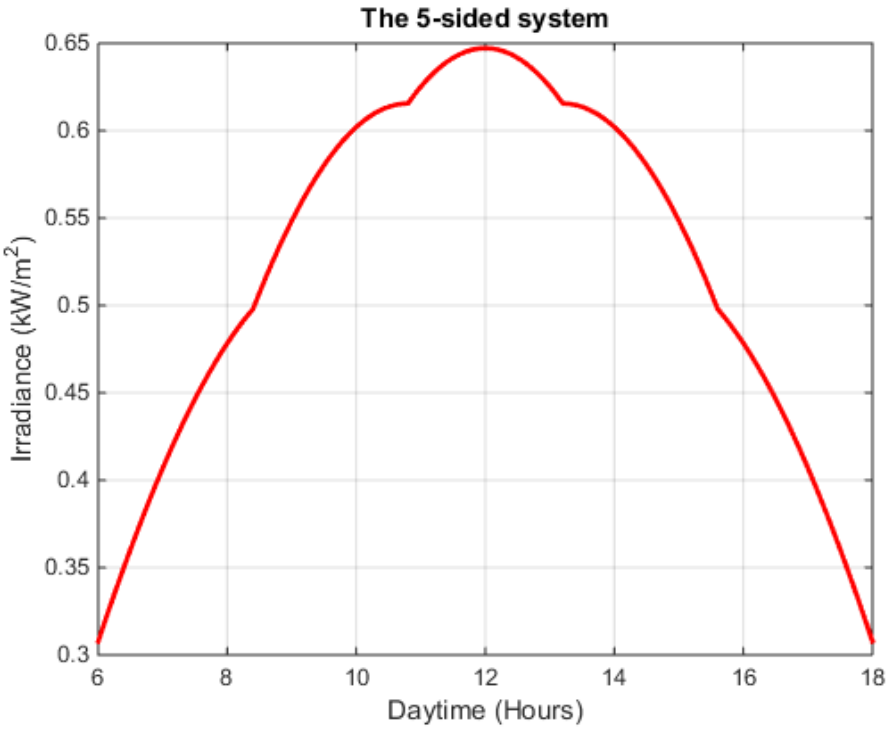

Figure 3. 7: Five-sided OSM irradiance dynamics

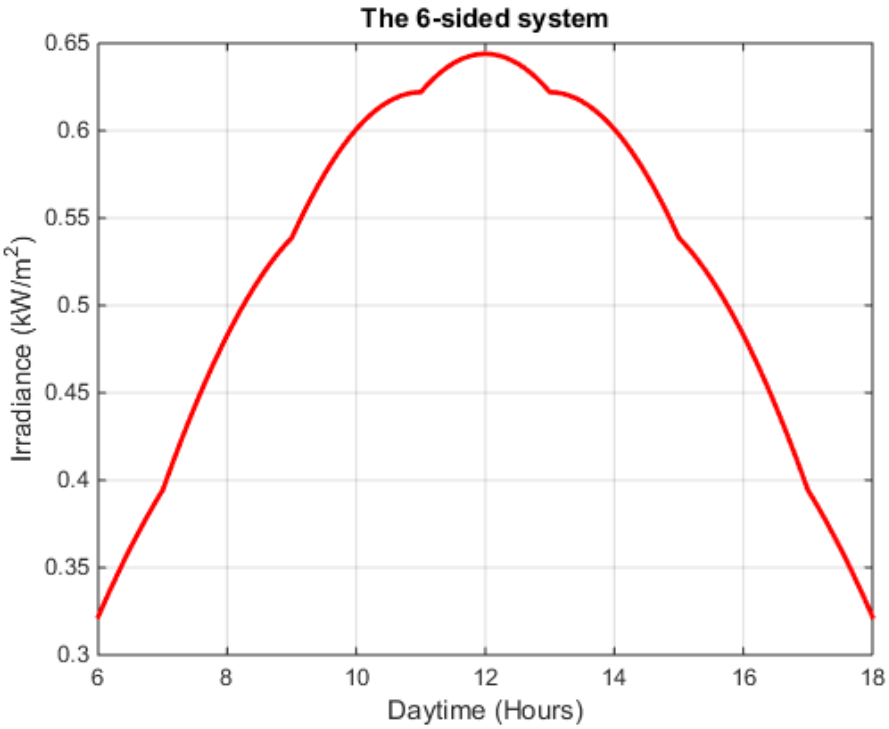

Figure 3. 8: Six-sided OSM irradiance dynamics

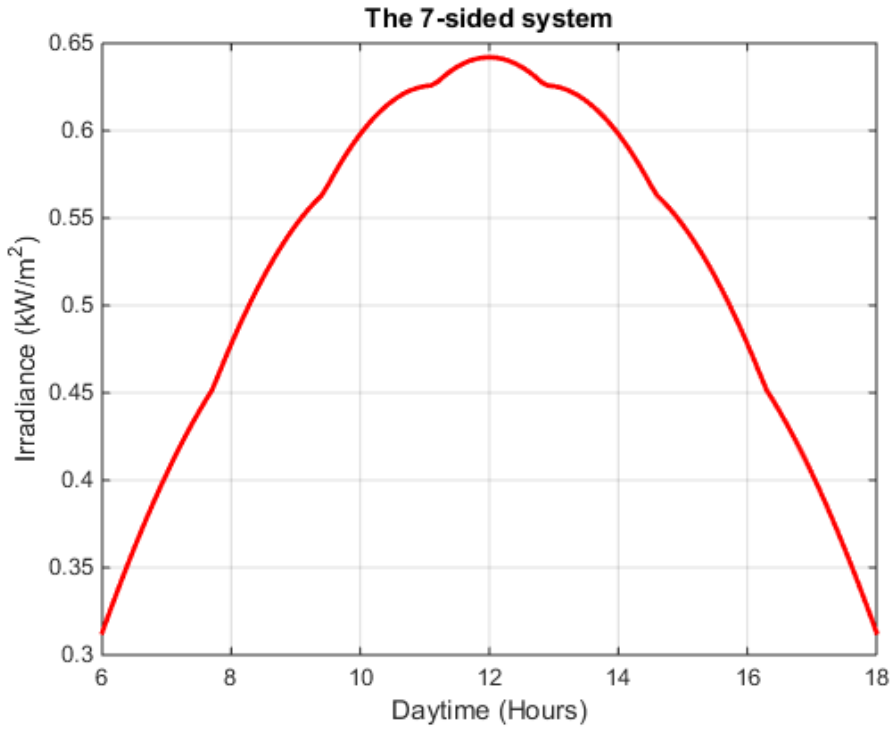

Figure 3. 9: Seven-sided OSM irradiance dynamics

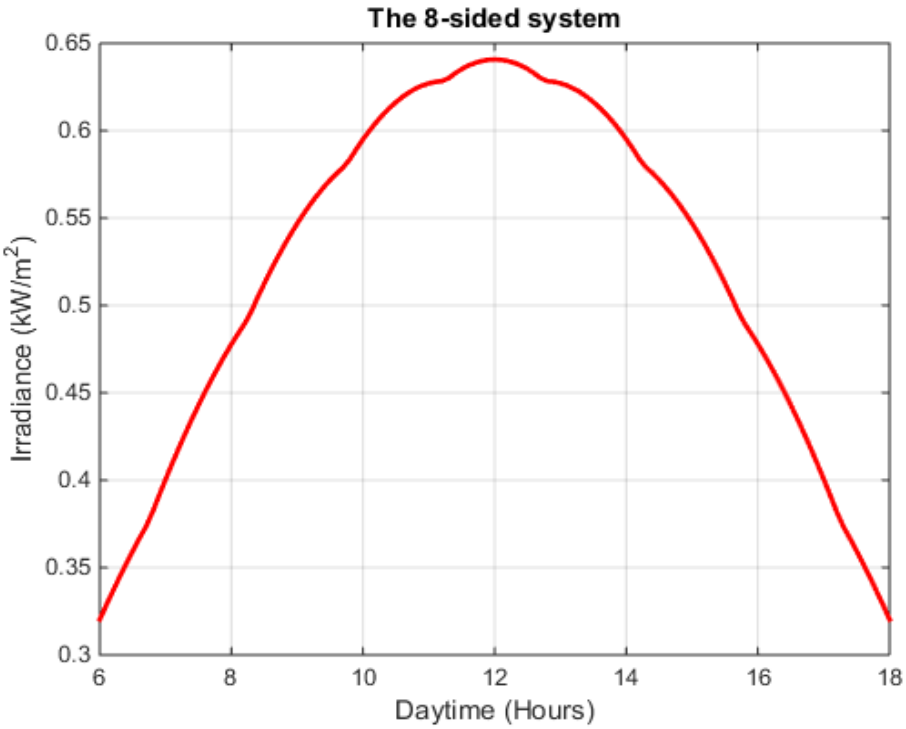

Figure 3. 10: Eight-sided OSM irradiance dynamics

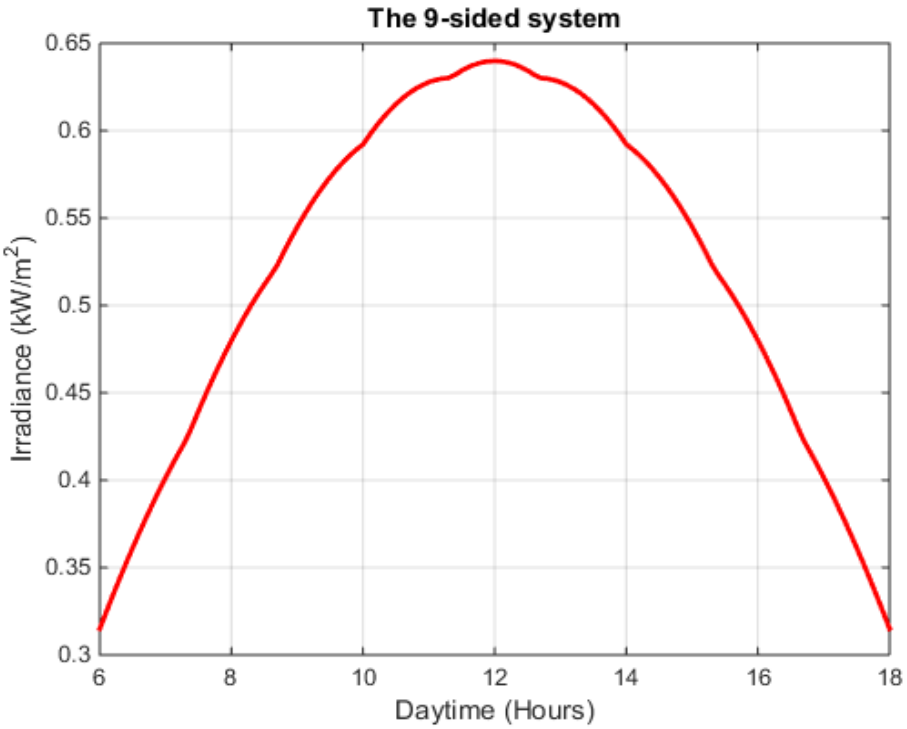

Figure 3. 11: Nine-sided OSM irradiance dynamics

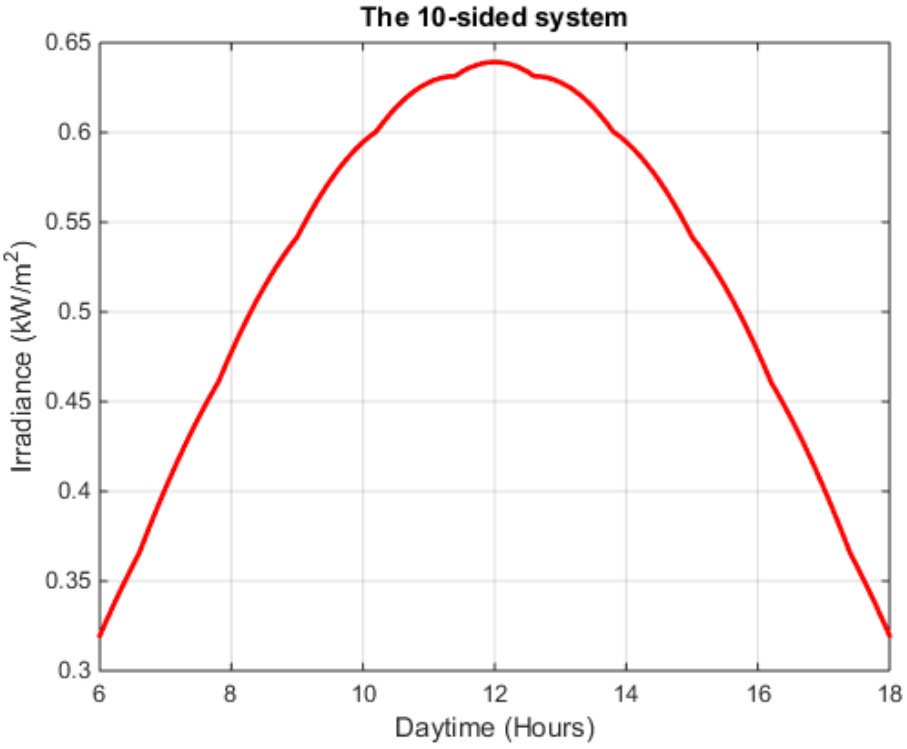

Figure 3. 12: Ten-sided OSM irradiance dynamics

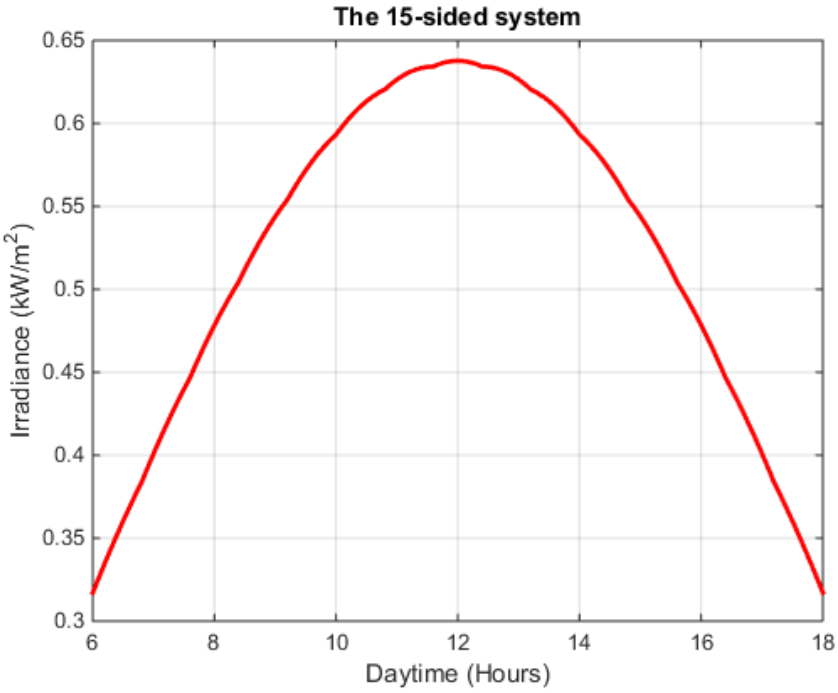

Figure 3. 13: Fifteen-sided OSM irradiance dynamics

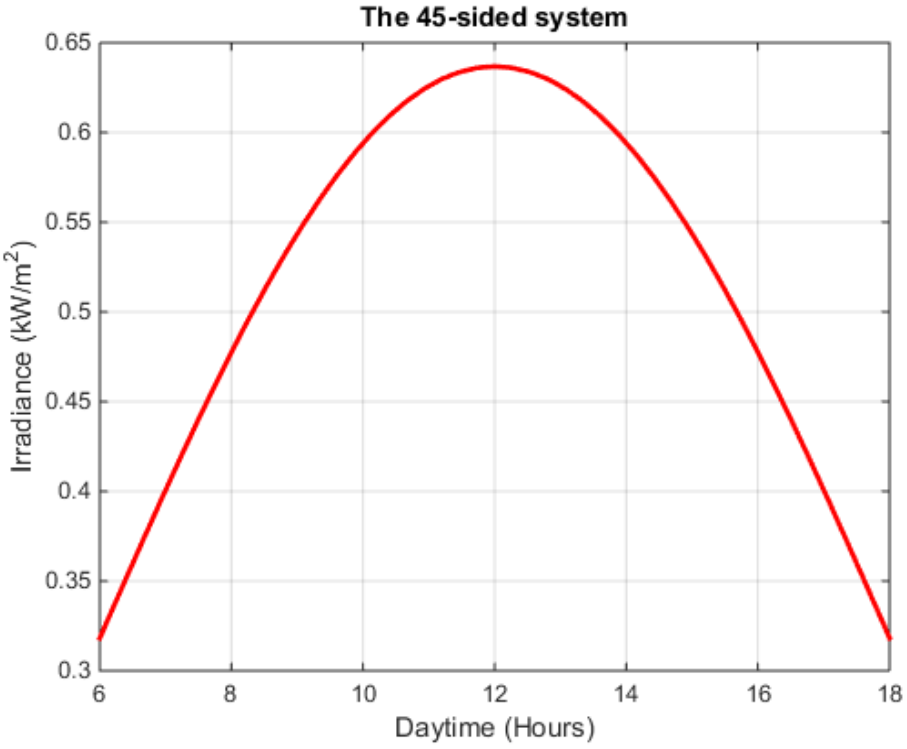

Figure 3. 14: Fourty-five-sided OSM irradiance dynamics

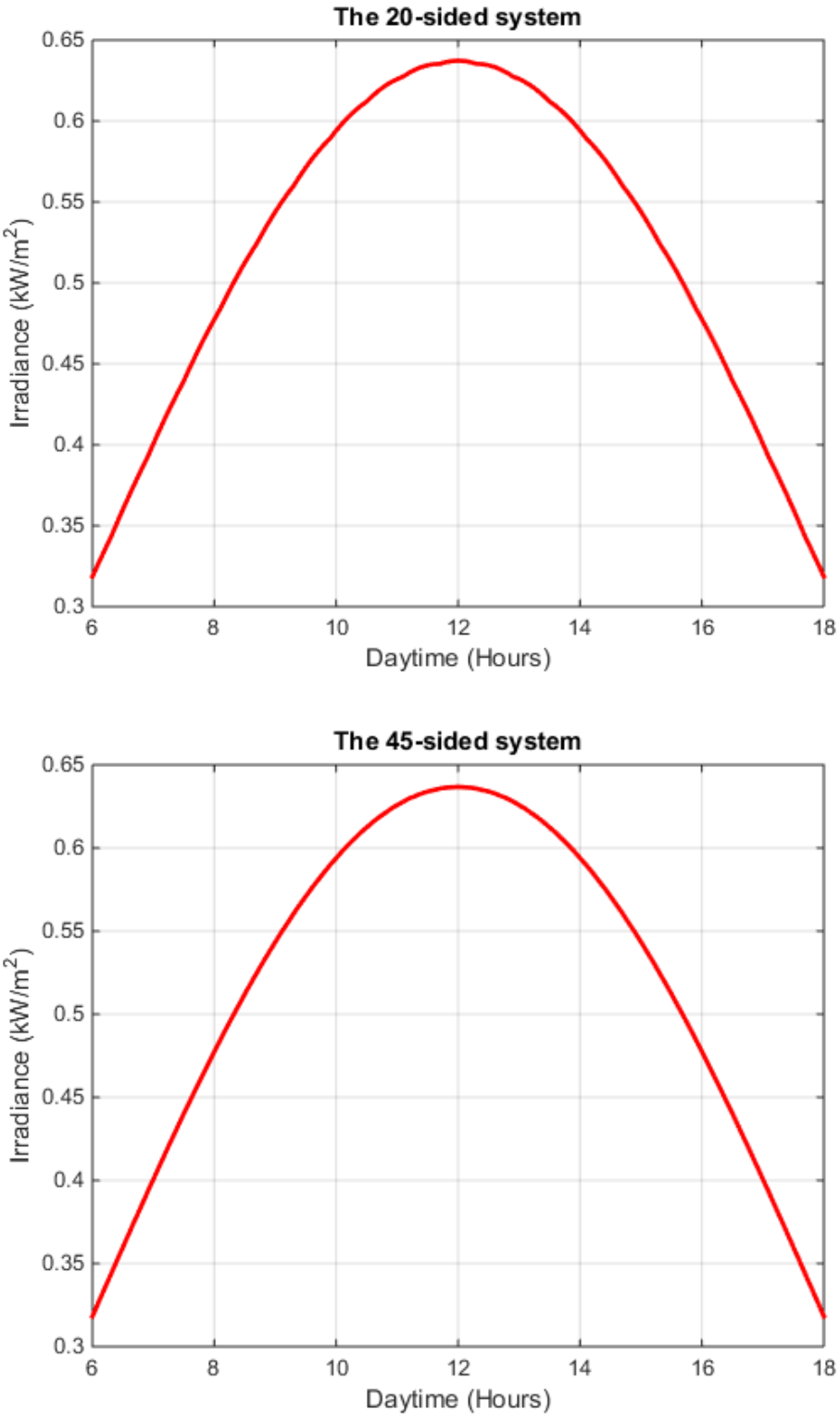

Figure 3. 15: Three-sided OSM irradiance dynamics

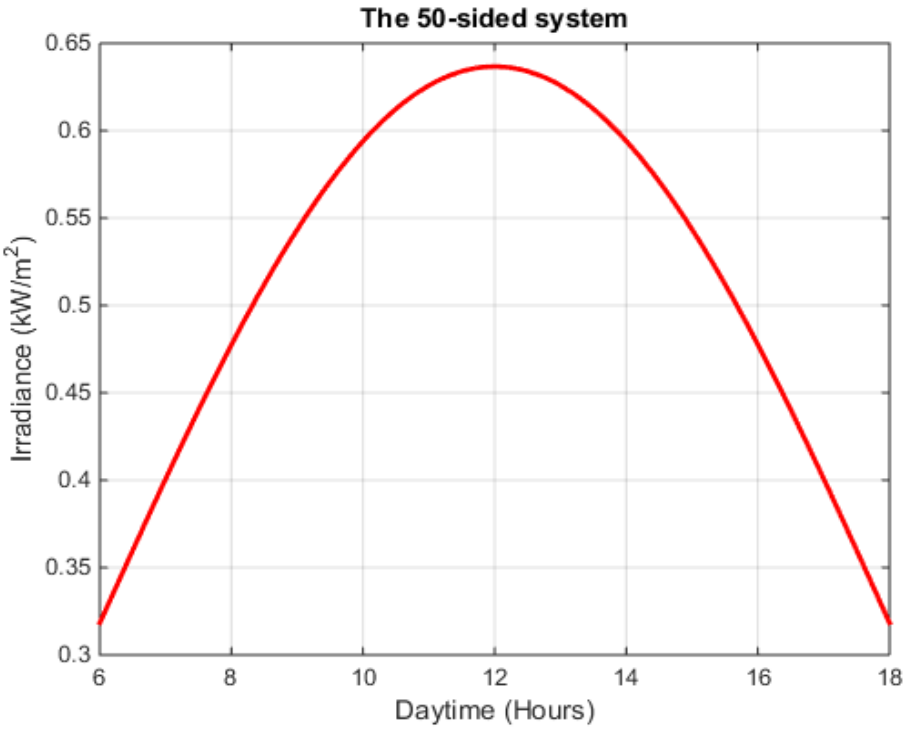

Figure 3. 16: Fifty-sided OSM irradiance dynamics

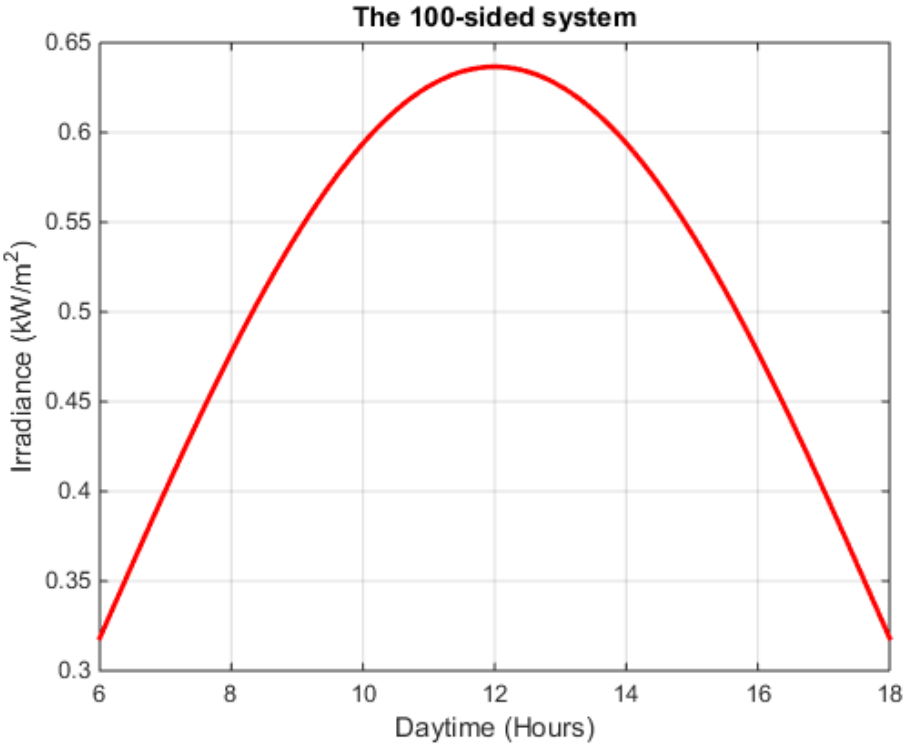

Figure 3. 17: Hundred-sided OSM irradiance dynamics

3.4.1. OSM sides' individual contributions

For a further understanding and visual clarity of irradiance profiles, individual contributions of sides to the overall irradiance were presented in separate figures.

Figure 3.18 through 3.32 depicts individual contributions to PV systems'outputs under study.

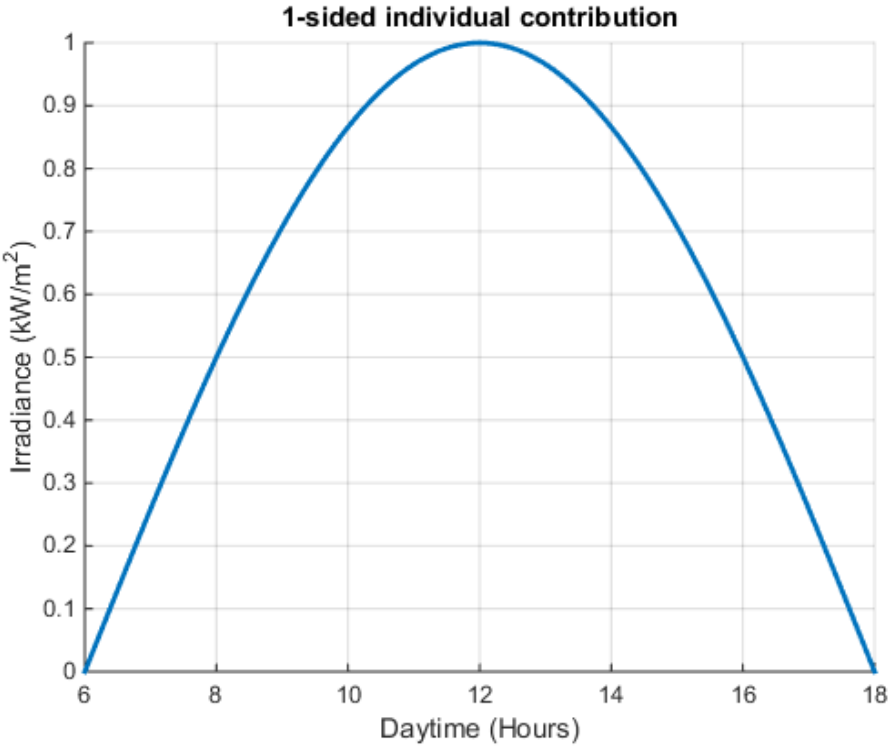

Figure 3. 18: Flat-fixed-tilt contribution

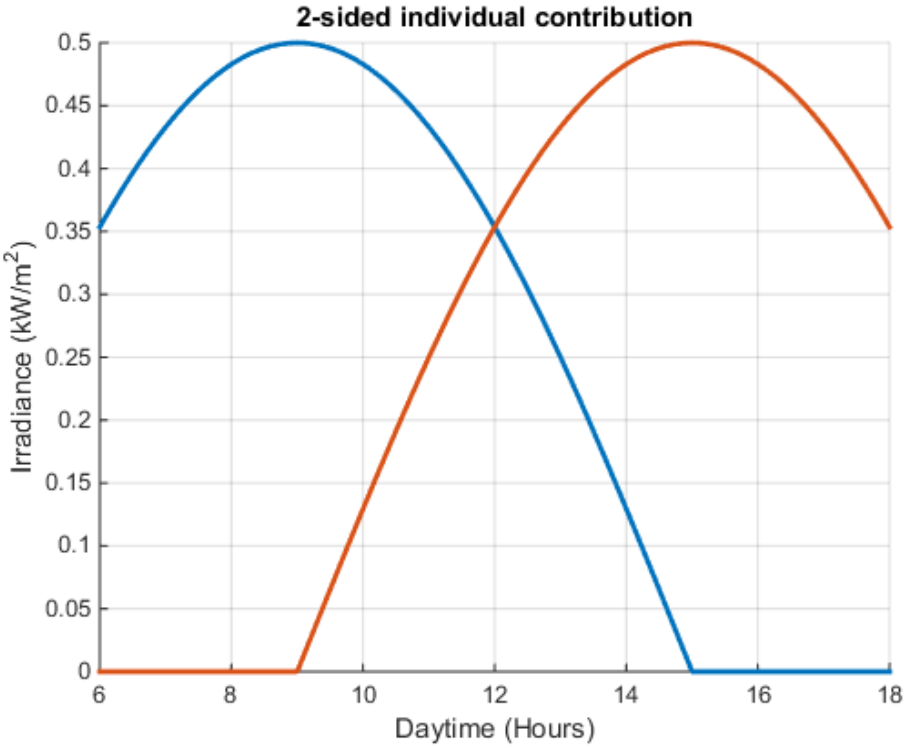

Figure 3. 19:Double-sided OSM sides' individual contributions

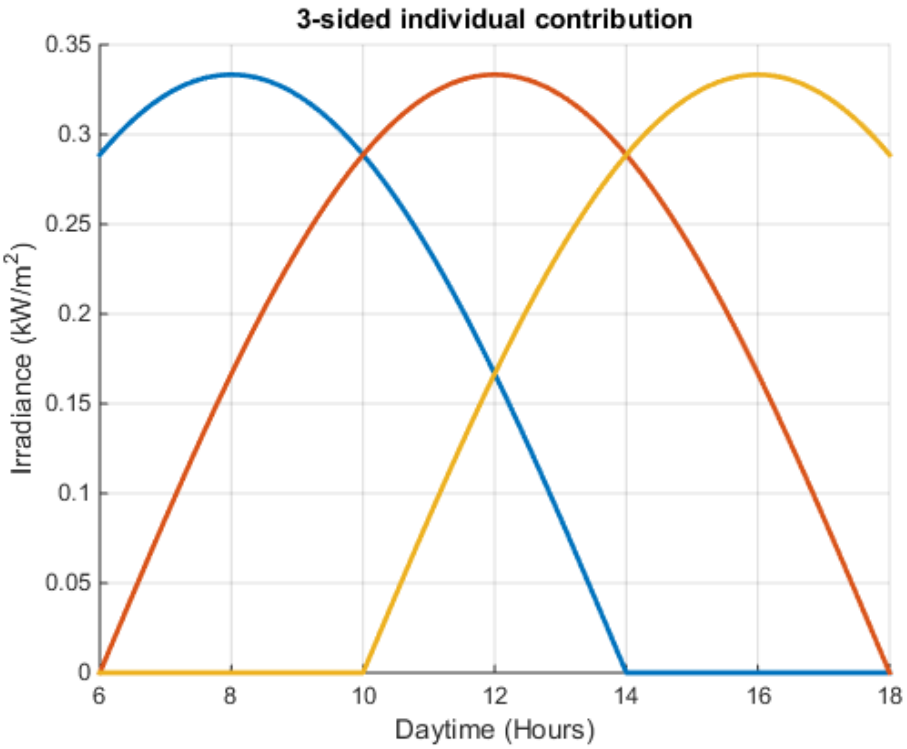

Figure 3. 20: Three-sided OSM sides' individual contributions

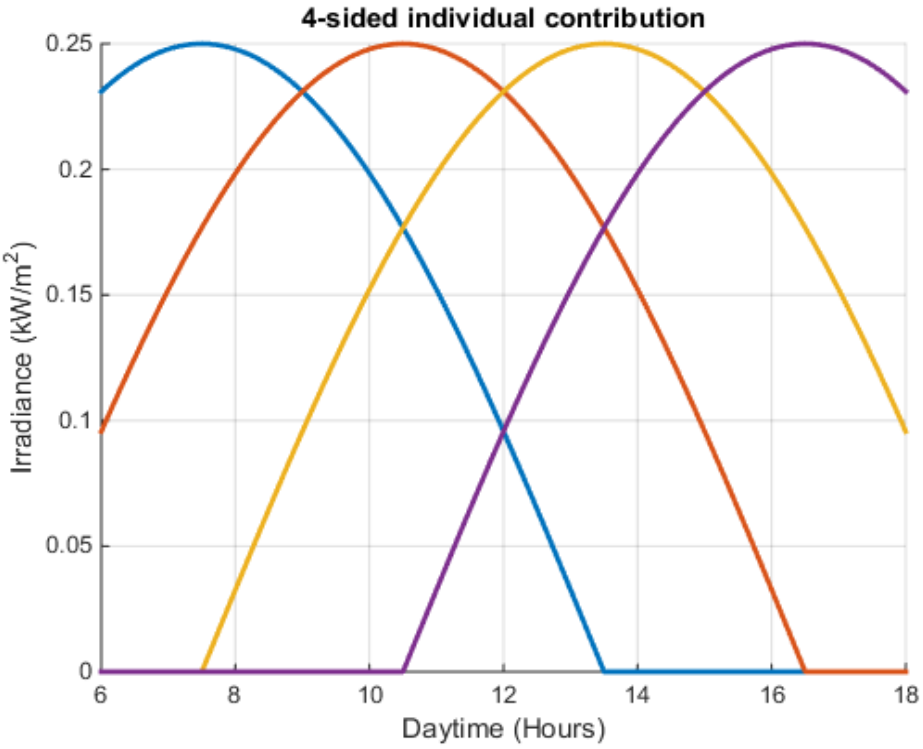

Figure 3. 21: Four-sided OSM sides' individual contributions

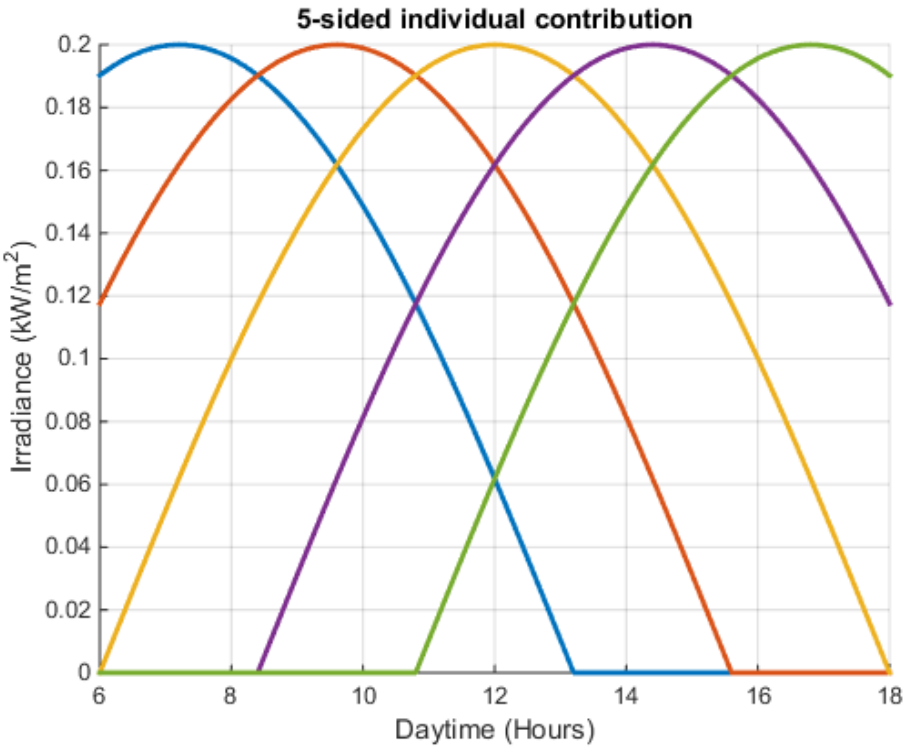

Figure 3. 22: Five-sided OSM sides' individual contributions

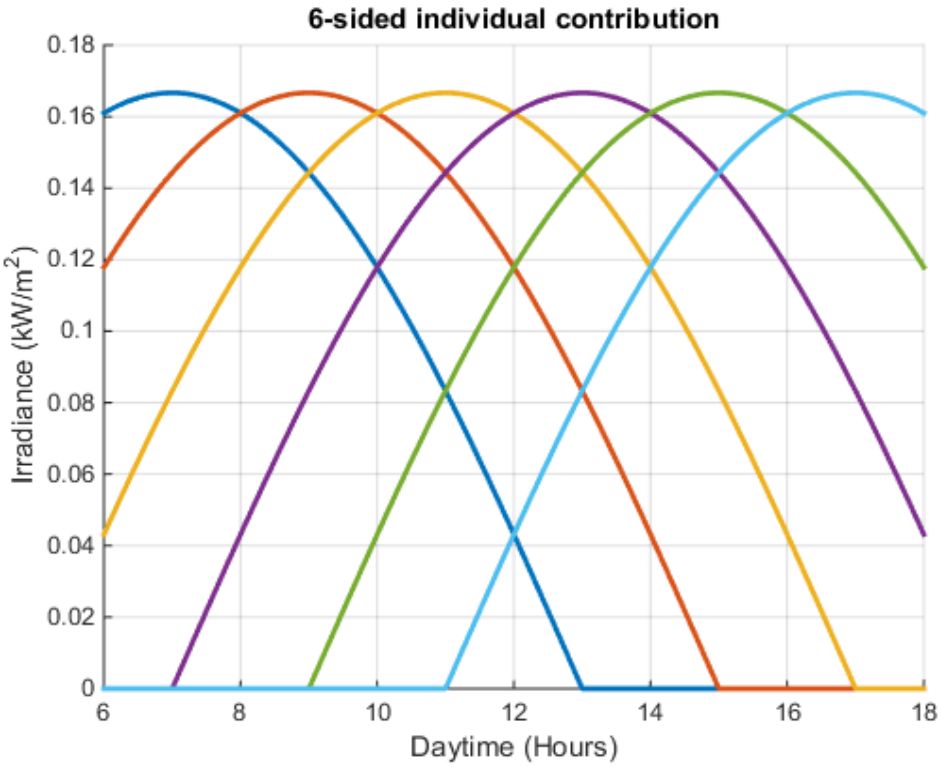

Figure 3. 23: Six-sided OSM sides' individual contributions

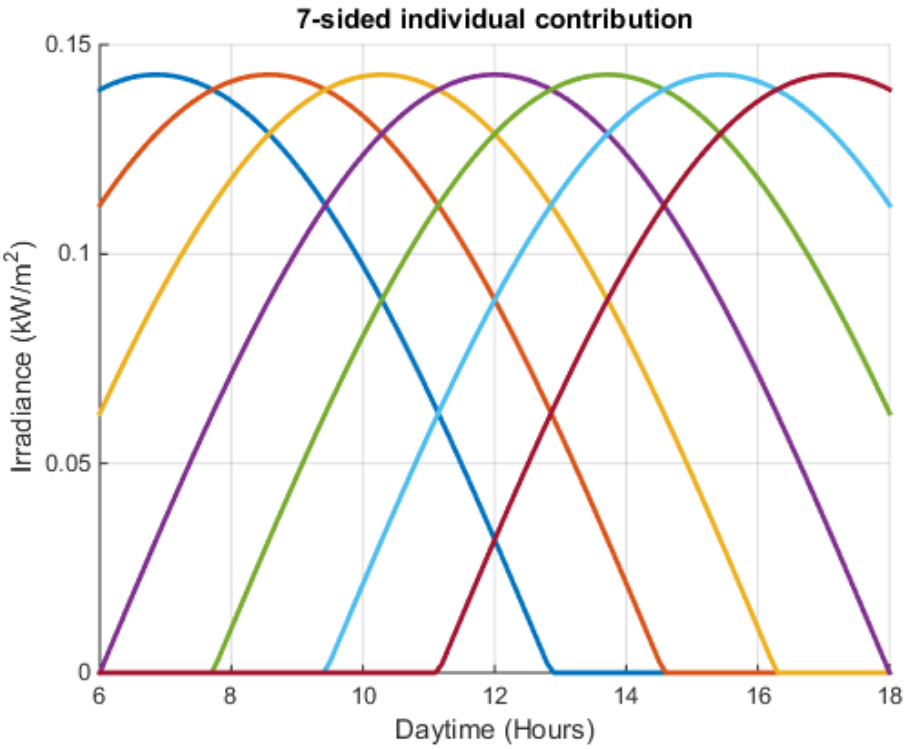

Figure 3. 24:Seven-sided OSM sides' individual contributions

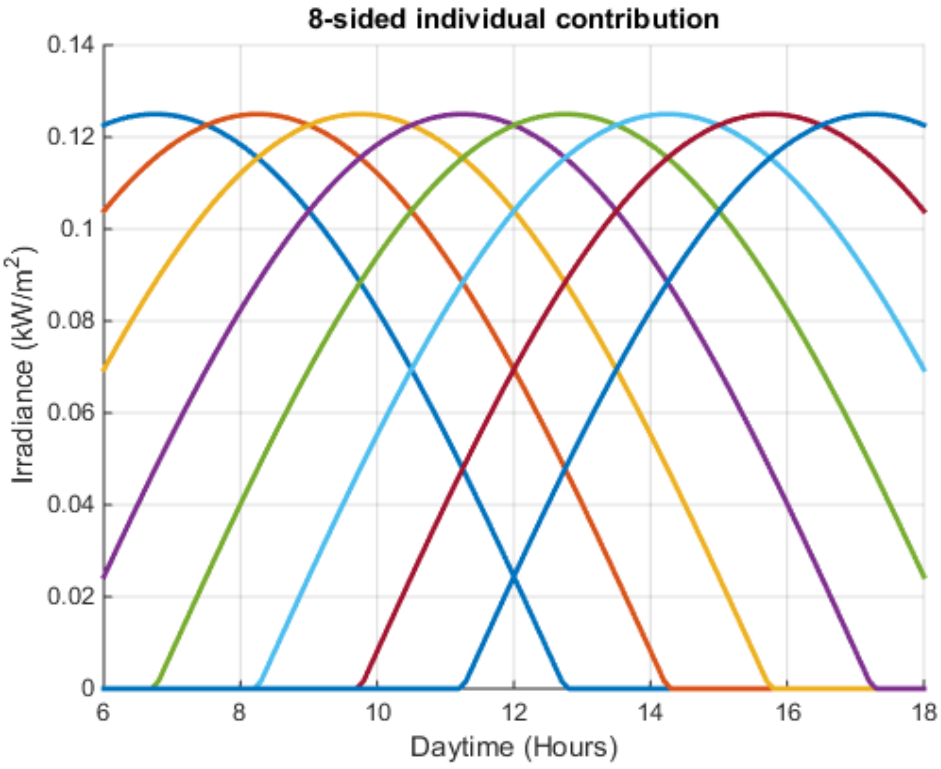

Figure 3. 25: Eight-sided OSM sides' individual contributions

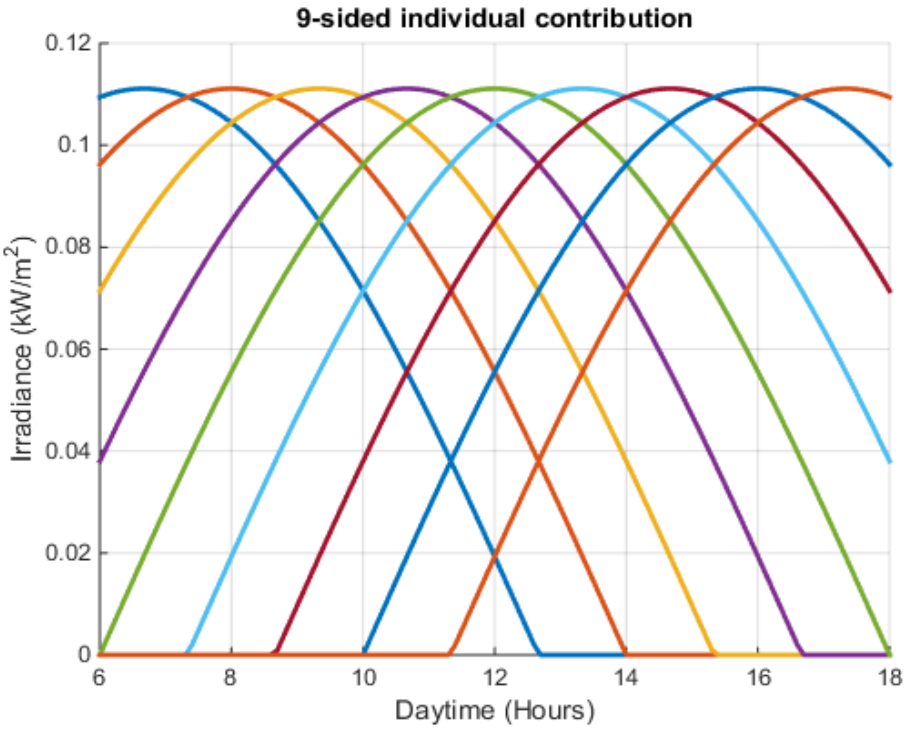

Figure 3. 26: Nine-sided OSM sides' individual contributions

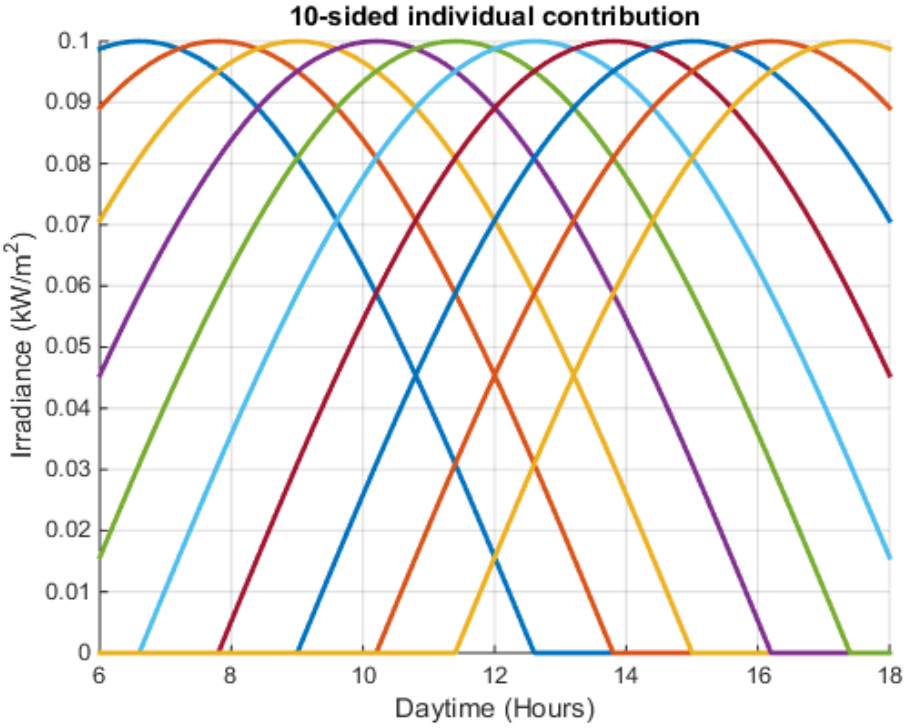

Figure 3. 27: Ten-sided OSM sides' individual contributions

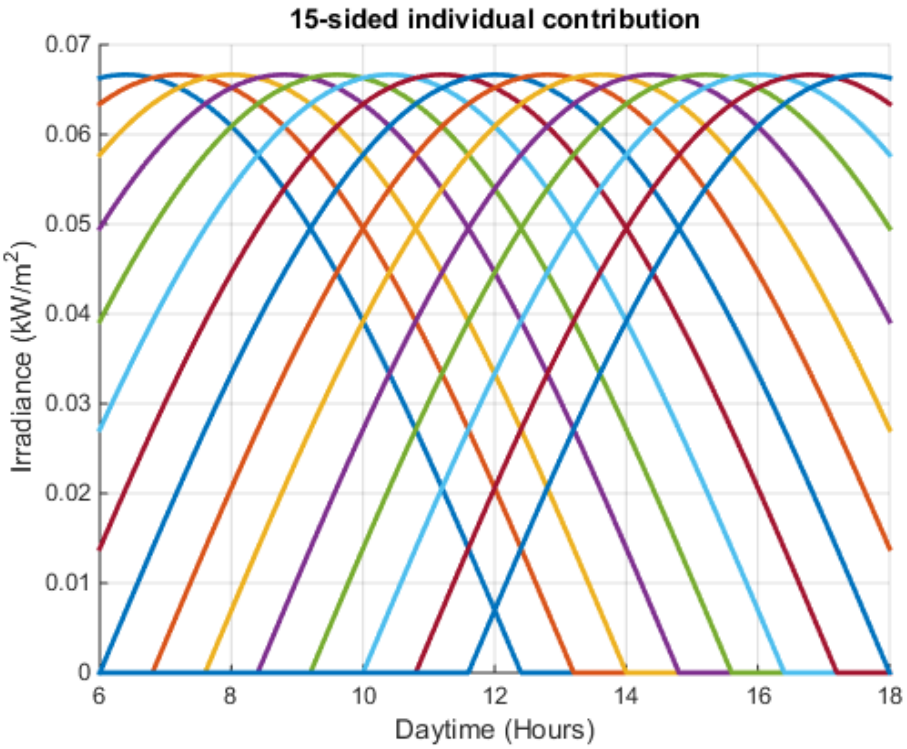

Figure 3. 28: Fifteen-sided OSM sides' individual contributions

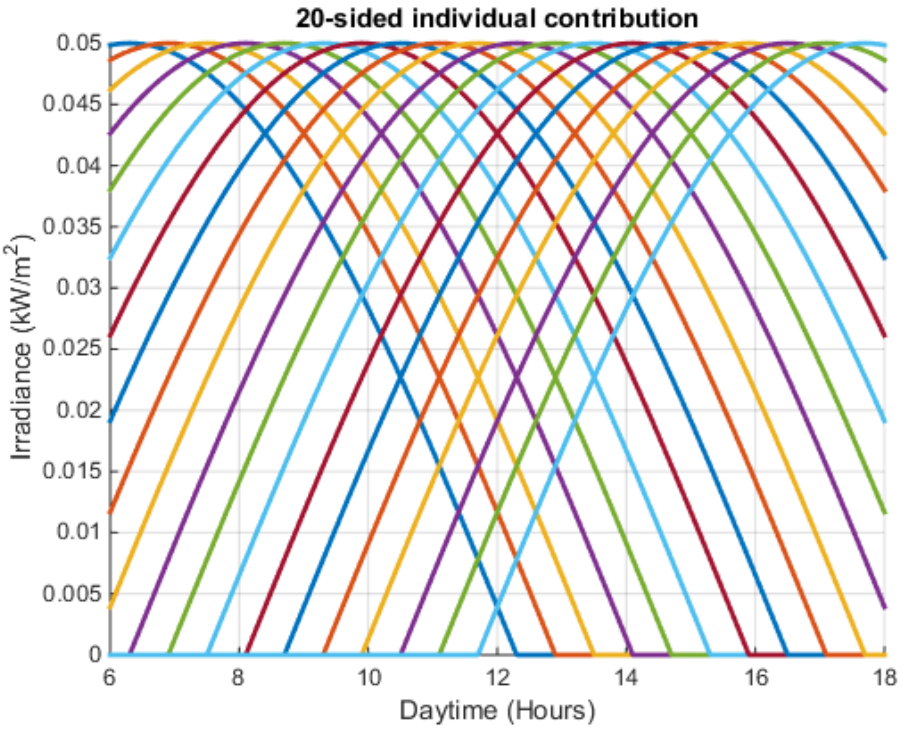

Figure 3. 29: Twenty-sided OSM sides' individual contributions

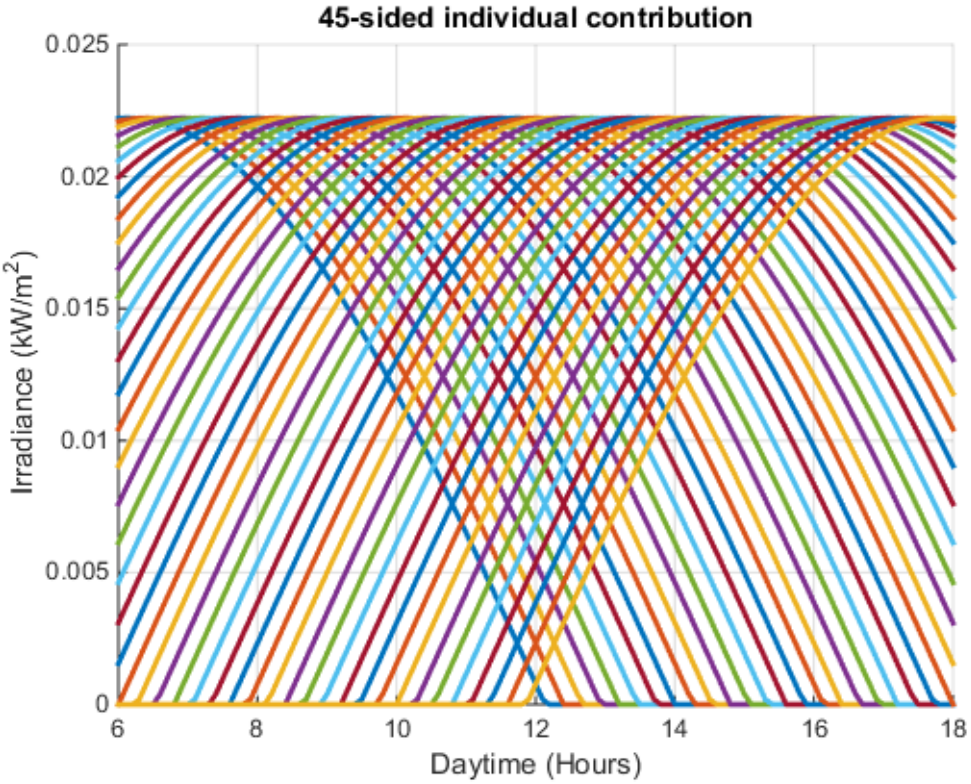

Figure 3. 30: Forty-five Five-sided OSM sides' individual contributions

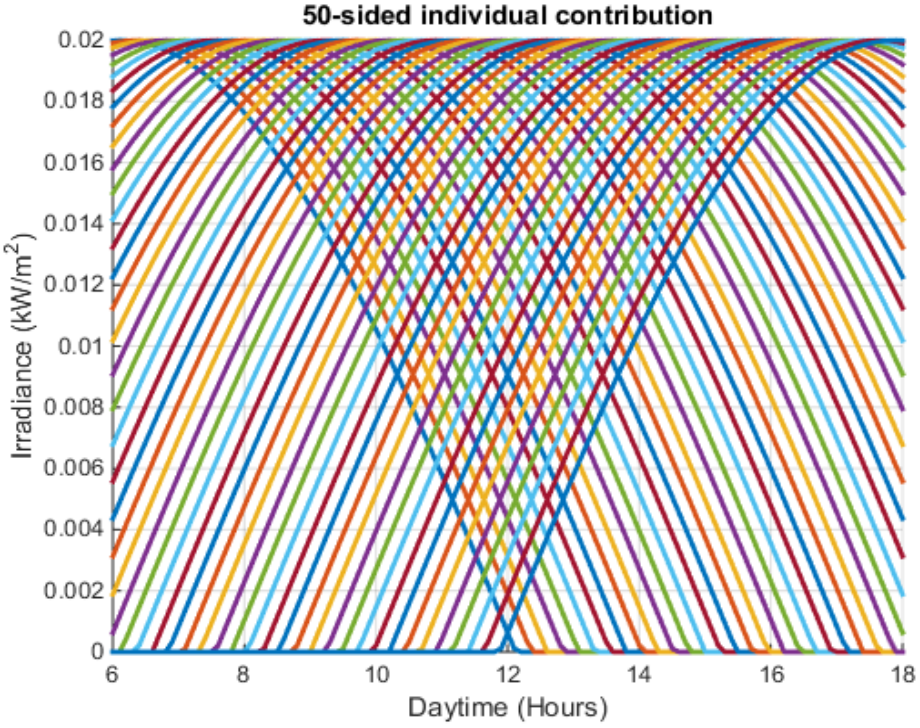

Figure 3. 31: Fifty-sided OSM sides' individual contributions

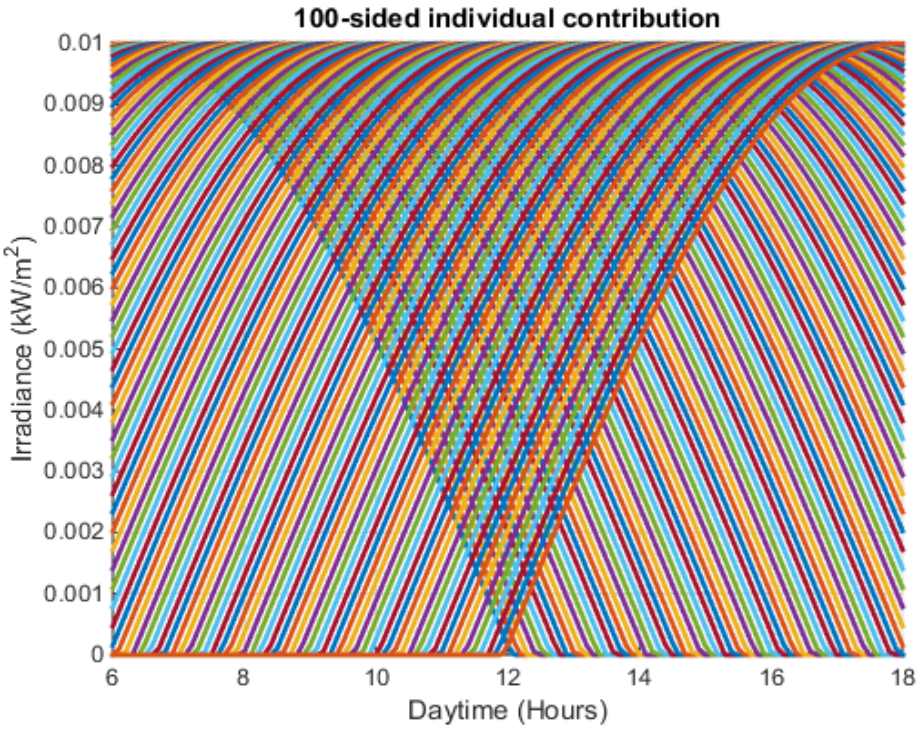

Figure 3. 32: Hundred-sided OSM sides' individual contributions

3.5. System evaluation parameters

Some key parameters from the irradiance dynamics were singled out towards the evaluation of the OSM PV systems' performance. Those parameters were picked from the irradiance dynamics and the values recorded in Table 3.1.

3.5.1. Average value

The average value is a commonly known indicator to quantities governed by sinusoidal functions and this is the case of PV systems under this study. For a half wave sine function, the average value, is defined as the peak value of the sine wave over π. Thus, since the sun describes a half-cycle during the day, the average value of the irradiance distribution over the daytime can be estimated as follows (Equation 3.5):

$$G_{avg} = \frac{G_M}{\pi}$$
$$G_{avg} = 0.318 G_M$$

Equation 3. 5

From the graphs in Figures 3 through 14, the irradiance of the whole PV system is dynamic and is established above a dc level located at 0. 318 on the irradiance axis i.e. 31.8 % of the nominal irradiance. For topologies with sides less or equal to ten, graphs have circumvolutions; the dynamics of the irradiance tend to become a perfect sinusoid, over a 0-to-π interval, and its peak value is π times smaller than the direct irradiance of 1 kW/m^2.

Figures 3.33 to 3.46 illustrate a comparison between the dynamic of a single sided PV system of which the peak value equals the nominal irradiance divided by π and the graph of the irradiance of which the initial constant level is omitted. The purpose of this comparison, is to circumvent the challenge that encountered in evaluating the average irradiance due to irregular-shaped dynamics of some multisided PV systems. Performing this exercise for selected sample has led to the conclusion that the dynamic part of the irradiance tends to conform to a half sinewave of 0.32 kW/m^2 amplitude.

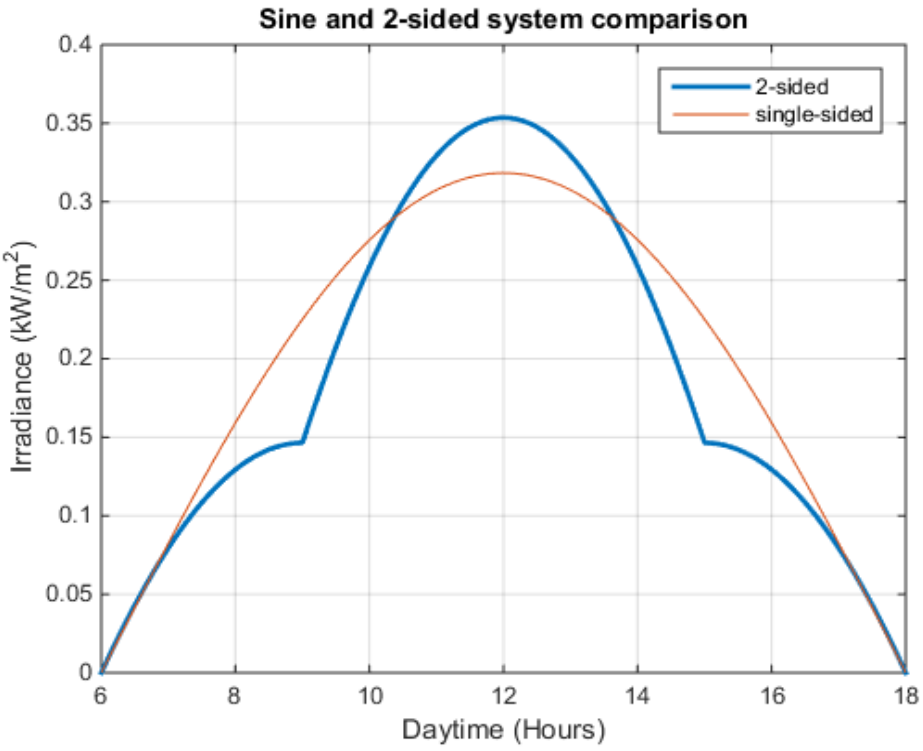

Figure 3. 33: Double-sided OSM vs sine comparison

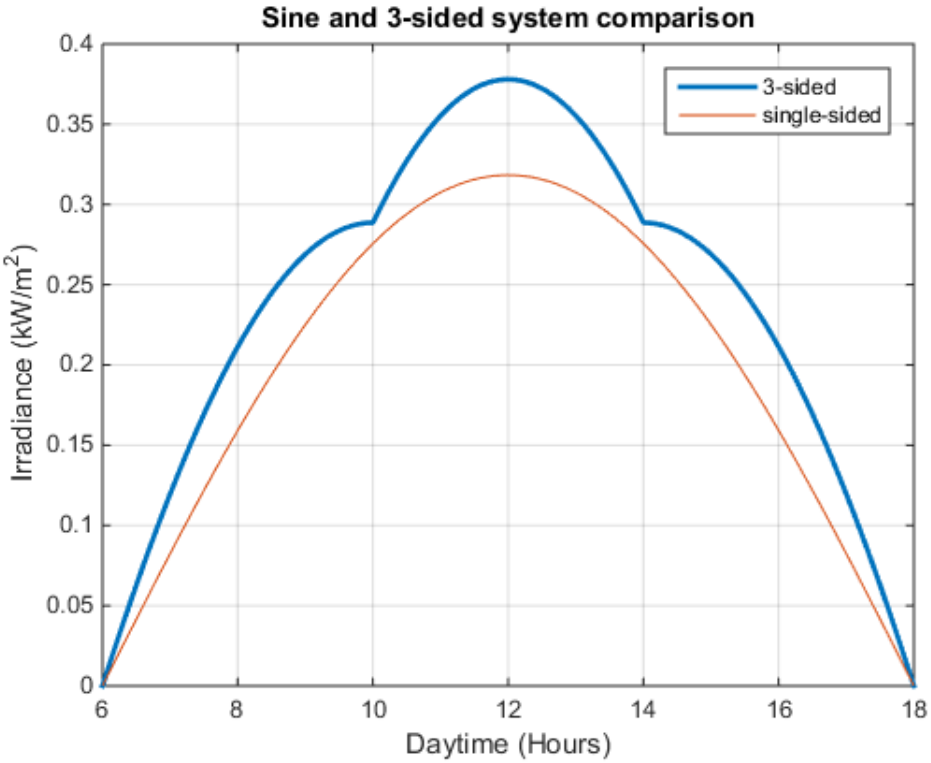

Figure 3. 34: Three-sided OSM vs sine comparison

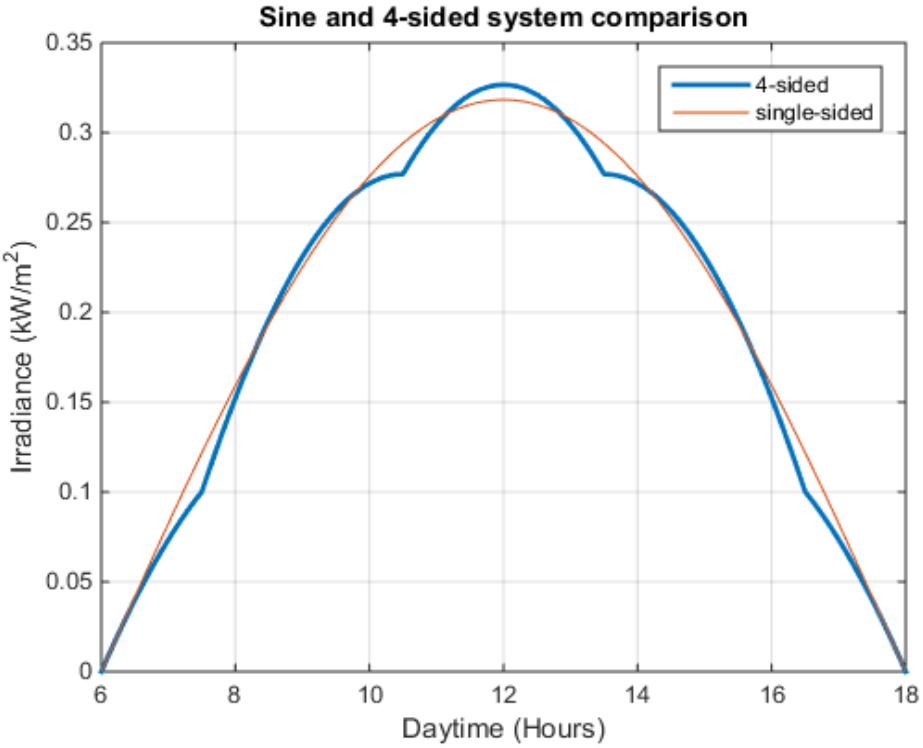

Figure 3. 35: Four-sided OSM vs sine comparison

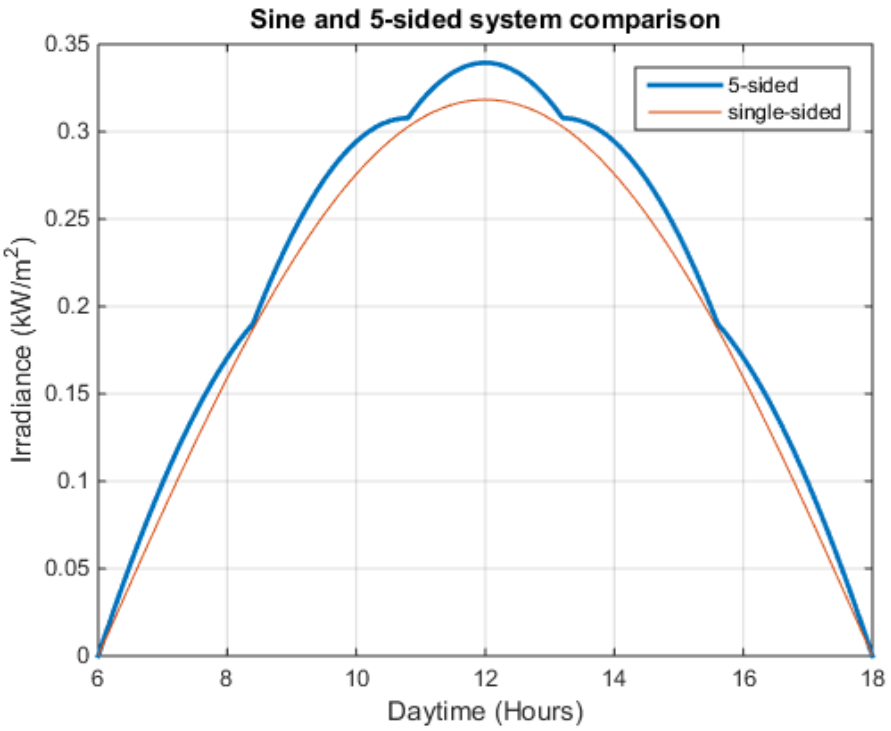

Figure 3. 36: Five-sided OSM vs sine comparison

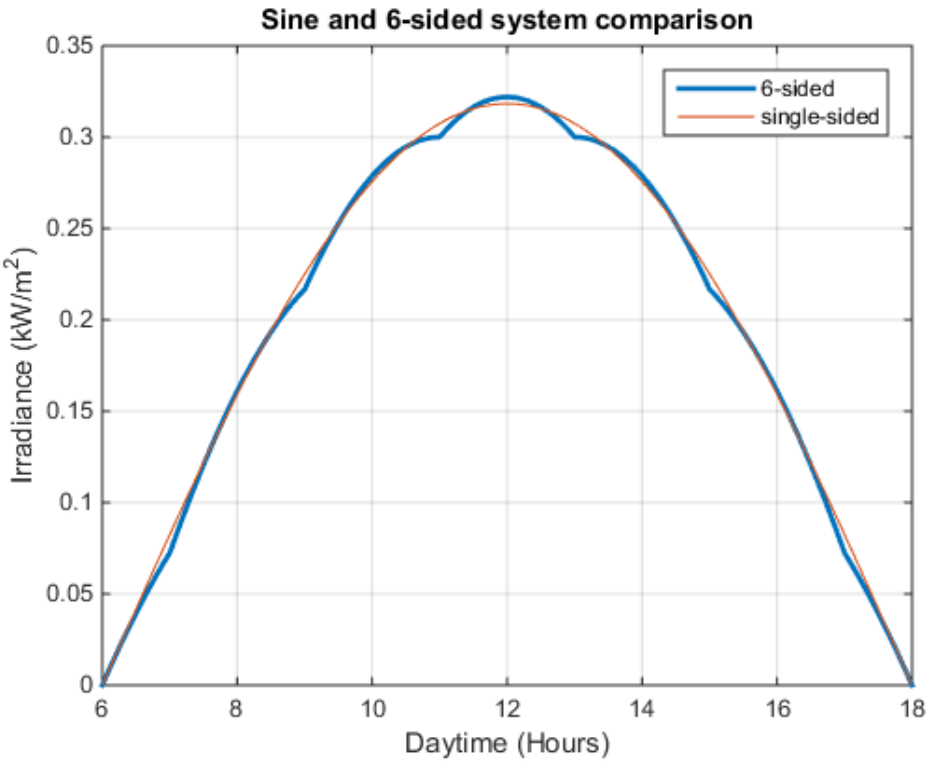

Figure 3. 37: Six-sided OSM vs sine comparison

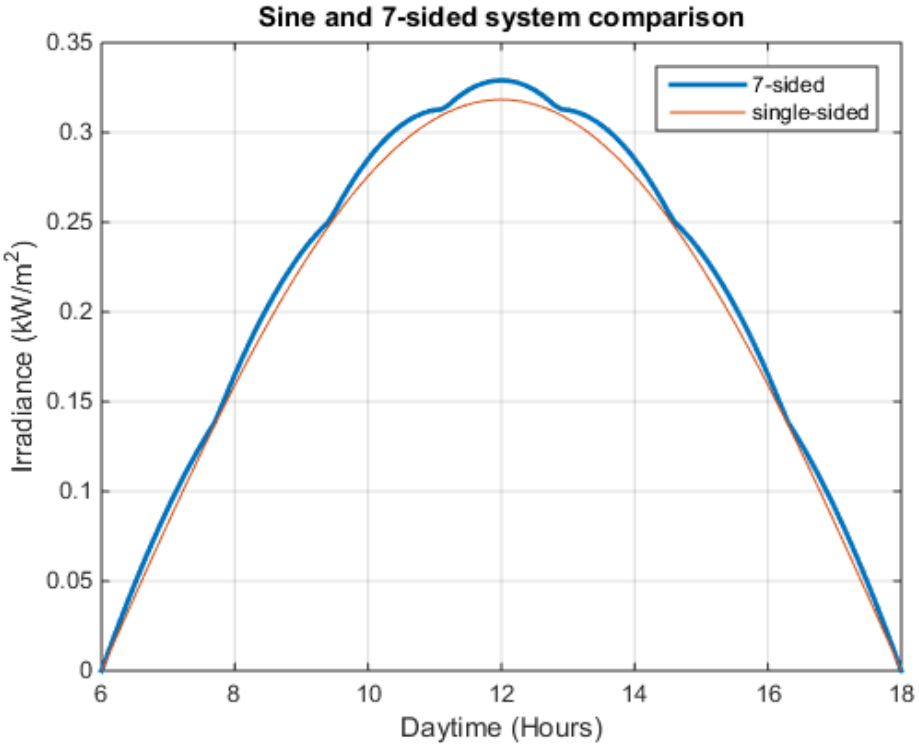

Figure 3. 38: Four-sided OSM vs sine comparison

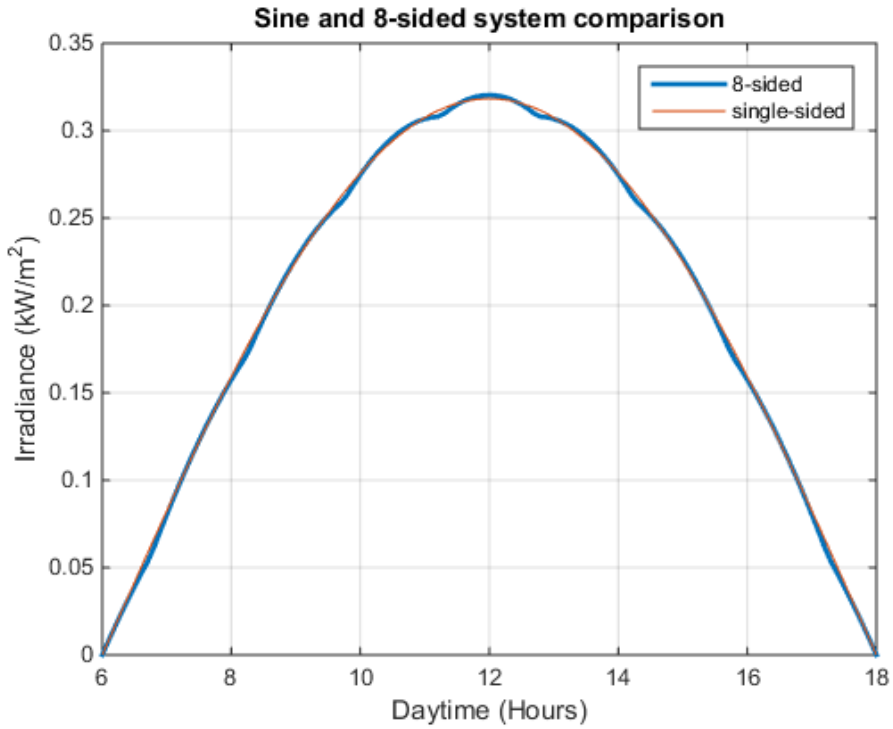

Figure 3. 39: Eight-sided OSM vs sine comparison

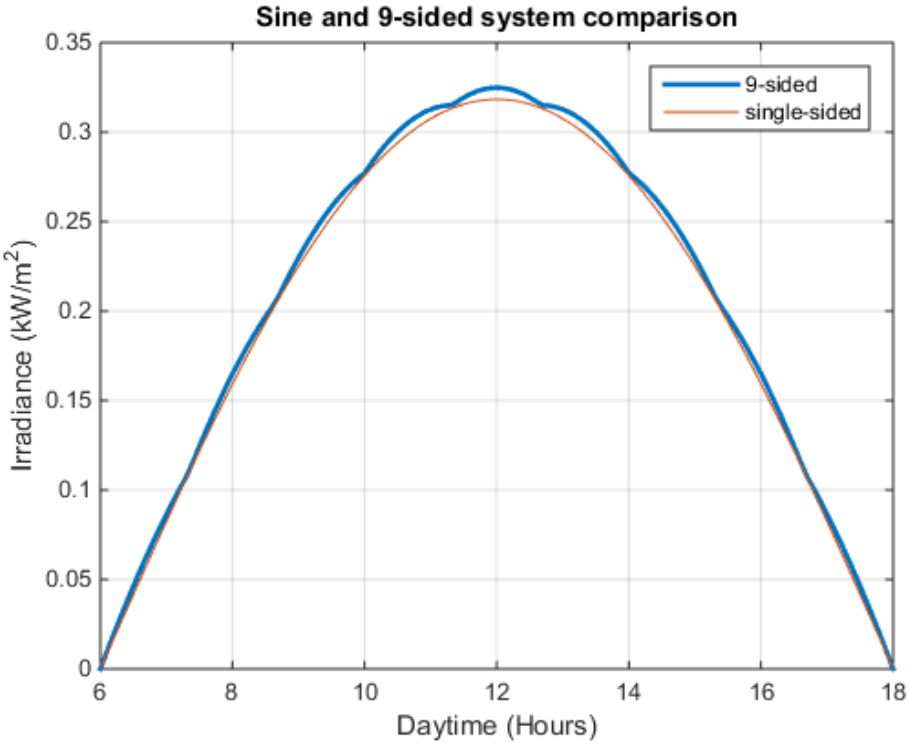

Figure 3. 40: Nine-sided OSM vs sine comparison

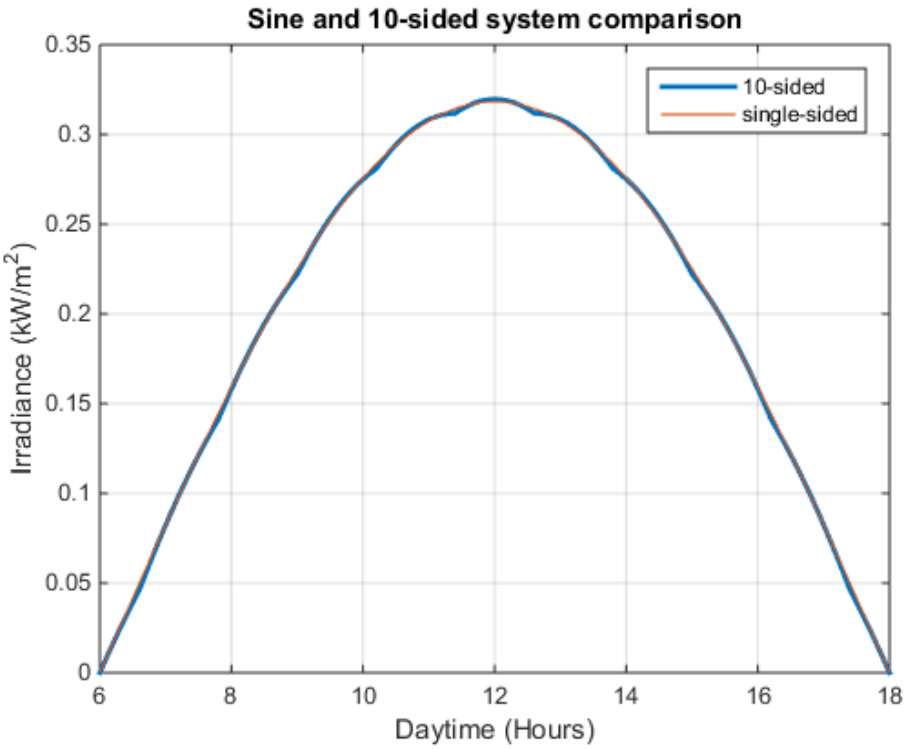

Figure 3. 41: Ten-sided OSM vs sine comparison

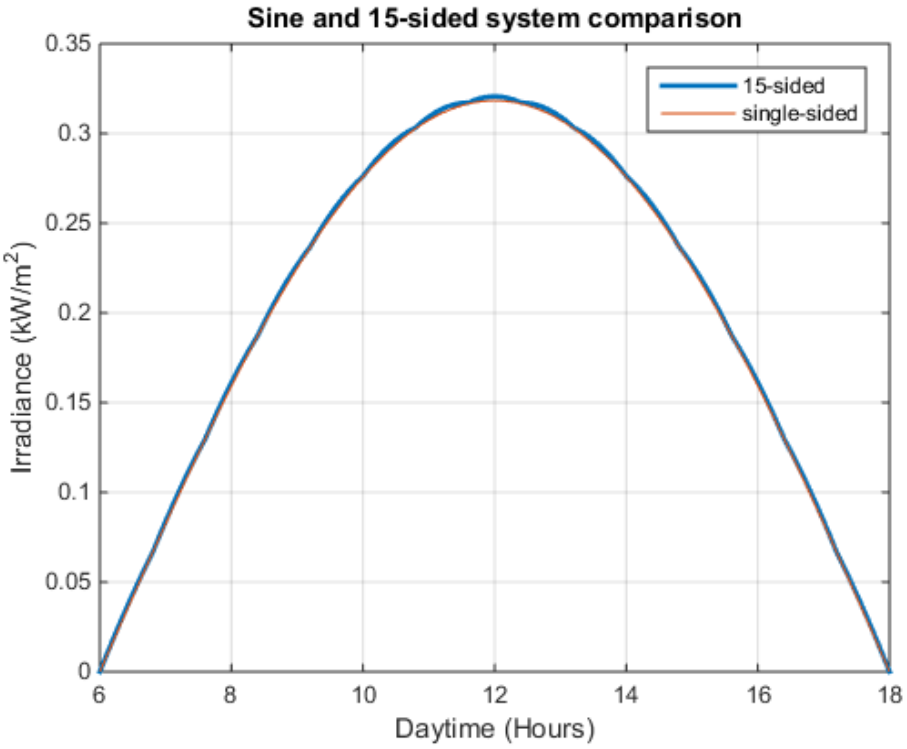

Figure 3. 42: Fifteen-sided OSM vs sine comparison

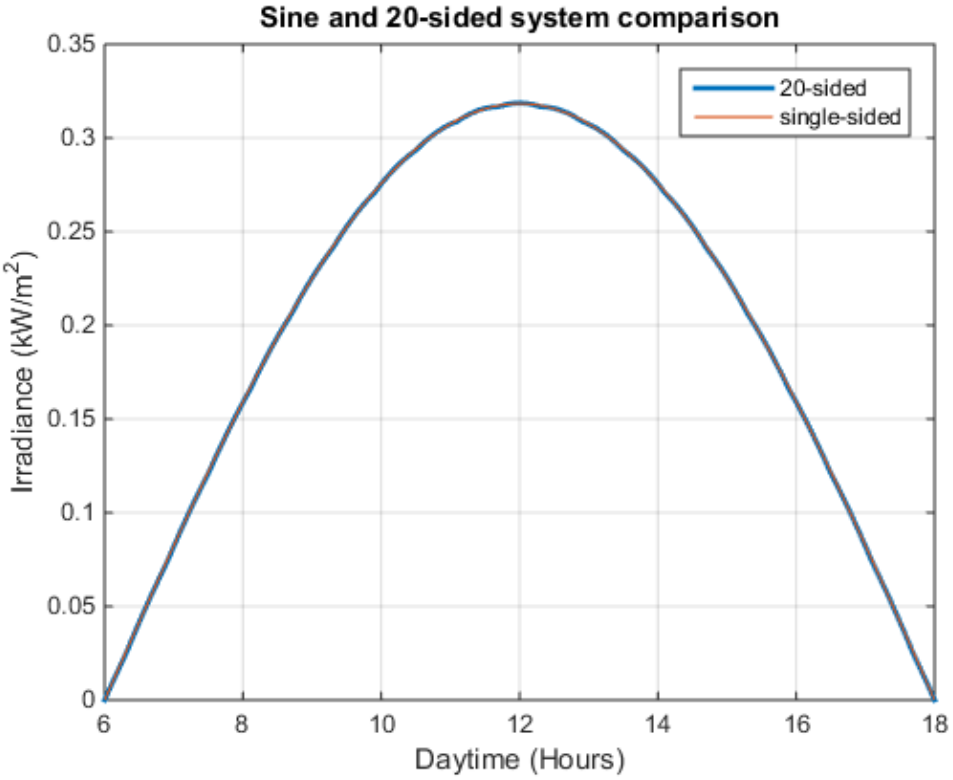

Figure 3. 43: Twenty-sided OSM vs sinewave comparison

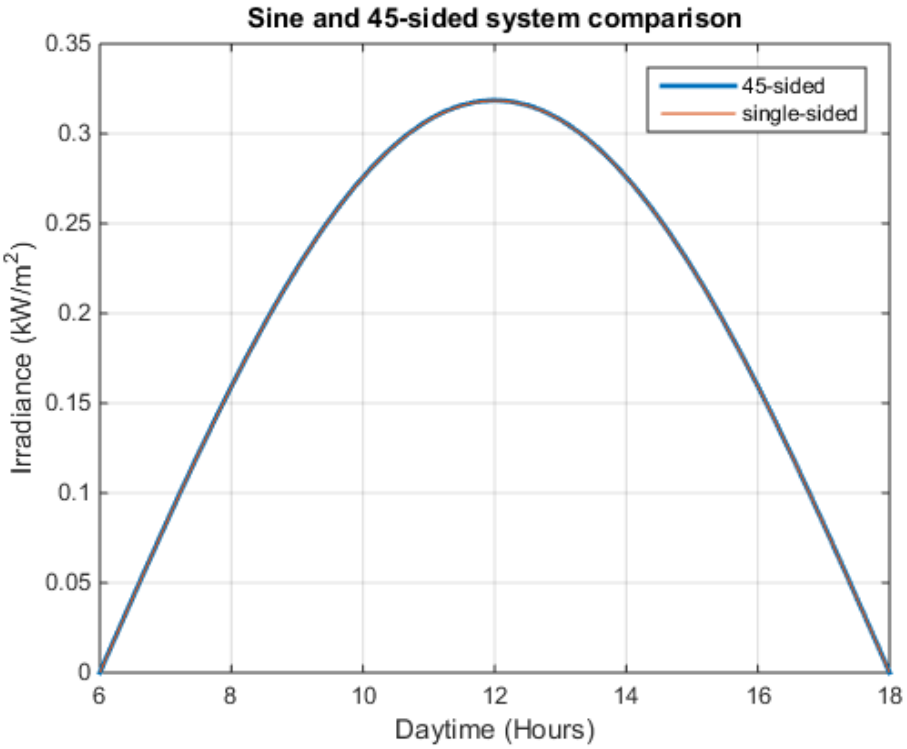

Figure 3. 44: Forty-five-sided OSM vs sine comparison

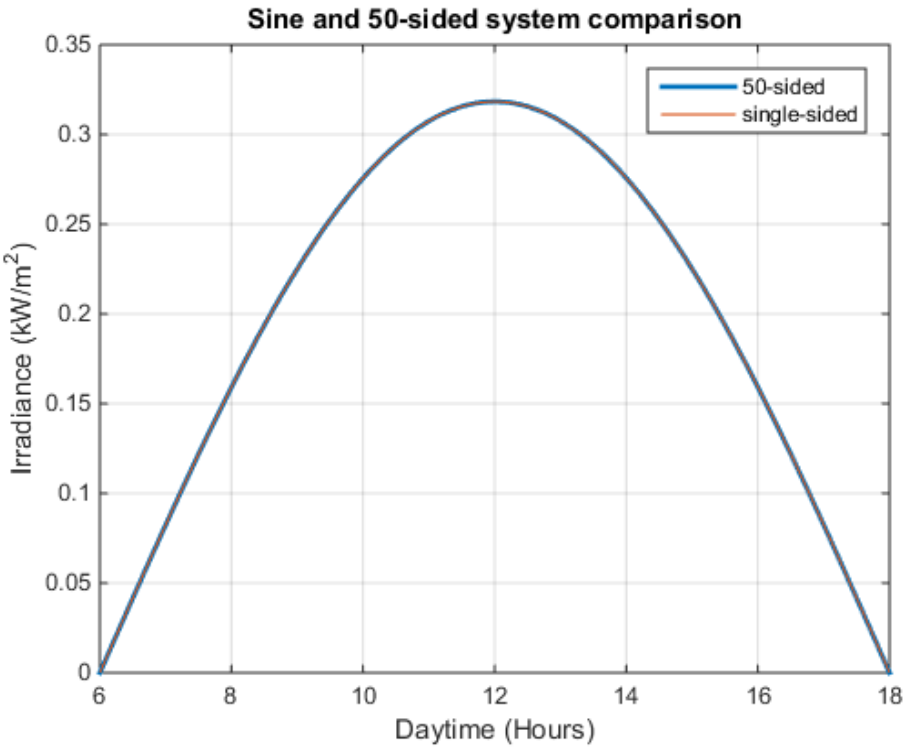

Figure 3. 45: Fifty-sided OSM vs sine comparison

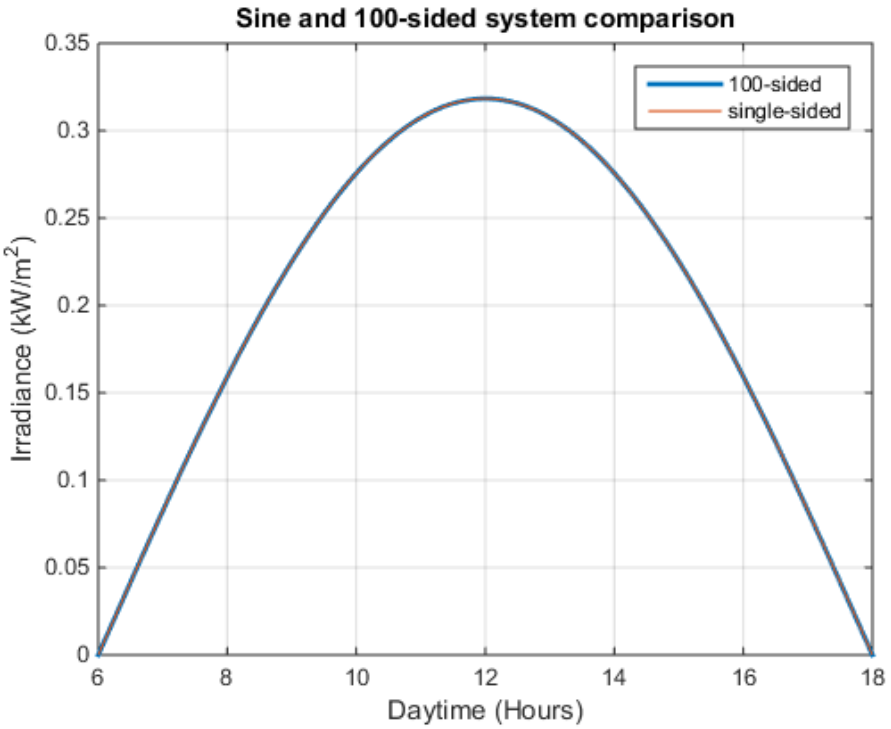

Figure 3. 46: Hundred-sided OSM vs sine comparison

The overall observation is that the dynamic part of the irradiance can be estimated to a sine wave as the number of sides increases. The irradiance function is therefore expected to be a perfect sinewave for a half-cylinder-shaped system. The overall

average irradiance for multisided PV systems could then be calculated as follows (Equation 3.6):

$$G_{avg} = 0.318G_M + \frac{0.318G_M}{\pi}$$ **Equation 3. 6**

For the direct irradiance of 1 kW/m^2, the average value of the multisided PV systems (0.420 kW/m^2) proves to be about 1.32 times greater than the average irradiance of 0.318 kW/m^2. On the right-hand side of equation 5, the first term corresponds to the dc level while the second term represents the average value of the dynamic part of the irradiance. To illustrate the increase, some graphs showing the average irradiance levels are displayed in Figures 3.47 through 3.62.

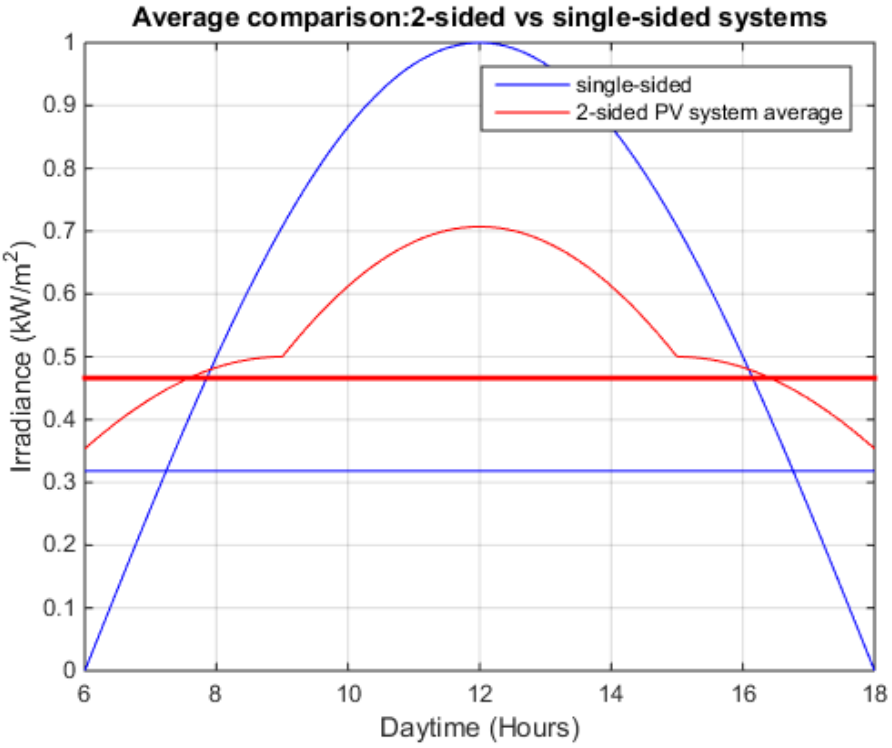

Figure 3. 47: Double-sided OSM vs single-sided average comparison

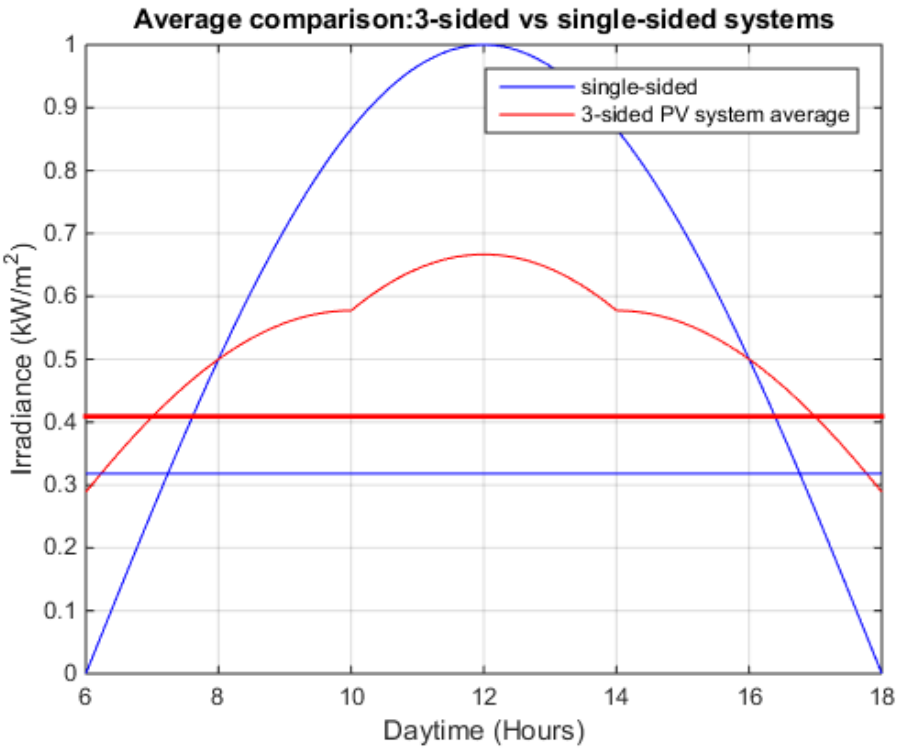

Figure 3. 48: Three-sided OSM vs single-sided average comparison

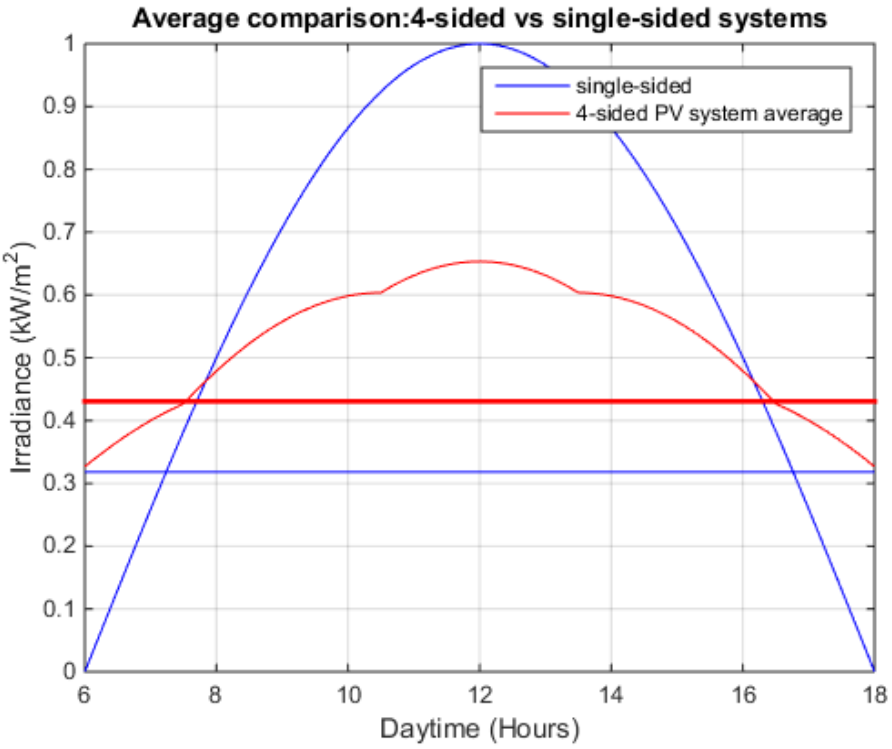

Figure 3. 49: Four-sided OSM vs single-sided average comparison

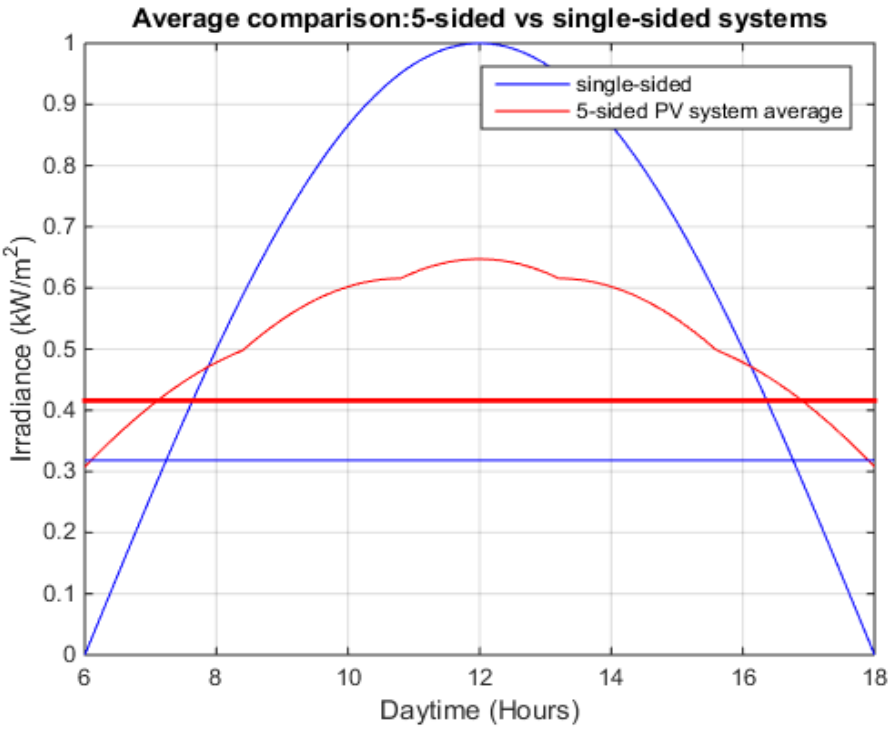

Figure 3. 50: Five-sided OSM vs single-sided average comparison

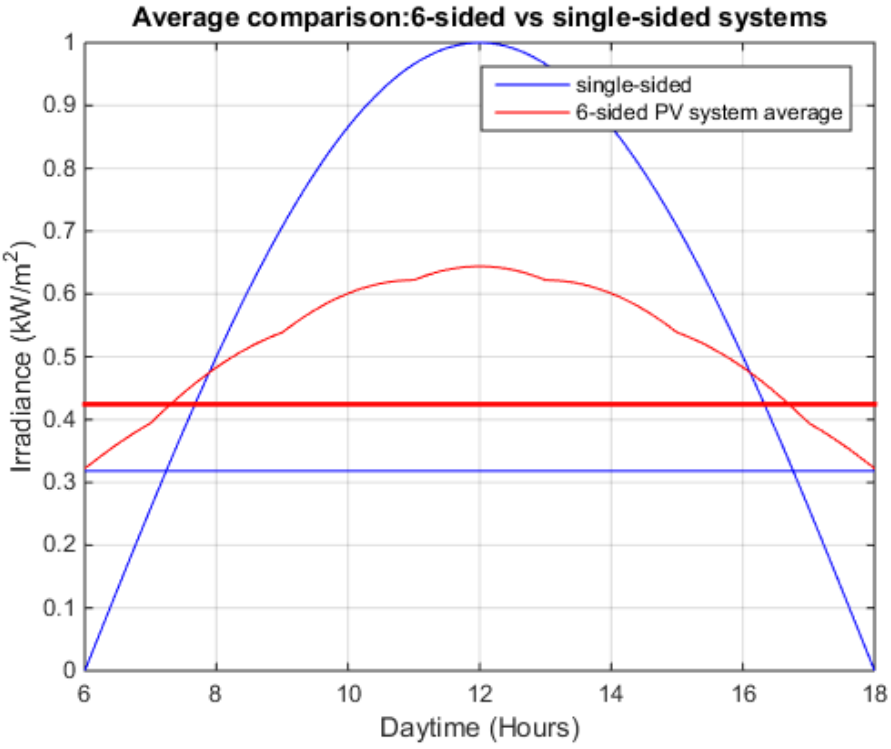

Figure 3. 51: Six-sided OSM vs single-sided average comparison

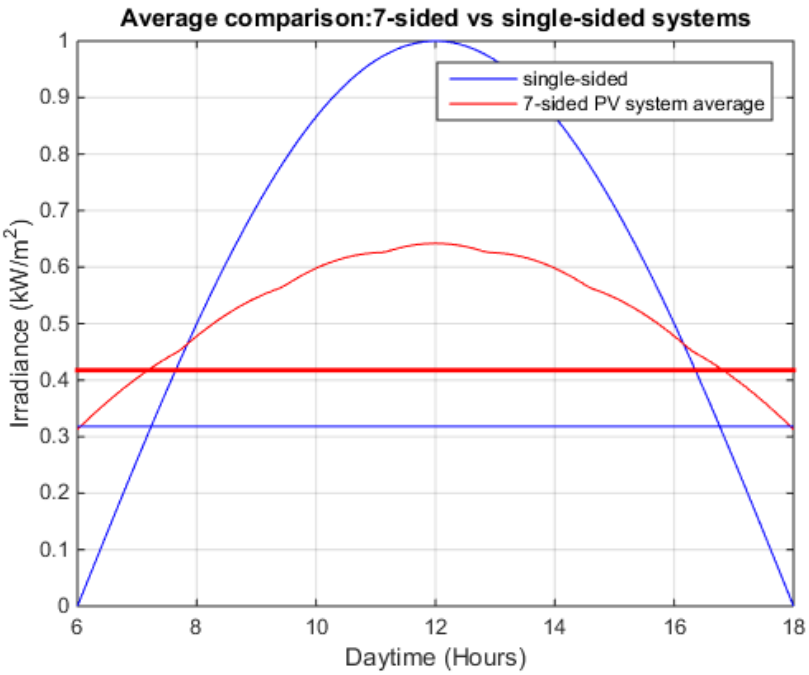

Figure 3. 52:Seven-sided OSM vs single-sided average comparison

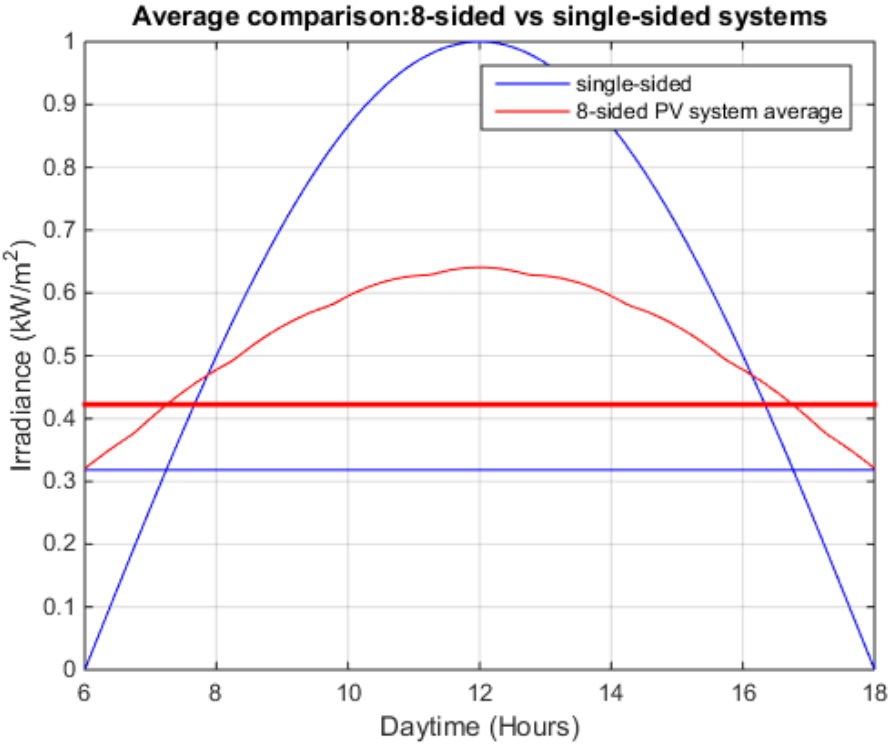

Figure 3. 53: Eight-sided OSM vs single-sided average comparison

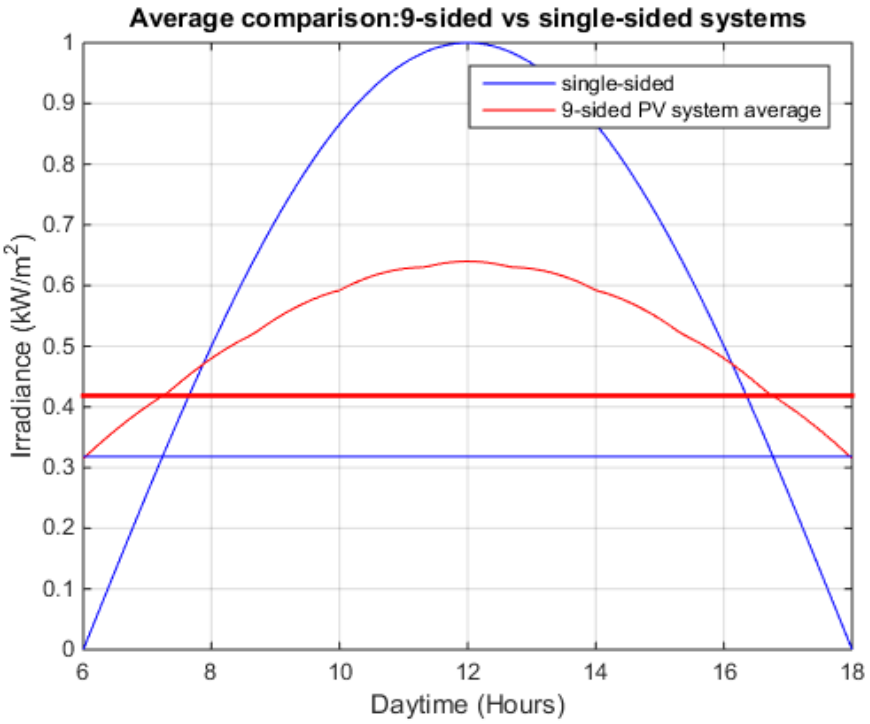

Figure 3. 54: Nine-sided OSM vs single-sided average comparison

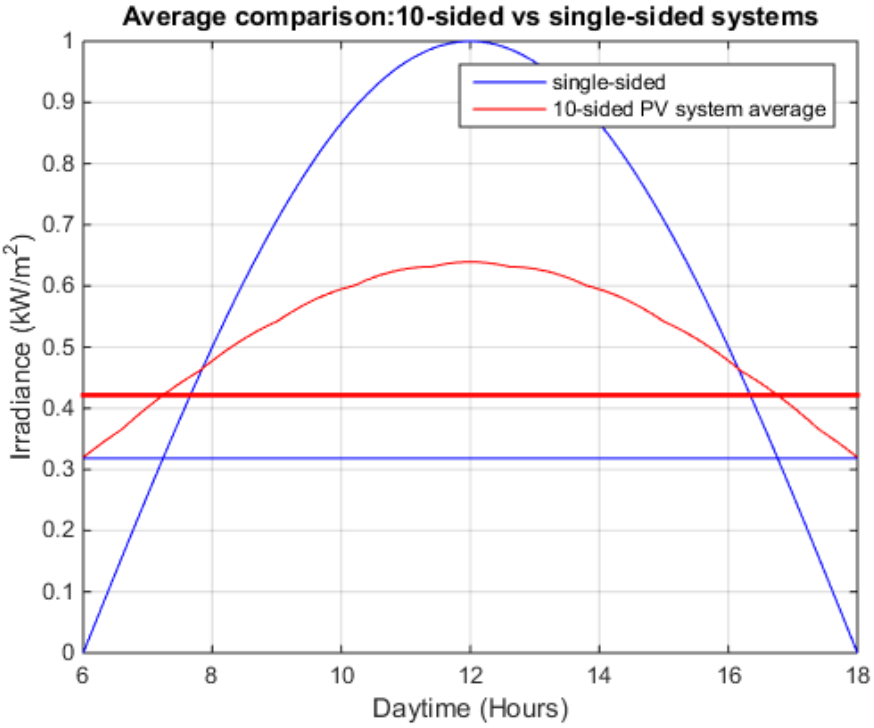

Figure 3. 55: Ten-sided OSM vs single-sided average comparison

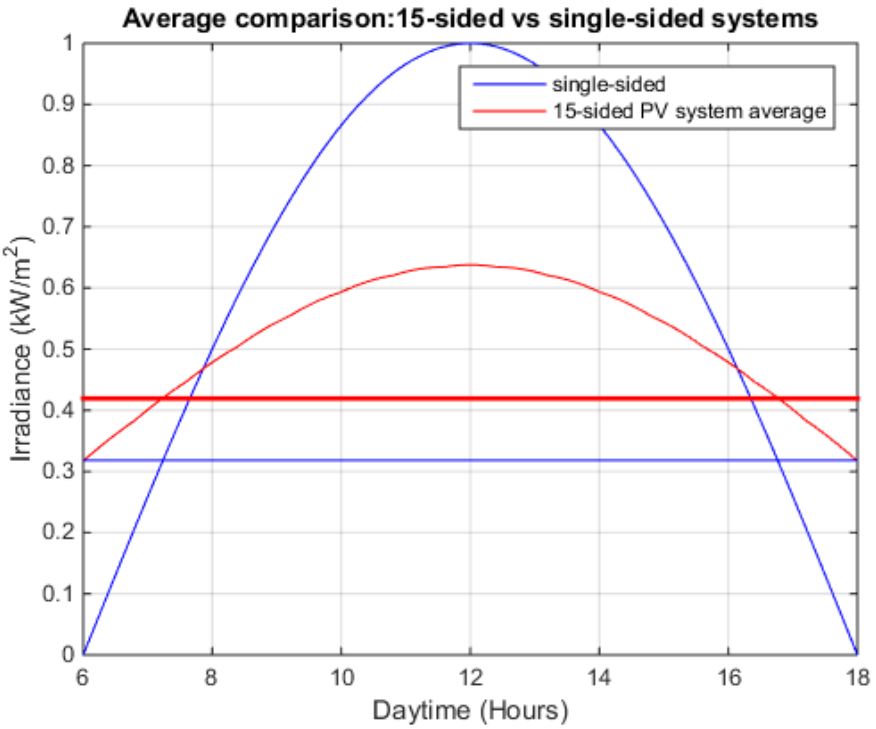

Figure 3. 56: Fifteen-sided OSM vs single-sided average comparison

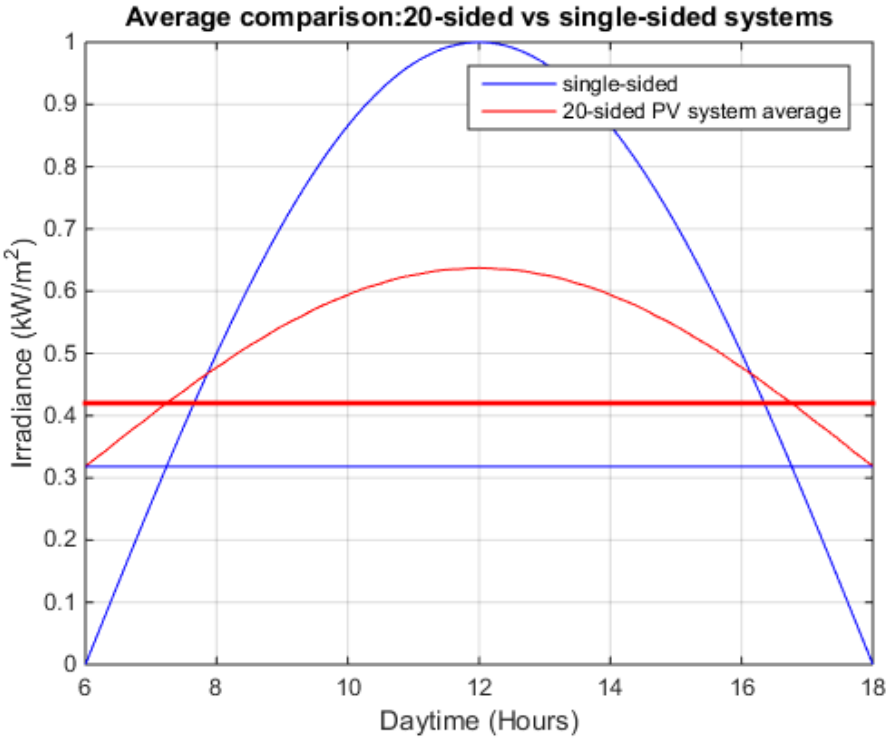

Figure 3. 57: Twenty-sided OSM vs single-sided average comparison

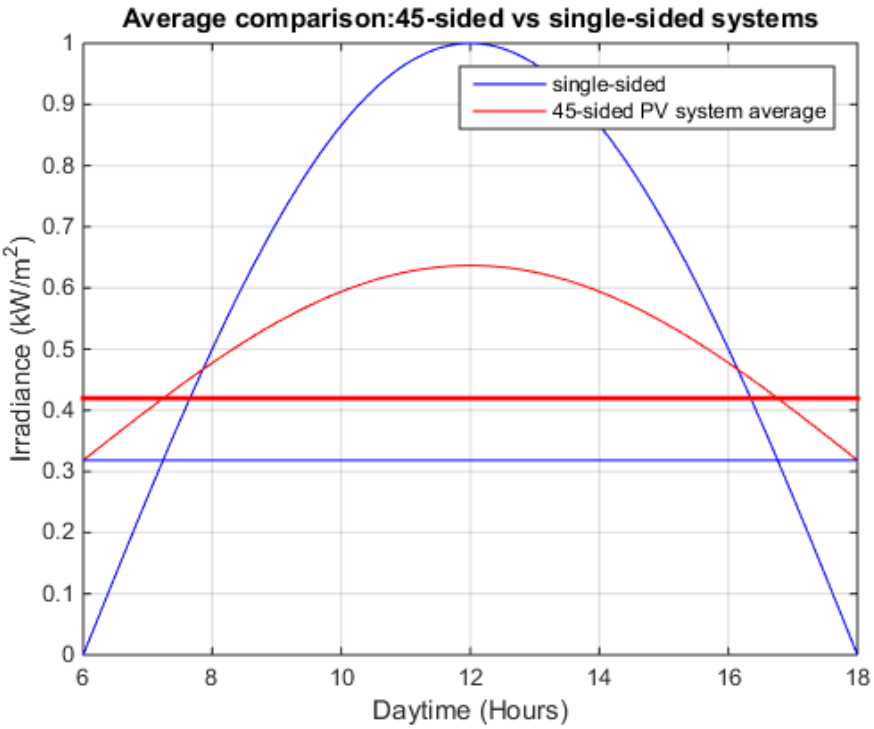

Figure 3. 58: Forty-five-sided OSM vs single-sided average comparison

3.5.2. Deviation

Deviation is an important parameter as it provides the information about the behaviour of the irradiance dynamics with respect to the mean value. PV system with a low deviation from the average value is the most desired since its irradiance dynamics will be close to the mean value; which is an advantage in the overall PV system supply as it requires little as regards power regulation process. Against 0.32 for the fixed-tilt panel, the highest deviation is 0.11 for the double-sided system whereas 0.099 deviation is the highest and remains same for systems with fifteen sides and more.

3.5.3. Irradiance collecting ratio

The irradiance capturing ratio is identified as a paramount indicator as well when it comes to evaluating the systems under study since it reflects PV systems' capacity of making use of the available irradiance. It is defined as the ratio of the irradiance collected by a multisided PV system over the irradiance gathered by a fixed-tilt solar panel of the same size and rating.

3.6. Results

The evaluation parameters of systematically selected OSM PV systems are synthetized gathered in Table 3.1. The peak and minimum values of the irradiance

give an indication on the irradiance extreme amplitudes whereas the deviation provides an insight on the system consistency in terms of collecting the available irradiance. Bar charts for described were then sketched so as to establish a comparison between different systems (Figures 3.50-3.54). Importantly, a ratio for irradiance collection was computed in the same Table.

Table 3. 1: Results Table

OSM Type	Average (kW/m^2)	Maximum (kW/m^2)	Minimum (kW/m^2)	Deviation (kW/m^2)	Ratio
One	0,3183	1,0000	0,0000	0,3132	1,0000
Two	0,4549	0,7071	0,3536	0,1091	1,4643
Three	0,3900	0,6667	0,2887	0,1069	1,2349
Four	0,4280	0,6533	0,3266	0,1021	1,3528
Five	0,4091	0,6472	0,3078	0,1018	1,3063
Six	0,4233	0,6440	0,3220	0,1008	1,3335
Seven	0,4143	0,6420	0,3129	0,1007	1,3122
Eight	0,4217	0,6407	0,3204	0,1003	1,3268
Nine	0,4164	0,6399	0,3151	0,1003	1,3146
Ten	0,4209	0,6393	0,3196	0,1001	1,3237
Fifteen	0,4185	0,6378	0,3171	0,0999	1,317
Twenty	0,4200	0,6373	0,3186	0,0998	1,3197
Forty-five	0,4195	0,6367	0,3186	0,0997	1,3182
Fifty	0,4197	0,6367	0,3184	0,0997	1,3185
Hundred	0,4196	0,6366	0,3183	0,0997	1,3184

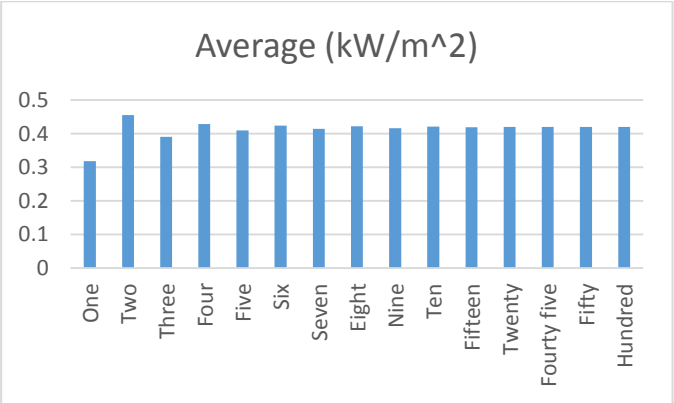

Figure 3. 59*:* Average values comparison

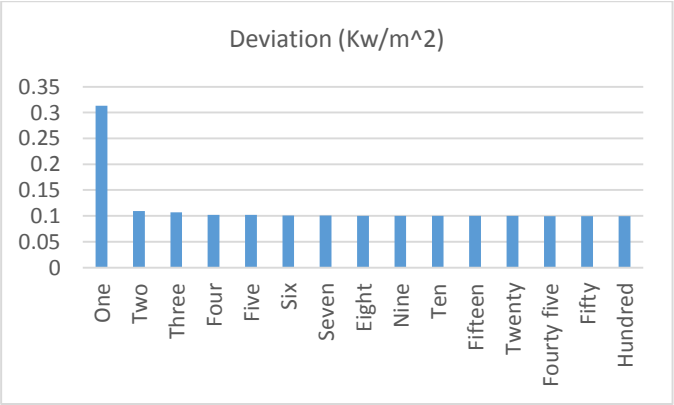

Figure 3. 60*:* comparison of deviation from the mean value

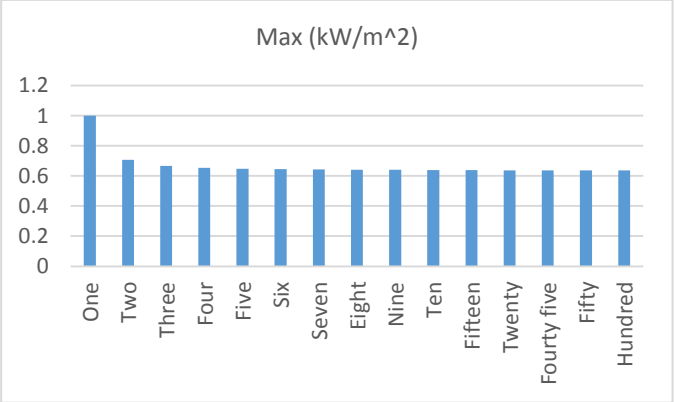

Figure 3. 61: Maximum values comparison

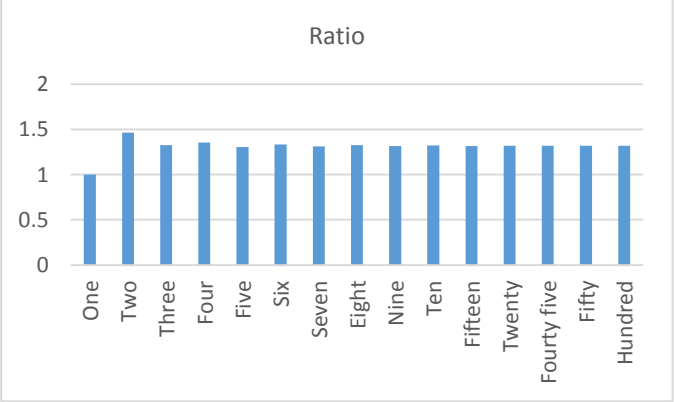

Figure 3. 62*:* OSM systems irradiance collection ratios

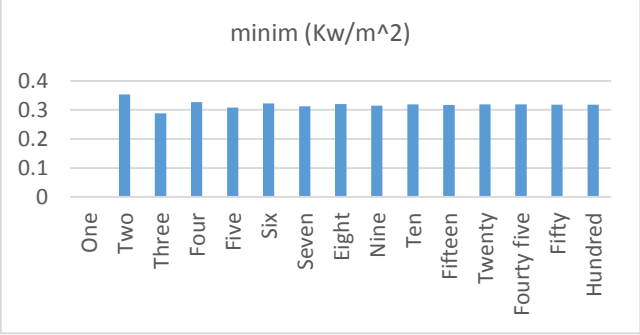

Figure 3. 63*:* Comparison of irradiance minimum values

3.7. Discussion of the Results

From the record in Table 3.1, the average level of the collected irradiance is found to be 0.4196 kW/m^2 for systems with 100 or more sides, the minimum level at 0.3182 Kw/m^2 and the maximum level at 0.6396 Kw/m^2. It can be observed that the maximum level observable at noon is double the minimum level occurring at sunrise and sunset. The question should be to know the reason why it is so. Firstly, looking at the OSM structure and the sunlight-receiving area, it can be observed that the area at sunrise and sunset is half the area at noon (Figures 3.55 and 3.56).

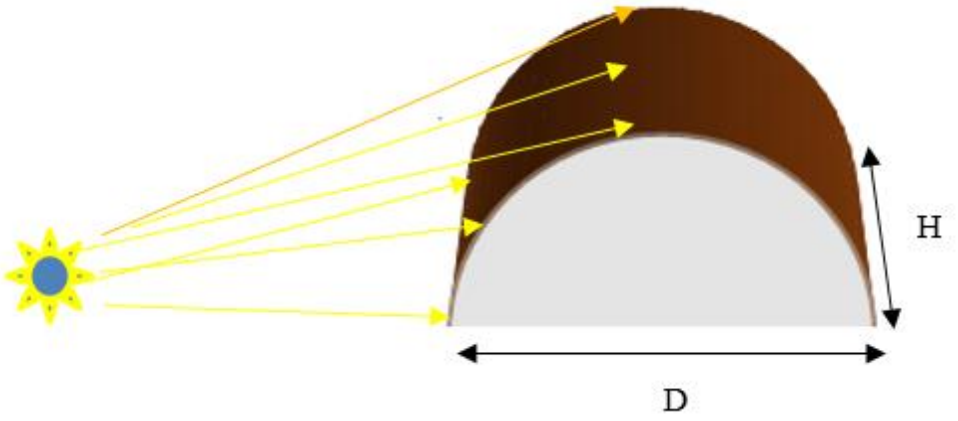

Figure 3. 64: Sunlight distribution at sunrise

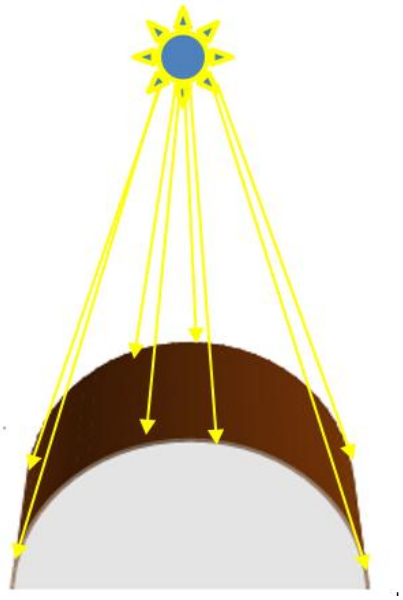

Figure 3. 65*:* Sunlight irradiance distribution at noon

In other words, the question should be to unfold the puzzle about the level figures and mathematics are used for the purpose. The PV system area is kept equal to 1 m^2 (1 m

x 1 m) same as the area of a flat panel for system-power-collection comparison. Thus, for the area of a hollowed half cylinder to be equal to that of a flat panel, the radius should be equal to 0.3183 m a circumference of 1m as per equation 3.7. The diameter should therefore be 0.6366 m (Figures 3.66 and 3.67).

$$r = \frac{1}{\pi} = 0.3183\,\mathrm{m} \qquad \textbf{Equation 3. 7}$$

Where *r* is the cylinder radius.

In terms of the area available for the sunlight at sunrise and sunset is 0.5 m^2 against 1 m^2 area for noon time. But, that area is only apparent given the curvature of the external surface of the PV system half-cylinder. In reality, the sunlight is received by an area equivalent to 0.3183 m^2 (0.3183 m x 1 m) at sunrises and sunsets. In other words, with 1 m^2-area, the power is reduced. At midday, the actual area exposed to the sun is 0.6366 m^2 (0.6366 m x 1 m), which gives the power of 0.3183 W and 0.6366 W at sunrise (sunset) and midday respectively.

This can also be mathematically corroborated through integral calculus. The power harvested by a solar panel is dependent on the incident angle of the sunlight angle on the panel as per equation 3.8 (Kamanzi & Kahn, 2015):

$$P = G_M * A\sin\theta \qquad \textbf{Equation 3. 8}$$

So, the sunlight power received by an infinitesimal portion of the half-cylindered OSM PV systems should be given by equation 3.9 and 3.10.

$$dP = G_M * dA\sin\theta d\theta \qquad \textbf{Equation 3. 9}$$

$$dA = H * r\sin\theta d\theta \qquad \textbf{Equation 3.10}$$

Where H is the height of the half-cylinder PV structure.

The boundary intervals of area exposure in terms of angles are 0 and $\frac{\pi}{2}$ at sunset, 0 and π at noon. Therefore, the power collected in the morning can be determined (Equation 3.11):

$$P_s = \int_0^{\pi/2} G_M * H * r\sin\theta d\theta\,[\mathrm{kW}] \qquad \textbf{Equation 3. 11}$$

Replacing $G_{M,}$ *H* and *r* by their values, we get:

$$P_s = 1*0.3183*1*\left[-\cos\theta\right]_0^{\pi/2}\,[\mathrm{kW}]$$

$$\therefore P_s = 0.3183\,\mathrm{kW}$$

Similarly, the power at noon will be found to be:

$$\therefore P_s = 0.6366\,\text{kW}$$

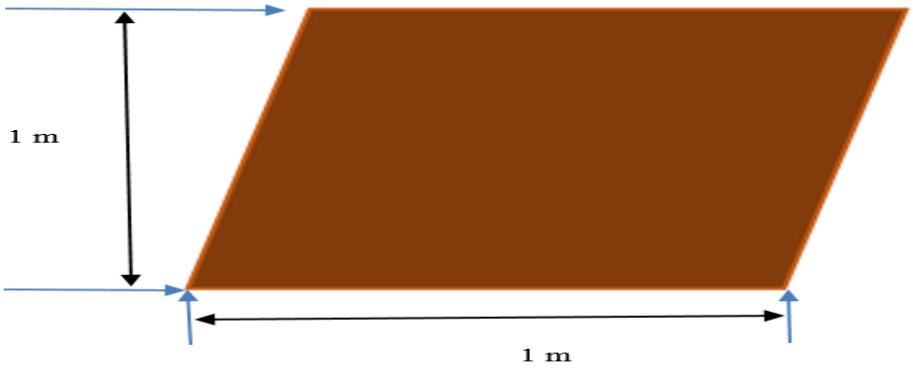

Figure 3. 66: Dimensions of Flat panel's dimensions

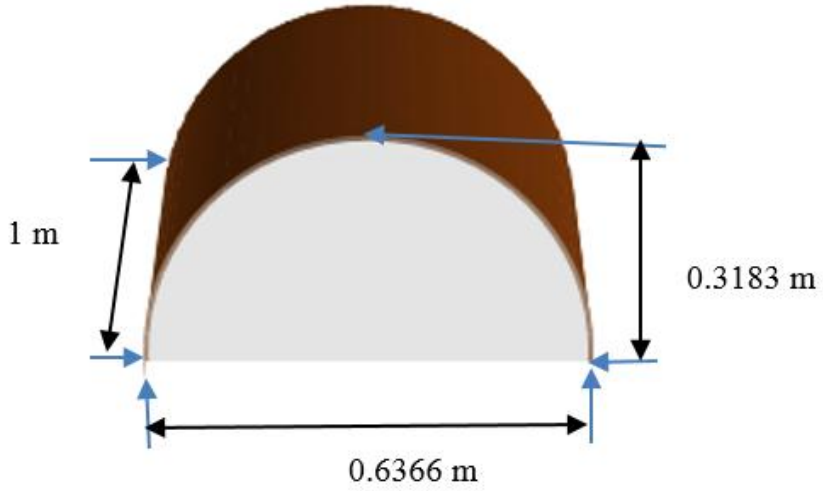

Figure 3. 67: Dimensions of 1 m^2-half-cylinder-structured PV system

Regarding the irradiance collection ratio, a consistent ratio of 1.32 is observed; and this is an indication that the OSM PV systems provide a boost of 32 % over flat and fixed-tilt solar panels under the same operating conditions. It is also noteworthy to notice that 32 % is a good increase in comparison with electronic-based sun-tracking systems. The proposed model exhibits a much even irradiance distribution, with the lowest and highest levels of 32 % and 64 % against 0 and 100 % of flat panels. Having half of the OSM PV system around sunrise and sunset is better than having the whole PV module at shade as it is the case for the fixed-tilt approach. Besides,

the OSM models offer reliability from the technical point of view since they involve no moving parts and thus require less in terms of maintenance.

Regarding applications, OSM PV systems are easy to implement especially given the general overview of building roof structures having sides in various directions with respect to the sun's movement. OSM PV models are therefore to be viewed as a novel, simple and cost-effective technology regarding optimizing the irradiance collection of solar panels for home and commercial power production. Their design and production is expected to be simple as it will consist of modifying the existing design of flat PV modules. OSM will not involve extra expertise to developed.

CHAPTER FOUR

CLOSED-STRUCTURE MULTISIDED PV SYSTEMS

4.1. Introduction

Chapter four explores addressing the problem of uneven distribution of sunlight collection using CSM PV systems. On a daily basis, the irradiance changes from zero in the morning, to peak at midday and comes back to zero in the evening. The CSM were therefore suggested as a solution. The same protocol as in chapter three was followed in terms of developing mathematical and structural models and results presentation. Graphical and tabulated results were obtained from a coded mathematical model and CSM PV models proved to keep the collected sunlight at a consistent level worth the average value of sunlight collected by a flat-fixed panel.

4.2. Background

Further to the global move to renewable energy (Bisseker, 2015), PV systems have gained popularity given their ability to comply with both economic and environmental needs. They are thus, deemed to lead the renewable energy sector by year 2030 (Photovoltaics, 2014) given investments and research uptakes focussed at PVs (Carter-brown et al., 2015; Wasiak & Hanzelka, 2010). In building power supply, PVs operate together with storage batteries and power regulators before the power is supplied to end-use by load (Jingcheng, 2010). However, with techniques being used, one can collect an unevenly distributed irradiance, even with the implementation of deservedly trusted automatic-controlled PV systems that track the sun (Bazyari et al., 2014) and this restrains batteries to short lifespans. Backup batteries that normally operate within a defined range have their effectiveness affected by long time charge-discharge cycles and the ideal should be to find a system that can ensure evenly distributed power when the sun is on.

In space engineering, spacecraft should be primarily supplied with a relatively regulated power for the sake of limiting the complexity, reliance on backup batteries and thus of lunch costs calculated per mass. As for batteries, it has been established that deep discharges and overcharges are the main sources of short battery's lifespan and this can result in short space missions (Ovchinnikov et al., n.d.). Consequently, for instance, costly NiH_2-based batteries with depth of discharge (DoD) ranging between 40 % and 60 % are to be deployed in a spacecraft built for long lifetime missions (a year and more). On the contrary, NiCd batteries are found suitable to short lifetime missions as a result of their low DoD (10 %-20 %) and of their short lifespan.

The OSM PV systems another chapter part of the current study, though providing a good average power output, they still lack the quality of supplying constant dc power

that would grant less fluctuations in battery charge-discharge cycles and the long lifespan for the electronics involved in power regulation.

4.3. Methodology

The CSM PV systems were thought of as a reliable solution since they can ensure the uniformly distributed irradiance over daytimes. The idea of using them in this research context was inspired from a work related to the study of PV system multisided topologies (Kamanzi & Kahn, 2015). The model of topologies was adapted to CSM systems, extensively modelled and explored to suit solar energy-based supply on rooftops for home, industry and spacecraft applications.

4.1.1. CSM PV system models

CSM PV systems were conceived in regular-shaped structures, in the form of prism precisely. So, the number of sides of a PV system is determined by the prism base. Isosceles, cubic, polygonal prisms and cylinder responded well to the CSM PV systems description. Some samples are shown in Figures 4.1-4.3.

Figure 4. 1:Illustration of a six-sided CSM PV system

Figure 4. 2: Illustration of a three-sided CSM PV system

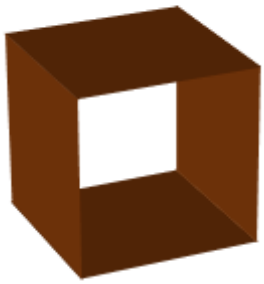

Figure 4. 3: Illustration of a four-sided CSM PV system

The CSM systems' performances were measured against the one for a fixed-tilt solar panel of the same surface area and type. This implies that for a CSM with *n* sides, each side' s area is *n* times smaller than the area of a single fixed tilted solar panel considered as a reference.

In the process of model development, assumptions were also outlined for the purpose of proper and accurate assessment of the functioning of these particular topologies. From sunrise and sunset, the sun's apparent movement plan is perpendicular to the CSM's plan which receives irradiance along the day. The nominal irradiance released by the sun is 1 kW/m^2 and the PV systems' area is 1 m^2, same as for the reference flat and fixed-tilt panel.

4.4. CSM PV profiles

The profiles for CSM PV systems were based on the aforesaid PV topologies' model and the algorithm towards their establishment was developed as to cover a larger number of multisided PV systems than in the study of topologies; thus increasing the expectation of reliable results. The governing mathematical model was established as per equations 4.1 and 4.2.

$$G = G_M \sum_{i=1}^{n} \frac{1}{n} \left(\sin(\omega t - i\varphi)\right) \qquad \textbf{Equation 4. 1}$$

$$\varphi = \frac{2\pi}{n} \qquad \textbf{Equation 4. 2}$$

$$i \in [1, n]$$

Where G is the irradiance, n is the number of sides, G_M is the nominal irradiance and φ is the phase angle between two consecutive sides. The profiles of strategically selected CSM PV systems are displayed in Figures 4.4-4.17. The

Figures are zoomed in so as to ensure an accurate view of the irradiance function levels and dynamics.

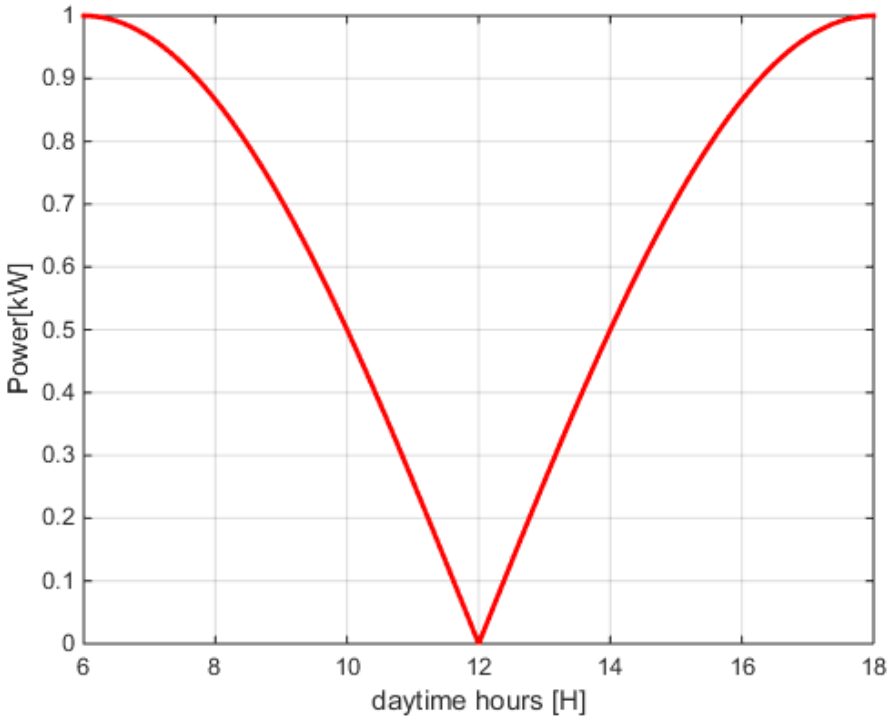

Figure 4. 4: Irradiance dynamics for a double-sided CSM

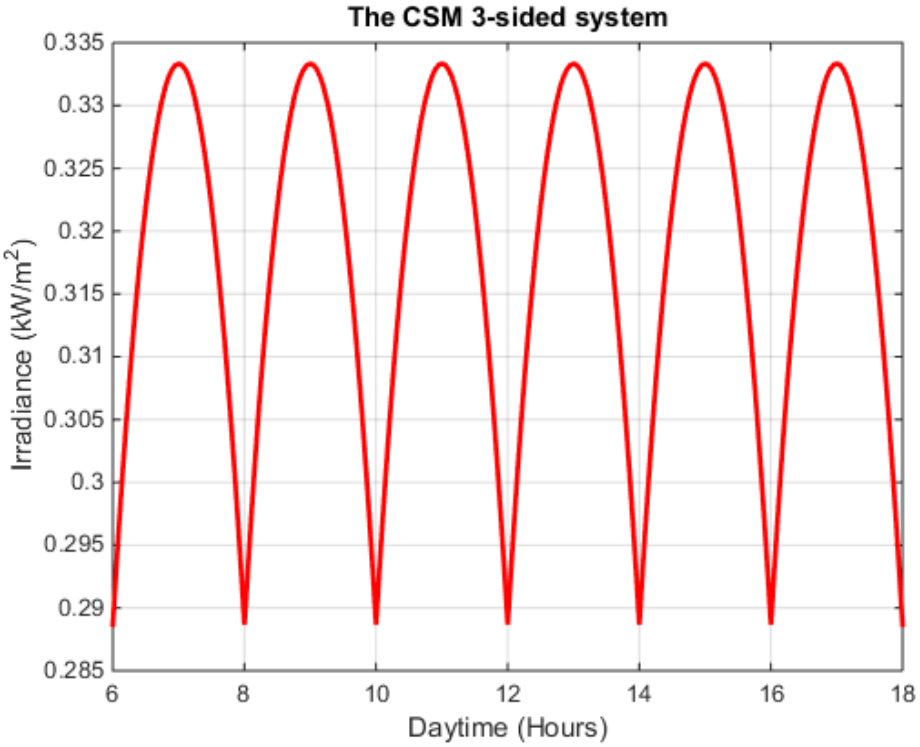

Figure 4. 5: Irradiance dynamics for a three-sided CSM

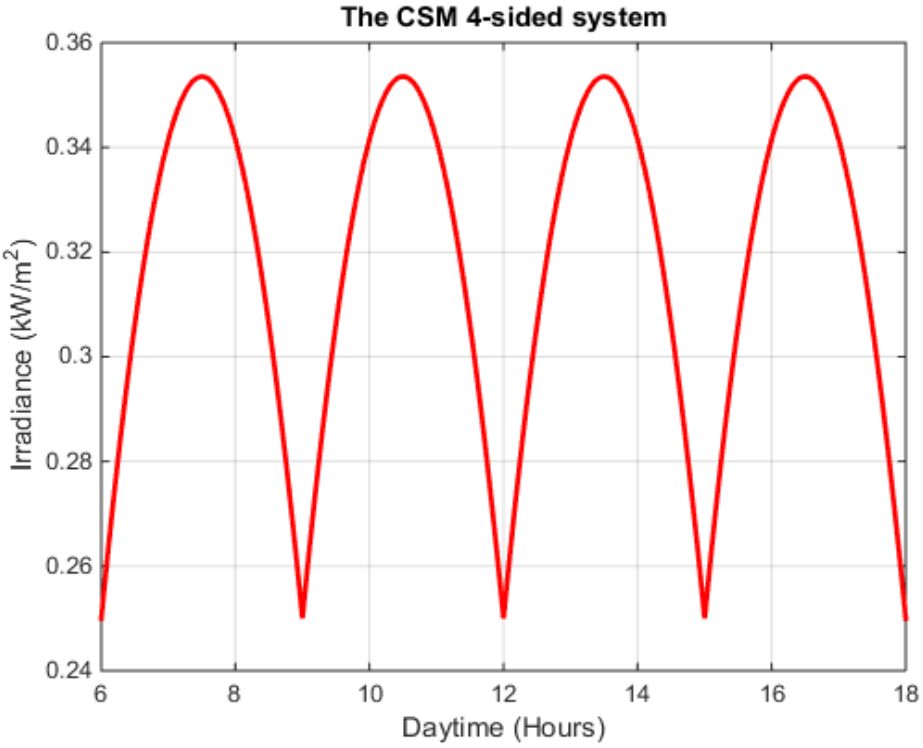

Figure 4. 6: Irradiance dynamics for a four-sided CSM

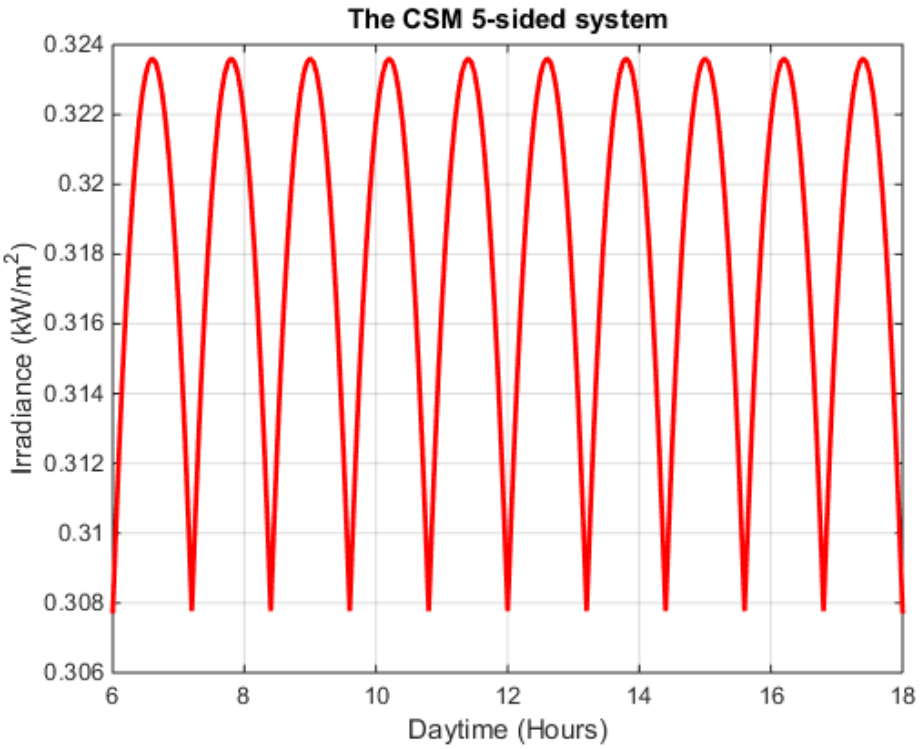

Figure 4. 7: Irradiance profile for a five-sided CSM

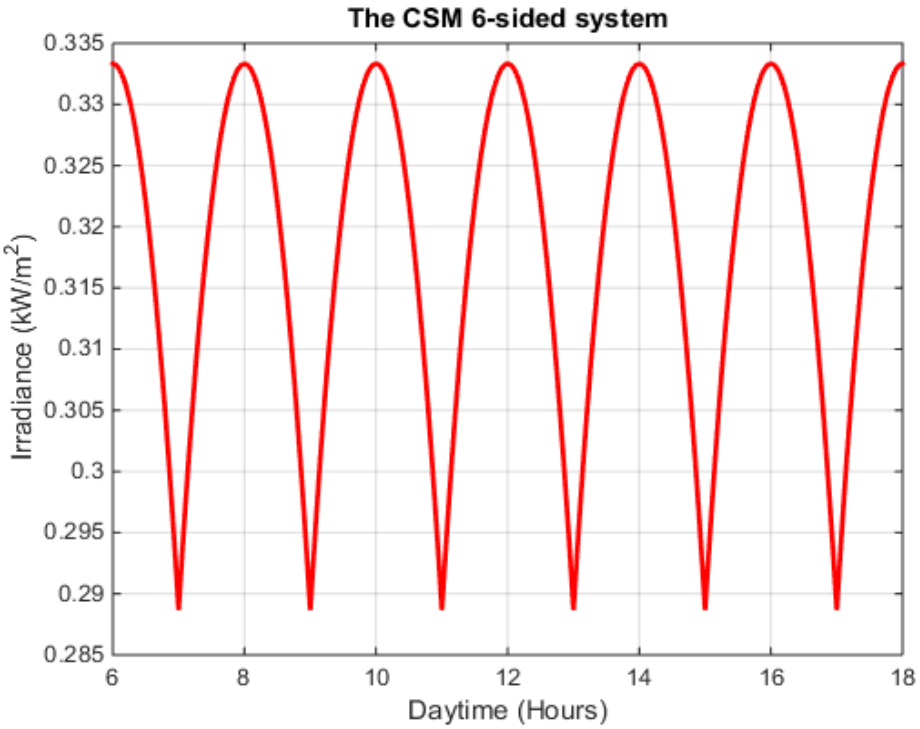

Figure 4. 8: Irradiance profile for a six-sided CSM

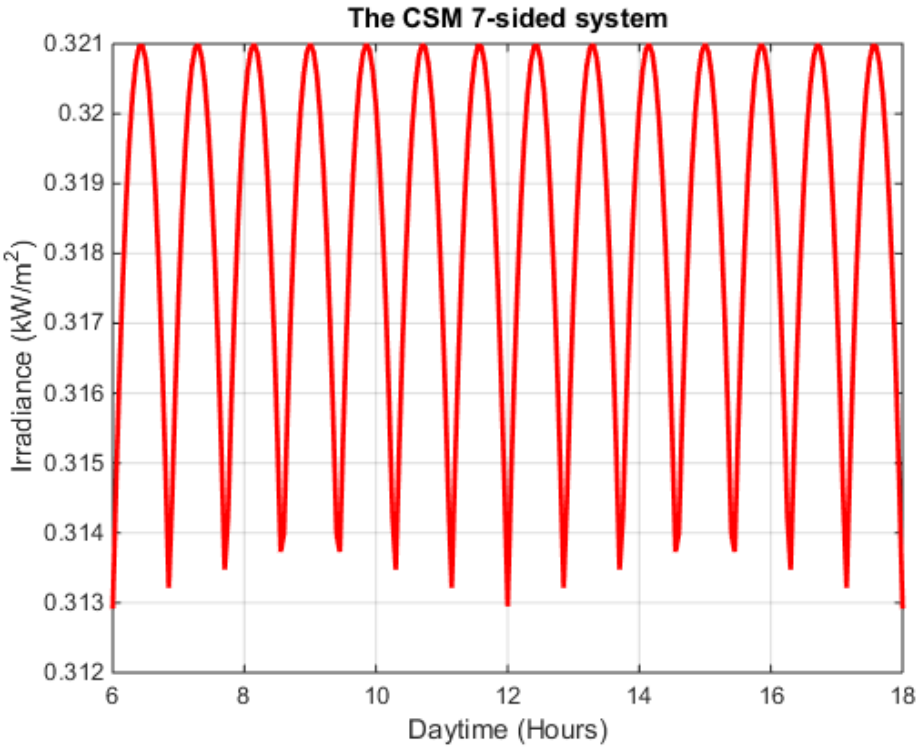

Figure 4. 9: Irradiance profile for a seven-sided CSM

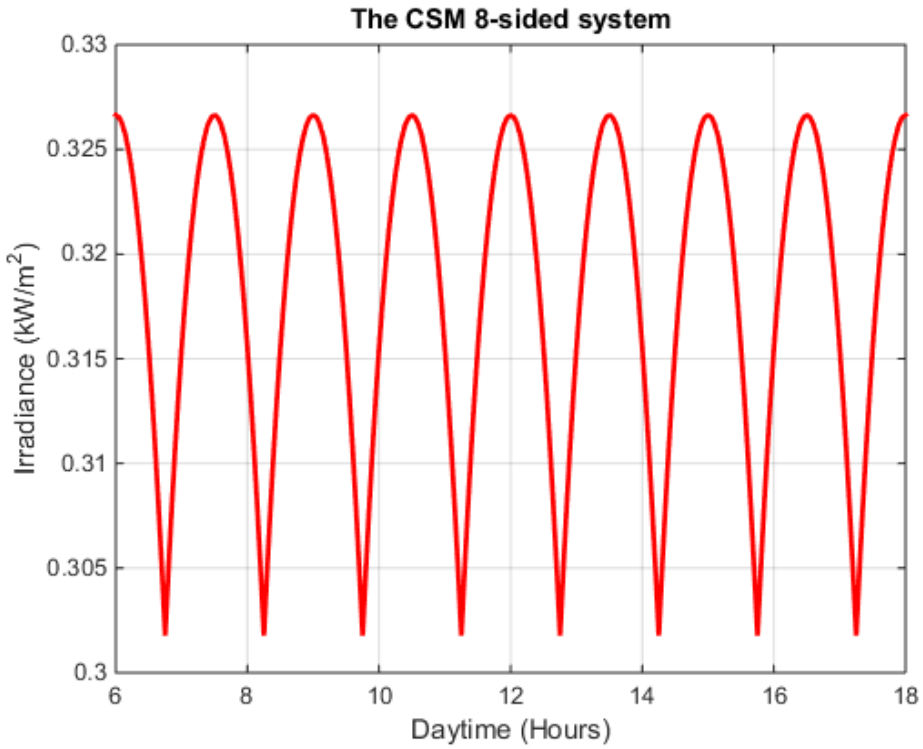

Figure 4. 10: Irradiance profile for an eight-sided CSM

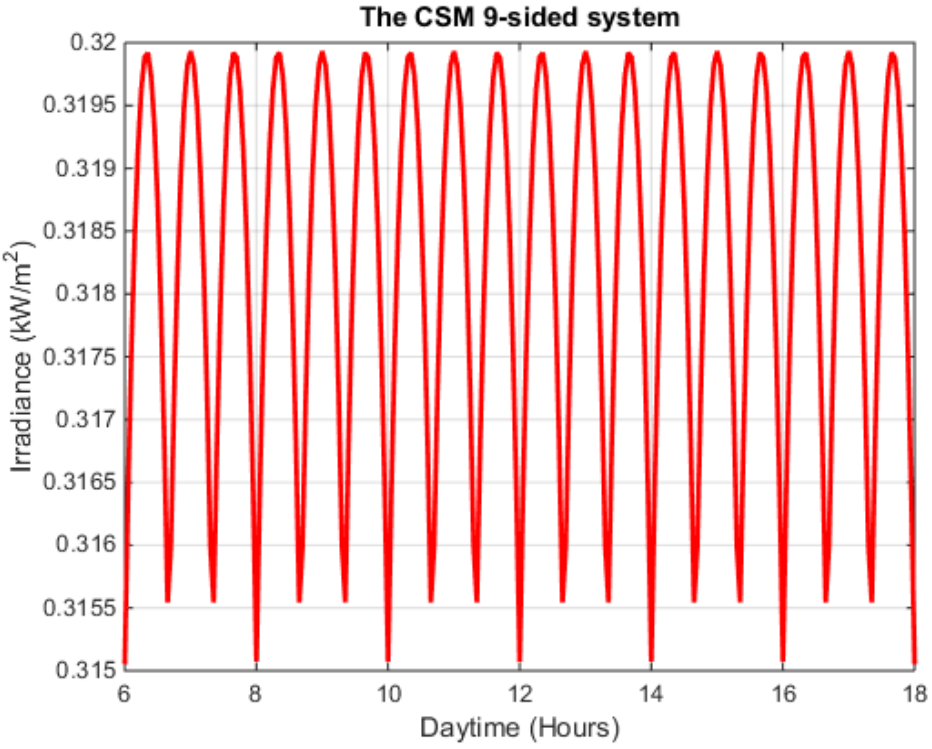

Figure 4. 11: Irradiance profile for a nine-sided CSM

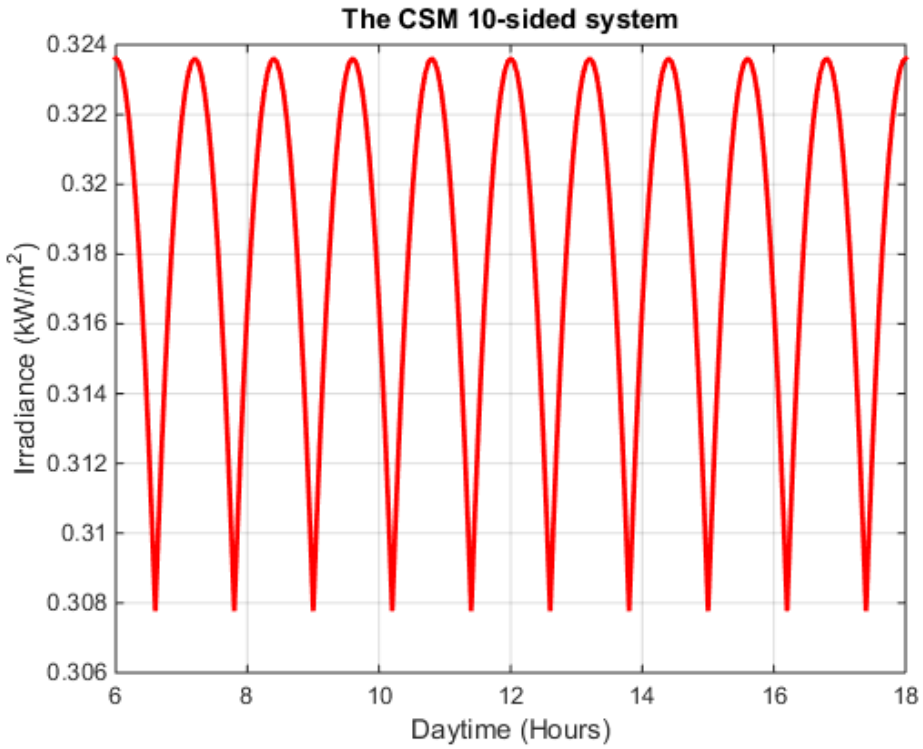

Figure 4. 12: Irradiance profile for a ten-sided CSM

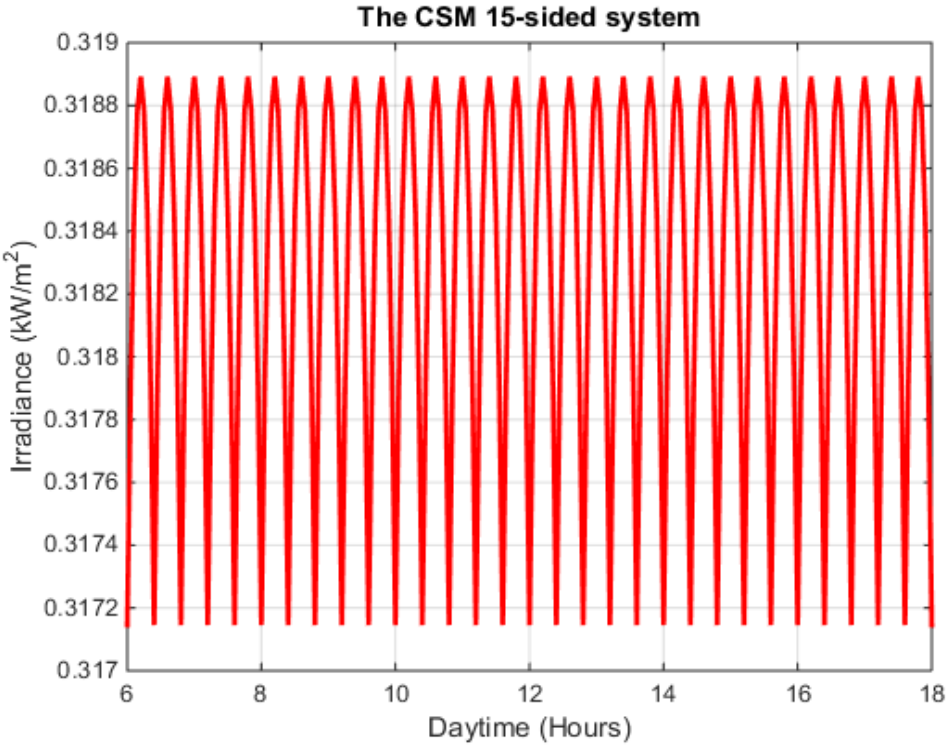

Figure 4. 13: Irradiance profile for a fifteen-sided CSM

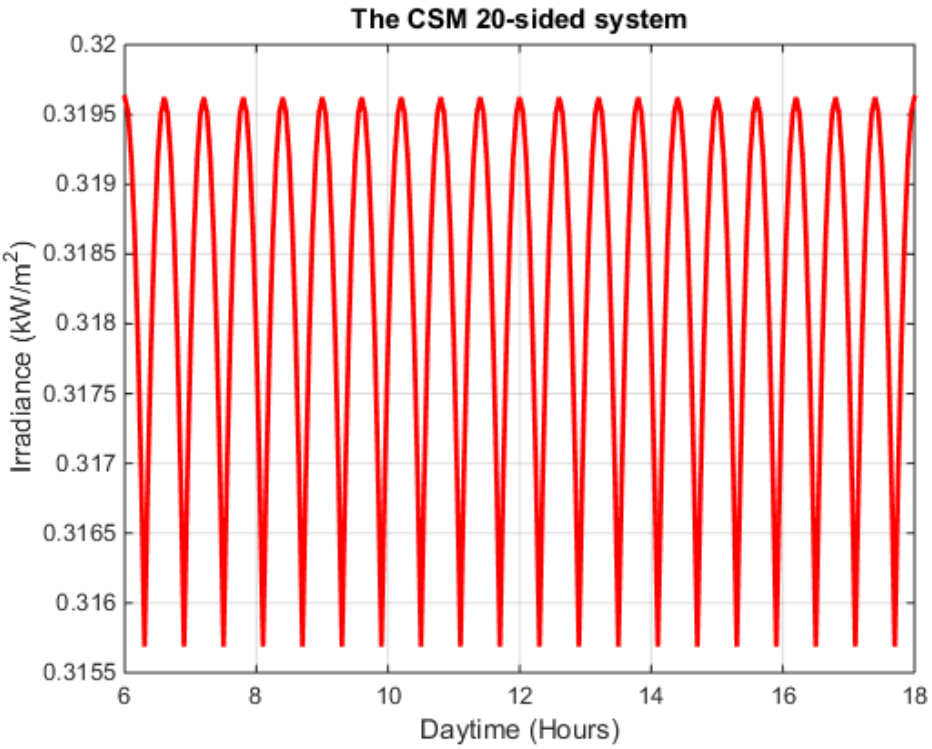

Figure 4. 14: Irradiance profile for a twenty-sided CSM

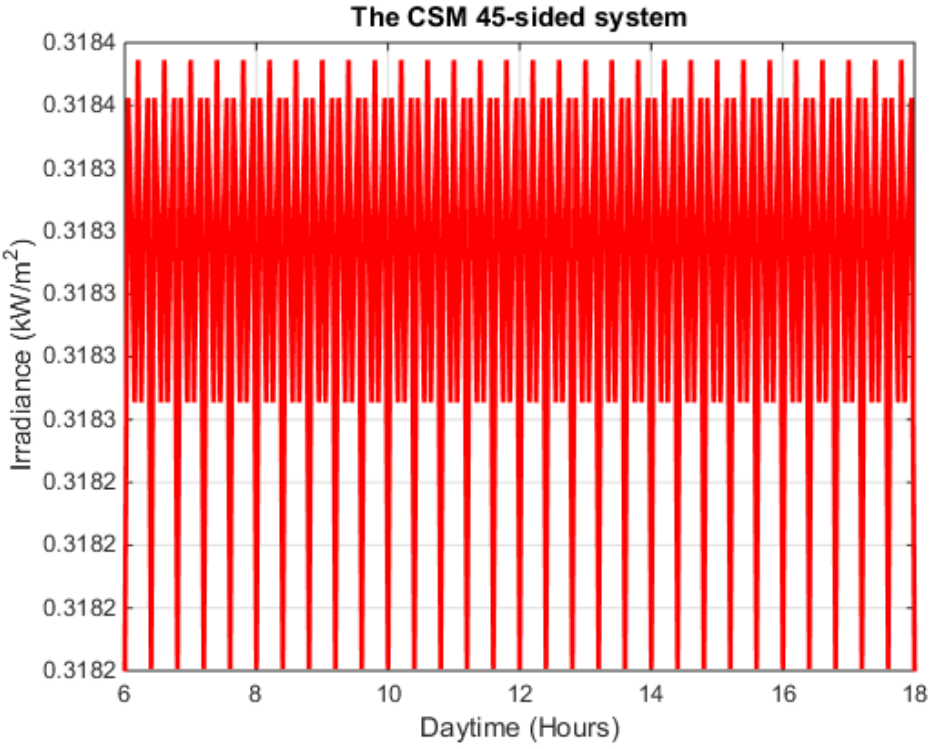

Figure 4. 15: Irradiance profile for a forty-five CSM

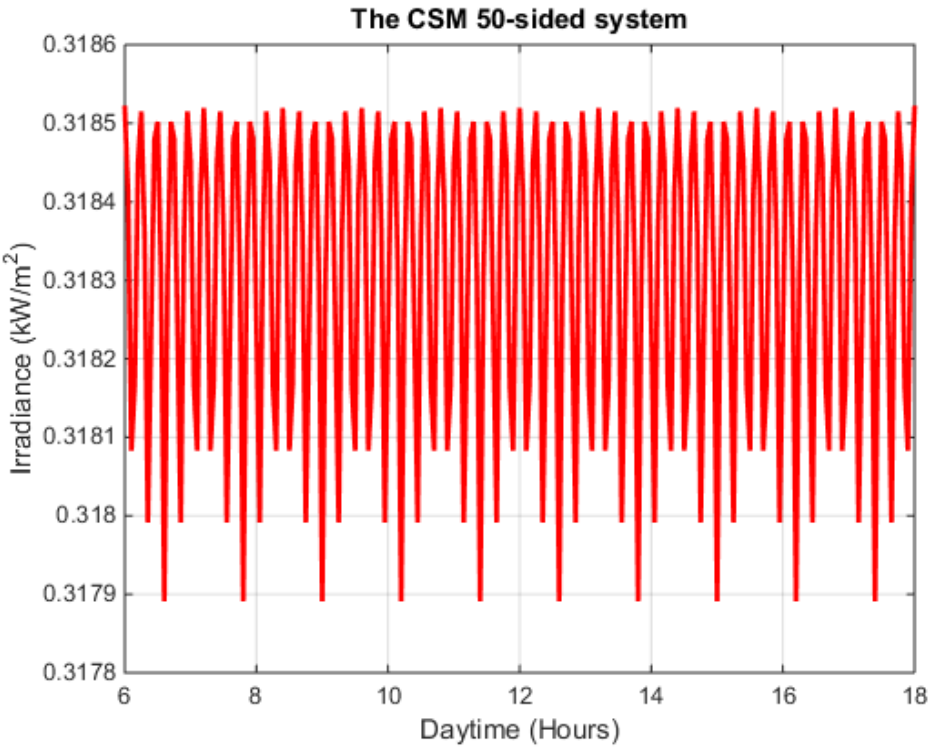

Figure 4. 16: Irradiance profile for a fifty-sided CSM

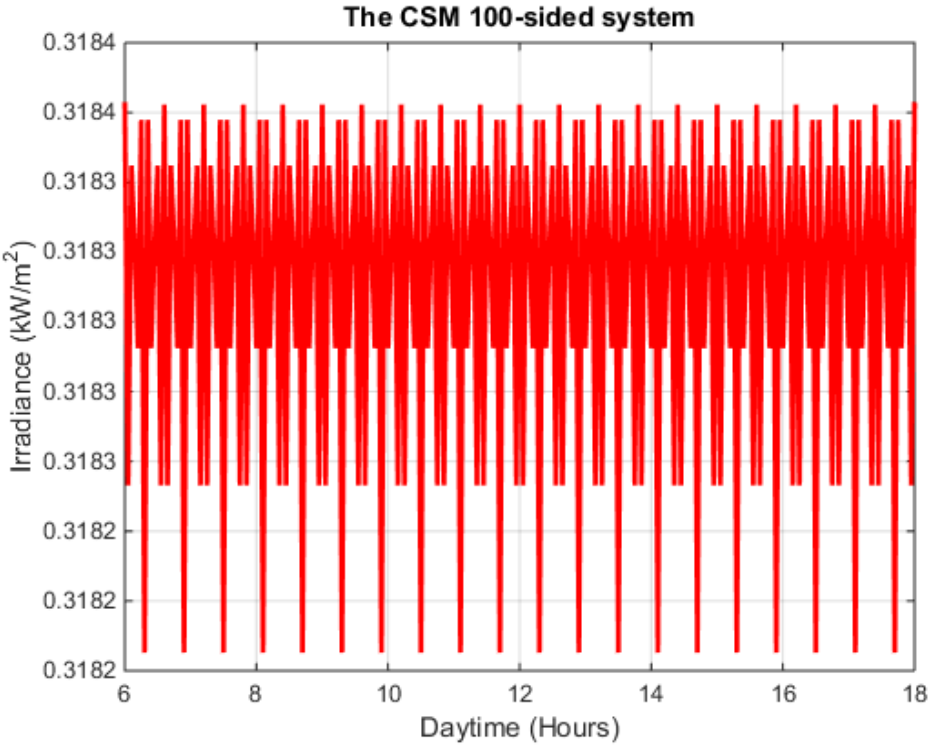

Figure 4. 17: Irradiance profile for a hundred-sided CSM

4.1.2. Side individual contributions

A close look into sides'individual contributions helps determine whether the model is behaving as expected. For instance, for a three-sided CSM PV system, the fundamental phase angle is 120^0. As such, side which will be fully exposed is meant to cover 6 hours. Looking at Figure 4.19, the curve in blue goes ON from 8:00 to 14:00. The phase angle in terms of daytime hours is equivalent to four hours. If 6 hours correspond to π, then 4 hours delay of the blue graph with respect to orange one, correspond to $2\pi/3$ and so is for higher order CSM individual contributions Figures 4.18- 4.31.

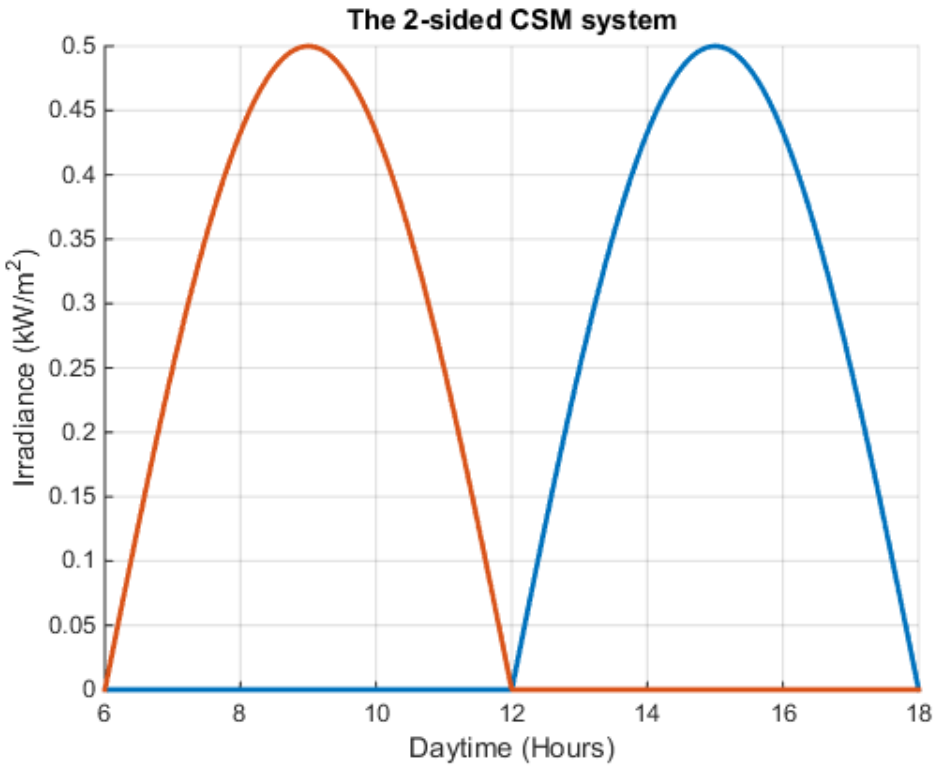

Figure 4. 18: Double-sided CSM individual contributions

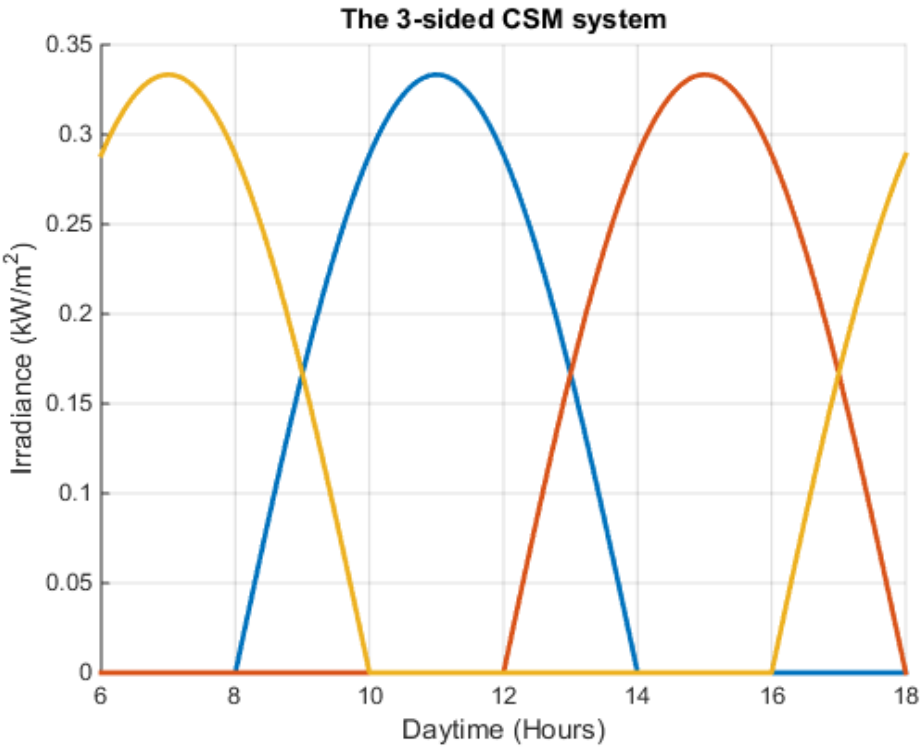

Figure 4. 19: Three-sided CSM individual contributions

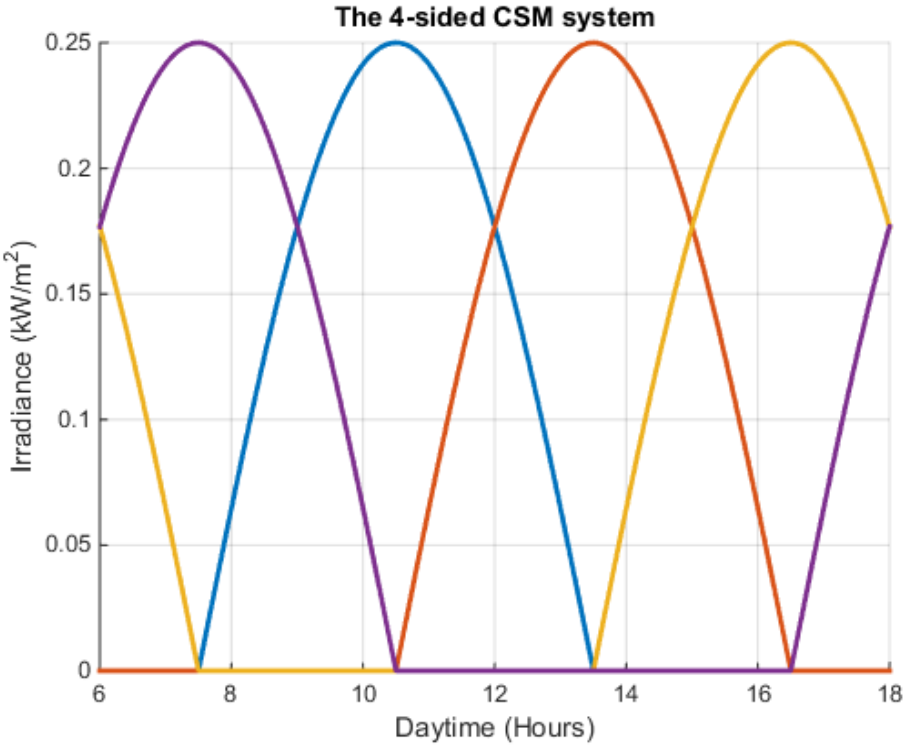

Figure 4. 20:Four-sided CSM individual contributions

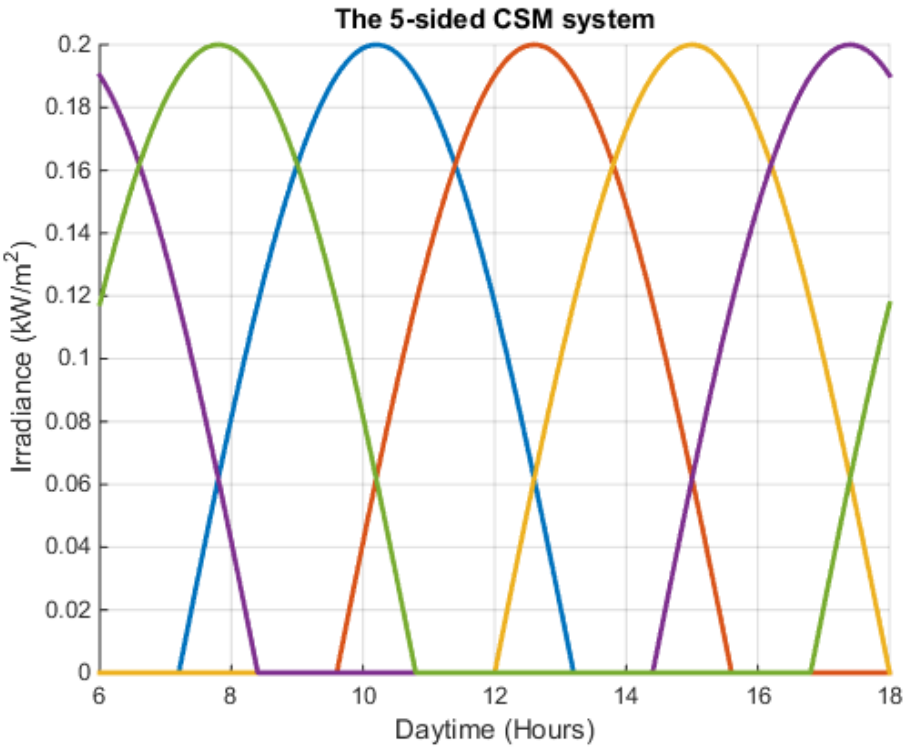

Figure 4. 21: Five-sided CSM individual contributions

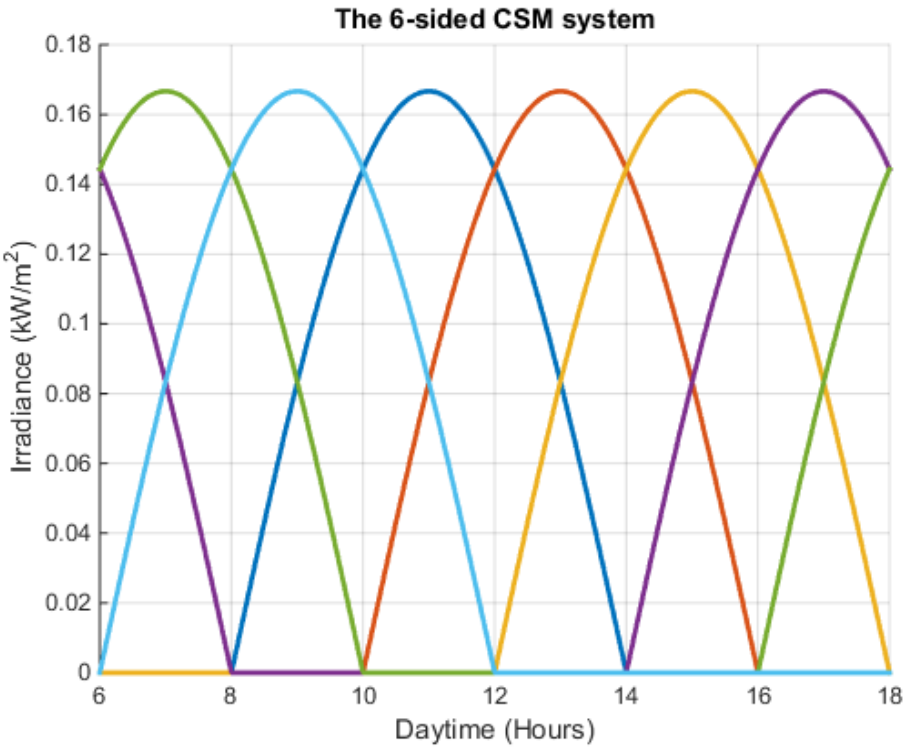

Figure 4. 22: Six-sided CSM individual contributions

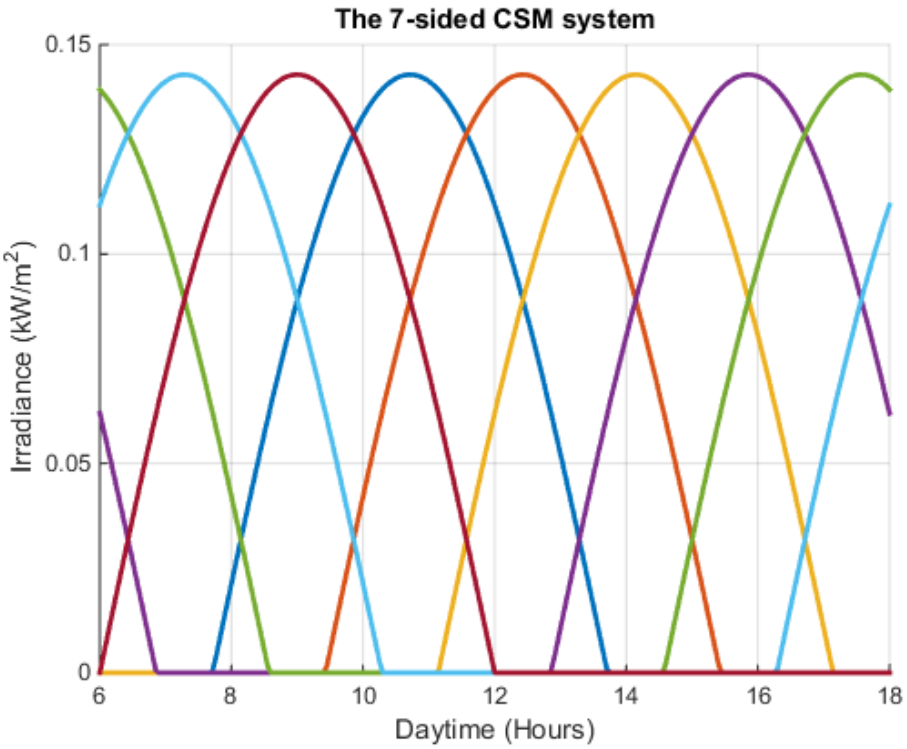

Figure 4. 23: Seven-sided CSM individual contributions

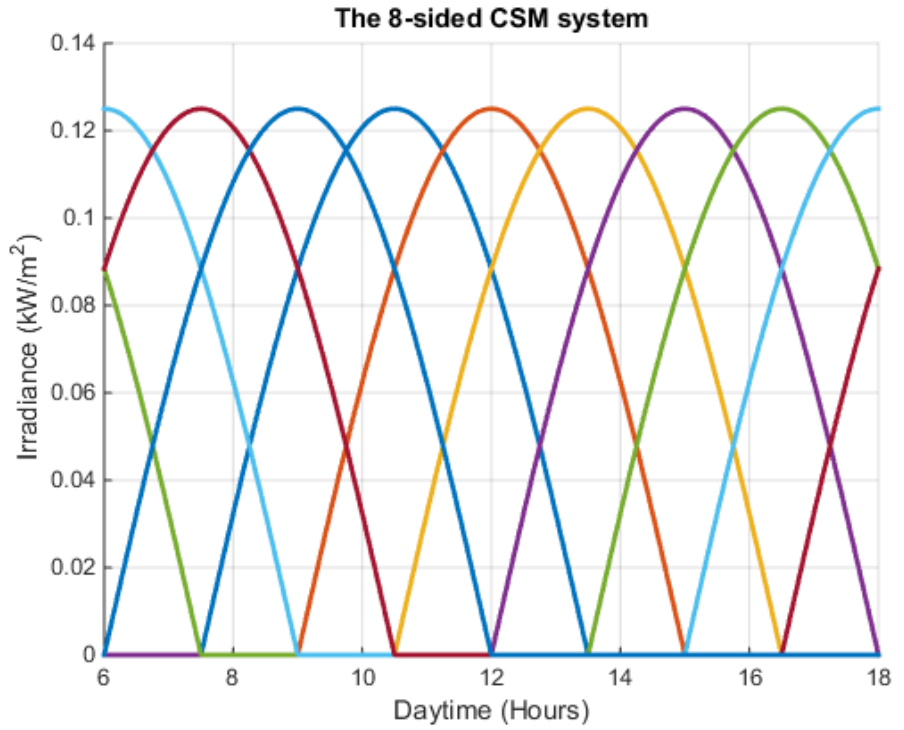

Figure 4. 24: Eight-sided CSM individual contributions

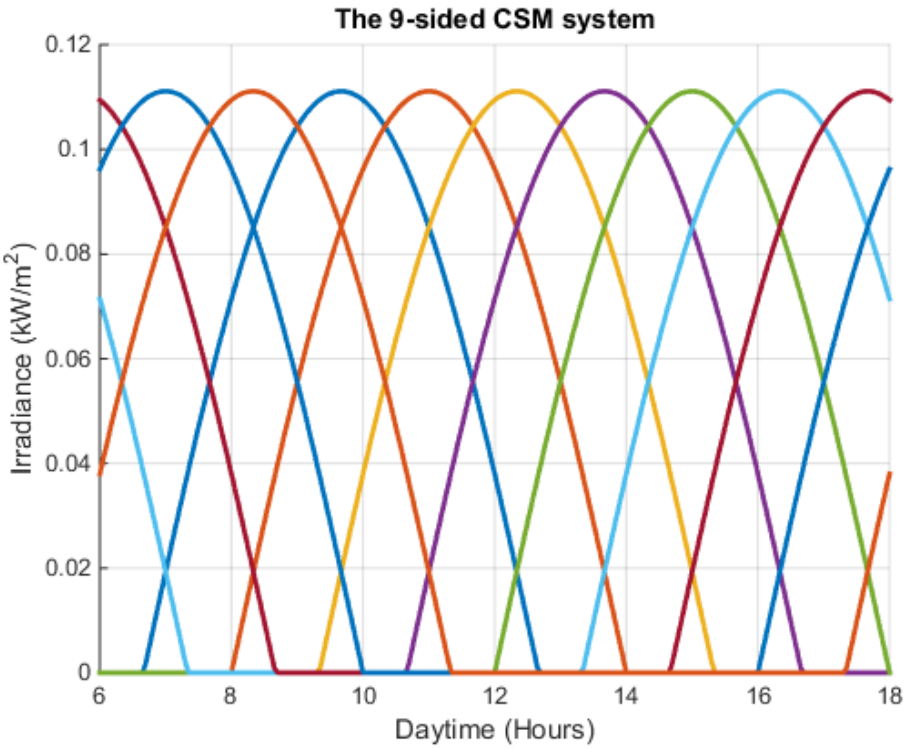

Figure 4. 25: Nine-sided CSM individual contributions

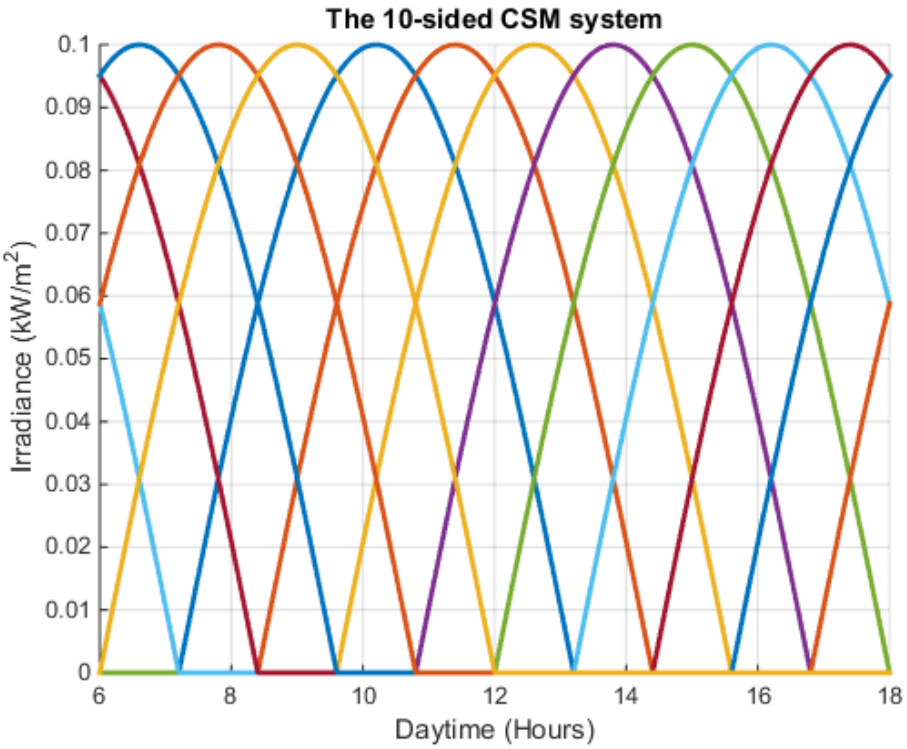

Figure 4. 26: Ten-sided CSM individual contributions

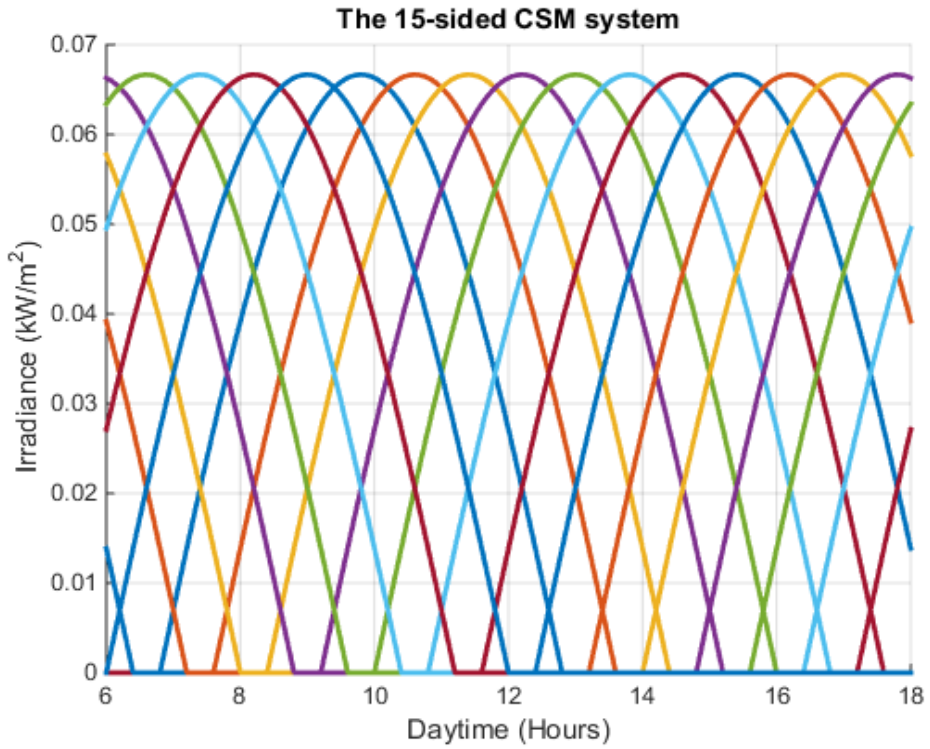

Figure 4. 27: Fifteen-sided CSM individual contributions

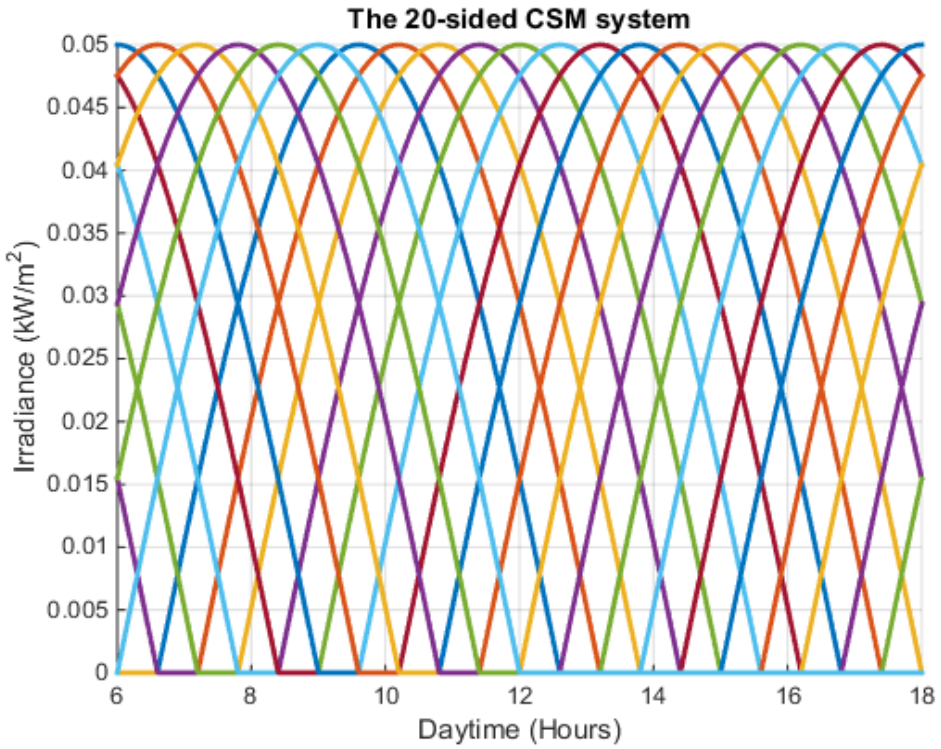

Figure 4. 28: Twenty-sided CSM individual contributions

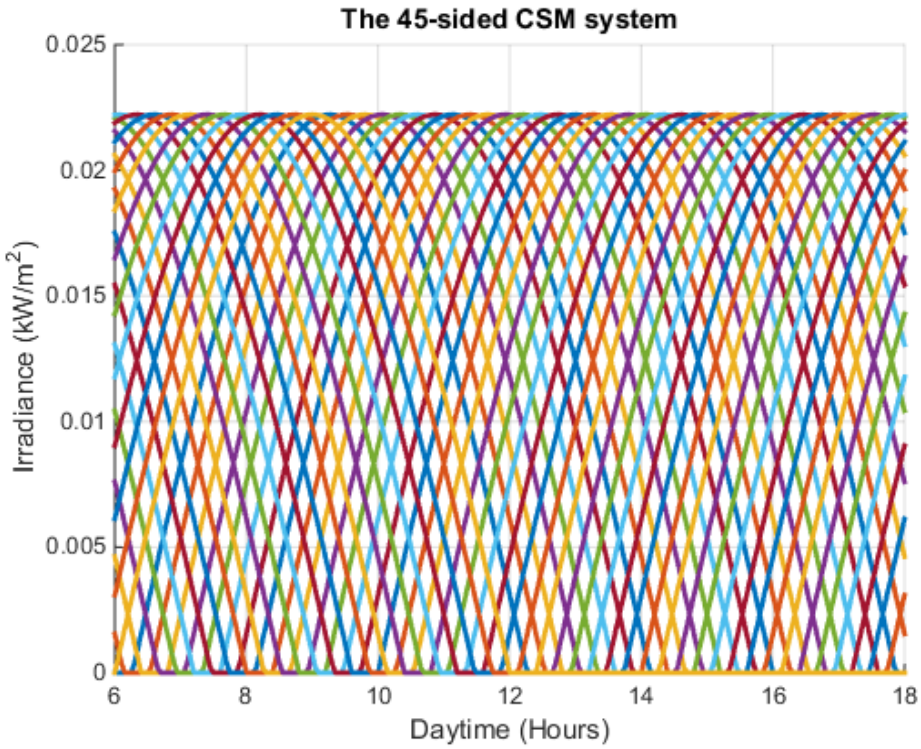

Figure 4. 29: Forty-five-sided CSM individual contributions

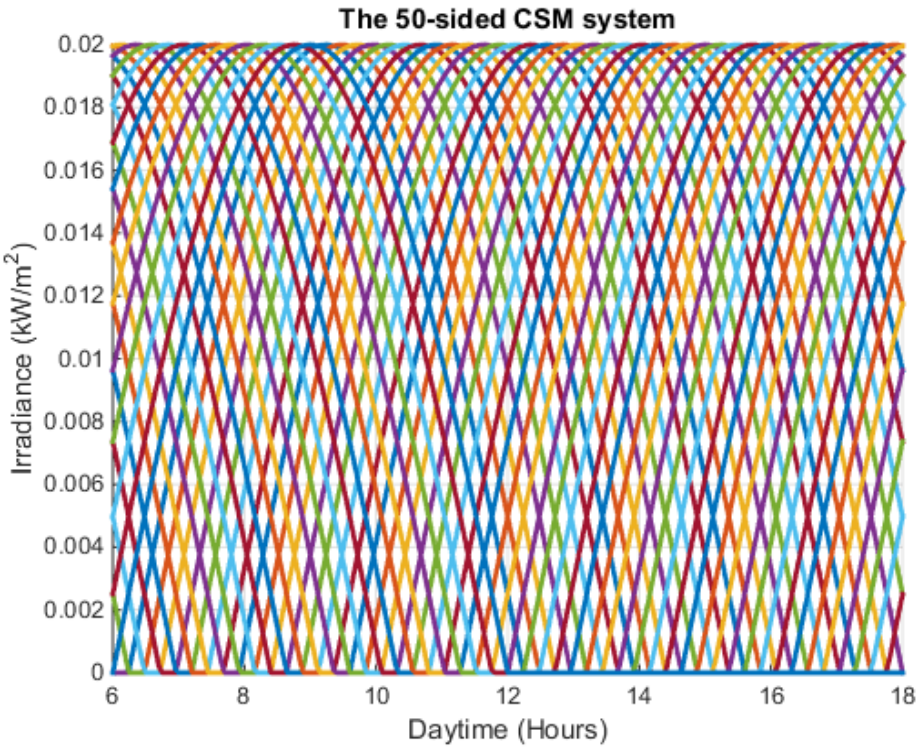

Figure 4. 30: Fifty-sided CSM individual contributions

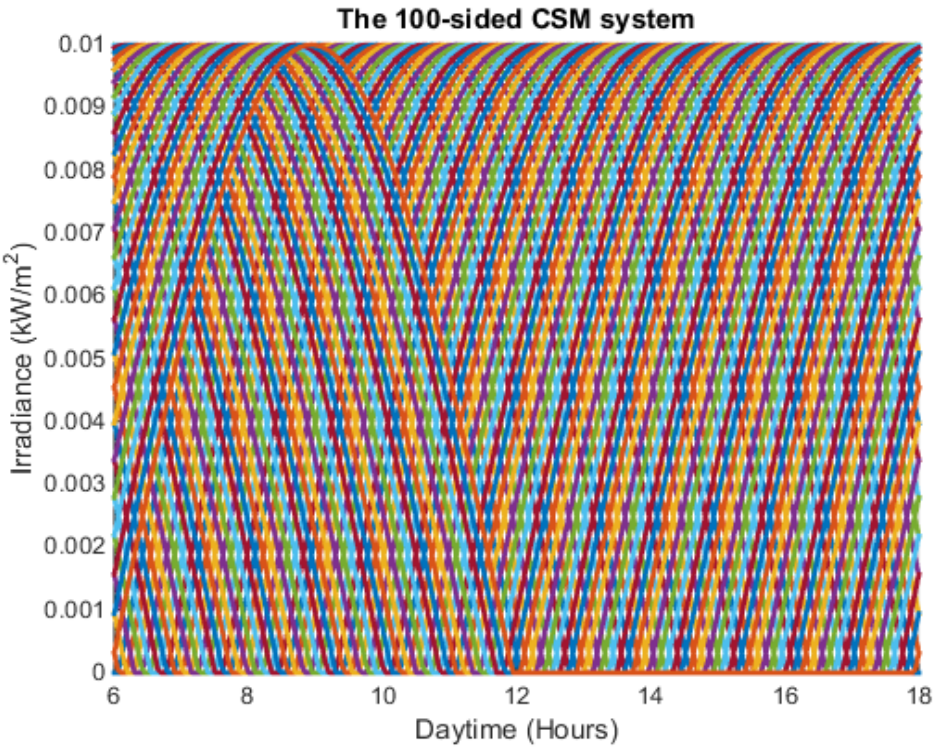

Figure 4. 31: Hundred-sided CSM individual contributions

4.5. CSM PV systems performance evaluation

The performance of the CSM PV systems was evaluated against the flat of the same area and ratings. As the aim this particular type of structure is to ensure the irradiance distribution is even, parameters such as irradiance average value, maxima and minima values along with the deviation from the mean were at the core of the evaluation criteria. With regard to the average value, profiles of selected PV systems were graphically represented in Figures 4.32-4.44.

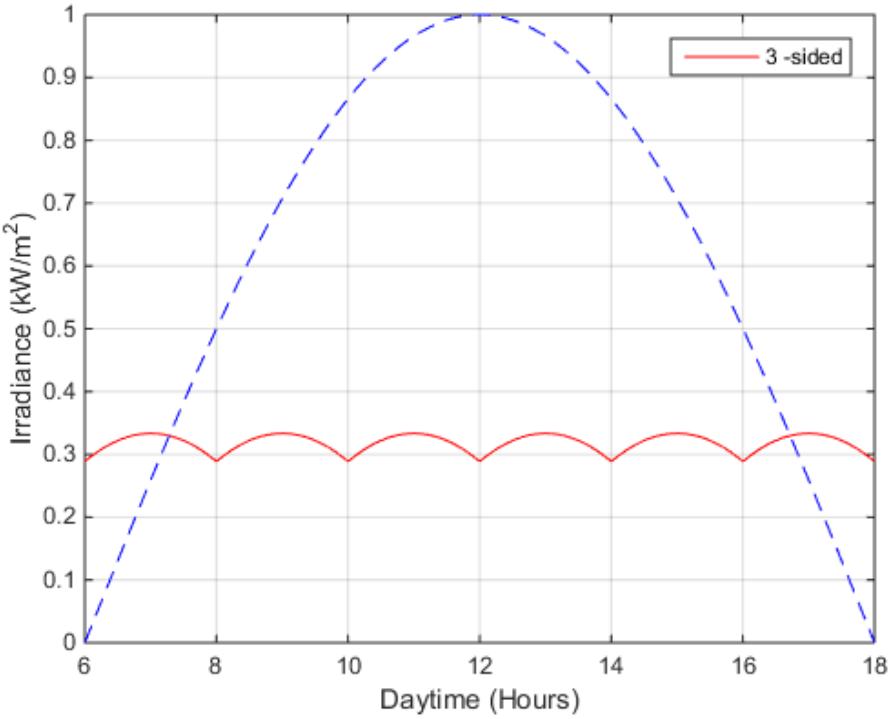

Figure 4. 32: Three-sided CSM vs flat single-sided profiles

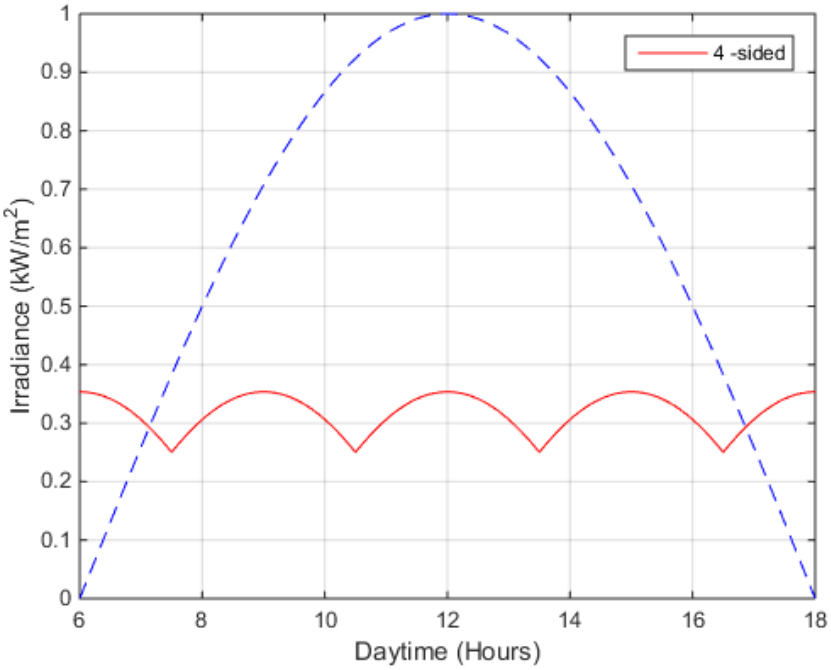

Figure 4. 33: Four-sided CSM vs flat single-sided profiles

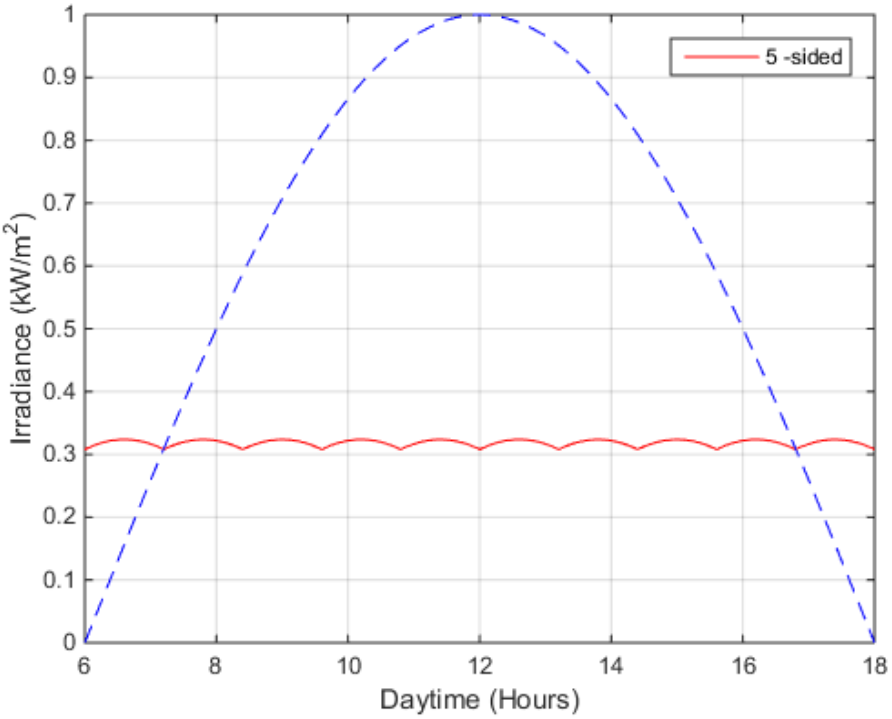

Figure 4. 34: Five-sided CSM vs flat single-sided profiles

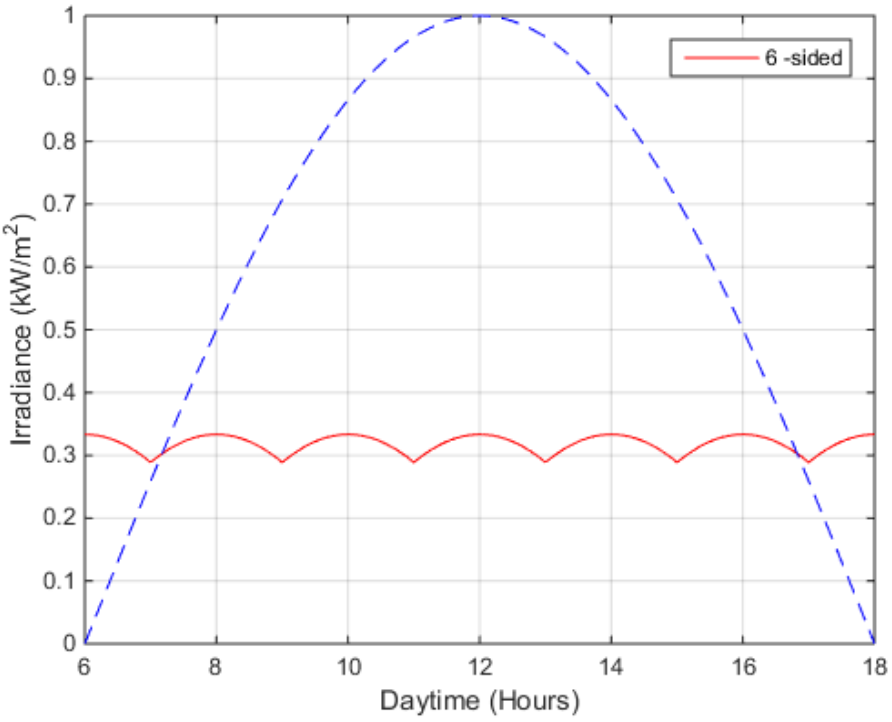

Figure 4. 35: Six-sided CSM vs flat single-sided profiles

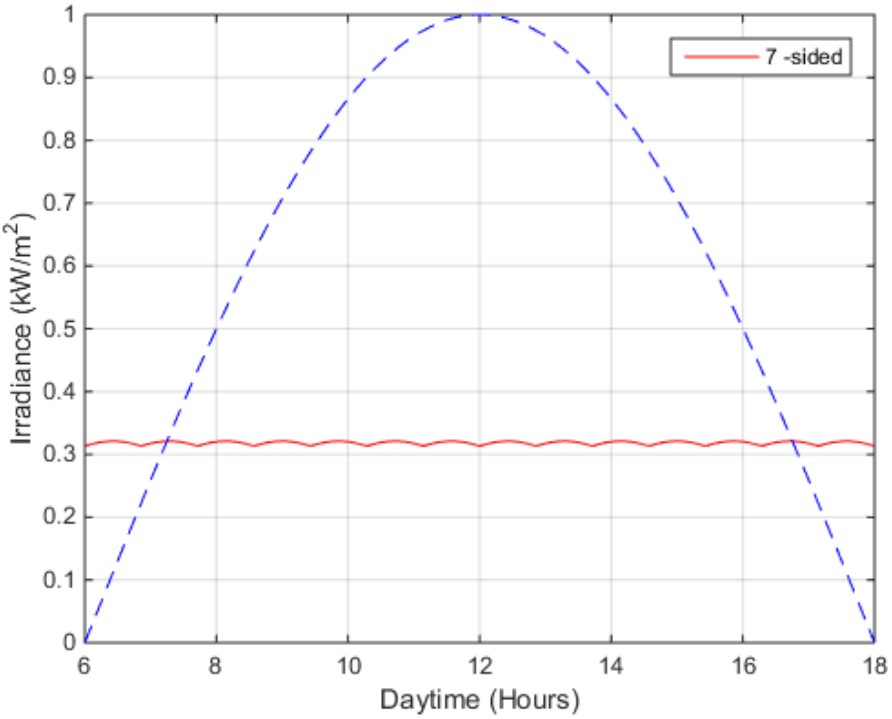

Figure 4. 36: Seven-sided CSM vs flat single-sided profiles

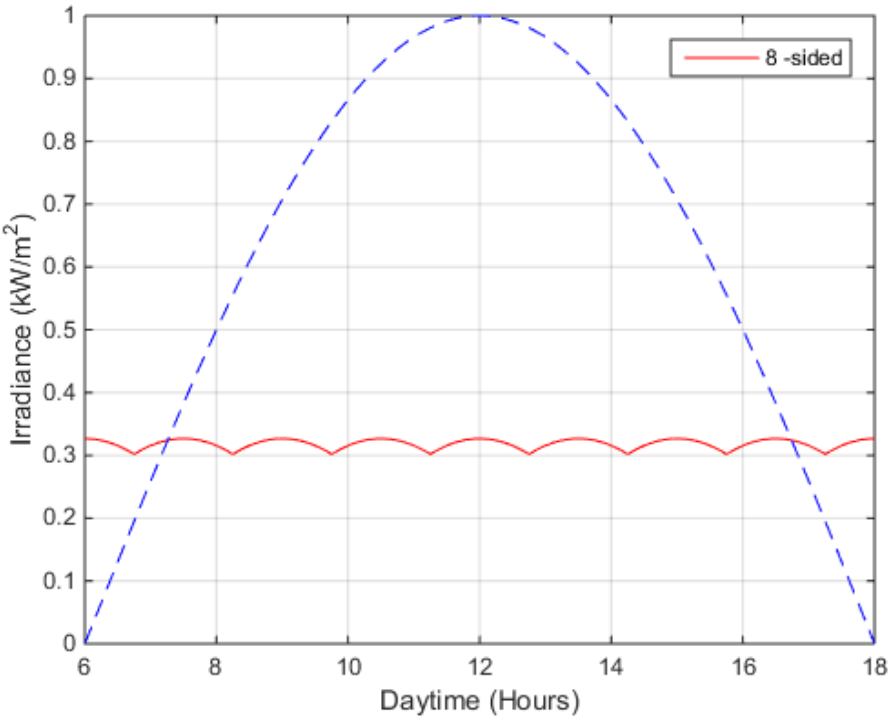

Figure 4. 37: Eight-sided CSM vs flat single-sided profiles

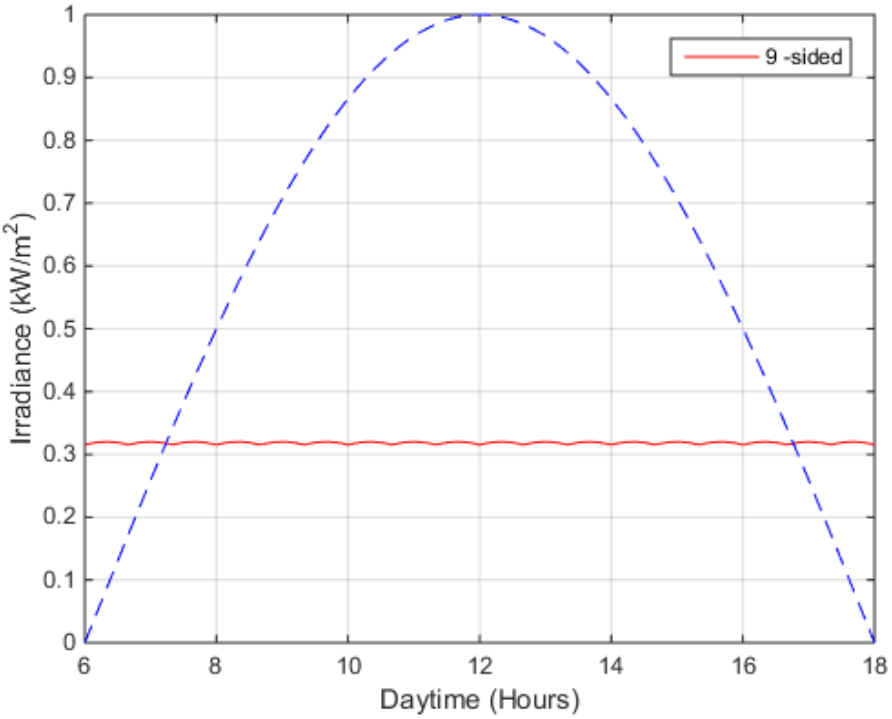

Figure 4. 38: Nine-sided CSM vs flat single-sided profiles

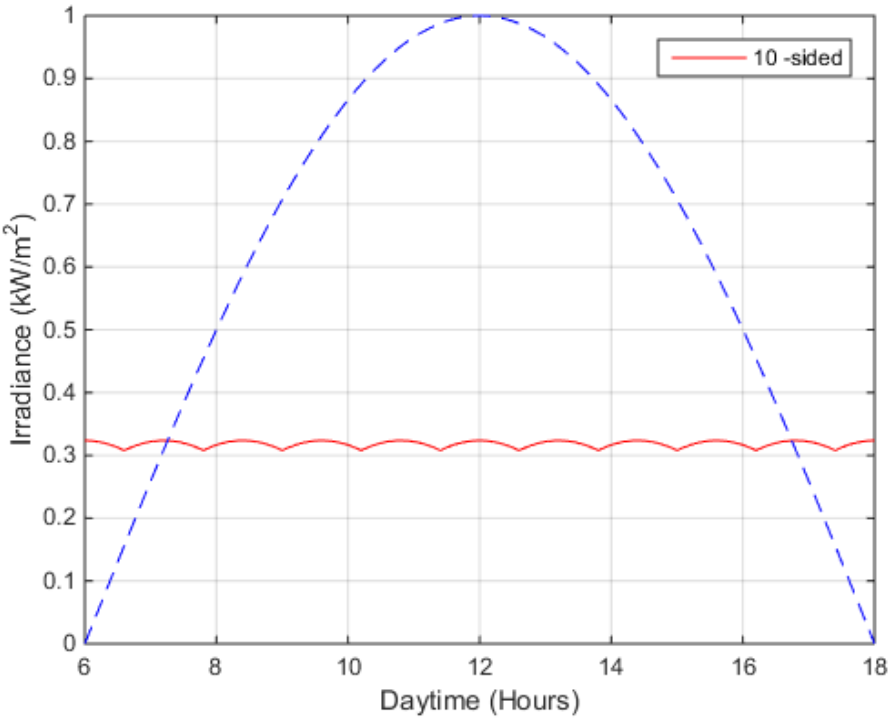

Figure 4. 39: Ten-sided CSM vs flat single-sided profiles

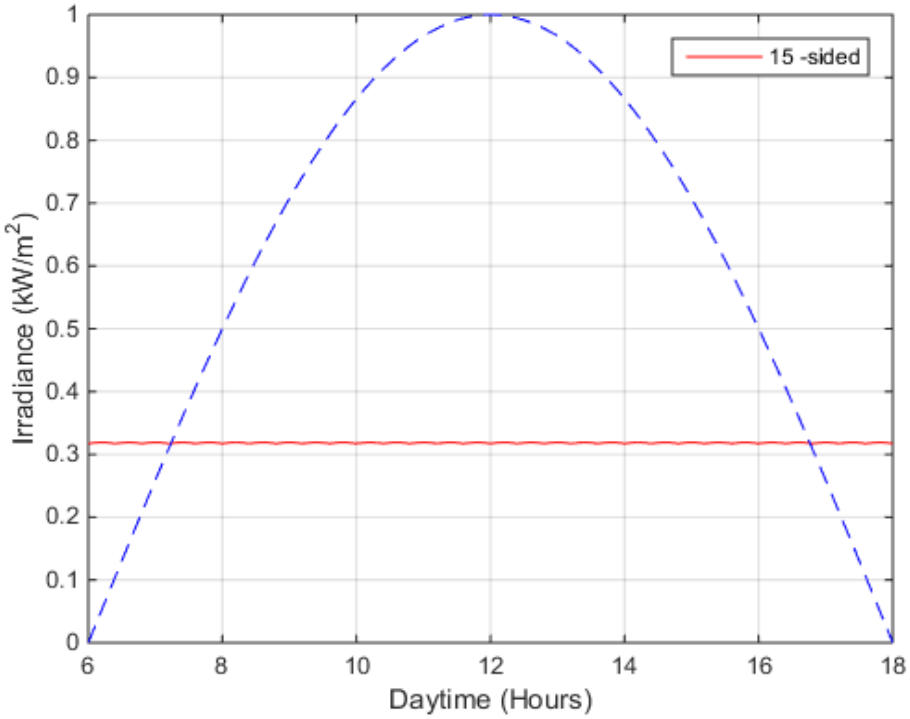

Figure 4. 40: Fifteen-sided CSM vs flat single-sided profiles

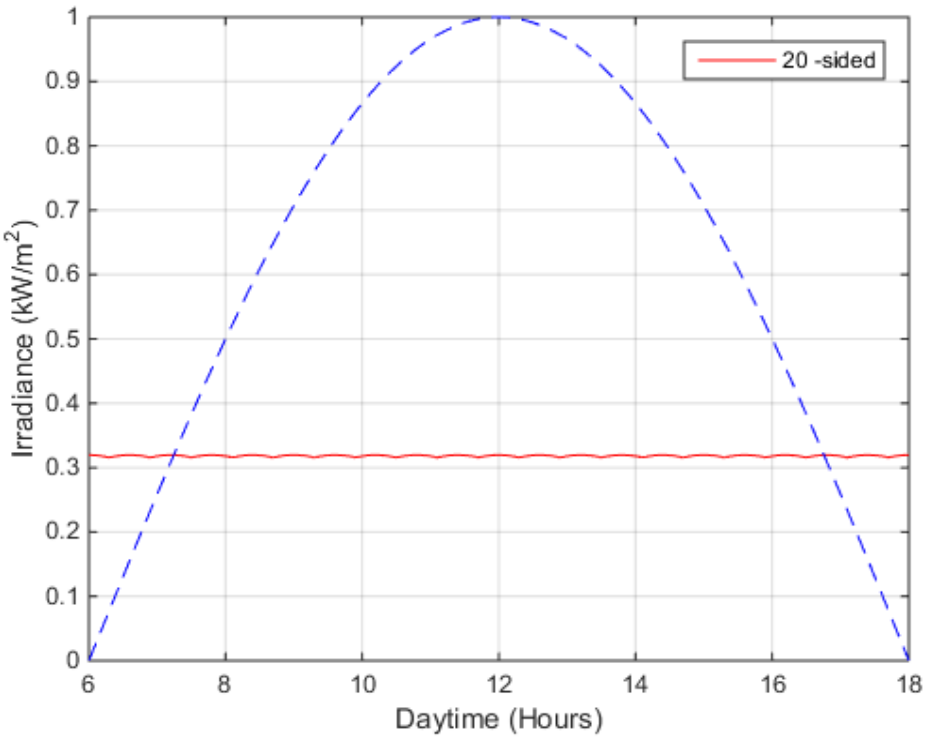

Figure 4. 41: Twenty-sided CSM vs flat single-sided profiles

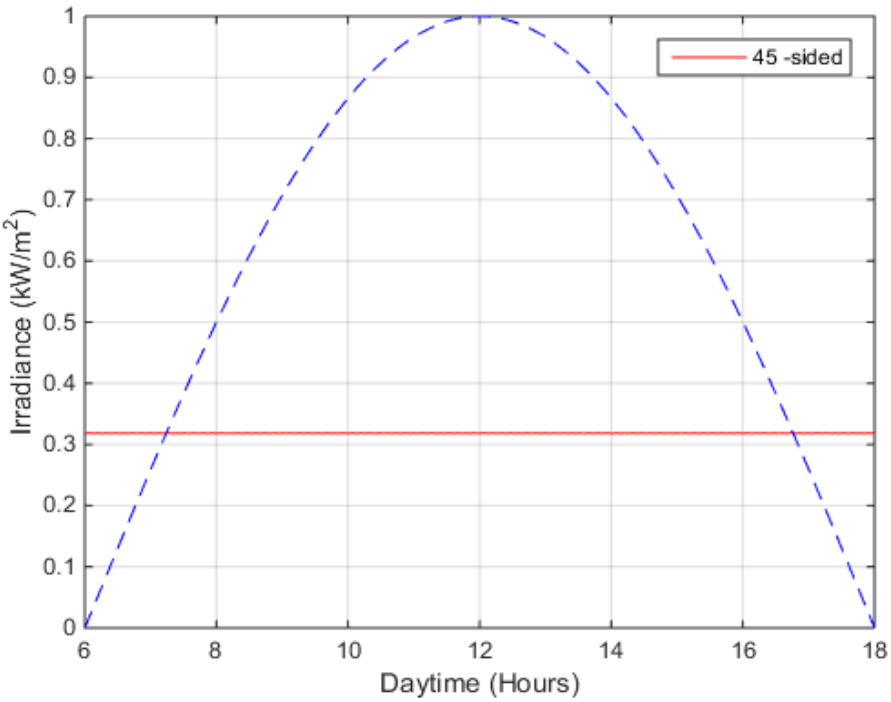

Figure 4. 42: Forty-five-sided CSM vs flat single-sided profiles

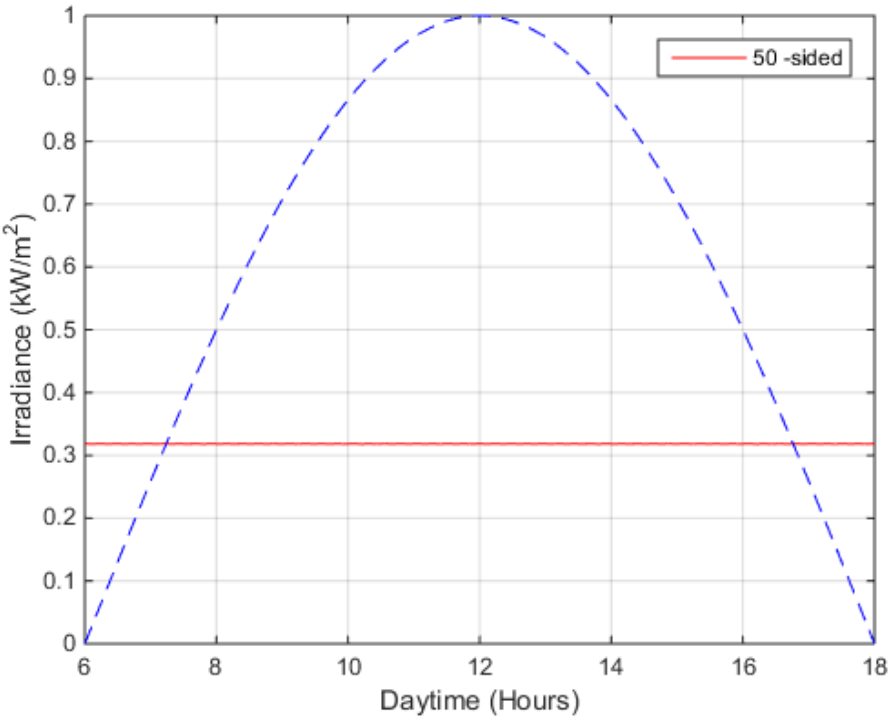

Figure 4. 43: Fifty-sided CSM vs flat single-sided profiles

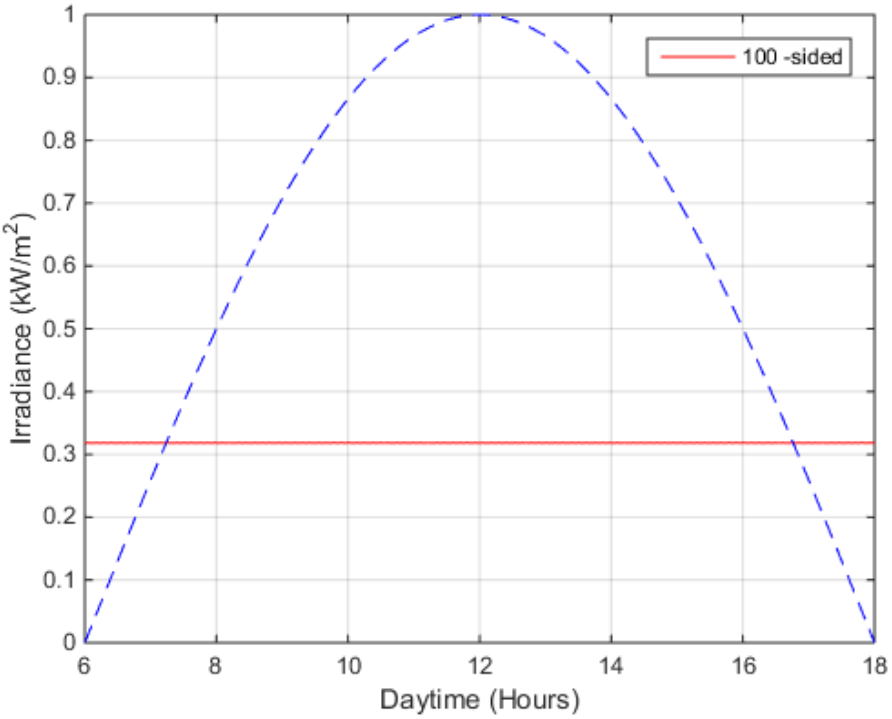

Figure 4. 44: Hundred-sided CSM vs flat single-sided profiles

4.6. Presentation of the results

The values of the key parameters are synthetized in Table 4.1. They are also translated in bar charts for a simultaneous comparison of parameter values (Figures 4.45-4.49).

Table 4. 1: Results summary

Type	Max (kW/m^2)	Min (kW/m^2)	Average (kW/m^2)	Ripple (kW/m^2)	Ratio
One	1,0000	0,0000	0,31818	1,0000	1,0000
Two	0,5000	0,0000	0,3157	0,2500	0,9922
Three	0,3333	0,2887	0,3180	0,0223	1,0073
Four	0,3537	0,2500	0,3177	0,0518	0,9991
Five	0,3236	0,3078	0,3182	0,0079	1,0016
Six	0,3333	0,2887	0,3180	0,0223	0,9994
Seven	0,3210	0,3129	0,3183	0,0040	1,0009
Eight	0,3266	0,3018	0,3182	0,0124	0,9997
Nine	0,3199	0,3151	0,3183	0,0024	1,0003
Ten	0,3236	0,3078	0,3182	0,0079	0,9997
Fifteen	0,3189	0,3171	0,3183	0,0009	1,0003
Twenty	0,3196	0,3157	0,3183	0,0020	1,0000
Forty-five	0,3184	0,3182	0,3183	0,0001	1,0000
Fifty	0,3185	0,3179	0,3183	0,00003	1,0000
Ninety-five	0,3183	0,3183	0,3183	0,00002	1,0000
Hundred	0,3184	0,3182	0,3183	0,00008	1,0000

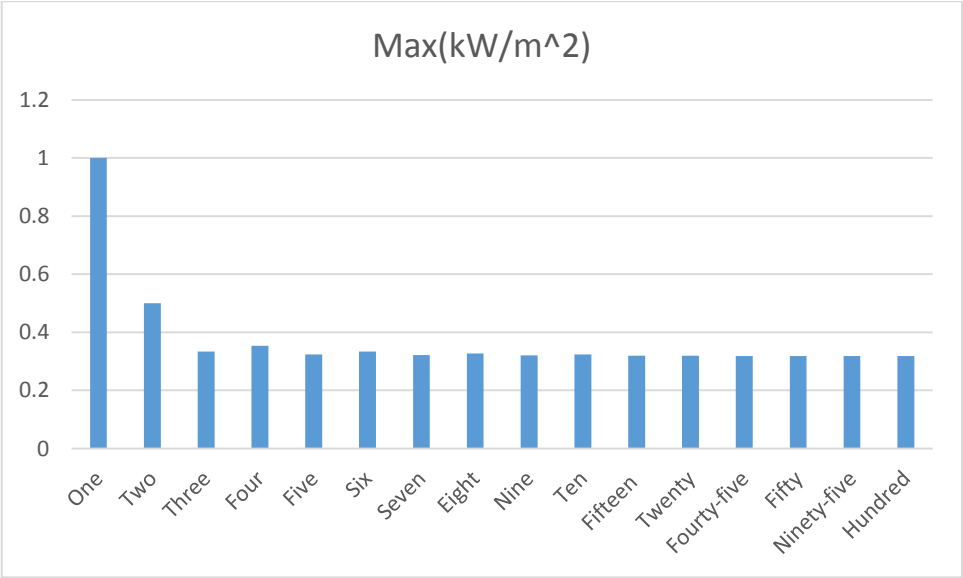

Figure 4. 45: Comparison of maxima irradiance

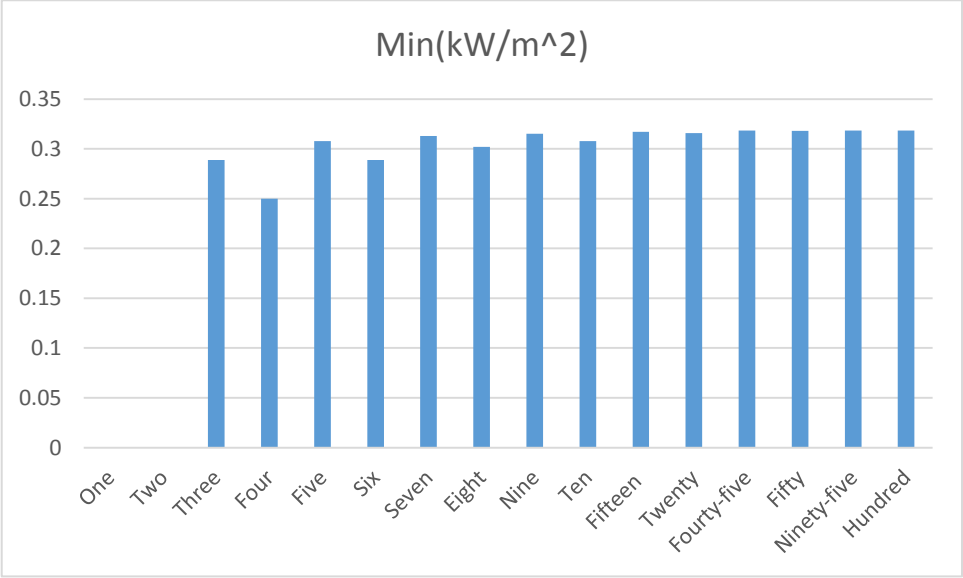

Figure 4. 46: Comparison of irradiance minima values

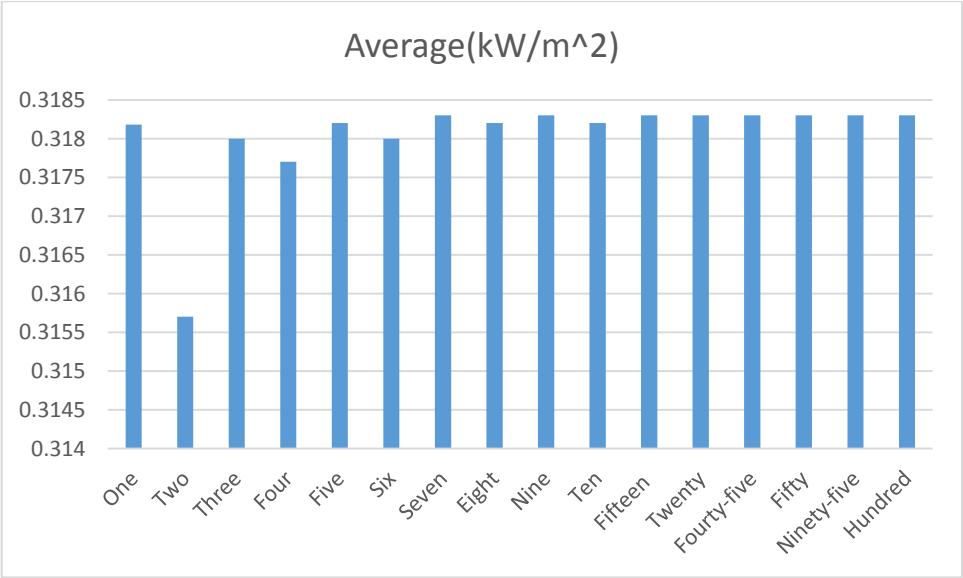

Figure 4. 47: Comparison of irradiance average values

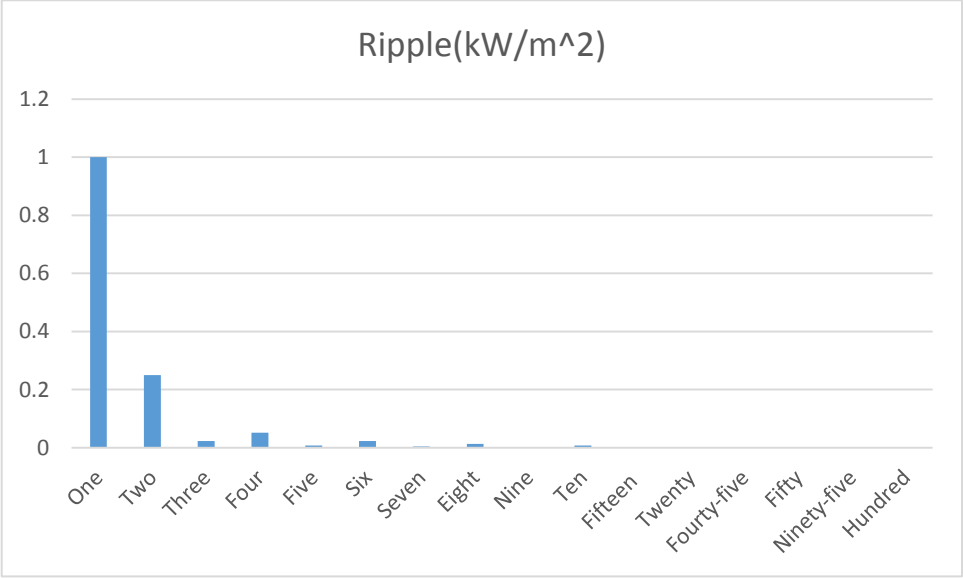

Figure 4. 48: Comparison of irradiance ripple values

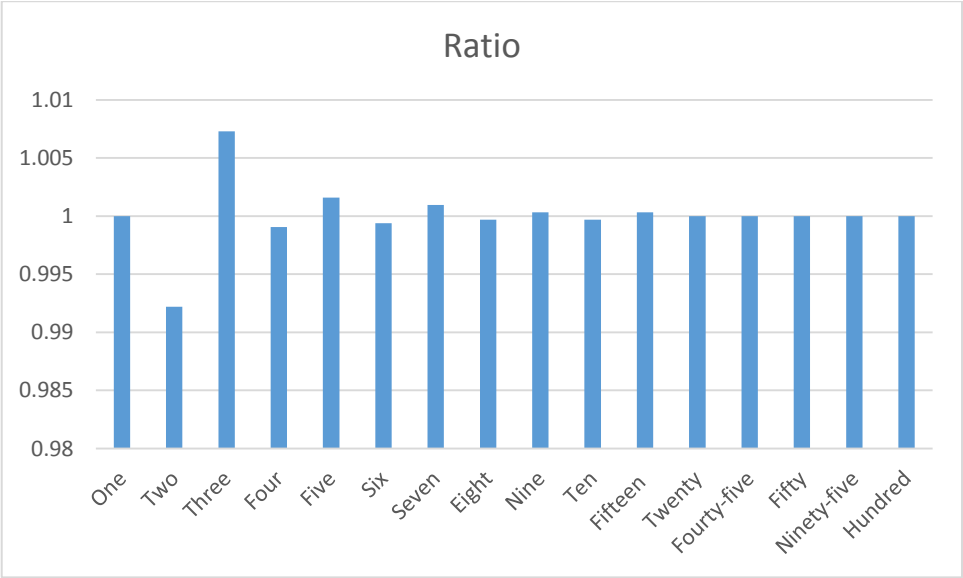

Figure 4. 49: Comparison of ratio (CSM/fixed tilt panel)

4.7. Results discussion and conclusions

A broad observation on the results in Table 4.1 and comparison graphs in Figures 4.48 to 4.52 lead to a conclusion that CSM PV systems have a better irradiance distribution than single-sided and fixed-tilt solar panel. With the increase of the number of sides, the CSM PV systems exhibit a much smoother irradiance of which the average level (0.3183 kW/m^2) equals the average of the single-sided PV systems of the same area. By deduction, this output is expected to be perfectly constant for cylindrical-shaped systems. With no fluctuations between minima and maxima values and with the average ratio equal to 1 (with respect to the reference average irradiance) CSM PV systems are believed to guarantee a constant electrical output power. This phenomenon can be explained by the fact that from sunrise to sunset a constant area equivalent to a half cylinder is exposed to the sunlight (Figure 4.53). Concerning the average level of 0.3183 kW/m^2, it is important to determine the area parameters of the CSM first. The height $H = 1\,\mathrm{m}$ whereas the diameter $D = 0.3183\,\mathrm{m}$ in order to have the base circumference equal to 1m (Figure 4.50). Therefore, the area exposed to the sun will be 0.3183 m^2, which makes the power level to be constant and equal to 0.3183 Kw (Figures 4.51.and 4.52).

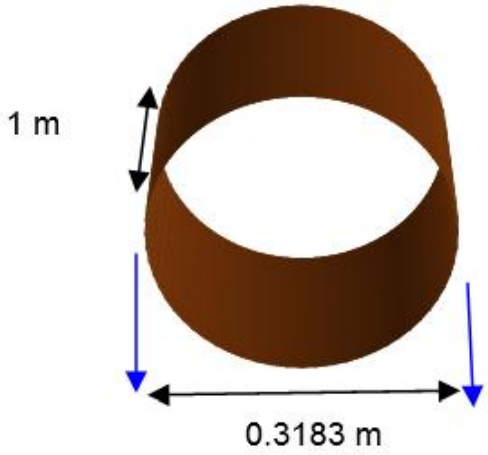

Figure 4. 50: Dimensions of an equivalent cylindrical-shaped system

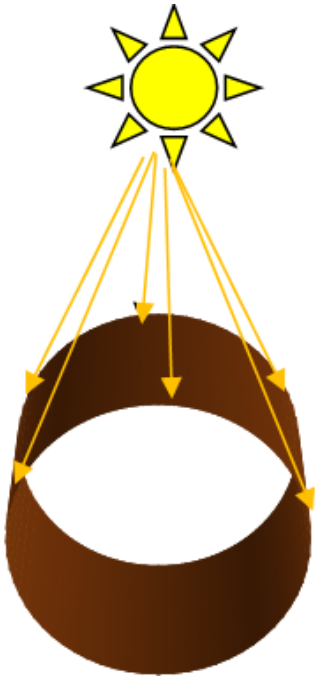

Figure 4. 51: Cylindrical shaped PV exposure at noon

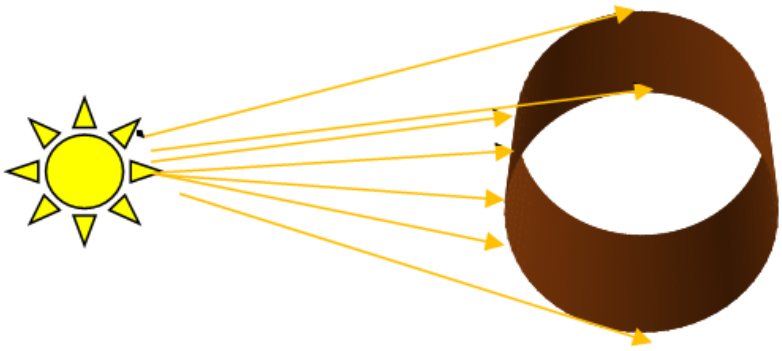

Figure 4. 52: Cylindrical shaped PV exposure at sunrise

Furthermore, a close look at the number of sides shows that systems with an odd number of sides produce smoother irradiance distributions than systems with an even

number of sides. A three-sided system has smaller ripples than the four sided and it remains so for the five and the six-sided, the seven and the eight-sided, the nine and the ten-sided systems. When evaluated based on the efficient utilisation of sides, irrespective of the irradiance dynamics evenness, three-sided CSM systems, simple in design, are best. Though a cylindrical-shaped CSM PV system is expected to evenly collect the irradiance since the exposed area is the same at any time of the day, it is however expected to require a meticulous, simple and efficient way of connecting sides, otherwise shading problems may negatively impact on the energy conversion and be complicated to implement. The inconvenience can be alleviated by designing PV systems such that the panel (sides) are independent from one another in terms of connections in one hand; and ensuring that panels are having less area in the shade on the other hand. Figure 4.53 depicts one possible approach design by dividing the whole PV system into four panels and connecting them in parallel. Eight-sided cylindrical PV system should minimize the shading problem but be a bit challenging in terms of connections.

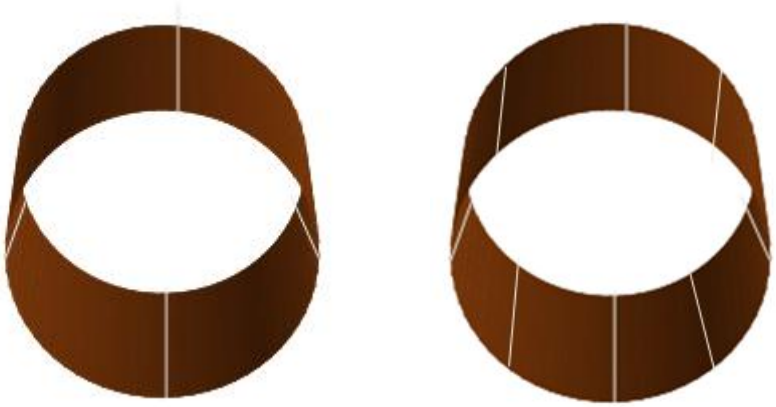

Figure 4. 53: Example of four-sided and eight-sided cylindrical CSM system

The choice of the CSM to adopt will depend on the application. Cylindrical-shaped systems would be recommended for applications where the level of output must be strictly kept constant whereas a three-sided should suit applications where the output level evenness allows for some degree of tolerance.

CHAPTER FIVE

THERMAL ELECTRIC SOLAR POWER PANEL DEVELOPMENT

5.1. Chapter summary

5.2. Design requirements

5.3. Sun-tracking scheme selection

5.4. Solidworks model

5.5. Solar cells connections

5.6. The cooling of solar cells

5.7. Power panel performance evaluation

5.7.1. Panel scale

5.7.2. Cell scale evaluation

5.8. Selection of TE device and performance evaluation

5.9. Overall system performance

5.10. Results discussion

5.1. Chapter summary

Stages of developing a thermal electric solar power panel are discussed in this chapter. Therefore, this chapter describes the roadmap towards the fulfilment of the research aim with a 3D printable model being the end-product for this first-time conducted study. Design requirements, limitations, constraints considered are also discussed. The design was done in two scales: the panel scale and cell scale. Firstly, at panel scale, two PV panels were assembled together with a 60^0 junction angle and their performance evaluated. With such configuration, the exposed area is double that of a laid-flat solar panel, so is the sunlight collected, beside the boost of OSM systems. Secondly, cells were assembled in the same way as at the panel scale, and then integrated on one solar panel. Thus, the PV panel was formed. TE conversion accompanied with the cooling followed. At the end, the performance comparison between the developed power panel and the flat-fixed-tilt solar panel was established, and the developed panel proved its worth in terms of efficiency.

5.2. Design requirements

The driving factors in the design are efficiency and lifespan. Narendrasinh Parmar et al. (2005) listed the factors affecting solar panels efficiency as follows:

Panel orientation: For a maximum sunlight reception, solar panels should be fitted on the roof side facing the sun's movement. This implies that solar panels should be installed facing the North in the southern hemisphere whereas they should face the South in the Northern hemisphere. Otherwise, solar panels not properly oriented would receive the sunlight for a limited number of hours per day.

Roof and panel pitch: The slope for solar panels and roof should be normal to the sun's apparent movement. Lower or higher pitch can result in solar panels' poor sunlight reception.

Temperature: The effect of temperature increase impacts on the efficiency and the lifespan of solar cells. This was thoroughly discussed in Chapter two.

Shade: Described as the enemy of the energy, a shade on one solar panel can shut down the energy production of the rest of the panels.

Sub-mentioned factors provide a guideline in the design process of the panel under development.

5.3. Sun-tracking scheme selection

One of the novelties of this research is the multisided PV system as means of tracking the sun. OSM and CSM PV systems were proposed and explored in the previous chapter. The two were found out to be more advantageous than the flat-fixed-tilt solar panel in terms of performance. From the efficiency perspective, the OSM systems yielded a raise of 32 % whereas CSM systems proved to collect the sunlight in even way throughout the daytime and hence to keep the same irradiance level.

In an attempt to seek simpler systems, a further examination into PV systems was done before the selection process. Simplicity was sought for given challenges that may be experienced while connecting sides. Sides should be connected in a way that gives no room of PV system shading. Two-sided OSM PV systems involve less design complexity in terms of sides numbers while producing a pretty steady irradiance input curve. Three-sided CSM PV systems were also found to produce a steady irradiance input using fewer sides though not as smooth as the cylinder-shaped PV systems. A two-sided was further explored by varying the junction angle (Kamanzi & Kahn, 2016). Figures 5.1 and 5.2 show the profile of double-sided OSM PV systems when the phase angle is respectively 60 and 90. When designed with a 60^0-junction angle, the two-sided CSM PV system collects the irradiance averaging around 42 % of the nominal irradiance. Thus, it offers a two-fold advantage.

Simplicity: the design of two sides makes it simple and therefore less connection work.

Average: with such configuration, the OSM PV systems with 60^0 junction angle produces an irradiance level increase of 32 % on the average level of a flat-fixed-tilt solar panel. In addition, with same average level, the design is better even over the CSM systems as it produces smoother irradiance dynamics.

Therefore, concerning this project, a design with a 60^0 junction is selected in the power panel development.

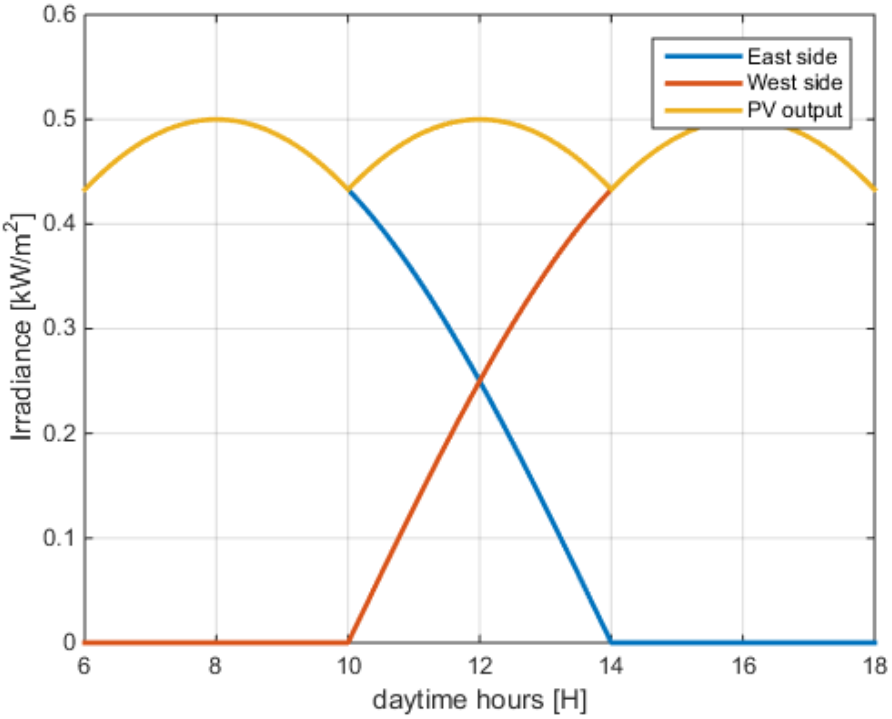

Figure 5. 1: Double-sided with 60^0 junction angle and 1 m^2 area

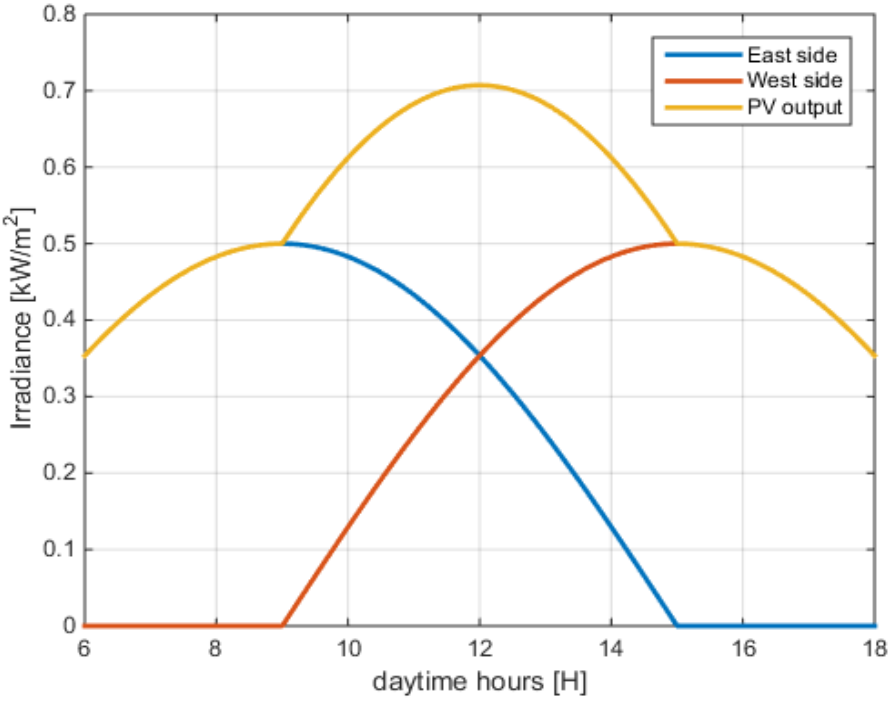

Figure 5. 2: Double-sided OSM with 90^0 junction angle and 1 m^2 area

5.4. Solidworks model

The power panel design was carried out in two scales: A panel scale in the first place and a cell scale in the second place. By panel scale design, it is meant a double-sided OSM PV

systems essentially made of two solar panels joined at 60^0; the whole assembly being held together by a stand (Figure 5.6). The cell scale design implies a solar panel made of two cells joined at 60^0 angle (in the place of one cell) and then integrated to form a solar panel (Figure). In either case the design process was done hierarchically, i.e. from the smallest element to largest element of the PV system. Cells of 200 mm x 300 mm each were laid on a solar base of 850 mm x 1250 mm in a 4-series- 4-parallel configuration. The 50 mm on the length and width cover the gap in-between the cells.

Concerning the double-sided design, the Solidworks project started with the cell (Figure 5.3), then the panel base (Figure 5.4) so as to form a solar panel (Figure 5.5). As for the cell scale design, a cell was structured to suit a double-sided compact structure as it was done at the panel scale. Thus obtained OSM PV cells are placed on the solar base of same area and structure as depicted in Figure 5.7.

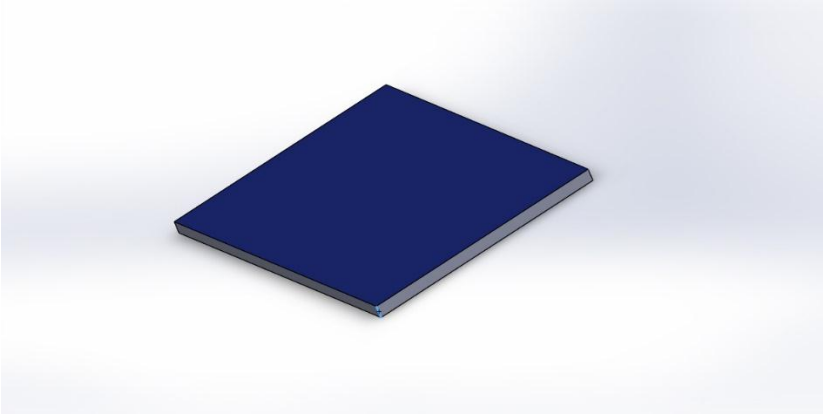

Figure 5. 3: Cell design

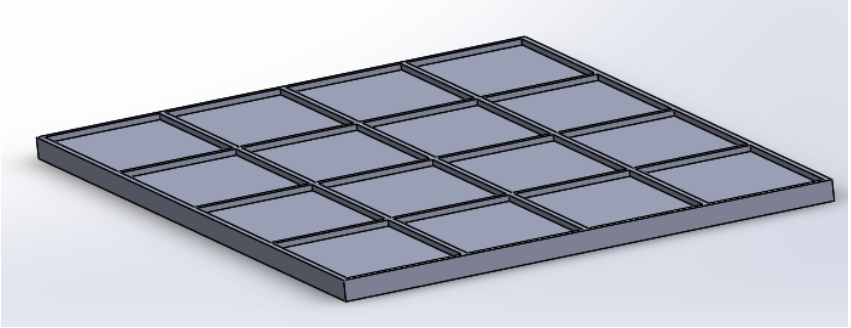

Figure 5. 4: Solar panel base design

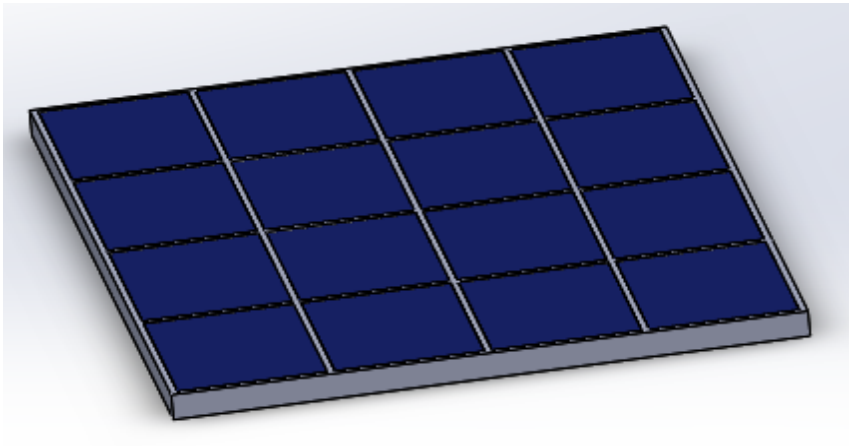

Figure 5. 5: Solidwork model of a PV panel

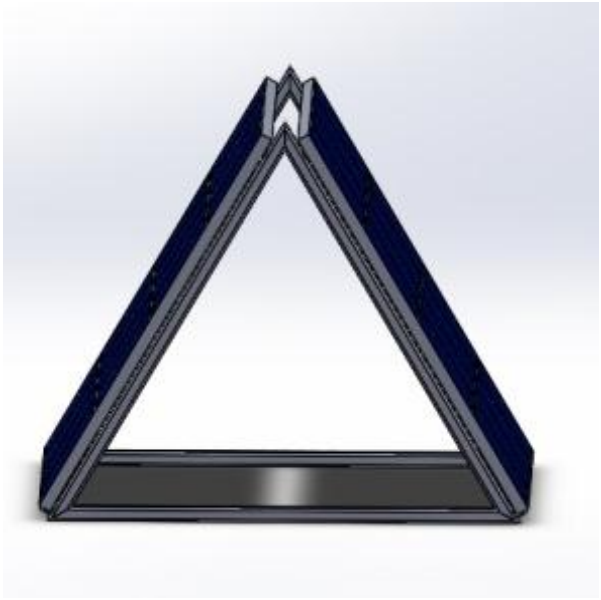

Figure 5. 6: Solidwork model of a double-sided OSM PV system with 60^0 junction angle

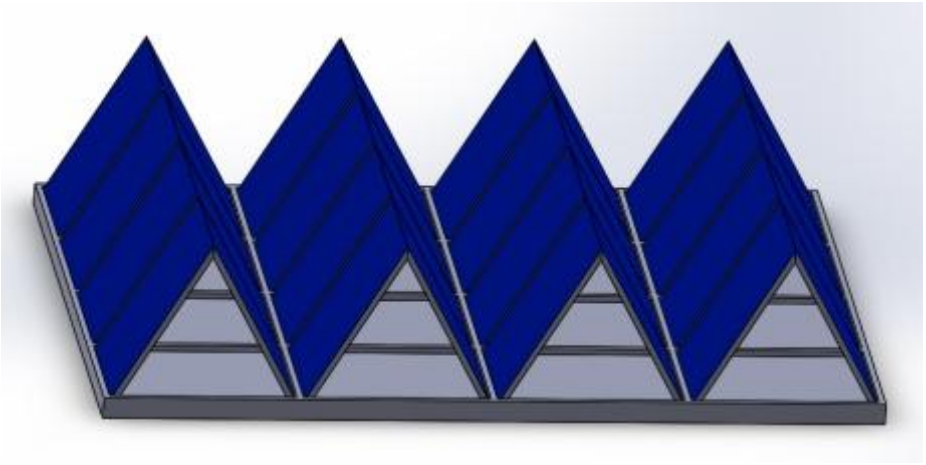

Figure 5. 7: Solidwork model of double-sided cells integrated in one panel

5.5. Solar cells connections

Though the developed panel is made of cells in a double-sided configuration assembled on solar panel base, cells should be connected in a way the panel does not suffer from shading effects. Cells are therefore put in two groups according to the orientation plane. There are cells that will be fully active in the morning whereas others will be at shade. The inverse scenario will take place in the afternoon. Considering the power panel to be row-column structured, cells in the same column were connected in series, then cells in the same plane were connected in parallel. This implies two output terminals connecting to next stages of electrical production process.

5.6. The cooling of solar cells

The power panel structure was made in a way that suits natural ventilation of cells. Furthermore, TE cooling devices were suggested to be applied at the back of each cell. TE devices also offer the advantage of producing electricity and the cooling effect at the same time. With the feature of converting temperature differences into electricity, TE devices are expected to perform well since the power panel is designed with ventilation.

5.7. Power panel performance evaluation

The performance of the power panel was evaluated from the PV and TE perspectives relative to the flat-fixed-tilt solar panel. The incoming sunlight being the main factor, the panel surface area was the determinant element in terms of quality. The area of the flat panel made of 16 cells of 60000 mm^2 each was found to be equal to 0.96 m^2. The power is then given by equation 5.1. With a 1000 W/ m^2, the PV power for the fat panel was evaluated at 960 W.

$$P(\mathrm{W}) = G_M(\mathrm{W/m^2}) * A(\mathrm{m^2}) \qquad \textbf{Equation 5. 1}$$

The average power collected by the flat panel could be determined as per equation 5.2. It was found to be 305.6 W.

$$P_{avg} = \frac{P_{peak}}{\pi} \qquad \textbf{Equation 5. 2}$$

Where P_{avg} is average power and P_{peak} is the peak power.

5.7.1. Panel scale

At panel scale, two panel are joined according to the chosen sun-tracking system. An OSM system with 60^0 junction angle was therefore implemented using two PV panels of 0.96 m^2 area each. With such a configuration, where one panel is set up facing the East and another faces the West, double PV active area could be fitted in the same space area as a horizontally laid solar panel. Hence, an active area of 1.920 m^2 could be gotten in the same space area as a flat-laid panel of 0.960 m^2. The parameters of the formation were graphically determined as follows:

- Peak power: 960 W,
- Minimum power: 0.831 W
- Average power: 916 W

Figure 5.8 shows the individual contributions of the sides whereas Figure 5.9 illustrate the overall collection of the sunlight by the formed panel.

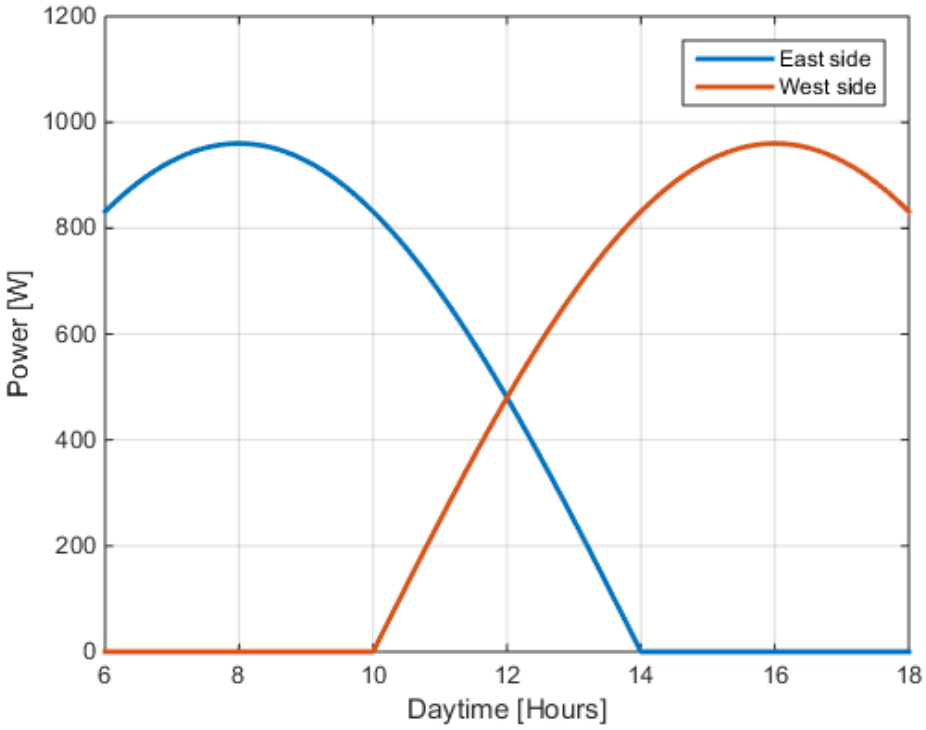

Figure 5. 8: Individual contributions of the side in sunlight collection

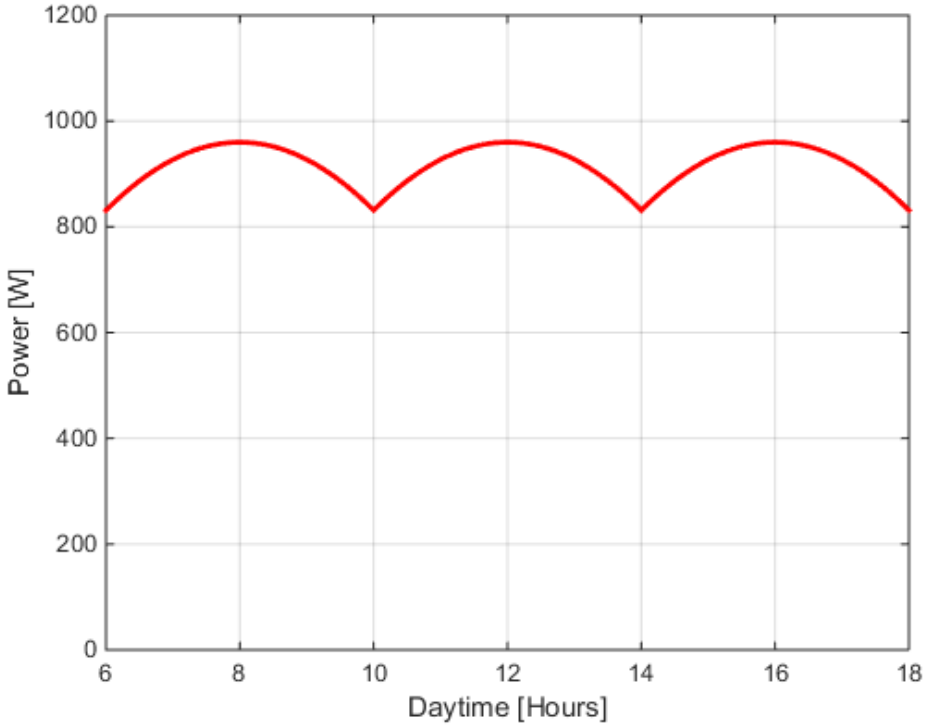

Figure 5. 9: Panel scale overall irradiance collection

5.7.2. Cell scale evaluation

For the thermal electric power panel, the area of the cells is double that of the flat solar panel since there are two cells in the place of one in the solar panel i.e. 1.920 m^2. There are cells facing East with a total area of 0.960 m^2 and cells facing the West with the same area. The formed OSM system ends up becoming the same as the one observed at panel-stage with same-value evaluation parameters.

Table 5. 1: Power performance comparison between designed OSM PV and reference flat panel

PV system type	Minimum (W)	Maximum (W)	Average (W)	Area (m^2)	Occupied flat area (m^2)
Flat panel	0	960	306	0.960	0.960
Proposed panel	831.6	960	916	1.920	0.960

Graphically, the designed panel is deemed to follow the 60^0-angled- double-sided function as in Figure 5.1. However, for practical reasons, various disturbances such

as weather-related, dusts and birds' droppings on PVs were randomly considered and the sunlight power captured by the panel would be expected to look as per Figure 5.10 and sides' individual contributions as in Figure 5.11.

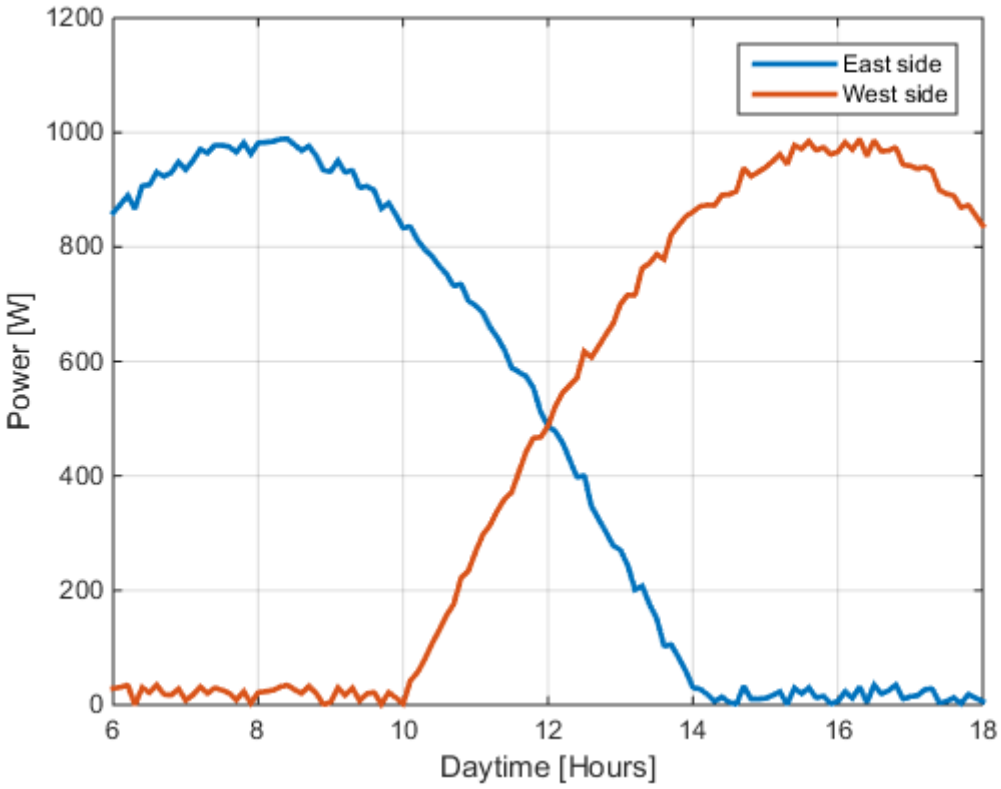

Figure 5. 10: The sunlight power collected per PV side

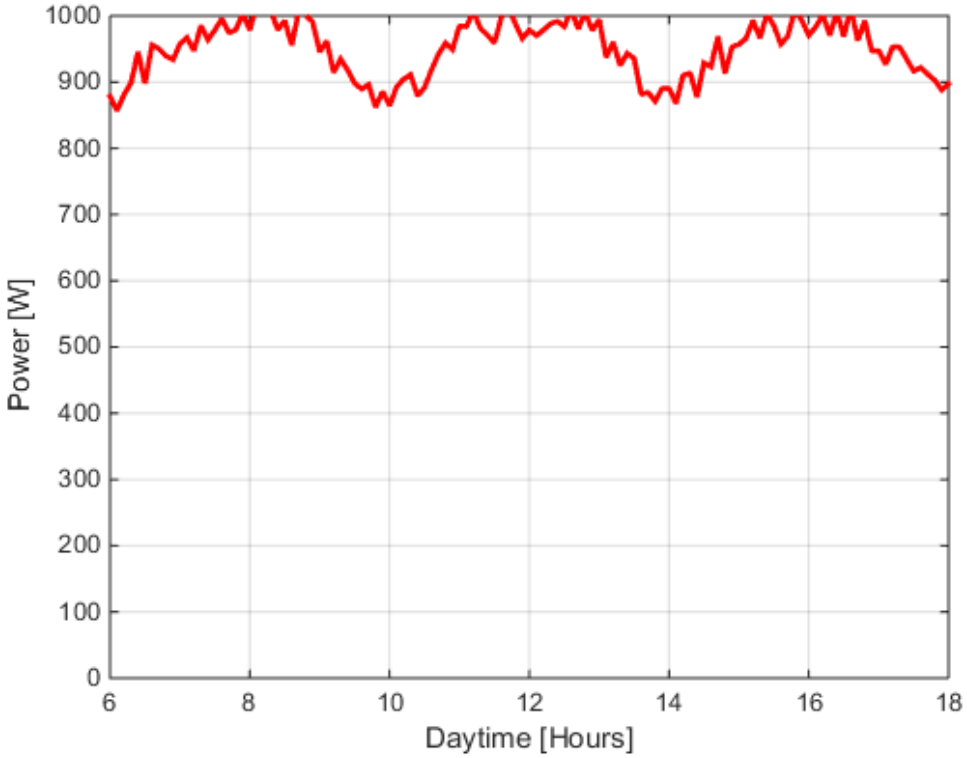

Figure 5. 11: Sunlight power collected by the designed panel

Regarding the electrical power output, the developed was assumed to have 15 % efficiciency. The peak electrical power was therefore evaluated at 144 W and graphically depicted in Figure 5.12.

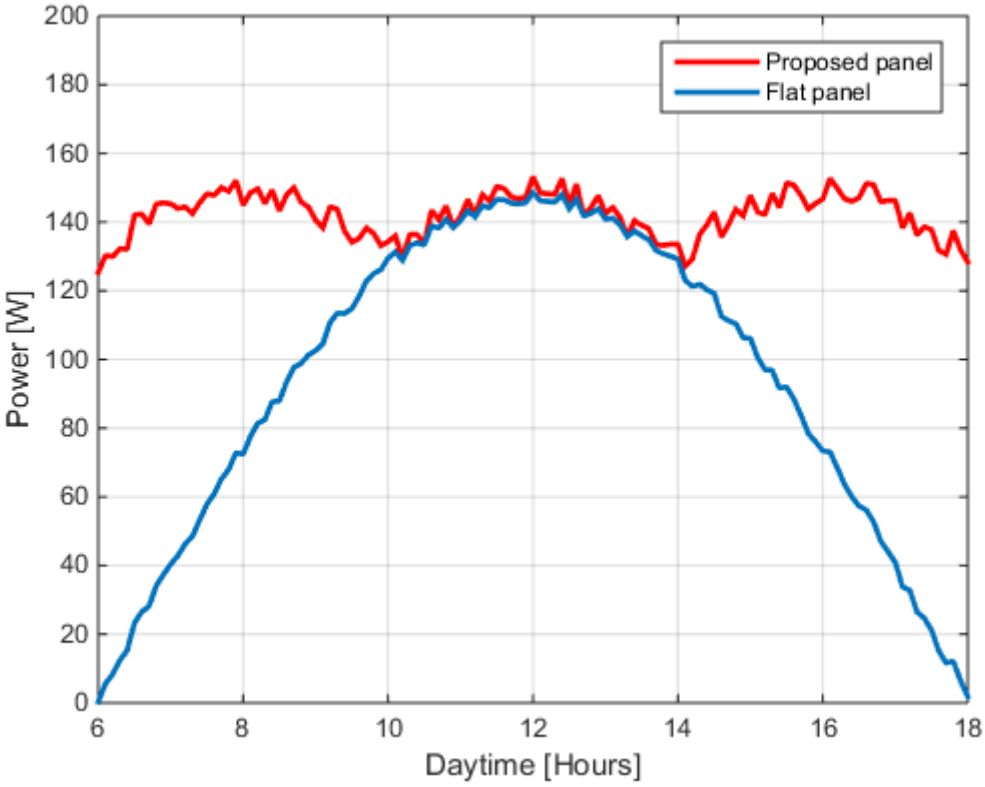

Figure 5. 12: Electrical power from the 15 %-efficient developed PV system

5.8. Selection of TE device and performance evaluation

After the design of a highly efficient solar panel, thermal electric conversion feature was still to be integrated. TE devices were therefore explored according to their size and energy conversion ability. Several TE technologies could be found from various vendors' catalogues in different sizes and ratings. (Schock et al., 2011) has on the market a TE device TEG 1-12661-6-0 that can produce the power of 14.2 W when operated with the cold temperature of 30^0 C and the hot temperature of 300^0 C. It is obvious that the hot temperature is too high especially for monocrystalline PV cells that reportedly can only heat up to 70^0 C (Zhang et al., 2015). The cooling power of the TEG device is rated at 11.6 W /cm^2. On the other hand, Module & Parameters, (n.d.) offer a variety of TE modules which are classified according to size, current, power and voltage outputs. They can handle temperature differences higher than 110^0 C and sizes that can fit the cells of the developed power panel. TEG 254-1.4-1.6, size 44 mm x 88 mm the hot side and 40 mm x 80 mm the hot side, can generate a matched power of 6.2 W. Full specifications are given in Table 5.2.

Table 5. 2: Specifications for TEG 254-1.4-1.6 at 110^0 C

Hot side (mm x mm)	Cold side (mm x mm)	Seebeck coefficient (V/K)	Open circuit voltage-Voc (V)	Load resistor (Ω)	Matched output voltage (Vout) (V)	Matched output power (Pout)(W)
40x80	44x88	0.11636	12.8	7.2	6.7	6.2

For the cooling of the power panel made of 200 mm x 300 mm-cells, the TEG 254-1.4-1.6 modules were chosen for they can be scaled up to cover the back side of the cells. Put in 2-series-2-parallel layout, 4 TEG modules can cover the cell are leaving a margin area and generate a matched output power of 28.8 W per cell if operated at 110^0 C temperature gradient. Since hottest temperatures for ordinary PVs are of order of 70^0 C while the lowest are of about 30^0 C (Zhang et al., 2015) for terrestrial applications, 40^0 C were rather used for temperature gradient in the calculation of the developed panel's power (Table 5.3). The matched power per TE device was evaluated at 1.49 W. Hence, considering that there were four TE devices per cell and sixteen cells per side, the total matched power generated by 16 cells facing either East or West is estimated at 95 W. Detailed specifications are gathered in Table 5.4.

Table 5. 3: Specification of the TE system per PV cell (4 TE devices) at 40^0 C

Hot side (mm x mm)	Cold side	Seebeck coefficient V/K	Open circuit voltage-Voc (V)	Load resistor (Ω)	Matched output voltage (Vout) (V)	Matched output power (Pout)(W)
80x160	88x176	0.11636	12.544	7.2	6.5	5.9

Table 5. 4: Specification of the TE system per same-direction facing cells at 40^0 C

Hot side (mm x mm)	Cold side	Seebeck coefficient (V/K)	Open circuit voltage-Voc (V)	Load resistor (Ω)	Matched output voltage (Vout) (V)	Matched output power (Pout)(W)
16x80x160	16x88x176	0.11636	12.544	7.2	26	95

However, the temperature distribution on TE devices depends on the level of exposure of cells to the incident radiation, a multisided approach was applied to determine the total TE generated power. If the TE sides were flat, the total power was

going to be 190 W. But due the non-uniformity in heat distribution as for OSM PV systems given the junction angle, the power was multiplied by 1.32, a ratio related to the heat collection this time. The same ratio as for OSM PV systems was used because cells receive the solar energy with the same ratio, they obviously release the energy with the same ratio. The TE system peak power was therefore evaluated at 105 W. By graph means, Figure 5.13 and 5.14 portray the variations of the TE power generated by the system.

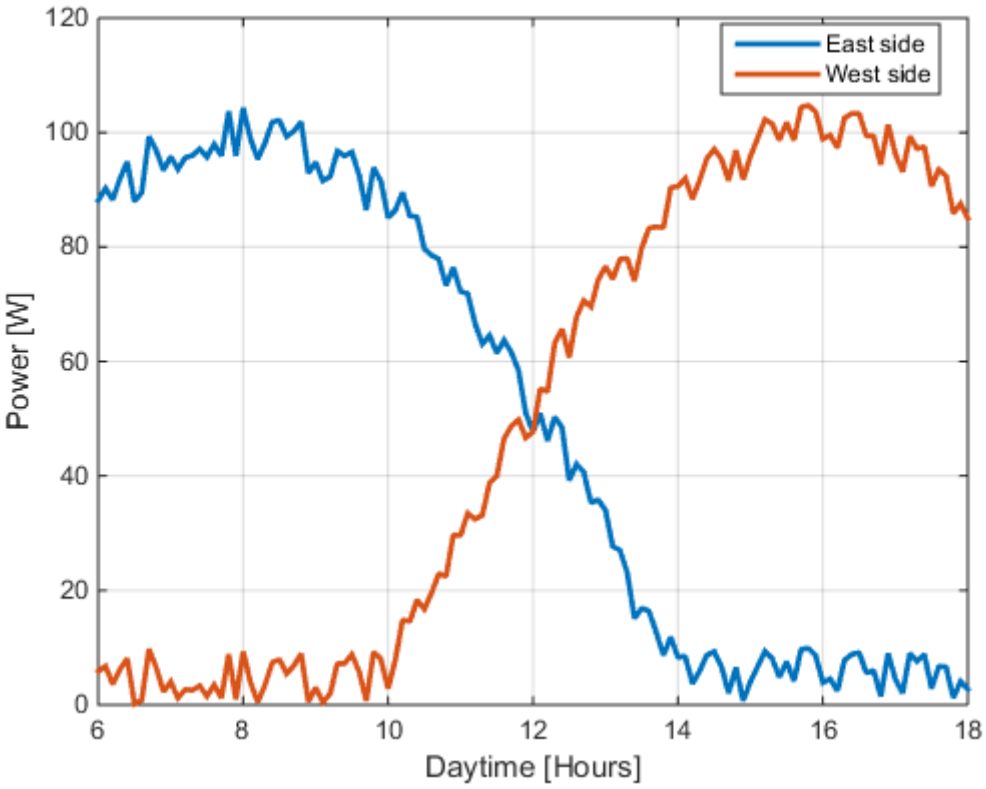

Figure 5. 13: Sides' contribution in TE power

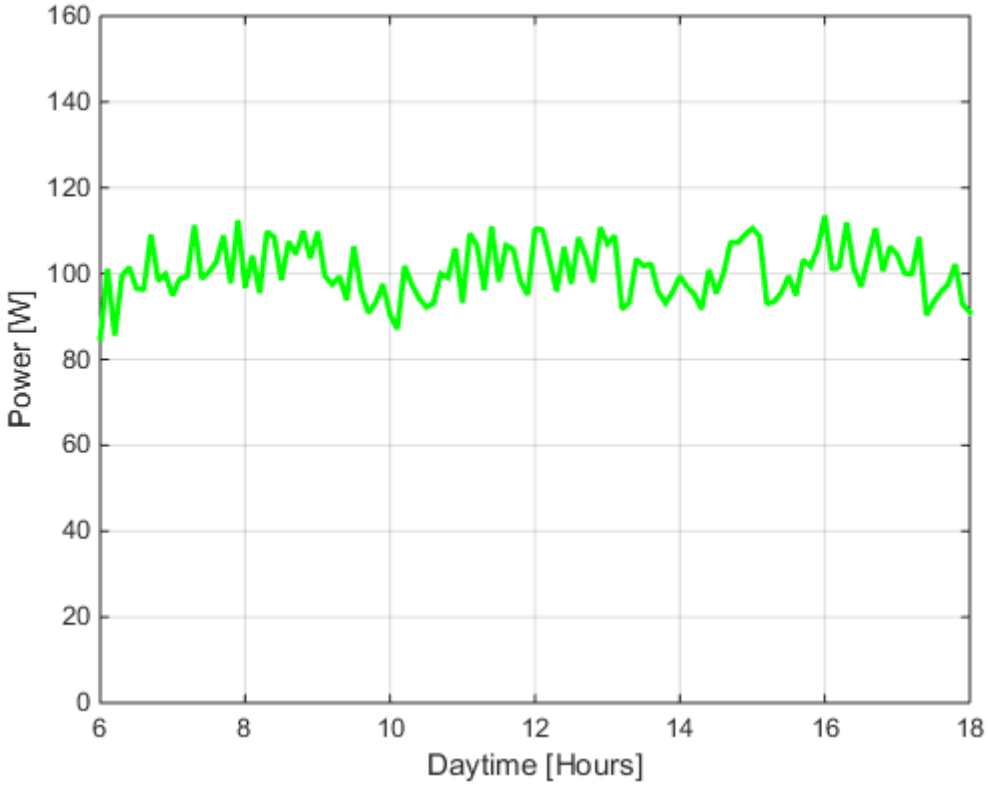

Figure 5. 14: TE system power dynamics

5.9. Overall system performance

The overall power was then calculated by adding the PV system power to the one of TE system. The peak, the average and the minimum power levels were found equal to 274.2 W, 247.8 W and 214.8 W respectively. The overall expected output power was plotted in Figure 5.15. Table 5.5 summarises key results with regards to developed model performance.

Table 5. 5: Summary of performance results

PV system	Power type	Minimum (W)	Maximum (W)	Average (W)	Area (m^2)	Occupied area (m^2)
Thermal electric solar conversion power panel	Collected	915	1073	921	1.920	0.960
	Electrical	126	153	142		
	TE	83	105	96		
	Total	209	258	238		
Uncooled flat panel	Electrical	0	144	46	0.960	0.960

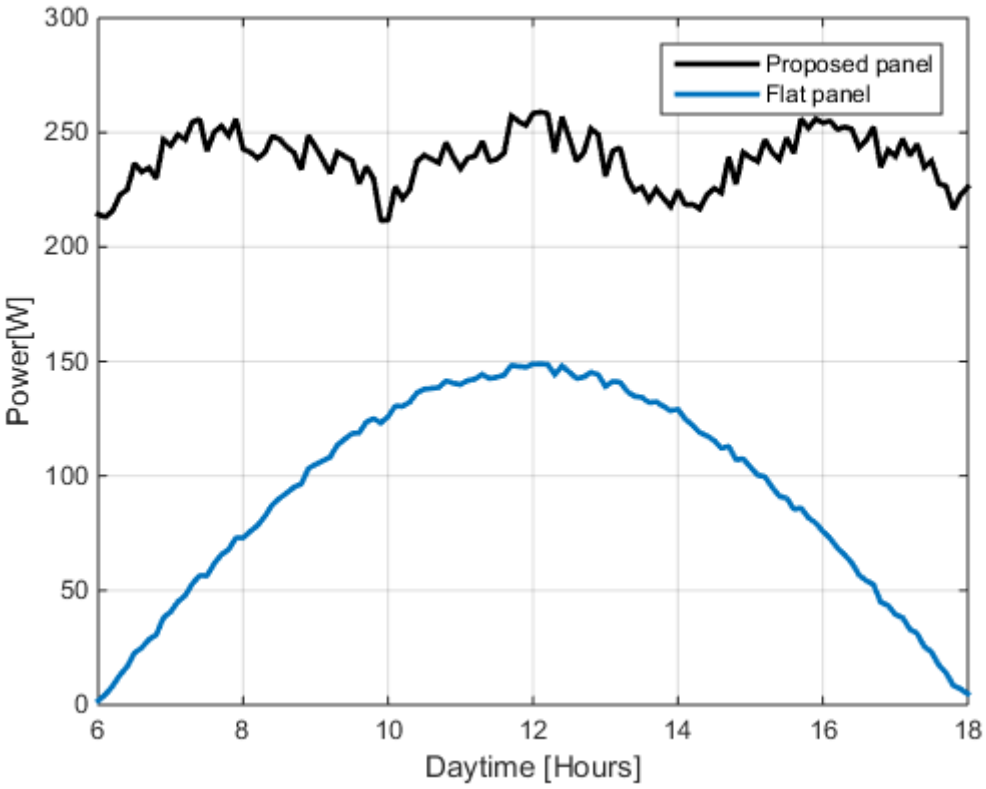

Figure 5. 15: Overall power panel electrical power dynamics

5.10. Results discussion

PV and TE aspects of the design were the drivers of the discussion of the results. From the PV point of view, the developed model exhibits several advantages including:

- Power boost: Average PV power which is 2.6 times boosted and smoother output as compared to a flat and fixed-tilt single panel while using the same space.
- High active area density: The PV active area is double the area of the flat-fixed-tilt single panel when the joint angle between the cells is set equal to 60^0. In other words, for the same surface area, the designed panel had the density of active material two times larger than that of a flat laid panel.
- Reliability: A system that is reliable from the functionality point of view since not containing any moving parts or heat-threatened electronics. The system is deemed to resist to mechanical forces if the cells junctions are tight.
- Cost-effectiveness: The designed PV system is believed to likely require less work in the post-installation maintenance given its reliability as per the above point.

From the TE perspective, the designed panel contributed a significant amount of power using a little area TE systems given the designed panel suits TE systems deployment because it offers high temperature gradients. Natural ventilation allows heat transfer between the top and the bottom sides of the cells of which the cold side temperature is naturally kept close to operating. As such, TE devices can be effectively made use of given the temperature gradient that result from the panel structural design. The structural design makes the developed suit the deployment and exploitation of TE devices unlike flat laid right on the roof with only the top side exposed to the atmosphere.

The future work will explore the implementation of the multisided technology. For residential power supply, especially in remote areas, the work will look on exploring the roofing features to effectively implement the novel technology contained in this thesis at lowest costs possible.

CHAPTER SIX

CONCLUSION AND RECOMMENDATIONS

6.1. Conclusions

The novel model of a thermal electrical solar power conversion panel geared at addressing the issues of PVs' poor efficiencies and alleviating global energy crises was completed based on novel, unique, efficient, reliable, cost-effective and recommendable approaches.

Open and closed-structure PV systems are new means of tracking the sun that improved PV efficiencies as compared to laid-flat solar. On one hand, 32 % extra sunlight power over that of fixed-tilt panels could be recovered through the implementation of OSM PV systems. OSM systems are therefore to be regarded as a successful and reliable way of tracking the sun since it does not involve moving parts and heat-susceptible electromechanical devices and require little in terms of maintenance. One the other hand, evenly distributed irradiance collection was found to be realizable through a CSM approach. A cylindrical-shaped PV system was deemed to absorb a perfectly constant level of the irradiance throughout the daytime in ideal conditions of clear sky and good-status solar arrays.

In the process of their development, OSM and CSM systems were firstly conceived in terms of how they could behave vis-à-vis the incident sunlight, then they were structurally designed. Such novel systems could be relevant only after their performance were quantifiable. Appropriate novel mathematical models for either system had then to be established and evaluation parameters to be determined. After mathematical models' verification and validation, the most challenging part was generating values for evaluation parameters for well-picked sample of proposed sun-tracking systems. As a powerful graphical and computing tool, MATLAB was resorted to. A code was developed and successfully implemented to generate graphs and results' tables for sun-tracking under study. Findings on multisided sun-tracking schemes were instrumental in pioneering a high-efficiency PV model with success.

A solar thermal electric power panel for improved energy conversion efficiency was then modelled from the electrical and thermal perspectives. Electrical wise, the findings on multisided schemes were further explored for the efficient utilisation of OSM and CSM while guarantying best efficiencies. A double-sided OSM with 60^0-junction angle was picked since only two PV sides were enough to bring a 32 % increase on power average level. Cells were then formed accordingly and the power

panel was designed. Two cells could fit in a space of one cell, which yielded 2.6 times the average level of a fixed-tilt solar panel occupying the same space area. The model is designed in a way that keeps cells cool through natural ventilation and suits the use of TE devices.

Thermal wise, few TE devices were included at the back of each cell and contributed a significant power amount given higher temperature gradients achievable from the developed panel.

Overall, the end-product of this research is a printable 3D model provided with measurements and specifications which can be referred in the development of a prototype. The research questions were answered and the aim was accomplished. Though the initial developing cost of the panel might be high, it would pay back with time through high energy generation, little post-installation costs and operation reliability.

6.2. Recommendations

Recommendations focused on other almost-unspoken factors that hinder PVs from collecting the available irradiance at full. It is commonplace that PVs are just mounted on roofs regardless of whether the roof pitch angle matches the optimum tilt angle or whether the roll angle caters for sun's motion coverage. This is mainly a consequence of having buildings conventionally laid out according to roads' plans and to the variety of roof shapes; while optimum solar exposure to the sun is not necessarily a driving factor for road planning and roof pitching.

Therefore, in line with poor-efficiency concerns, the authors suggest that PVs be mounted on roofs considering the regional PVs' optimum angle especially for fixed-tilt solar panels; which also applies for the power panel proposed in this research. Also, mounting PVs a bit up from the roof would allow heat transfer from them to the atmosphere, thus allowing natural ventilation to take place and keep PVs' temperature close to nominal operational temperatures.

The future work would explore the implementation and the exploitation of the multisided technology. For residential power supply, especially in remote areas, the work would look on exploring the possible features for efficient implementation of the novel technology contained in this thesis at lowest costs possible.

REFERENCES

Ã, H.Z., Wei, J., Wang, K., Wu, D., Al-Hasan, A.Y., Altermatt, P.P., Kiesewetter, T., Ellmer, K., Tributsch, H., Atwater, H. a, Polman, A., Boudreault, P.-L.T., Najari, A., Leclerc, M., Catchpole, K.R., Chow, T.T., Dang, M.T., Hirsch, L. & Wantz, G. 2011. The history of solar. *Solar Energy Materials and Solar Cells*, 93: 1461–1470.

Bagnall, D.M. & Boreland, M. 2008. Photovoltaic technologies. *Energy Policy*, 36(12): 4390–4396.

Bazyari, S., Keypour, R., Farhangi, S., Ghaedi, A. & Bazyari, K. 2014. A Study on the Effects of Solar Tracking Systems on the Performance of Photovoltaic Power Plants. *Journal of Power and Energy Engineering*, (April): 718–728.

Bhushan, S. 1999. Impurities and defects in photovoltaic Si devices: a review. In *Tenth International Workshop NREL*. Delhi: 1–59.

Bisseker, C. 2015. *South Africa's Energy Crisis: Eskom 2008-2005*. Rosebank: Times Medial Books.

Camargo, J.R., Claudia, M. & Oliveira, C. De. 2011. Principles of Direct Thermoelectric Conversion. http://www.intechopen.com/download/get/type/pdfs/id/20001.

Campbell, W.M., Jolley, K.W., Wagner, P., Wagner, K., Walsh, P.J., Gordon, K.C., Schmidt-mende, L., Nazeeruddin, M.K., Wang, Q., Grtzel, M. & Officer, D.L. 2007. Highly Efficient Porphyrin Sensitizers for Dye-Sensitized Solar Cells Highly Efficient Porphyrin Sensitizers for Dye-Sensitized Solar Cells. , 36(3): 11760–11762.

Carter-brown, C., Marais, R., Leask, K., Vrey, D. & Melesi, R. 2015. Transmission network integration of renewable energy in South Africa. *Energize*, 3: 18–23.

Chow, T.T. 2010. A review on photovoltaic / thermal hybrid solar technology. *Applied Energy*, 87(2): 365–379.

Clifford, M.J. & Eastwood, D. 2004. Design of a novel passive solar tracker. *Solar Energy*, 77(3): 269–280.

Crabtree, G.W. & Lewis, N.S. 2007. Solar energy conversion. *CaltechAuthors*: 37–42.

Dharmadasa, I., Bingham, P., Echendu, O., Salim, H., Druffel, T., Dharmadasa, R., Sumanasekera, G., Dharmasena, R., Dergacheva, M., Mit, K., Urazov, K., Bowen, L., Walls, M. & Abbas, A. 2014. Fabrication of CdS/CdTe-Based Thin Film Solar Cells Using an Electrochemical Technique. *Coatings*, 4(3): 380–415.

http://www.mdpi.com/2079-6412/4/3/380/.

Diamandis, P. 2015. Smart-grid technologies for automation and control in a grid connected wind energy facility in South Africa. *Energize*, 3(June): 35–38.

Ekama, G.A., Sötemann, S.W., Wentzel, M.C., Ekama, G.A. & Eurelectric. 2003. Efficiency in Electricity Generation. *Water Research*, 32(3): 297–306.

Feuermann, D. & Gordon, J.M. 2001. High-concentration photovoltaic designs based on miniature parabolic dishes. *Solar Energy*, 70(5): 423–430.

Floyd, T.L. 2012. *Electronic Devices: Conventional Current Version*. 9th ed. San Francisco: Prentice Hall.

Fraas, L.M. 2014. Low-Cost Solar Electric Power. *Springer International Publishing*: 1–181.

Grätzel, M. 2003. Dye-sensitized solar cells. *Journal of Photochemistry and Photobiology C: Photochemistry Reviews*, 4(2): 145–153.

Green, M.A. 2002. Photovoltaic principles. *Physica E: Low-Dimensional Systems and Nanostructures*, 14(1–2): 11–17.

Green, M.A. 2011. Third Generation Photovoltaics: First Generation Wafers / Ribbons. *Photovoltaics-Electricity from Sunlight*: 1–18.

Green, M.A., Emery, K., Hishikawa, Y. & Warta, W. 2011. Solar cell efficiency tables (version 37). *Prog. Photovolt:Res.App*, (19): 84–92.

Hasan, A., Alnoman, H. & Shah, A. 2016. Energy Efficiency Enhancement of Photovoltaics by Phase Change Materials through Thermal Energy Recovery. *Energies*, 9(10): 782. http://www.mdpi.com/1996-1073/9/10/782.

Hegedus, S. 2005. Amorphous Silicon Solar Cells Thin Film Amorphous Silicon Solar Cells Solar Cell Design and Processing. *Handbook of Photovoltaics Science and Engineering*: 23–30.

Ibrahim, A. 2011. Analysis of Electrical Characteristics of Photovoltaic Single Crystal Silicon Solar Cells at Outdoor Measurements. *Smart Grid and Renewable Energy*, 2(2): 169–175. http://www.scirp.org/journal/PaperDownload.aspx?DOI=10.4236/sgre.2011.22020.

Ismail, B. & Ahmed, W. 2009. Thermoelectric Power Generation Using Waste-Heat Energy as an Alternative Green Technology. *Recent Patents on Electrical Engineeringe*, 2(1): 27–39.

Jäger-waldau, A. 2017. Snapshot of Photovoltaics — March 2017. , (March): 1–9.

Jiao, Y., Zhang, F. & Meng, S. 1991. Dye Sensitized Solar Cells Principle and New Desi.

International Journal of Molecular Sciences, 11(3): 5–37.

Jingcheng, L. 1959. Application of solar energy. *Solar Energy*, 3(3): 48.

Jones-albertus, R., Feldman, D., Fu, R., Horowitz, K. & Woodhouse, M. 2016. Technology advances needed for photovoltaics to achieve widespread grid price parity. : 1–12.

Jordan, D.C. & Kurtz, S.R. 2013. Photovoltaic degradation rates - An Analytical Review. *Progress in Photovoltaics: Research and Applications*, 21(1): 12–29.

Juang, J. & Radharamanan, R. 2014. Design of a Solar Tracking System for Renewable Energy. *Proceedings of 2014 Zone 1 Conference of the American Society for Engineering Education*.

Kamal, M.A. 2012. An Overview of Passive Cooling Techniques in Buildings : Design Concepts and Architectural Interventions. , 55(1).

Kamanzi, J. & Kahn, M. 2015. Development of a Renewable Energy-Based Cooling System for a Mobile Ground Station. *IEEE Aerospace and Electronic Systems Magazine*, 30(2): 6–13.

Kamanzi, J. & Kahn, M. 2016. Multisided approach for photovoltaics regulated outputs : computer-based simulations. *Journal of Energie Challenges and Mechanics*, 3(2): 93–99.

Kibria, M.T., Ahammed, A., Sony, S.M. & Hossain, F. 2014. A Review : Comparative studies on different generation solar cells technology. In *International Conference on Environmental Aspects of Bangladesh*. Dhaka: 51–53.

Kim, J., Bahk, J.H., Hwang, J., Kim, H., Park, H. & Kim, W. 2013. Thermoelectricity in semiconductor nanowires. *Physica Status Solidi - Rapid Research Letters*, 7(10): 767–780.

Kim, Y.J., Joshi, Y.K. & Fedorov, A.G. 2008. An absorption based miniature heat pump system for electronics cooling. *International Journal of refrigeration*, 31(2008): 23–33.

King, R.R., Bhusari, D., Larrabee, D., Liu, X., Rehder, E., Edmondson, K., Cotal, H., Jones, R.K., Ermer, J.H., Fetzer, C.M., Law, D.C. & Karam, N.H. 2012. Solar cell generations over 40 % ef fi ciency. *Prog.Photovolt: Res.Appl*: 1–15.

Lain, M. & Hensen, J. 2006. Passive and low energy cooling techniques in buildings. In *Proceedings of the 17th Int . Air-conditioning and Ventilation Conference*. Prague: 1–7.

Lapidot, D., Dror, R., Vered, E., Mishli, O., Levy, D. & Helman, Y. 2014. Automatic Solar Tracking System. *Plant Pathology*, 1(7): 192–195.

Lee, C.-Y., Chou, P.-C., Chiang, C.-M. & Lin, C.-F. 2009. Sun Tracking Systems: A Review. *Sensors*, 9(5): 3875–3890. http://www.mdpi.com/1424-8220/9/5/3875/.

Leite, E.P. 2010. *Matlab - Modelling, Programming and Simulations*. http://www.intechopen.com/books/matlab-modelling-programming-and-simulations.

Lin, S., Li, W., Chen, Z., Shen, J., Ge, B. & Pei, Y. 2016. Tellurium as a high-performance elemental thermoelectric. *Nature Communications*, 7: 10287. http://www.nature.com/doifinder/10.1038/ncomms10287.

Long, J. & Memik, S.O. 2010. A Framework for Optimizing Thermoelectric Active. In *DAC10-June 13-18*. Anaheim: 591–596.

Marco, T.G. 1849. Photovoltaic Panels : a Review of the Cooling. , 1(1): 63–74.

Megahed, S. Cooling Techniques for High Density Electronics. *Electronics Cooling Methods in Industry*: 71–81.

Meneses-Rodríguez, D., Horley, P.P., González-Hernández, J., Vorobiev, Y. V. & Gorley, P.N. 2005. Photovoltaic solar cells performance at elevated temperatures. *Solar Energy*, 78(2): 243–250.

Mittal V, Kasana KS, T.N. 2005. The study of solar absorption air-conditioning systems. *Journal of Energy in Southern Africa*, 16(4): 59–66.

Module, S.-T. & Parameters, E. Thermoelectrics module specifications (TEC1-00703). *Everredtronics Limited Specifications*, (89). http://www.everredtronics.com/thermoelectric.TEC1.html [15/10/2016].

Moharram, K.A., Abd-Elhady, M.S., Kandil, H.A. & El-Sherif, H. 2013. Enhancing the performance of photovoltaic panels by water cooling. *Ain Shams Engineering Journal*, 4(4): 869–877.

Narendrasinh Parmar, A.J., Parmar, A.N. & Gautam, V.S. 2015. Passive Solar Tracking System. *International Journal of Emerging Technology and Advanced Engineering Website: www.ijetae.com ISO Certified Journal*, 5(1): 67–88.

Natarajan, S.K., Mallick, T.K., Katz, M. & Weingaertner, S. 2011. Numerical investigations of solar cell temperature for photovoltaic concentrator system with and without passive cooling arrangements. *International Journal of Thermal Sciences*, 50(12): 2514–2521.

Ovchinnikov, M., Mckenna-lawlor, S., Psychology, S., Kanas, N., Manuy, D., Larson, W.J. & Wertz, J.R. *Space Mission Analysis and Design .*

Pachpande, S.G. & Jalgaon. 2012. Studying The Effect of Shading on Solar Panel using

MATLAB. *International Journal of Science and Applied Information Technology*, 1(2): 46–51.

Parida, B., Iniyan, S. & Goic, R. 2011. A review of solar photovoltaic technologies. *Renewable and Sustainable Energy Reviews*, 15(3): 1625–1636. http://dx.doi.org/10.1016/j.rser.2010.11.032.

Photovoltaics, F. 2014. GLOBAL MARKET.

Rawal, N., Vaishaly, A.G., Sharma, H. & Mathew, B.B. 2016. Dye Sensitized Solar Cells : The Emerging Technology Dye Sensitized Solar Cells : The Emerging Technology. *Energy and Power Engineering Science*, 2(2): 46–52.

Rekioua, D. & Matagne, E. 2012. *Optimization of photovoltaic power systems: Modelization, Simulation and Control*.

Royne, A. & Dey, C.J. 2007. Design of a jet impingement cooling device for densely packed PV cells under high concentration. *Solar Energy*, 81(8): 1014–1024.

Sabri, L., Benzirar, M. & Student, P.G. 2007. Effect of Ambient Conditions on Thermal Properties of Photovoltaic Cells: Crystalline and Amorphous Silicon. *International Journal of Innovative Research in Science, Engineering and Technology (An ISO Certified Organization)*, 3297(12): 17815–17821.

Santra, P.K. & Kamat, P. V. 2012. Mn-Doped Quantum Dot Sensitized Solar Cells: A Strategy to Boost Efficiency over 5%. *J.Am Chem Soc*, 134(5): 23–26.

Schock, H., Caillet, T., Case, E., Fleurial, J., Hogan, T., Lyle, M., Maloney, R., Moran, K., Ruckle, T., Sakamoto, J., Shih, T., Thompson, T., Timm, E., Zhang, L. & Zhu, G. 2011. Thermoelectric Conversion of Waste Heat to Electricity in an IC Engine Powered Vehicle Objectives and Relevance to DOE Goals. *Energy Efficiency Renewable Energy*: 1–25.

Seebeck, T. & Coefficient, S. 1821. Thermopower (Seebeck Effect).

Segal, A., Epstein, M. & Yogev, A. 2004. Hybrid concentrated photovoltaic and thermal power conversion at different spectral bands. *Solar Energy*, 76(5): 591–601.

Solesvik Oppedal, K. 2013. A Study of the Staebler-Wronski Effect and Amorphous Silicon Solar Cells.

Steinfeld, A., Haueter, P. & Weidenkaff, A. 2010. Conversion of Simulated Solar Radiation into Electrical Energy. : 2801–2814.

Sthel, M.S. 2013. Current energy crisis and its economic and environmental consequences:

Intense human cooperation. *Natural Science*, 5(2): 244–252. http://www.scirp.org/journal/PaperInformation.aspx?PaperID=28343.

Sunpower. 2008. More power. A better investment. : 1–10.

Systems, P.R.E. 2015. The sun shines , but not always …. *Energize*, 3: 51–53.

Thompson, C.P., Hegedus, S.S., Shafarman, W.N. & Desai, D. 2008. Temperature dependence of V oc in CdTe and Cu (InGa)(SeS) 2–based solar cells. *33rd IEEE Photovoltaic Specialists Conference (PVSC)*, (1): 1–6. http://www.udel.edu/iec/Publications/33rdIEEE/Thompson.pdf.

Wang, Y. & Chen, X. 2009. Advanced Electronic Cooling Technologies. : 149–152.

Wasiak, I. & Hanzelka, Z. 2010. Integration of distributed energy sources with electrical power grid. *Bulletin of the Polish Academy of Sciences: Technical Sciences*, 57(4): 297–309.

Wright, J. 2015. Electrical energy storage to make wind and solar PV resources disptatchable. *Energize*: 54–59.

Yilmaz, S., Riza Ozcalik, H., Dogmus, O., Dincer, F., Akgol, O. & Karaaslan, M. 2015. Design of two axes sun tracking controller with analytically solar radiation calculations. *Renewable and Sustainable Energy Reviews*, 43(September 2016): 997–1005.

Yılmaz, M. & Kentli, F. 2015. Increasing of Electrical Energy with Solar Tracking System at the Region which Has Turkey's Most Solar Energy Potential. *Journal of Clean Energy Technologies*, 3(4): 287–290. http://www.jocet.org/index.php?m=content&c=index&a=show&catid=39&id=499.

You, L.J., Hao, L.J. & Adele, L.S. Sun and Architecture. *GEK 1506 Heavenly Mathematics*.

Zeng, W., Cao, Y., Bai, Y., Wang, Y., Shi, Y., Zhang, M., Wang, F., Pan, C. & Wang, P. 2010. Efficient dye-sensitized solar cells with an organic photosensitizer featuring orderly conjugated ethylenedioxythiophene and dithienosilole blocks. *Chemistry of Materials*, 22(5): 1915–1925.

Zhang, Q.X., Yu, H.Y., Zhang, Q.Y., Zhang, Z.Y., Shao, C.H. & Yang, D. 2015. A solar automatic tracking system that generates power for lighting greenhouses. *Energies*, 8(7): 7367–7380.

Zhang, X. & Zhao, L.-D. 2015. Thermoelectric materials: Energy conversion between heat and electricity. *Journal of Materiomics*, 1(2): 92–105.

Zhu, L., Boehm, R.F., Wang, Y., Halford, C. & Sun, Y. 2011. Water immersion cooling of PV

cells in a high concentration system. *Solar Energy Materials and Solar Cells*, 95(2): 538–545.

Zhu, L., Wang, Y., Fang, Z., Sun, Y. & Huang, Q. 2010. Solar Energy Materials & Solar Cells An effective heat dissipation method for densely packed solar cells under high concentrations. *Solar Energy Materials and Solar Cells*, 94(2): 133–140.

Zhu, W., Deng, Y., Wang, Y., Shen, S. & Gulfam, R. 2016. High-performance photovoltaic-thermoelectric hybrid power generation system with optimized thermal management. *Energy*, 100(April): 91–101.

Zondag, H.A. 2008. Flat-plate PV-Thermal collectors and systems: A review. *Renewable and Sustainable Energy Reviews*, 12(4): 891–959.